Hidden non–n-locality in linear networks

Kaushiki Mukherjee[1,*] Soma Mandal[2,†] Tapaswini Patro[3,‡] and Nirman Ganguly[3,§]
[1]*Department of Mathematics, Government Girls' General Degree College, Ekbalpore, Kolkata-700023, India*
[2]*Department of Physics, Government Girls' General Degree College, Ekbalpore, Kolkata-700023, India*
[3]*Department of Mathematics, Birla Institute of Technology and Science Pilani, Hyderabad Campus, Telangana-500078, India*

(Received 16 March 2023; revised 3 July 2023; accepted 6 September 2023; published 19 September 2023)

We study hidden nonlocality in a linear network with independent sources. In the usual paradigm of Bell nonlocality, there are certain states which exhibit nonlocality only after the application of suitable local filtering operations, which, in turn, are some special stochastic local operations assisted with classical communication (SLOCC). In the present work, we introduce the notion of hidden non n-locality. The notion is detailed using a bilocal network. We provide instances of hidden nonbilocality and nontrilocality, where we notice quite intriguingly that nonbilocality is observed even when one of the sources distributes a mixed two-qubit separable state. Furthermore, a characterization of hidden nonbilocality is also provided in terms of the Bloch-Fano decomposition, wherein we conjecture that, to witness hidden nonbilocality, one of the two states (used by the sources) must have nonnull local Bloch vectors. Noise is inevitable in practical scenarios, which makes it imperative to study any possible method to enhance the possibility of detecting nonclassicality in the presence of noise in the network. We find that local filtering enhances the robustness to noise, which we demonstrate using bit-flip and amplitude-damping channels.

DOI: 10.1103/PhysRevA.108.032416

I. INTRODUCTION

The study on correlations unachievable within the classical realm has both foundational [1] and pragmatic [2] implications. Bell nonlocality [1,3] constitutes one of the most profound correlations that a quantum state has to offer. The fact that measurements done by spatially separated parties give rise to correlations that cannot be explained by local hidden variables is the mainstay of such nonlocal correlations [1]. Correlations that do not admit a local hidden variable (LHV) description will hence violate a suitably chosen Bell's inequality [1]. Thus the violation of the Bell's inequality bears the signature of Bell nonlocality. Apart from foundational interest, Bell nonlocality also plays significant roles in practical tasks like device-independent quantum cryptography [4] and random number generation [5].

In a standard (n, m, k) measurement scenario, each of n parties sharing a given state repeatedly makes a random and independent choice of one measurement from a collection of m measurements which are each k valued. It is then checked whether the correlations generated therein violate Bell's inequality. Violation of at least one Bell's inequality thus guarantees the nonlocal nature of such correlations. Entanglement is considered a necessity for the violation of Bell's inequalities. However, there are several states, which although entangled, do not violate any Bell's inequality [3,6]. Some of those states violate Bell's inequality when subjected to sequential measurements. In such a sequential measurement scenario, the measurements are applied in multiple stages. Initially, the parties are allowed to perform local operations assisted with classical communication (LOCC). In the final step, the parties perform local measurements as in the usual (n, m, k) scenario.

Speaking of sequential measurements, the application of local filtering operations followed by local measurements deserves special mention in the context of Bell nonlocality. Local filtering operations constitute an important class of stochastic local operations and classical communication (SLOCC [6,7]). Any state which violates Bell's inequality after being subjected to suitable filtering operations is said to exhibit hidden nonlocality [8,9]. Over the years, multiple probes observed various instances of hidden nonlocality [8–11]. In [8,9], the authors gave instances of Bell–Clauser-Horne-Shimony-Holt (CHSH) [12] local [3] entangled states which exhibit hidden nonlocality when subjected to suitable local filters. In [10], the authors showed that even states admitting a LHV model can generate hidden nonlocality under a suitable measurement context. In a broader sense, the present work characterizes hidden nonlocality in the purview of a linear network (which we briefly state below with the details given in Sec. II B).

In the last decade, the study of nonlocality has been extended beyond the usual paradigm of a Bell scenario to accommodate and analyze network correlations arising in different experimental setups involving multiple independent sources [13–20]. Network scenarios, characterized by source independence (*n-local*) assumption are commonly known as *n-local networks* [16]. In such scenarios, each of the sources

*kaushiki.wbes@gmail.com
†soma2778.wbes@gmail.com
‡p20190037@hyderabad.bits-pilani.ac.in
§nirmanganguly@hyderabad.bits-pilani.ac.in

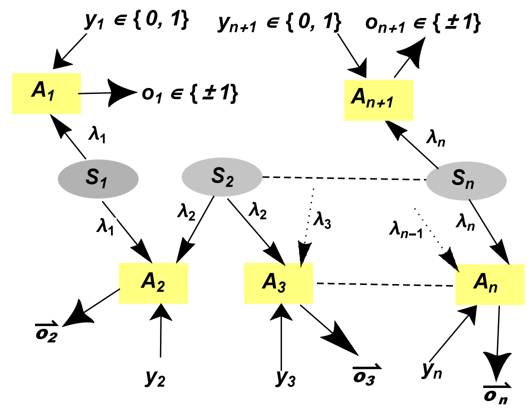

FIG. 1. Schematic diagram of a linear n-local network [16].

sends particles to a subset of distant parties forming the network. Owing to n-local assumption, some novel quantum correlations are observed in a network that are not witnessed in the standard Bell scenario [17,21]. For example, nonclassical correlations (non–n-local correlations) are generated across the entire network even though all the parties do not share any common past. Moreover, in the measurement scenario associated with a network, some or all the parties perform a fixed measurement. This is also in contrast to the standard Bell scenario, where the random and free choice of inputs by each party is crucial to demonstrate Bell nonlocality.

Different research activities have been conducted which provide for the characterization of quantum correlations in n-local networks [14–16,22–38]. Much like the usual Bell nonlocality experiments, violation of an n-local inequality indicates the presence of n-nonlocal correlations. However, when a particular n-local inequality is satisfied, we remain inconclusive. It has been shown that in a network if each source distributes a two-qubit pure entangled state then a violation is observed [23]. The same conclusion does not hold in case the source generates some mixed entangled states. The n-local inequality fails to capture nonlocality even though there may be some non–n-local correlations. Thus, it becomes imperative to probe whether local filtering operations can reveal hidden non–n-local correlations. The present work addresses this question.

In this work, we introduce the notion of *hidden non–n-locality*. We analyze the nature of quantum correlations in a n-local network where at least one party performs local filtering operations after the distribution of qubits by the sources. For a detailed discussion, we consider the simplest n-local network, namely, a bilocal network ($n = 2$ [15]). We then characterize the set of hidden nonbilocal correlations. The characterization is also given in terms of the Bloch-Fano decomposition. It is observed that to witness hidden nonbilocality in a network, at least one of the two states must have nonnull local Bloch vectors, which we state as a conjecture. Interestingly, hidden nonbilocality is detected even when one of the sources distributes a two-qubit mixed separable state. Environmental noise is ubiquitous in any implementation of quantum information processing protocols. In this context, it is thus important to explore ways which can enhance the detection of non–n-local correlations. We find that appropriately chosen local filters are effective in this scenario. We demonstrate this phenomenon using bit-flip and amplitude damping channels.

The rest of the work is organized in the following manner. In Sec. II, we briefly discuss the prerequisites for our work. In Sec. III, we discuss the n-local network scenario where now the parties may perform filtering operations thereby introducing the notion of hidden non–n-locality. Hidden non–n-local correlations are then analyzed in Sec. IV. Characterization of hidden non–n-locality in terms of Bloch parameters is provided next in Sec. V. The utility of filtering operations in increasing bilocal inequality's robustness to noise is discussed with a few examples in Sec. VI. We then summarize our work with a discussion on possible future courses of work.

II. PRELIMINARIES

A. Bloch-Fano decomposition of a density matrix

Let ρ denote an arbitrary two-qubit state. In the Bloch-Fano decomposition ρ is given as

$$\rho = \frac{1}{4}\Bigg(\mathbb{I}_2 \times \mathbb{I}_2 + \vec{a}\cdot\vec{\sigma}\otimes\mathbb{I}_2 + \mathbb{I}_2\otimes\vec{b}.\vec{\sigma} + \sum_{j_1,j_2=1}^{3} \mathfrak{w}_{j_1 j_2}\sigma_{j_1}\otimes\sigma_{j_2}\Bigg), \tag{1}$$

where $\vec{\sigma} = (\sigma_1, \sigma_2, \sigma_3)$, σ_{j_k} stand for Pauli operators along three mutually perpendicular directions ($j_k = 1, 2, 3$). $\vec{a} = (a_1, a_2, a_3)$ and $\vec{b} = (b_1, b_2, b_3)$ denote local bloch vectors ($\vec{a}, \vec{b} \in \mathbb{R}^3$) corresponding to the party Alice (A) and Bob (B), respectively, with $|\vec{a}|, |\vec{b}| \leqslant 1$ and $(\mathfrak{w}_{i,j})_{3\times3}$ denotes correlation tensor $\mathcal{W}$ (real). Matrix elements $\mathfrak{w}_{j_1 j_2}$ are given by $\mathfrak{w}_{j_1 j_2} = \mathrm{Tr}[\rho\, \sigma_{j_1}\otimes\sigma_{j_2}]$.

$\mathcal{W}$ can be diagonalized by subjecting it to suitable local unitary operations [39,40]. The transformed state is then given by

$$\rho' = \frac{1}{4}\Bigg(\mathbb{I}_2 \times \mathbb{I}_2 + \vec{u}\cdot\vec{\sigma}\otimes\mathbb{I}_2 + \mathbb{I}_2\otimes\vec{z}\cdot\vec{\sigma} + \sum_{j=1}^{3} s_j\sigma_j\otimes\sigma_j\Bigg), \tag{2}$$

$T = \mathrm{diag}(s_1, s_2, s_3)$ denote the correlation matrix in Eq. (2) where s_1, s_2, s_3 are the eigen values of $\sqrt{\mathcal{W}^T\mathcal{W}}$, i.e., singular values of $\mathcal{W}$. It is important to note here such local unitary transforms do not affect the nonlocality exhibited by the state.

B. Linear *n*-local networks

Here we give a brief overview of linear n-local networks [16]. Let us consider a linear network arrangement of n sources $\mathbf{S}_1, \mathbf{S}_2, \ldots, \mathbf{S}_n$ and $n+1$ parties $\mathbf{A}_1, \mathbf{A}_2, \ldots, \mathbf{A}_{n+1}$ (see Fig. 1). $\forall i = 1, 2, \ldots, n$, source $\mathbf{S}_i$ independently sends physical systems to $\mathbf{A}_i$ and $\mathbf{A}_{i+1}$. Each of $\mathbf{A}_2, \mathbf{A}_3, \ldots, \mathbf{A}_n$ receives two particles and is referred to as *central* parties. The other two parties $\mathbf{A}_1$ and $\mathbf{A}_{n+1}$ are referred to as *extreme* parties. Each of the extreme parties receive one particle. Each of the sources $\mathbf{S}_i$ is characterized by variable λ_i. The sources being independent, joint distribution of the variables $\lambda_1, \dots, \lambda_n$ is factorizable

$$q(\lambda_1, \dots, \lambda_n) = \Pi_{i=1}^{n} q_i(\lambda_i), \tag{3}$$

where $\forall i$, q_i denotes the normalized distribution of λ_i. Equation (3) represents the n-local constraint.

$\forall i = 2, 3, \dots, n-1$ the central party $\mathbf{A}_i$ performs a single measurement y_i on the joint state of the two subsystems that are received from $\mathbf{S}_{i-1}$ and $\mathbf{S}_i$. Each of the two extreme parties ($\mathbf{A}_1$, $\mathbf{A}_{n+1}$) selects from a collection of two dichotomous inputs. The $n+1$-partite network correlations are local if those can be decomposed as

$$p(o_1, \vec{o}_2, \dots, \vec{o}_n, o_{n+1}|y_1, y_2, \dots, y_n, y_{n+1}) = \int_{\Lambda_1}\int_{\Lambda_2}\cdots\int_{\Lambda_n} d\lambda_1 d\lambda_2 \dots d\lambda_n\, q(\lambda_1, \lambda_2, \dots, \lambda_n) P, \quad \text{with}$$
$$P = p(o_1|y_1, \lambda_1)\Pi_{i=2}^{n} p(\vec{o}_i|y_i, \lambda_{i-1}, \lambda_i) p(o_{n+1}|y_{n+1}, \lambda_n). \tag{4}$$

The notations appearing in Eq. (4) are detailed below.

(1) $\forall i$, Λ_i denotes the set of all possible values of λ_i.

(2) $y_1, y_{n+1} \in 0, 1\}$ label inputs of $\mathbf{A}_1$ and $\mathbf{A}_{n+1}$, respectively.

(3) $o_1, o_{n+1} \in \{0, 1\}$ denote outputs of $\mathbf{A}_1$ and $\mathbf{A}_{n+1}$, respectively.

(4) $\forall i$, $\vec{o}_i = (o_{i1}, o_{i2})$ labels four outputs of input y_i for $o_{ij} \in \{0, 1\}$.

$n+1$-partite correlations are n-local if they satisfy both Eqs. (3) and (4). Hence, any set of correlations that do not satisfy both Eqs. (3) and (4), are termed as non–n-local.

An n-local inequality [16] corresponding to linear n-local network is given by

$$\sqrt{|I|} + \sqrt{|J|} \leqslant 1, \quad \text{where} \quad I = \frac{1}{4}\sum_{y_1, y_{n+1}} \langle O_{1,y_1} O_2^0 \dots O_n^0 O_{n+1,y_{n+1}} \rangle,$$
$$J = \frac{1}{4}\sum_{y_1, y_{n+1}} (-1)^{y_1 + y_{n+1}} \langle O_{1,y_1} O_2^1 \dots O_n^1 O_{n+1,y_{n+1}} \rangle, \ \text{with}$$
$$\langle O_{1,y_1} O_2^i \dots O_n^i O_{n+1,y_{n+1}} \rangle = \sum_{\mathcal{D}} (-1)^{\mathbf{o}_1 + \mathbf{o}_{n+1} + \mathbf{o}_{2i} + \cdots \mathbf{o}_{ni}} N_2,$$
$$\text{where} \quad N_2 = p(\mathbf{o}_1, \vec{o}_2, \dots, \vec{o}_n, \mathbf{o}_{n+1}|y_1, y_{n+1}), \ i = 0, 1,$$
$$\text{and} \quad \mathcal{D} = \{\mathbf{o}_1, \mathbf{o}_{21}, \mathbf{o}_{22}, \dots, \mathbf{o}_{n1}, \mathbf{o}_{n2}, \mathbf{o}_{n+1}\}. \tag{5}$$

Violation of Eq. (5) guarantees that the corresponding correlations are non–n-local.

C. Quantum linear n-local network scenario

In a linear n-local network, let $\mathbf{S}_i (i = 1, 2, \dots, n)$ generate an arbitrary two-qubit state ϱ_i. Each of the central parties thus receives two qubits: one of ϱ_{i-1} and another of ϱ_i. Extreme parties $\mathbf{A}_1$ and $\mathbf{A}_{n+1}$ receive a single qubit of ϱ_1 and ϱ_n, respectively. Let each of the central parties perform the projective measurement in Bell basis $\{|\psi^{\pm}\rangle, |\phi^{\pm}\rangle\}$. Let each of $\mathbf{A}_1$ and $\mathbf{A}_{n+1}$ perform projective measurements along any one of two arbitrary directions. For these measurement settings, non–n-local correlations are ensured by violation of Eq. (5), i.e., if [29]

$$\mathbf{B}_{lin} = \sqrt{\Pi_{i=1}^{n} t_{i1} + \Pi_{i=1}^{n} t_{i2}} > 1, \tag{6}$$

with t_{i1}, t_{i2} denoting the largest two singular values of correlation tensor (T_i) of ϱ_i $(i = 1, 2, \dots, n)$. If Eq. (6) is not satisfied, nothing can be concluded about the n-local nature of the corresponding correlations.

D. Filtering operations

As noted before, filtering operations [6] are used to reveal the hidden nonlocality. Let ϱ_{AB} denote a bipartite state shared between two distant parties Alice and Bob. A local filtering operation by one of the two parties, say, Alice may be defined as a local measurement (F_A) having two outcomes $\{\mathfrak{F}_A, \bar{\mathfrak{F}}_A\}$ such that $\mathfrak{F}_A^{\dagger}\mathfrak{F}_A + \bar{\mathfrak{F}}_A^{\dagger}\bar{\mathfrak{F}}_A = \mathbb{I}$. Hence, $\mathfrak{F}_A^{\dagger}\mathfrak{F}_A \leqslant \mathbb{I}$. Local filtering operation F_B can be defined similarly. Let Alice and Bob perform F_A and F_B on their respective subsystems. After the parties apply the filtering operations, four possible output states can be obtained. On being allowed to communicate over the classical channel, Alice and Bob postselect the state corresponding to output pair $(\mathfrak{F}_A, \mathfrak{F}_B)$, i.e., they keep the state

$$\varrho'_{AB} = \frac{(\mathfrak{F}_A \otimes \mathfrak{F}_B)\varrho_{AB}(\mathfrak{F}_A \otimes \mathfrak{F}_B)^{\dagger}}{\mathrm{Tr}[(\mathfrak{F}_A \otimes \mathfrak{F}_B)\varrho_{AB}(\mathfrak{F}_A \otimes \mathfrak{F}_B)^{\dagger}]}. \tag{7}$$

The probability of obtaining ϱ'_{AB} as the output state is given by $\mathrm{Tr}(\mathfrak{F}_A \otimes \mathfrak{F}_B \varrho_{AB} \mathfrak{F}_A^{\dagger} \otimes \mathfrak{F}_B^{\dagger})$.

The postselected state ϱ'_{AB} is usually referred to as the *filtered state*. As indicated in [6,10], for the qubit case the diagonal form of the local filters turns out to be most relevant:

$$\mathfrak{F} = \epsilon|0\rangle\langle 0| + |1\rangle\langle 1|, \epsilon \in [0, 1]. \tag{8}$$

For our purpose, we use this particular form of local filter.

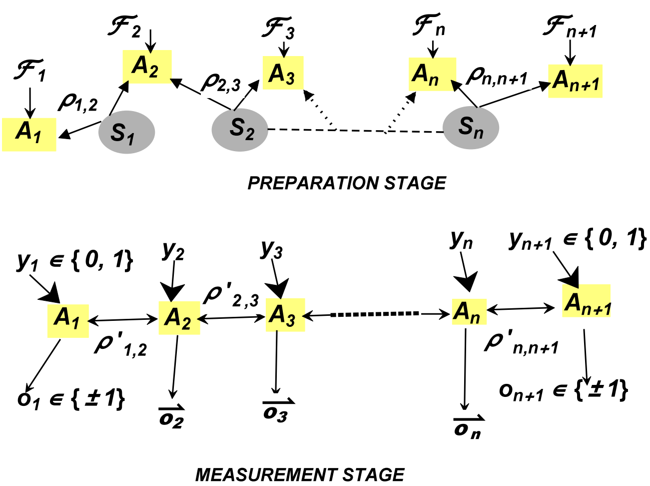

FIG. 2. Schematic diagram of the sequential linear n-local network. The overall quantum state shared between the parties in the preparation stage is ρ_{initial} [Eq. (9)]. In this stage, each of the parties performs local filtering operations [Eqs. (10) and (11)]. ρ_{filtered} [Eq. (12)] is the overall state in the measurement stage.

III. SEQUENTIAL LINEAR n-LOCAL NETWORK

We now consider an n-local linear network where the parties are allowed to perform local filtering operations. The entire network scenario (see Fig. 2) is now divided into two stages: the *preparation stage* and the *measurement stage*.

A. Preparation stage

As in usual linear n-local network (Sec. II C), let each of n sources $\mathbf{S}_i$ distribute a two-qubit quantum state $\rho_{i,i+1}$ between $\mathbf{A}_i$ and $\mathbf{A}_{i+1} (i = 1, 2, \dots, n)$. The overall state of the particles shared by all the parties across the entire network is thus given by

$$\rho_{\text{initial}} = \otimes_{i=1}^{n} \rho_{i,i+1}. \tag{9}$$

On receiving the particles, let each of the parties now perform local filtering operations on their respective subsystems. The local filter applied on a single qubit by each of $\mathbf{A}_1$ and $\mathbf{A}_{n+1}$ is of the form given by Eq. (8)

$$\mathfrak{F}_j = \epsilon_j |0\rangle\langle 0| + |1\rangle\langle 1|, \; j = 1, n+1, \text{ and } \epsilon_j \in [0, 1]. \tag{10}$$

Clearly, in case $\epsilon_j = 1$, then $\mathbf{A}_j$ $(j = 1, n+1)$ does not apply any filtering operation. Each of the $n-1$ intermediate parties performs local filters on the joint state of the two qubits (received from two sources). Form of the local filter applied by $\mathbf{A}_j (j = 2, 3, \dots, n-1)$ is given by

$$\mathfrak{F}_j = \otimes_{i=1}^{2} \big(\epsilon_j^{(i)} |0\rangle\langle 0| + |1\rangle\langle 1|\big), \quad \epsilon_j^{(i)} \in [0, 1]. \tag{11}$$

If $\epsilon_j^{(1)} = \epsilon_j^{(2)} = 1$, then $\mathbf{A}_j$ $(j = 2, 3, \dots, n)$ does not apply any filtering operation.

The filtered state shared across all the parties takes the form

$$\rho_{\text{filtered}} = N\big(\otimes_{j=1}^{n+1} \mathfrak{F}_j\big) \rho_{\text{initial}} \big(\otimes_{j=1}^{n+1} \mathfrak{F}_j\big)^{\dagger},$$
$$\text{where} \quad N = \frac{1}{\text{Tr}\big[\big(\otimes_{j=1}^{n+1} \mathfrak{F}_j\big) \rho_{\text{initial}} \big(\otimes_{j=1}^{n+1} \mathfrak{F}_j\big)^{\dagger}\big]}. \tag{12}$$

In Eq. (12), N denotes the probability of obtaining ρ_{filtered}. To this end, one may note that, in the preparation stage, at least one of the $n+1$ parties performs a filtering operation.

B. Measurement stage

In this stage each of the parties now performs local measurements on their respective share of particles forming the state ρ_{filtered}. Measurement context is same as in the usual linear n-local network scenario (Sec. II C). To be precise, each of the central parties $\mathbf{A}_2, \mathbf{A}_3, \dots, \mathbf{A}_n$ performs projective measurement in Bell basis $\{|\psi^{\pm}\rangle, |\phi^{\pm}\rangle\}$. $\forall i = 2, 3, \dots, n$, let $\mathbf{B}_i$ denote the Bell-state measurement (BSM [15]) of $\mathbf{A}_i$. Let each of $\mathbf{A}_1$ and $\mathbf{A}_{n+1}$ perform projective measurements $(\mathbf{M}_0, \mathbf{M}_1)$ and $(\mathbf{N}_0, \mathbf{N}_1)$, respectively, along any one of two arbitrary directions: $\{\vec{m}_0 \cdot \vec{\sigma}, \vec{m}_1 \cdot \vec{\sigma}\}$ for $\mathbf{A}_1$ and $\{\vec{n}_0 \cdot \vec{\sigma}, \vec{n}_1 \cdot \vec{\sigma}\}$ for $\mathbf{A}_{n+1}$ with $\vec{m}_0, \vec{m}_1, \vec{n}_0, \vec{n}_1 \in \mathbb{R}^3$. Correlations generated due to the local measurements are then used to test a violation of the n-local inequality [Eq. (13)].

The measurement settings considered here is the same as that considered for usual linear n-local network [29]. For these setups the n-local inequality [Eq. (5)] takes the form

$$\frac{1}{2} \sum_{h=0}^{1} \sqrt{\langle f_h(\mathbf{M}_0, \mathbf{M}_1, \mathbf{N}_0, \mathbf{N}_1)\rangle} \leqslant 1,$$
$$\text{where} \quad f_h(\mathbf{M}_0, \mathbf{M}_1, \mathbf{N}_0, \mathbf{N}_1) = A(\mathbf{M}) \otimes_{r=2}^{n-1} \sigma_{2+(-1)^h} \otimes A(\mathbf{N})$$
$$\text{with} \quad A(\mathbf{X}) = \left(\sum_{j=0}^{1} (-1)^{h.j} \mathbf{X}_j\right), \quad h = 0, 1. \tag{13}$$

For the rest of the work Eq. (13) will be referred to as the n-local inequality. Note that, it is the preparation stage where the scenario considered here differs from that of the usual linear n-local network scenario. In the usual scenario, the parties do not perform any operation in this stage. The overall state used in the measurement stage of the usual scenario is thus ρ_{initial}, in contrast to the postselected state ρ_{filtered} in the sequential scenario. Such a state is formed due to local operation and classical communication (Sec. II D) performed by at least one of $n+1$ parties in the preparation stage of the sequential network scenario.

Having introduced the sequential linear n-local network scenario, we now proceed to characterize the non–n-locality of the correlations generated therein.

IV. CHARACTERIZATION OF HIDDEN NON n-LOCALITY

Consider a sequential linear n-local network (Fig. 2) with the filtering operations [Eqs.(10) and (11)] and measurement context as specified in Sec. III. To be specific each of $\mathbf{A}_1$ and $\mathbf{A}_{n+1}$ performs projective measurements whereas each of $n-1$ intermediate parties perform Bell basis measurement. Before analyzing the hidden non–n-locality, we first give a formal definition of hidden non–n-local correlations in such a sequential linear n-local network.

Definition 1. With each of the extreme parties performing projective measurements in anyone of two possible directions and each of the intermediate parties performing a fixed projective measurement in Bell basis, under the n-local constraint [Eq. (3)], if $n+1$-partite correlations generated in the sequential linear n-local network are inexplicable in the form given by Eq. (4), then such correlations are said to be *hidden non–n-local correlations* and the corresponding notion of nonlocality is defined as *hidden non–n-locality*.

To characterize non–n-locality in sequential network, the term *"hidden"* is used in the same spirit as in [8]. Consider a set of n two-qubit states such that non–n-locality cannot be detected by the violation of n-local inequality [Eq. (13)] in the usual n-local network. However, the same set of states, when used in the sequential n-local network, may generate non–n-local correlations. This corresponds to the detection of hidden non–n-locality. Violation of the n-local inequality Eq. (13) acts as a sufficient criterion to detect hidden non–n-local behavior (if any) of the corresponding set of correlations generated in the sequential network scenario.

Before progressing further, we would like to note that our entire analysis of non–n-locality detection will rest upon violation of n-local inequality. As already mentioned in Sec. I, violation of such an inequality acts as a sufficient criterion to detect non–n-locality. It may happen that given a set of n two-qubit states in the n-local network, the correlations fail to violate n-local inequality. Such correlations may still be non–n-local. We can rule out non–n-locality only if we show that the state admits a n-local hidden variable model. However, owing to the obvious complexity in giving any such proof, we rather focus on the detection issue via the violation of n-local inequality. To be precise, when no violation of n-local inequality is observed in the usual n-local scenario, we use the given set of states in the sequential n-local network and test for violation of the same inequality. If the violation is observed, then hidden non–n-locality is detected. However, one remains inconclusive if no violation is observed.

Another important fact to be noted here is that the phenomenon of observing hidden non–n-locality is stochastic. In a sequential n-local network, apart from uncertainty due to measurements (measurement stage), an extra level of uncertainty arises in the preparation stage. As already discussed in Sec. III, such uncertainty is due to the probability N in obtaining the state ρ_{filtered} [Eq. (12)] as the selected output corresponding to the local filtering operations made by the parties. Such a form of uncertainty is absent in the usual non–n-locality paradigm. Ignoring measurement uncertainty (common in both usual and sequential n-local networks), we will refer to the probability term N [Eq. (12)] as the *probability of success for observing hidden non–n-locality*.

To provide instances of hidden non–n-locality, we start with the simplest sequential bilocal network.

A. Examples of hidden nonbilocality

Let $\mathbf{S}_1$ and $\mathbf{S}_2$ generate $\varrho_{1,2}$ and $\varrho_{2,3}$, respectively, from the following family of two-qubit states [41,42]

$$\begin{aligned}\varrho_{i,i+1} = {} & v_i|00\rangle\langle 00| + (1-v_i)[\sin^2 x_i|01\rangle\langle 01| \\ & + \cos^2 x_i|10\rangle\langle 10| \\ & + \sin x_i \cos x_i(|01\rangle\langle 10| + |10\rangle\langle 01|)], \\ & i=1,2, \quad v_i \in [0,1] \text{ and } x_i \in \left[0, \frac{\pi}{4}\right]. \end{aligned} \tag{14}$$

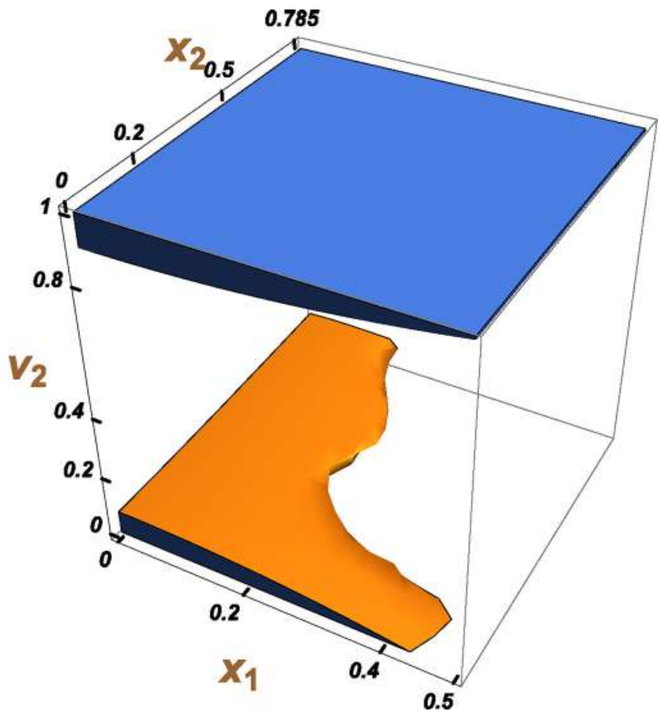

FIG. 3. Shaded region gives state parameters for which hidden nonbilocality is observed for $v_1 = 0.1$ with not less than 60% probability when only $\mathbf{A}_2$ performs local filtering operations [Eq. (11)] for $(\epsilon_2^{(1)}, \epsilon_2^{(2)}) = (0.8, 0.97)$.

Let only the intermediate party $\mathbf{A}_2$ perform local filtering operations [Eq. (11)] on the joint state of two qubits received from $\mathbf{S}_1, \mathbf{S}_2$. For suitable values of local filter parameters $(\epsilon_2^{(1)}, \epsilon_2^{(2)})$ and suitable directions of projective measurements $(\vec{m}_0, \vec{m}_1, \vec{n}_0, \vec{n}_1)$ by $\mathbf{A}_1$ and $\mathbf{A}_{n+1}$, hidden nonbilocality is observed (see Fig. 3). For instance, consider two particular states from the above family [Eq. (14)] specified by $(x_1, x_2, v_1, v_2) = (0.23, 0.44, 0.1, 0.99)$. When used in the usual bilocal scenario, the left-hand side (L.H.S.) of Eq. (6) takes the value 0.8871. Hence, no violation of the bilocal inequality [Eq. (13) for $n=2$] is obtained. But for $(\epsilon_2^{(1)}, \epsilon_2^{(2)}) = (0.8, 0.97)$, and for suitable measurement settings, the L.H.S. of the same inequality [Eq. (13)] gives the value 1.081 with approximately 62% success probability. So the violation reveals hidden nonbilocality. It is interesting to observe that, for states from the same family [Eq. (14)] with $x_1 = 0.23$, $x_2 = 0.34$, $v_2 = 0.15$, hidden nonbilocality cannot be detected if only $\mathbf{A}_2$ applies local filters. When such states are used in the network, hidden nonbilocality can be detected only if all the three parties apply suitable local filters (see Fig. 4).

B. Examples of hidden nontrilocality

Let us now consider a trilocal sequential network. Let each of $\mathbf{S}_1, \mathbf{S}_2, \mathbf{S}_3$ distribute states from the above family of states [Eq. (14)]. Let each of the two intermediate parties $\mathbf{A}_2, \mathbf{A}_3$ perform local filtering operations on their respective share of particles whereas the extreme parties do not perform any filtering operation. Hidden nontrilocality is observed in the network (see Fig. 5). For example, consider the specific state parameters: $(x_1, x_2, x_3, v_1, v_2, v_3) =$

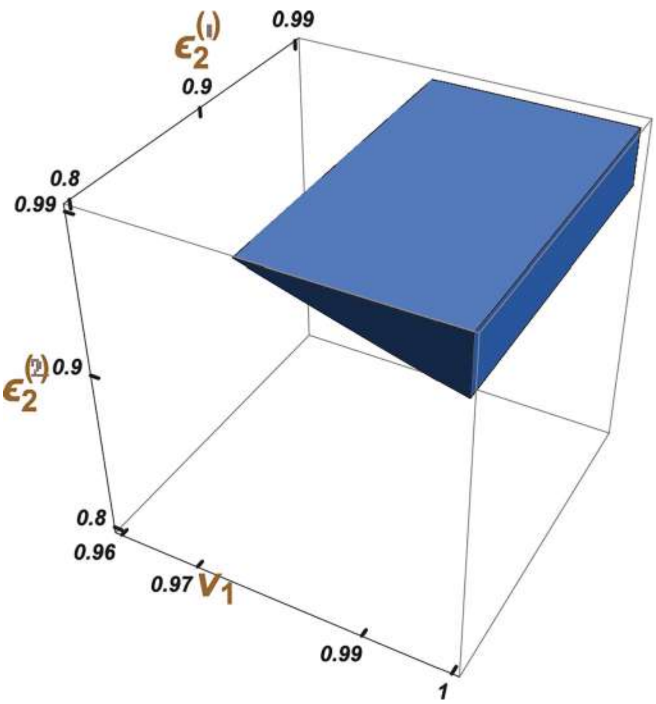

FIG. 4. Let us consider specific members from the family [Eq. (14)]: $x_1 = 0.23$, $x_2 = 0.34$, $v_2 = 0.15$. Shaded region gives state parameter v_1 and parameters of local filters $(\epsilon_2^{(1)}, \epsilon_2^{(2)})$ applied by $\mathbf{A}_2$ for which hidden non bilocality is observed with not less than 30% probability approximately when all the parties apply local filters with extreme parties performing specific local filters for $(\epsilon_1, \epsilon_4) = (0.95, 0.76)$. It may be noted that nonbilocality cannot be detected if these states are used in the usual bilocal network.

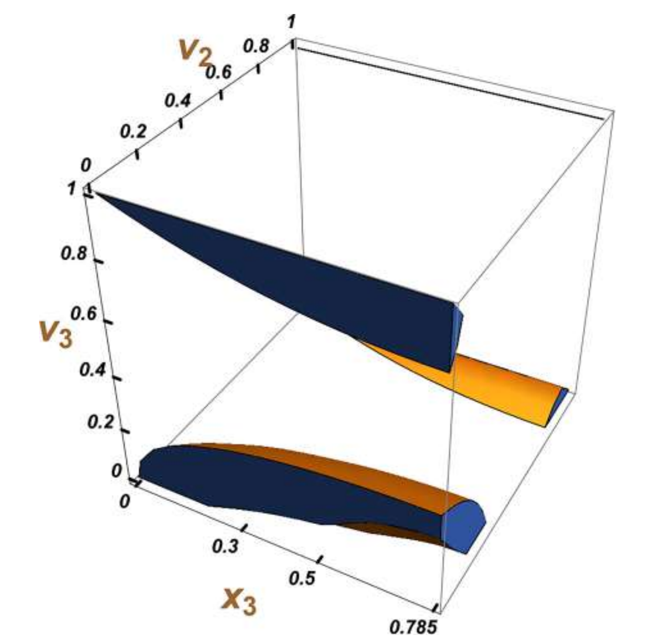

FIG. 5. For specific values of state parameters $(x_1, x_2, v_1) = (0.3455, 0.5586, 0.1)$, and specified local filters: $(\epsilon_2^{(1)}, \epsilon_2^{(2)}, \epsilon_3^{(1)}, \epsilon_3^{(2)}) = (0.6362, 0.99, 0.989, 0.989)$, shaded region gives state parameters x_3, v_2, v_3 and parameters for which hidden nontrilocality is observed with not less than 44% probability. In case these states are used in the usual trilocal network, nontrilocality cannot be detected.

(0.3455, 0.5586, 0.7799, 0.1, 0.12, 0.1). Nontrilocality is not detected when these three states are used in the usual trilocal network [the L.H.S. of Eq.(6) takes value 0.9888]. However, under suitable measurement settings and specific filtering parameters $(\epsilon_2^{(1)}, \epsilon_2^{(2)}, \epsilon_3^{(1)}, \epsilon_3^{(2)}) = (0.6362, 0.99, 0.989, 0.989)$, the L.H.S. of Eq. (13) gives 1.2332 with approximately 44% success probability.

C. Entanglement and hidden non–n-locality

If the mixed states are allowed in the network, all the sources need not distribute entangled states. For example, let us consider a sequential bilocal network. Let $\mathbf{S}_1$ generate the mixed entangled state $\varrho_{1,2}$ from the family of states given by Eq. (14). Let $\mathbf{S}_2$ distribute the separable Werner state [3,8]

$$\varrho_{2,3} = \frac{(1-p_2)}{4}\mathbb{I}_{4\times 4} + p_2(|01\rangle\langle 01| + |10\rangle\langle 10| - (|01\rangle\langle 10| + |10\rangle\langle 01|)), \; p_2 \in [0.25, 0.30]. \tag{15}$$

When $\mathbf{A}_2$ applies a suitable local filtering operation in the preparation stage, then hidden nonbilocality is detected for suitable local measurement settings applied in the measurement stage of the network [see Fig. 6(a)]. However, no violation of bilocal inequality [Eq. (13) for $n = 2$] is observed when the same states are used in the usual bilocal network [23].

Let us now consider a sequential trilocal network. Let $\mathbf{S}_1, \mathbf{S}_3$ each generate a mixed entangled state from the same family of states [Eq. (14)] whereas $\mathbf{S}_2$ generates a separable Werner state [Eq. (15)]. Under a suitable measurement context, hidden nontrilocality can be observed in the network [see Fig. 6(b)]. This was noted in [36] while considering the usual network nonlocality, however, we observe this phenomenon also in the pursuit to reveal hidden non–n-locality.

All these instances imply that not all the sources need to generate entanglement in a sequential n-local network for detecting hidden non–n-locality.

Comparison with observations in [29]

As already discussed in Sec. III, the measurement settings considered here are the same as that considered in usual linear n-local network [29]. As per the arguments presented in [29], nonbilocality (nontrilocality) can be observed when one (two) maximally entangled state(s) are used along with any generic two-qubit state which does not exhibit the Bell-CHSH violation. However, in our sequential network scenario, nonbilocal (nontrilocal) correlations are generated even when one (two) mixed, hence nonmaximally entangled states are used with a separable state. Consequently, our results, as discussed above in Sec. IV C, clearly points out the utility of applying suitable filtering operations in the context of simulating non n-locality in linear networks.

D. No violation of Eq. (13) while using product of mixed states

Next, let us consider the case when only product of two single-qubit mixed states are used in the sequential n-local network. Let each party be allowed to perform local filters as mentioned in Sec. III. Hidden non–n-locality cannot be

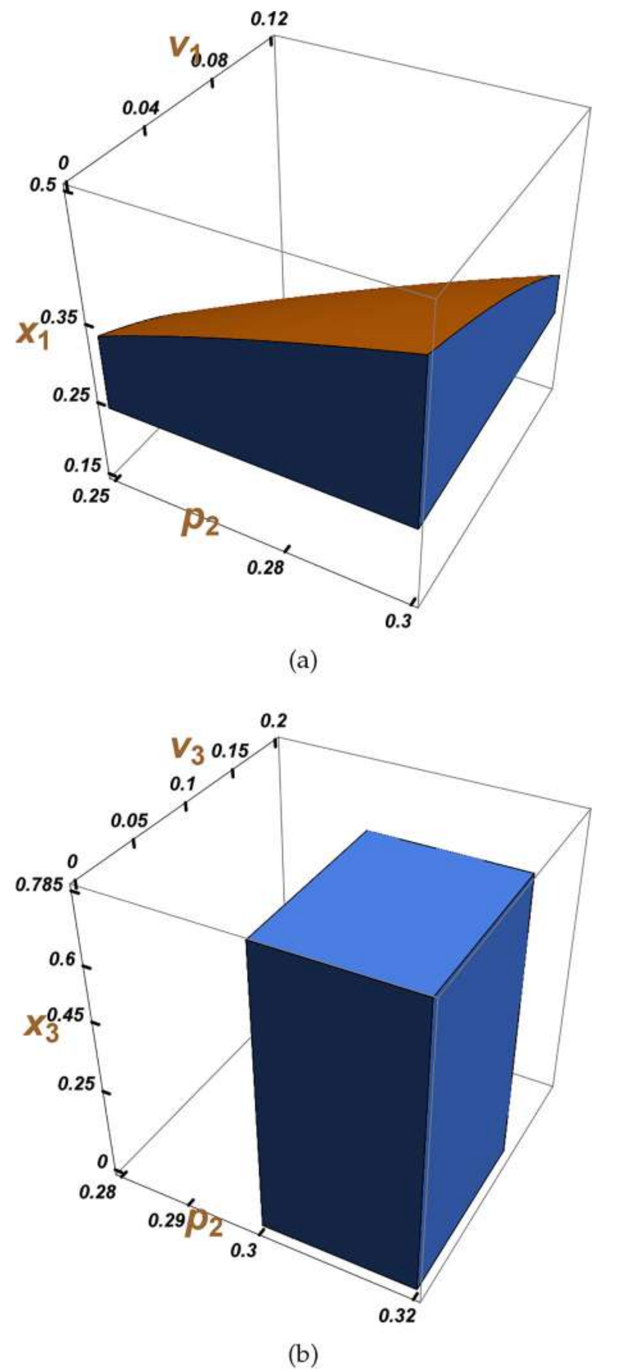

FIG. 6. In both subfigures, the shaded portions indicate regions in the parameter space $[(v_1, x_1, p_2)$ in (a) and (v_3, x_3, p_2) in (b)] for which hidden non–n-locality is observed for $n = 2$ (a) and $n = 3$ (b). Specifications used in (a) are $(\epsilon_2^{(1)}, \epsilon_2^{(2)}) = (0.46, 1)$. Specifications used in (b) are $(\epsilon_2^{(1)}, \epsilon_2^{(2)}, \epsilon_3^{(1)}, \epsilon_3^{(2)}, x_1, v_1) = (0.762, 0.038, 0.038, 1, 0.3, 0.07)$. In each of these two cases, violation of n-local inequality [Eq. (13) for $n = 2, 3$] is not observed in the usual n-local network.

detected if at least one of the sources distributes a product of two single-qubit mixed states. The result is formalized as follows.

Theorem 1. In a sequential n-local network, with each extreme party performing projective measurements and each of the intermediate party measuring in Bell basis, for any $i \in \{1, 2, \ldots, n\}$, if ith source generates a product of two arbitrary single-qubit mixed states and if the parties perform local filters of the form given by Eqs. (10) and (11), then a violation of n-local inequality [Eq. (13)] is impossible for any finite n.

Proof. See the Appendix. ■

V. CHARACTERIZATION IN TERMS OF BLOCH PARAMETERS

Here we intend to analyze hidden non–n-locality detection from density matrix formalism of the states used in the corresponding network. Examples of hidden nonbilocality and nontrilocality illustrated in Secs. IV A and IV B, involve members from a particular family of two-qubit states [Eq. (14)]. Now it may be noted that any member ϱ_i from this family has nonnull local Bloch vectors

$$u_i = [0, 0, v_i - (1 - v_i)\cos(2x_i)],$$
$$z_i = [0, 0, v_i + (1 - v_i)\cos(2x_i)].$$

Again, as discussed in Sec. IV C, hidden non–n-locality (for $n = 2, 3$) is observed when one of the states is a Werner state. It may be noted that Werner state does not have any local Bloch vector. Combining these two observations from Secs. IV A, IV B, and IV C, it is clear that hidden non–n-locality can be observed when at least one of the states used in the corresponding network has local Bloch vector. At this junction, we conjecture that hidden non–n-locality cannot be detected via the violation of Eq. (13) when none of the states used in the network has local Bloch vectors (see the Appendix).

A. Closed form of upper bound of Eq. (13)

In the absence of filtering operations, there exists a closed form in terms of state parameters [$\mathbf{B}_{\text{lin}}$ in Eq. (6)] of the upper bound of linear n-local inequality [Eq. (13)]. Following the method discussed in the Appendix, the upper bound of Eq. (13) in the linear sequential network scenario maintains the same structure as that of $\mathbf{B}_{\text{lin}}$ in Eq. (6)

$$\mathbf{B}_{\text{seq}} = \sqrt{\Pi_{j=1}^{n} t''_{j1} + \Pi_{j=1}^{n} t''_{j2}}, \tag{16}$$

where $\forall j = 1, 2, \ldots, n$, the two largest singular values t''_1, t''_2 of the normalized postselected states $\rho''_{j,j+1}$ [Eq. (A7)] are functions of the filtering parameters $\epsilon_1, \epsilon_{n+1}, \epsilon_k^{(1)}, \epsilon_k^{(2)} (k = 2, 3, \ldots, n-1)$, the singular values of the correlation tensor and also local bloch vectors of $\rho_{j,j+1}$. So, unlike $\mathbf{B}_{\text{lin}}$, the closed form of the upper bound of the n-local inequality [Eq. (13)] depends on state parameters and also on the filtering parameters. Equation (13) is thus violated if

$$\mathbf{B}_{\text{seq}} > 1. \tag{17}$$

For any given set of initial states $\rho_{j,j+1} (j = 1, 2, \ldots, n)$, hidden non–$n$-local correlations can be simulated in case there exist suitable filters such that Eq. (6) is violated but Eq. (17) is satisfied.

B. Illustration

Let us consider the following family of two qubit states [43]:

$$\chi(x_1, x_2, x_3, x_4) = x_1|00\rangle\langle 00| + x_2|01\rangle\langle 01| + x_3|11\rangle\langle 11| + x_4(|00\rangle\langle 11| + |11\rangle\langle 00|),$$
$$\text{with} \quad x_1 + x_2 + x_3 = 1$$
$$0 \leqslant x_1, \quad x_2, \quad x_3 \leqslant 1,\ x_4^2 \leqslant x_1x_3.$$

This family forms a subclass of X state [43]. Singular values of the correlation matrix [Eq. (2)] of this class are

$$s_1 = 2|x_4|,$$
$$s_2 = s_1,$$
$$s_3 = |x_1 - x_2 + x_3|. \tag{18}$$

Local Bloch vectors are given by

$$\vec{u} = (0, 0, x_1 + x_2 - x_3),$$
$$\vec{z} = (0, 0, x_1 - x_2 - x_3). \tag{19}$$

Let any two states from this class of states [Eq. (18)] be used in the usual bilocal network: $\rho_{i,i+1} = \chi(x_{i1}, x_{i2}, x_{i3}, x_{i4})$, $i = 1, 2$. For that network, the bilocal inequality is not violated if $\mathbf{B}_{\text{lin}}$ then turns out to be

$$\mathbf{B}_{\text{lin}} \leqslant 1 \text{ where} \tag{20}$$

$$\mathbf{B}_{\text{lin}} = \text{Max}[\sqrt{2L_1},\ \sqrt{L_1 + L_2},\ \sqrt{L_1 + L_3},\ \sqrt{L_2 + L_3},\ \times\sqrt{L_1 + L_4}], \quad \text{with}$$
$$L_1 = 4|x_{14}.x_{24}|,$$
$$L_2 = 2|(x_{11} - x_{12} + x_{13})x_{24}|,$$
$$L_3 = 2|(x_{21} - x_{22} + x_{23})x_{14}|,$$
$$L_4 = \Pi_{i=1}^2|(x_{i1} - x_{i2} + x_{i3})|. \tag{21}$$

Now let $\chi(x_{i1}, x_{i2}, x_{i3}, x_{i4})(i = 1, 2)$ be used in a sequential bilocal network where all the parties are applying the same filtering operation, i.e., $\epsilon_1 = \epsilon_2^{(1)} = \epsilon_2^{(2)} = \epsilon_3 = \epsilon$. After the preparation stage, the correlation tensor of the normalized postselected states $\rho''_{i,i+1}$ [Eq. (A7)] turns out to be

$$s''_{i1} = \frac{2|x_{i4}|\epsilon^2}{|x_{i3} + \epsilon^2(x_{i2} + x_{i1}\epsilon^2)|},$$
$$s''_{i2} = s''_{i1},$$
$$s''_{i3} = \frac{|x_{i3} + \epsilon^2(-x_{i2} + x_{i1}\epsilon^2)|}{|x_{i3} + \epsilon^2(x_{i2} + x_{i1}\epsilon^2)|}. \tag{22}$$

The probability of success is given by $\Pi_{i=1}^2[x_{i3} + \epsilon^2(x_{i2} + x_{i1}\epsilon^2)]$.

As discussed above, $\mathbf{B}_{\text{seq}}$ is obtained by using the largest two of these singular values [Eq. (22)] of each of $\rho''_{1,2}$ and $\rho''_{2,3}$. Violation of the bilocal inequality [Eq. (13) for $n = 2$] is obtained if

$$\mathbf{B}_{\text{seq}} > 1, \quad \text{where} \tag{23}$$

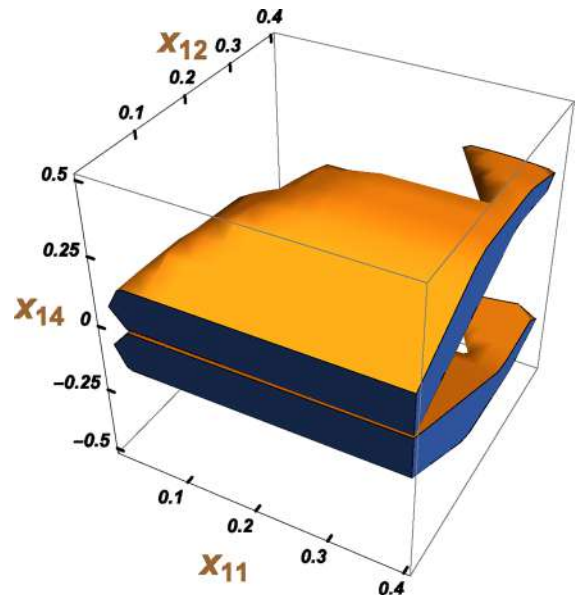

FIG. 7. Shaded region gives the specifications of the state parameters of $\chi(x_{11}, x_{12}, x_{13}, x_{14})$ [Eq. (18)], which, when used with $\chi(0.2, 0.1, 0.7, 0.15)$ in the sequential bilocal network, simulates hidden nonbilocal correlations in case each of the four parties perform apply the same local filters specified by $\epsilon = 0.75$. It may be noted that nonbilocality cannot be detected when $\chi(0.2, 0.1, 0.7, 0.15)$ and $\chi(x_{11}, x_{12}, x_{13}, x_{14})$ corresponding to any point in the shaded region, are used in the usual bilocal network.

$$\mathbf{B}_{\text{seq}} = \frac{1}{\sqrt{L_8}}\text{Max}\Big[\sqrt{2L_5},\ \sqrt{L_5 + L_6},\ \sqrt{L_5 + L_7},\ \sqrt{L_6 + L_7},\ \times\sqrt{L_5 + \frac{L_6.L_7}{4x_{14}x_{24}\epsilon^4}}\Big], \quad \text{with}$$
$$L_5 = 4|x_{14}x_{24}\epsilon^4|,$$
$$L_6 = 2|x_{24}\epsilon^2[x_{13} + \epsilon^2(-x_{12} + x_{11}\epsilon^2)]|,$$
$$L_7 = 2|x_{14}\epsilon^2[x_{23} + \epsilon^2(-x_{22} + x_{21}\epsilon^2)]|,$$
$$L_8 = \Pi_{i=1}^2[x_{i3} + \epsilon^2(x_{i2} + x_{i1}\epsilon^2)]. \tag{24}$$

For a suitable value of the filtering parameter ϵ, there exist states from this subclass of X states [Eq. (18)], which satisfy both the above relations [Eqs. (20) and (23)] for which hidden nonbilocal correlations are simulated in sequential bilocal network, but nonbilocality cannot be detected in the usual bilocal network (see Fig. 7). For a numeric instance, let us consider $\chi(0.2, 0.1, 0.7, 0.15)$ and $\chi(0.86, 0, 0.14, 0.33)$. For these two states $\mathbf{B}_{\text{lin}} = 0.999$. Hence, no violation of Eq. (13) observed in usual bilocal network. However, in the sequential bilocal network, when all the parties perform filtering with $\epsilon = 0.77$, violation of the same is observed (with approximately 37% success probability) as $\mathbf{B}_{\text{seq}} = 1.023$.

VI. ENHANCEMENT IN ROBUSTNESS TO NOISE

A linear n-local network scenario underlies different entanglement distribution protocols involving quantum repeaters [36]. In an idealistic situation pure entangled states are supposed to be communicated among the distant observers (often referred to as *nodes* [44]) in any such network structure. However, in practical situations, due to unavoidable interaction with the environment, entanglement is transferred across noisy channels [45]. It is thus significant to study any possible method to enhance possibility of detecting nonclassicality in the presence of noise in the network. Hence, from practical perspectives, it becomes interesting to explore procedures that can increase resistance to noise of the n-local inequality for detecting non–n-local correlations. Applying suitable local filters turns out to be effective in this context. To be specific it is observed that nonbilocality can be detected over a wider range of noise parameter in sequential linear bilocal network in comparison with the usual bilocal network. In support of our claim, we provide with illustration considering communication over two specific noisy channels.

A. Communication through bit-flip channel [45]

Let each of the two sources $\mathbf{S}_1, \mathbf{S}_2$ generate a pure entangled state

$$|\Psi(\theta)\rangle = \cos\theta|01\rangle + \sin\theta|10\rangle,\ \theta \in \left(0, \frac{\pi}{4}\right). \tag{25}$$

Let each of the two qubits generated from $\mathbf{S}_i$ be passed through a bit-flip channel parameterized by $p_i(i = 1, 2)$. $\forall i = 1, 2,\ p_i$ denotes the probability with which the state of a single qubit is flipped from $|0\rangle$ to $|1\rangle$ and vice versa. Each of $\rho_{1,2}$ and $\rho_{2,3}$ is thus a two-qubit mixed entangled state

$$\begin{aligned}\rho_{i,i+1} = {} & p_i(1-p_i)[|00\rangle\langle 00| + \sin 2\theta(|00\rangle\langle 11| + |11\rangle\langle 00|)] \\ & + [(1-p_i)^2\cos^2\theta + p_i^2\sin^2\theta]|01\rangle\langle 01| \\ & + [(1-p_i)^2\sin^2\theta + p_i^2\cos^2\theta]|10\rangle\langle 10| \\ & + \left(1 - 2p_i + 2p_i^2\right)\cos\theta\sin\theta(|10\rangle\langle 01| + |01\rangle\langle 10|), \\ & i = 1, 2. \end{aligned} \tag{26}$$

On application of suitable local filters by the parties, hidden nonbilocal correlations are simulated over an enhanced range of noise parameters (p_1, p_2) compared to the range of (p_1, p_2) for which nonbilocality is detected in usual bilocal network (see Fig. 8). For a specific instance, consider two identical copies of $|\Psi(0.62)\rangle$ [Eq. (25)]. As discussed above, let these states be passed through bit flip channels, with $\rho_{1,2}$ and $\rho_{2,3}$ [Eq. (26)] being characterized by $p_1 \in (0, 0.4)$ and $p_2 = 0.15$, respectively. In case the parties do not apply filtering, $\mathbf{B}_{\text{lin}} > 1$ if $p_1 \in (0, 0.214]$. Now, in the sequential bilocal network, when $\mathbf{A}_2$ applies filtering operations specified by $\epsilon_2^{(1)} = 0.98$, $\epsilon_2^{(2)} = 0.79$, $\mathbf{B}_{\text{seq}} > 1$ is obtained for $p_1 \in (0, 0.235]$. Hence, for this particular instance, when $p_1 \in [0.215, 0.235]$, nonbilocality can be detected in sequential network but not in the usual bilocal network.

B. Communication through amplitude damping channel [45]

Let each of $\mathbf{S}_1, \mathbf{S}_2$ generate an identical copy of the pure entangled state $|\Psi(\theta)\rangle$ [Eq. (25)]. Each of the qubits of $|\Psi(\theta)\rangle$, generated from $\mathbf{S}_i$, are distributed through identical amplitude damping channels characterized by damping parameter $\gamma_i(i = 1, 2)$. The mixed entangled states thus distributed in the network are given by

$$\begin{aligned}\rho_{i,i+1} = {} & \gamma_i(|00\rangle\langle 00| + (1-\gamma_i)(\cos^2\theta(|01\rangle\langle 01| \\ & + \cos\theta\sin\theta((|10\rangle\langle 01| + (|01\rangle\langle 10|) \\ & \times \sin^2\theta(|10\rangle\langle 10|)\ i = 1, 2. \end{aligned} \tag{27}$$

It is observed that there exists range of damping parameters (γ_1, γ_2) for which the hidden nonbilocality can be exploited under effect of suitable filtering operations in contrast to the

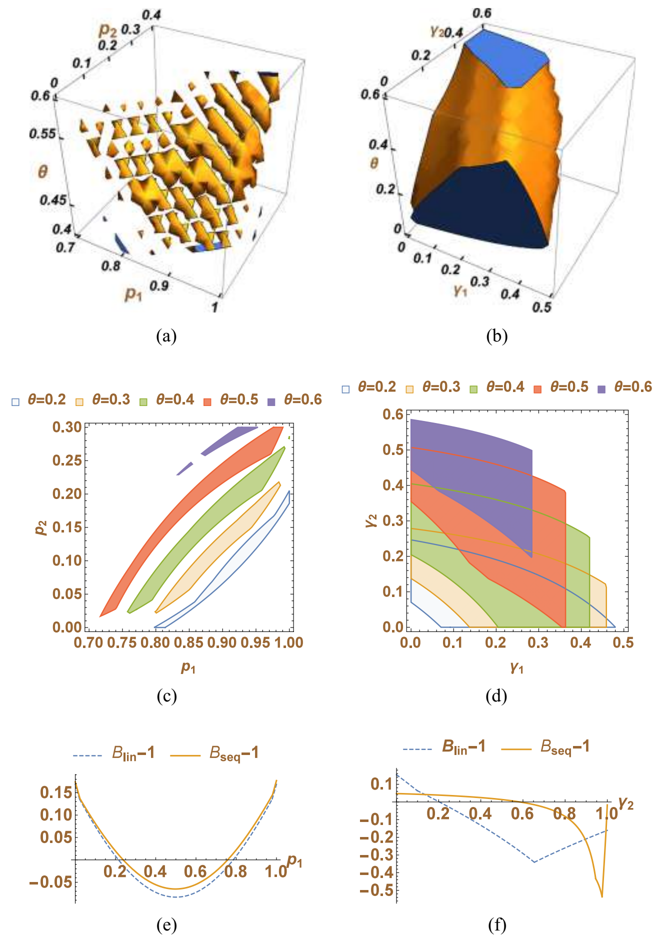

FIG. 8. All the subfigures in this figure point out the utility of applying suitable filters in perspective of increasing the bilocal inequality's resistance to noise when qubits are distributed across bit-flip channel (all subfigures in left-hand side panel) and amplitude damping channel (subfigures in right-hand side panel). In the context of exploiting hidden nonbilocality, in each of left and right panels: (i) the topmost one gives the possible region of both state and noise parameters; (ii) the middle one gives the region of noise parameters for different pure entangled states [Eq. (25)], i.e., for different values of θ; and (iii) the bottom one gives the range of one noise parameter for a fixed value of the other noise parameter and state parameter for which the violation of bilocal inequality [Eq. (13)] is observed both with and without filtering operations. Details of the filtering parameters in each of the subfigures are as follows: $\epsilon_2^{(1)} = 0.68$, $\epsilon_2^{(2)} = 0.78$ in subfigures (a) and (c); $\epsilon_1 = 0.78$, $\epsilon_2^{(1)} = 0.22$, $\epsilon_2^{(2)} = 0.15$, $\epsilon_3 = 0.73$ in subfigures (b) and (d); $\epsilon_2^{(1)} = 0.98$, $\epsilon_2^{(2)} = 0.79$, $(\theta, p_2) = (0.58, 0.15)$ in subfigure (e); and $\epsilon_1 = 0.78$, $\epsilon_2^{(1)} = 0.22$, $\epsilon_2^{(2)} = 0.1$, $\epsilon_3 = 0.79$, $(\theta, \gamma_1) = (0.55, 0.21)$ in subfigure (f).

usual bilocal network where no violation of bilocal inequality [Eq. (13)] can be observed (see Fig. 8).

For example, consider the following: $|\Psi(0.55)\rangle$ and amplitude damping channels with $\gamma_1 = 0.21$ and $\gamma_2 \in (0, 1)$. With these specifications, $\mathbf{B}_{\text{lin}} > 1$ for $\gamma_2 \in (0, 0.2]$. Now, for $\epsilon_1 = 0.78, \epsilon_3 = 0.79$, $\epsilon_2^{(1)} = 0.22$, and $\epsilon_2^{(2)} = 0.1$, $\mathbf{B}_{\text{seq}} > 1$ for $\gamma_2 \in (0, 0.54]$. (0.2,0.54] thus turns out to be the enhanced range of visibility for detecting the violation of the bilocal inequality under effective filtering operations.

VII. DISCUSSION

A sequential linear n-local network was introduced in our present work. In the preparation stage of such a protocol, the parties are allowed to perform local filtering operations which constitute a specific form of stochastic local operations assisted with classical communication (SLOCC). Keeping analogy with hidden Bell nonlocality, non–n-locality obtained in such protocols was referred to as a hidden non–n-locality. Several instances of hidden non–n-locality are demonstrated. This, in turn, points to the fact that filtering operations are significant in revealing hidden non–n-locality. It is also observed that, in some situations, the sequential framework is more robust against noise than the usual network non–n- locality.

Interestingly, it is observed that hidden non–n-locality can be observed even when one of the sources does not distribute entanglement. However, the same is not the case when one of the sources generates a product state. To this end, one may note that we used a specific class of local filters, which is, however, considered the most useful form of local filters in the standard Bell scenario [6,10]. It will be interesting to characterize hidden non–n-locality considering the general form of local filtering operations. Also, apart from applying local filters, considering other sequential measurement strategies to explore non–n-locality can also be considered as a potential direction of future research. In addition, we applied sequential measurement techniques in the linear n-local network scenario. It will be interesting to analyze similar techniques in the nonlinear n-local networks.

ACKNOWLEDGMENTS

T.P. would like to acknowledge the support from DST-Inspire fellowship No. DST/INSPIRE Fellowship/2019/IF190357. N.G. acknowledges support from the project grant received under the SERB-MATRICS scheme vide file number MTR/2022/000101. We thank the anonymous referees for their insightful suggestions which helped us to improve the overall quality of the manuscript.

APPENDIX

We first analyze the upper bound of n-local inequality [Eq. (13)] in the sequential n-local network.

$\forall j = 1, 2, \ldots, n$, let source $\mathbf{S}_i$ generate an arbitrary two-qubit state $\rho_{j,j+1}$ [Eq. (2)]. In the preparation stage of the sequential network (Sec. III) $\mathbf{A}_j, (j = 1, 2, \ldots, n+1)$ applies the local filter of the form given by Eqs. (10) and (11). It may be noted that local filter $\mathfrak{F}_j$ [Eq. (11)] applied by each of $n-1$ intermediate parties $\mathbf{A}_j (j = 2, \ldots, n)$ is of the form

$$\mathfrak{F}_j = \mathfrak{F}_j^{(1)} \otimes \mathfrak{F}_j^{(2)} \text{ where} \tag{A1}$$

$$\mathfrak{F}_j^{(k)} = \epsilon_j^{(k)} |0\rangle\langle 0| + |1\rangle\langle 1| \quad \text{for} \quad k = 1, 2 \text{ and } j = 2, 3, \ldots, n. \tag{A2}$$

As discussed in the main text (Sec. III), $n+1$-partite correlations generated at the end of the measurement stage are used to test the n-local inequality [Eq. (13)].

The n-local inequality [Eq. (13)] is given by

$$\frac{1}{2} \sum_{h=0}^{1} \sqrt{\text{Tr}[f_h(\mathbf{M}_0, \mathbf{M}_1, \mathbf{N}_0, \mathbf{N}_1)\rho_{\text{filtered}}]} \leqslant 1. \tag{A3}$$

In the usual n-local network, Eq. (13) is given by

$$\frac{1}{2} \sum_{h=0}^{1} \sqrt{\text{Tr}[f_h(\mathbf{M}_0, \mathbf{M}_1, \mathbf{N}_0, \mathbf{N}_1)\rho_{\text{initial}}]} \leqslant 1,$$

$$\frac{1}{2} \sum_{h=0}^{1} \sqrt{\text{Tr}[f_h(\mathbf{M}_0, \mathbf{M}_1, \mathbf{N}_0, \mathbf{N}_1) \otimes_{i=1}^{n} \rho_{i,i+1}]} \leqslant 1. \tag{A4}$$

As discussed in Sec. II C, the upper bound ($\mathbf{B}$, say) of the above inequality [Eq. (A4)], is given by [29]

$$\mathbf{B} = \sqrt{\Pi_{i=1}^{n} t_{i1} + \Pi_{i=1}^{n} t_{i2}}, \tag{A5}$$

where t_{i1}, t_{i2} denotes the largest two singular values of the correlation tensor (T_i) of $\rho_{i,i+1}$ $i = 1, 2, \ldots, n$). Now let us analyze the state ρ_{filtered} used in the above Eq. (A3). As mentioned in Sec. III, ρ_{filtered} [Eq. (12)] is given by

$$\begin{aligned}
\rho_{\text{filtered}} &= N\big(\otimes_{j=1}^{n+1} \mathfrak{F}_j\big)\rho_{\text{initial}}\big(\otimes_{j=1}^{n+1} \mathfrak{F}_j\big)^{\dagger}, \\
&\quad \text{where} \quad N \text{ is given by Eq. (12)} \\
&= N \otimes_{j=1}^{n} \rho'_{j,j+1} \quad \text{where} \\
\rho'_{1,2} &= \big(\mathfrak{F}_1 \otimes \mathfrak{F}_2^{(1)}\big)\rho_{1,2}\big(\mathfrak{F}_1 \otimes \mathfrak{F}_2^{(1)}\big)^{\dagger}, \\
\rho'_{j,j+1} &= \big(\mathfrak{F}_j^{(2)} \otimes \mathfrak{F}_{j+1}^{(1)}\big)\rho_{j,j+1}\big(\mathfrak{F}_j^{(2)} \otimes \mathfrak{F}_{j+1}^{(1)}\big)^{\dagger} \\
&\quad \forall j = 2, 3, \ldots, n-1, \\
\rho'_{n,n+1} &= \big(\mathfrak{F}_n^{(2)} \otimes \mathfrak{F}_{n+1}\big)\rho_{n,n+1}\big(\mathfrak{F}_n^{(2)} \otimes \mathfrak{F}_{n+1}\big)^{\dagger}.
\end{aligned} \tag{A6}$$

It may be noted that $\forall j = 1, 2, \ldots, n$, $\rho'_{j,j+1}$ is unnormalized. Let $\rho''_{j,j+1}$ denote the normalized state corresponding to $\rho'_{j,j+1}$:

$$\rho''_{j,j+1} = N_{j,j+1}\rho'_{j,j+1}, \tag{A7}$$

where the normalization factor $N_{j,j+1}$ is given by

$$\begin{aligned}
N_{1,2} &= \frac{1}{\text{Tr}\big[\big(\mathfrak{F}_1 \otimes \mathfrak{F}_2^{(1)}\big)\rho_{1,2}\big(\mathfrak{F}_1 \otimes \mathfrak{F}_2^{(1)}\big)^{\dagger}\big]}, \\
N_{j,j+1} &= \frac{1}{\text{Tr}\big[\big(\mathfrak{F}_j^{(2)} \otimes \mathfrak{F}_{j+1}^{(1)}\big)\rho_{j,j+1}\big(\mathfrak{F}_j^{(2)} \otimes \mathfrak{F}_{j+1}^{(1)}\big)^{\dagger}\big]} \\
&\quad \forall j = 2, 3, \ldots, n-1, \\
N_{n,n+1} &= Tr\big[\big(\mathfrak{F}_n^{(2)} \otimes \mathfrak{F}_{n+1}\big)\rho_{n,n+1}\big(\mathfrak{F}_n^{(2)} \otimes \mathfrak{F}_{n+1}\big)^{\dagger}\big].
\end{aligned} \tag{A8}$$

Now, Eq. (A6) gives

$$\begin{aligned}\rho_{\text{filtered}} &= N \otimes_{j=1}^{n} \rho'_{j,j+1}\\ &= N \otimes_{j=1}^{n} \frac{1}{N_{j,j+1}}(N_{j,j+1}\rho'_{j,j+1})\\ &= \left(\frac{N}{\otimes_{j=1}^{n} N_{j,j+1}}\right) \otimes_{j=1}^{n} \rho''_{j,j+1}\\ &= \otimes_{j=1}^{n}\rho''_{j,j+1} \text{ using } \mathrm{Tr}\big[\otimes_{i=1}^{n} R_i\big]\\ &= \Pi_{i=1}^{n}\mathrm{Tr}[R_i], \text{ for any finite } n. \end{aligned} \tag{A9}$$

Using Eq. (A9), Eq. (A3) becomes

$$\frac{1}{2}\sum_{h=0}^{1}\sqrt{\mathrm{Tr}\big[f_h(\mathbf{M}_0, \mathbf{M}_1, \mathbf{N}_0, \mathbf{N}_1) \otimes_{j=1}^{n} \rho''_{j,j+1}\big]} \leqslant 1. \tag{A10}$$

A comparison of Eq. (A4) with Eq. (A10) points out that, on maximizing over measurement parameters (used in the measurement stage), the upper bound ($\mathbf{B}_{\text{seq}}$, say) of the above inequality and consequently that of the n-local inequality [Eq. (13)] in the sequential n-local network is given by Eq. (16) with t''_{j1}, t''_{j2} denoting the largest two singular values of correlation tensor (T''_j) of $\rho''_{j,j+1}$ ($j = 1, 2, \dots, n$). It may be noted that $\mathbf{B}_{\text{seq}}$ is a function of the Bloch parameters of $\rho_{j,j+1} \forall j = 1, 2, \dots, n$ and the filtering parameters $\epsilon_1, \epsilon_{n+1}, \epsilon_j^{(1)}, \epsilon_j^{(2)}$ ($j = 2, 3, \dots, n$). Using Eq. (16), we next give the proof of the theorem.

1. Proof of Theorem 1

Let one of the n sources generate the product of two single-qubit mixed states. Without loss of generality (W.L.O.G.) let $\mathbf{S}_1$ generate

$$\rho_{1,2} = \tfrac{1}{4}(\sigma_0 + \vec{m}\cdot\vec{\sigma}) \otimes (\sigma_0 + \vec{n}\cdot\vec{\sigma}) \quad \text{where} \tag{A11}$$

$\vec{m}, \vec{n}$ are three-dimensional vectors with length less than or equal to unity. Singular values of the correlation tensor of $\rho_{1,2}$ are $(|\vec{m}||\vec{n}|, 0, 0)$. The magnitude of the singular values of any correlation tensor is always less than unity [46]. Hence when $\rho_{1,2}$ is used in the usual n-local network, $\mathbf{B} \leqslant 1$. Consequently no violation of Eq. (13) is obtained. Now, in a sequential n-local network, the correlation tensor of $\rho''_{1,2}$ has only one non-zero singular value. So, from Eq.(16), we get $\mathbf{B}_{\text{seq}} \leqslant 1$. Consequently, the violation of Eq. (13) turns out to be impossible in the sequential n-local network. Hence, if at least one of the sources generates the product of two single-qubit mixed states, non–n-locality cannot be detected in a sequential n-local network for any finite n. This completes the proof of Theorem 1. ∎

2. Justification in support of conjecture made in Sec. V

As per the condition, n-local inequality is not violated in the usual n-local network. Hence, by Eq. (A5)

$$\sqrt{\Pi_{j=1}^{n} t_{j1} + \Pi_{j=1}^{n} t_{j2}} \leqslant 1. \tag{A12}$$

Let us focus on any one of the n states $\rho_{j,j+1}$($j = 1, 2, \dots, n$). W.L.O.G., let us consider $\rho_{1,2}$. Local bloch vectors of $\rho_{1,2}$ are considered to be null. Singular values of $\rho''_{1,2}$ turn out to be

$$\begin{aligned} t''_{1,1} &= \frac{\epsilon_1\epsilon_2^{(1)} t_{11}}{c_1},\\ t''_{1,2} &= \frac{\epsilon_1\epsilon_2^{(1)} t_{12}}{c_1}, \end{aligned} \tag{A13}$$

$$t''_{1,3} = \frac{(1-\epsilon_1^2)\big[1-\big(\epsilon_2^{(1)}\big)^2\big] + t_{13}(1+\epsilon_1^2)\big[1+\big(\epsilon_2^{(1)}\big)^2\big]}{4c_1}$$

where

$$c_1 = t_{13}(1-\epsilon_1^2)\big[1-\big(\epsilon_2^{(1)}\big)^2\big] + (1+\epsilon_1^2)\big[1+\big(\epsilon_2^{(1)}\big)^2\big]. \tag{A14}$$

Singular values of $\rho''_{j,j+1}$($j = 2, 3, \dots, n$) have analogous forms. For these forms of singular values, the numerical maximization of Eq. (16), under the constraint that Eq. (A12) holds, yields 1. Consequently, Eq. (13) is not violated in case none of $\rho_{j,j+1}$ has local Bloch vectors.

[1] J. S. Bell, Physics 1, 195 (1964); J. S. Bell, *Speakable and Unspeakable in Quantum Mechanics*, 2nd ed. (Cambridge University Press, Cambridge, England, 2004).
[2] P. Zoller *et al.*, Eur. Phys. J. D **36**, 203 (2005).
[3] N. Brunner, D. Cavalcanti, S. Pironio, V. Scarani, and S. Wehner, Bell nonlocality, Rev. Mod. Phys. **86**, 419 (2014).
[4] A. Acín, N. Brunner, N. Gisin, S. Massar, S. Pironio, and V. Scarani, Phys. Rev. Lett. **98**, 230501 (2007).
[5] S. Pironio *et al.*, Nature (London) **464**, 1021 (2010).
[6] F. Hirsch, Hidden nonlocality, Master thesis, University of Geneva (2013), http://cms.unige.ch/sciences/physique/wpcontent/uploads/Travail-de- Master.pdf.
[7] R. Horodecki, P. Horodecki, M. Horodecki, and K. Horodecki, Rev. Mod. Phys. **81**, 865 (2009).
[8] S. Popescu, Phys. Rev. Lett. **74**, 2619 (1995).
[9] N. Gisin, Phys. Lett. A **210**, 151 (1996).
[10] F. Hirsch, M. T. Quintino, J. Bowles, and N. Brunner, Phys. Rev. Lett. **111**, 160402 (2013).
[11] B. Paul, K. Mukherjee, and D. Sarkar, Phys. Rev. A **94**, 052101 (2016).
[12] J. F. Clauser, M. A. Horne, A. Shimony, and R. A. Holt, Phys. Rev. Lett. **23**, 880 (1969).
[13] T. Fritz, New J. Phys. **14**, 103001 (2012).
[14] C. Branciard, N. Gisin, and S. Pironio, Phys. Rev. Lett. **104**, 170401 (2010).
[15] C. Branciard, D. Rosset, N. Gisin, and S. Pironio, Phys. Rev. A **85**, 032119 (2012).
[16] K. Mukherjee, B. Paul, and D. Sarkar, Quant. Info. Proc. **14**, 2025 (2015).
[17] M. O. Renou, E. Baumer, S. Boreiri, N. Brunner, N. Gisin, and S. Beigi, Phys. Rev. Lett. **123**, 140401 (2019).
[18] S. Wehner, D. Elkouss, and R. Hanson, Science **362**, eaam9288 (2018).

[19] C. M. Lee and M. J. Hoban, Phys. Rev. Lett. **120**, 020504 (2018).

[20] W. Kozlowski, S. Wehner, *Proceedings of the Sixth Annual ACM International Conference on Nanoscale Computing and Communication, NANOCOM '19* (Association for Computing Machinery, New York, 2019).

[21] A. Tavakoli, P. Skrzypczyk, D. Cavalcanti, and A. Acín, Phys. Rev. A **90**, 062109 (2014).

[22] K. Mukherjee, B. Paul, and D. Sarkar, Quant. Info. Proc. **15**, 2895 (2016).

[23] N. Gisin, Q. Mei, A. Tavakoli, M. O. Renou, and N. Brunner, Phys. Rev. A **96**, 020304(R) (2017).

[24] F. Andreoli, G. Carvacho, L. Santodonato, M. Bentivegna, R. Chaves, and F. Sciarrino, Phys. Rev. A **95**, 062315 (2017).

[25] K. Mukherjee, B. Paul, and D. Sarkar, Phys. Rev. A **96**, 022103 (2017).

[26] F. Andreoli *et al.*, New J. Phys. **19**, 113020 (2017).

[27] K. Mukherjee, B. Paul, and D. Sarkar, Quant. Info. Proc. **18**, 212 (2019).

[28] K. Mukherjee, B. Paul, and A. Roy, Phys. Rev. A **101**, 032328 (2020).

[29] A. Kundu, M. K. Molla, I. Chattopadhyay, and D. Sarkar, Phys. Rev. A **102**, 052222 (2020).

[30] A. Tavakoli, N. Gisin, and C. Branciard, Phys. Rev. Lett. **126**, 220401 (2021).

[31] A. Pozas-Kerstjens, N. Gisin, and A. Tavakoli, Phys. Rev. Lett. **128**, 010403 (2022).

[32] I. Supic, J. D. Bancal, and N. Brunner, Phys. Rev. Lett. **125**, 240403 (2020).

[33] S. K. Liao, W. Q. Cai, J. Handsteiner, B. Liu, J. Yin, L. Zhang, D. Rauch, M. Fink, J. G. Ren, W. Y. Liu *et al.*, Phys. Rev. Lett. **120**, 030501 (2018).

[34] J. Aberg, R. Nery, C. Duarte, and R. Chaves, Phys. Rev. Lett. **125**, 110505 (2020).

[35] E. Wolfe, A. Pozas-Kerstjens, M. Grinberg, D. Rosset, A. Acin, and M. Navascues, Phys. Rev. X **11**, 021043 (2021).

[36] A. Tavakoli, A. P. Kerstjens, M. X. Luo, and M. O. Renou, Rep. Prog. Phys. **85**, 056001 (2022).

[37] K. Hansenne, Z. P. Xu, T. Kraft, and O. Guhne, Nat. Commun. **13**, 496 (2022).

[38] K. Mukherjee, I. Chakrabarty, and G. Mylavarapu, Phys. Rev. A **107**, 032404 (2023).

[39] O. Gamel, Entangled Bloch spheres: Bloch matrix and two-qubit state space, Phys. Rev. A **93**, 062320 (2016).

[40] S. Luo, Quantum discord for two-qubit systems, Phys. Rev. A **77**, 042303 (2008).

[41] A. Wojcik, J. Modlawska, A. Grudka, and M. Czechlewski, Phys. Lett. A **374**, 4831 (2010).

[42] W. Klobus, W. Laskowski, M. Markiewicz, and A. Grudka, Phys. Rev. A **86**, 020302(R) (2012).

[43] S. Rana and P. Parashar, Quant. Info. Proc. **13**, 2815 (2014).

[44] W. Dai, T. Peng, and M. Z. Win, IEEE J. **38**, 3 (2020).

[45] I. Chuang and M. Nielsen, *Quantum Information Science* (Cambridge University Press, 2000).

[46] S. Cheng and M. J. W. Hall, Phys. Rev. Lett. **118**, 010401 (2017).

Vol. 17, No.2 (II),
April - June2023

ISSN: 2229 - 5348

JME

JOURNAL OF MANAGEMENT & ENTREPRENEURSHIP

CONTENTS

XIME

Xavier Institute of Management & Entrepreneurship

Contents

JOURNAL OF MANAGEMENT AND ENTREPRENEURSHIP
ISSN : 2229-5348
UGC CARE Group 1 Journal

AN ANALYSIS ON LINKAGE BETWEEN FOREST ECOSYSTEM AND ECONOMIC EMPOWERMENT

Mousumi Bhar, Associate Professor, Department of Economics, Govt. Girls General Degree College, Ekbalpur, Kolkata, West Bengal, India, prof.mousumibhar@gmail.com
Mukul Kanti Gole, Registrar, Mahatma Gandhi University, Purba Midnapore, West Bengal, India, writetoomkg@gmail.com

ABSTRACT
In developing country, forests provides a significant socio-economic benefits at all level. Forest is an important renewable, natural resource, which greatly influences the socio-economic development in any rural community. Business and trade have coexistence for thousands of years and ultimately which are referred as economics by some elite peoples. Natural resource is our common future. Within the natural resource, the forestry sector has gained importance. Forest ecosystem has played multiple roles of global as well as local levels and provides a range of economic, social goods for the well beings of the poor communities. Development of natural resource management to the local community level, particularly at the forestry sector, is important to improve community livelihoods and economic empower. Both primary and secondary forest products showed a good contribution on local, regional and international economy. Forest ecosystem has an ecological impact. Economic evaluation has always played an important role in studies of how plants are used by local peoples and how that attains importance in global or regional markets to possess contribute on national and community development. Mangrove forestry has been considered for economic empowerment purposes. A highlight has been made on the rural and tribal population those are highly dependent upon forests.

In this communication an attempt has been made to scrutinize the role of forest ecosystem on economic development. An attempt has already been consider to discuss about participatory forest management by local community.

KEYWORDS: Wild Biodiversity, Forest Ecosystem, Economic Empowerment, Forest Products, Medicinal and Aromatic Plants, Natural Resources, Mangrove Forestry.

INTRODUCTION

The world commission report on 'our common future' (**Brundland, 1987**) formed the basis for the United Nations Conferences on Environment and Development in Rio de Janeiro in 1992. This conference brought into a sharp focus that the natural system was over burdened with concurrent human activities. The first principle of the Rio declaration stressed that human beings were entitled with healthy and productive life in harmony with nature (**UN, 1993**). The resulting Agenda 21 took this principle of sustainable development further. Despite ongoing efforts, the United Nations General Assembly expressed concern over continuing declaration of the environment and called Johannesburg World Summit in 2002 to focus on the status of Agenda 21. There was a gradual shift in thinking from Rio to Johannesburg .The first shift was that unlike Agenda 21, Johanesburg summit recognized poverty as the running theme linked to multiple dimensions from access to energy, water and sanitation to equitable distribution of benefits of biodiversity. The second shift was the summit emphasized on the integration of social. economic and environmental needs of people for sustainable development. Third shift was called for business group participation in financing sustainable development projects. People seek to manage natural resources for two reasons. First, management of natural resources improves their conditions of livelihood. Second, environmental degradations are threatening, either to life sustaining processes through deforestation, fuel shortage, etc., or to people's aesthetic value. Natural resources can be held under any one of the four property rights regimes: open access, common property, private property. and state property. In practice, natural resources are rarely managed by one of these alone. Open access regime entails the absence of property rights. With the demands for rapid socio-economics development. complete nonviolence on nature is impossible. Use and conservation of natural resources simultaneously can help attaining well being of people on sustainable basis. At

ISSN 0972-8945

SOUTH INDIA JOURNAL OF SOCIAL SCIENCES

A.P. ACADEMY OF SOCIAL SCIENCES

Vol. XXI, No.38, January – June 2023

CONTENTS

SOUTH INDIA JOURNAL OF SOCIAL SCIENCES
ISSN: 0972 – 8945

STUDIES ON MEDICINAL PLANTS AS LIVELIHOOD SECURITY AND ECONOMIC EMPOWERMENT

Mousumi Bhar, Associate Professor, Department of Economics, Govt. Girls General Degree College, Ekbalpur, Kolkata, West Bengal, India, prof.mousumibhar@gmail.com
Mukul Kanti Gole, Registrar, Mahatma Gandhi University, Purba Midnapore, West Bengal, India, writetoomkg@gmail.com (Corresponding author)

Abstract
Natural resource is our common future. Within the natural resource, the forestry sector has gained importance. Overall trades in forest product are currently estimated to makeup 2-3 percent of the total merchandise trade. Both primary and secondary forest products showed a good contribution on local, regional and international economy. Development of natural resource management to the local community level, particularly at the forestry sector, is important to improve community livelihoods and economic empower. Economic evaluation has always played an important role in studies of how plants are used by local peoples and how that attains importance in global or regional markets to posses contribute on national and community development.

In this communication, an attempt has been made to scrutinize the role of medicinal plants, a non-timber forest products as a source of income of the poor. Information are collected from different secondary data and with contact of some native forests dwellers.

Key words:
Natural Resources, Forest Ecology, Economic Development, Non Timber Forest Products, Medicinal Plants.

Introduction

The United Nations Conferences on Environment and Development in Rio de Janeiro in 1992, brought into sharp focus that the natural system was over burdened with concurrent human activities. The first principle of the Rio declaration stressed that human beings were entitled with healthy and productive life in harmony with nature (**UN, 1993**). The resulting Agenda 21 took this principle of sustainable development further. People seek to manage natural resources for two reasons. First, management of natural resources improves their conditions of livelihood. Second, environmental degradations are threatening, either to life sustaining processes through deforestation, fuel shortage, etc., or to people's aesthetic value. Natural resources can be held under any one of the four property rights regimes: open access, common property, private property, and state property. In practice, natural resources are rarely managed by one of these alone. Use and conservation of natural resources simultaneously can help attaining well being of people on sustainable basis.

Over the last two decades, a profound change has been witnessed in the area of natural resource management especially in the forestry sector, with countries at least partially developing right and responsibilities over their natural resources to the users (**Edmonds, 2002, Larsen and Ribort, 2004**) with the hope that forest resources will be better conserved and at the same time livelihood systems of forest dependent people will be involved. India has been at the forefront of developing natural resources management to the local community level, particularly in the forestry sector, for more than a decade. In a follow-up documents issued in 1990, the central government issued guidelines to all the state governments to implements ' joint forest management systems'(JFM) by devolving everyday forest use and management rights to the community. It has been observed that almost all the states have formally resolved to implement JFM and making it one of the largest of such programs in the world (**Kumar, 2002; Behera and Engel, 2006**).

UGC CARE LIST No. 135
ISSN 0030 - 5324

Journal of The Oriental Institute

Vol. 72, Issue. 03, No.1,
July – September: 2023

सत्यं शिवं सुन्दरम्
Estd. 1949

Accredited Grade 'A' by NAAC

Oriental Institute

The Maharaja Sayajirao University of Baroda
[illegible]dodara

Editor
Sweta Prajapati

INDEX

Journal
of the
Oriental Institute
M.S. University of Baroda
ISSN: 0030-5324

ROLE OF HEALTH FINANCING ON HUMAN HEALTH DEVELOPMENT- AN ANALYSIS

MousumiBhar, Associate Professor, Department of Economics, Govt. Girls General Degree College, Ekbalpur, Kolkata, West Bengal, India, prof.mousumibhar@gmail.com
MukulKantiGole, Registrar, Mahatma Gandhi University, PurbaMidnapore, West Bengal, India, writetoomkg@gmail.com (Corresponding author)

Abstract

Health is a complex and multi-dimensional concept. It is not only function on medical core but also the overall integrated development of society. Health is influenced by income of the households, educational level of the family members, as well as food, housing, basic sanitations, social practices, environmental hazards, communicable diseases and government spendingon in clinical and public health. India's socioeconomic characters are largeand extremely heterogeneous characters. India today remains a country of stark contrasts and striking disparities. Commencing with independence in 1947, India has indeed make some gains in health.Development must be holistic that encompasses not only advancement of economic parameters but also achievements in health, education, environmental sustainability, etc. Amongst all, social sector development assumes the centre stage and is an integral part of the development process. It primarily includes education, health, and food and nutrition security. It is found that India is shouldering least responsibility regarding the health of its people. So, in India, there is a need to increase the share of public finances for health sector.

An analysis has been made in this communication on the above mentioned issues with reference to the secondary data sources.These secondary data are collected from Government reports and other different reports, publications.

Keywards: Human Health Development, Health tax, Economic development,Public private health expenditure. Gross Domestic Product (GDP)

Introduction

Health is a form of human capital.It facilitates economic development of nation in very many ways. As the poverty level has declined in post-liberalization period, the income level of the people has gone up. This has resulted in the expansion of health seeking behavior of the people. Even after the allocation of huge amount of funds through different programmes, public expenditure as a percent of Gross Domestic Product (GDP) has reached 1.37 percent in 2010- 2011.As the public sector has failed to cope up with rise in health care demand, the private sector dominates the health care market which is evident from the fact that the private sector provides 76 percent of the healthcare in India. Rising cost of diagnosis, medicines and hospitalizations push millions of Indians below the poverty line. India has one of the highest proportions of out-of-pocket spending on healthcare in the world. The enhanced rate of economic growth has failed to address certain issues of vital importance which includes dynamic of labors market, progress of the agricultural sector, gender equality, caste representations, cultural developments, environmental protections and health (Aghionand Bolton, 1992, Gopalan,1994, Greese, 1997, Senghor, 1987).

UGC CARE LISTED PERIODICAL
ISSN : 2278 - 6864

Education and Society

Since 1977

Vol-46, Issue-4, No.05, July-September: 2023

EQUALITY • EDUCATION • DEVELOPMENT

भा. सं.

Indian Institute of Education

J. P. Naik Path, 128/2, Kothrud, Pune-411 038

INDEX

Education and Society (शिक्षण आणि समाज)
(UGC Care Journal)
ISSN: 2278-6864
Vol-46, Issue-4, No.05, July-September: 2023

CHOICE BASED CREDIT SYSTEM: A LEAF AT THE REFORMS IN INDIAN HIGHER EDUCATION

Mukul Kanti Gole, Registrar, Mahatma Gandhi University, Purba Midnapore, West Bengal, India, writetoomkg@gmail.com (Corresponding author)
Sidhartha Sankar Laha, Associate Professor, Department of Lifelong Learning & Extension, University of North Bengal, Darjeeling, West Bengal, sidharthasankar09@gmail.com
Mousumi Bhar, Associate Professor, Department of Economics, Govt. Girls General Degree College, Ekbalpur, Kolkata, West Bengal, India, prof.mousumibhar@gmail.com

Abstract
Education play a key stone in the process of nation building. India is the ancient land where wisdom made its home before it went into any other country. Education system of India is full of intricacies of different nature. Several attempts have been taken to lessen complexities. Several commission have been constituted in India to improve the quality and uniformity in the Indian education system. These commission have also been constituted for removal of different anomalies within the Indian education system. In all over India, the present education system are divided in the form of primary education, secondary education and tertiary education. The tertiary education is consider as the higher education. Higher education is considered as the back bone of the nation. Higher education is a noble exercise for creation and dissemination of knowledge, understanding and skill. University Grants Commission (UGC) is the premier policy framing, decision making and funding agency for universities and institution of higher learning in India. A reform in the higher education in India is made by University Grants Commission (UGC) which is annual to semester system and then to Choice Based Credit System (CBCS). This reform was brought to bring flexibility in higher education. It is a student- centric education and it helps the students to pursue the courses of their choice which are from interdisciplinary, intra-disciplinary and skill based courses. This system would help the Indian education system to match with the international education pattern.
The traditional cohort system does not cater to the expectations of all stakeholders of education. The Choice Based Credit System (CBCS) is going popularity among the higher education institutions in India slowly as it allows the students to customize the programme to suit their requirements. The programme under the Choice Based Credit System (CBCS) is meant to cater to requirements of the customer i.e. the students. The main parameters of Choice Based Credit System (CBCS) are course of choice, pedagogy, course timings, approach, faculty, etc. Academic reforms in India are being introduced with a goal of increasing quality standards in tandem with initiatives designed to broaden access. The University Grants Commission (UGC) has initiated several measures to bring equity, efficiency and the excellency in the higher education system in country. The important measure has taken to enhance academic standards and quality in higher education which includes innovation and improvements in curriculum, teaching – learning process, examination and evaluation systems, governance and other related matters. The main features of Choice Based Credit System(CBCS) are ability to meet student's scholastic needs and aspirations, improvement in quality education, flexibility for working students, standardization and compatibility, part completion of the programme at the institution of enrolment and part completion at specialized, intra- institution transferability.
In this communication an attempt has been made to analyses different aspects of Choice Based Credits System (CBCS) including reforms and new initiatives taken for the higher education system in India including new education policy.

Keywords: *Choice Based Credit System (CBCS), University Grants Commission (UGC), Indian Higher Education system, New Education Policy.*

Introduction

Education is the key stone of nation building. The levels of education reflect the status of a nation. Education is a process which facilitates learning and equipped the learners to the knowledge and confidence, instilling values, changing attitudes and behavior by which they become well - adjusted

قسم العربية، جامعة كاليكوت، كيرالا
ISSN 2278-764X

مجلّة كاليكوت
KALIKOOT

المجلد الثاني عشر – العدد الثالث: سبتمبر – ديسمبر ٢٠٢٢

انعكاس الإيديولوجية وصراعها في ثلاثية القاهرة لنجيب محفوظ

عبد المتين وسيم الدين، الباحث بقسم اللغة العربية وآدابها، جامعة عالية، كولكاتا، الهند؛ والأستاذ المساعد بكلية الشهادات العامة الحكومية للبنات التابعة لجامعة كلكتة، الهند

المدخل:

الإيديولوجية هي ملمح فكري وميدان رحب للبحث في الدراسات الأدبية، ويسع معظم مجالات الحياة الاجتماعية والثقافية والسياسية والنفسية والتربوية والاقتصادية والإعلامية، وعقيدة تتصل بقيم ثقافية واجتماعية وسياسية، ولا تتكون بقرار ولا تأتي من العدم، وإنما هي ضرب من الولادة عبر عملية تاريخية معقدة. وعلاقتها بالعمل الأدبي الروائي علاقة وثيقة، فهي الجزء الرئيس في خلق تناقضات الرواية. فالكاتب لا يكتب من فراغ، بل كتابته جزء من إيديولوجيته وثقافته، ومضمونه مستمد من بيئته ومحيطه. وكانت علاقة نجيب محفوظ بمصر وطيدة، فنجده في معظم أعماله يناجيها ويستمع إلى نبضها، فرواياته انعكاس واضح لتاريخ وأماكن وحوادث مصر. وأما ثلاثية القاهرة فهي عمل روائي ضخم يمثل واقع الشعب المصري عبر ثلاثة أجيال، ويبرز ثلاثة أطوار فكرية تمثل المجتمع المصري، فالجزء الأول بين القصرين يمثل حقيقة الإيمان بالأشياء والاستسلام لها في ميدان الدين والسياسة، أما الجزء الثاني قصر الشوق فهو ميدان الشك والتردد والحيرة بكل القيم والحقائق بالعلم والإيمان والحب والأب. وأما الجزء الثالث السكرية فهو الانتماء والوعي للقيم والمبادئ، والأفكار هو شعارها.

الكلمات المفتاحية:

نجيب محفوظ، وثلاثية القاهرة، والإيديولوجية، والمجتمع، والانتماء الإيديولوجي، والخلاف الإيديولوجي، والصراع الفكري، والدين وأتباعه، والشيوعية، وجماعة الإخوان المسلمين، والاتجاهات والأفكار، والعلم والإيمان.

نبذة عن الروائي:

أ – حياته: هو نجيب محفوظ روائي وكاتب مصري، وأول أديب عربي نال جائزة نوبل في الأدب. وُلد ونشأ في حي الحسين عام ١٩١١، وتلقى تعليمه الابتدائي في مدرسة الحسينية بالقاهرة ثم أتم مرحلته الثانوية في مدرسة فؤاد الأول الثانوية، وحصل على ليسانس الآداب من قسم الفلسفة عام ١٩٣٤، وكان هو الأصغر لستة أشقاء. وعمل معظم حياته بالوظائف

الحكومية بدءا بالجامعة المصرية فوزارة الأوقاف ثم مصلحة الفنون ثم مؤسسة السينما ورئيسا لمجلس الإدارة وفي الأخير عضوا في جريدة الأهرام. وأحيل على المعاش سنة ١٩٧١ بموقع مستشار وزارة الثقافة لشؤون السينما. وعمر طويلا وتوفي عام ٢٠٠٦.[١] وقد نال أول جائزة أدبية على مستوى الدولة عام ١٩٤٠ جائزة قوت القلب الدمرداشية، ثم جائزة مجمع اللغة العربية عام ١٩٤٣، ونال يوم الخميس ١٣ أكتوبر عام ١٩٨٨ جائزة نوبل للآداب التي منحته شهرة واسعة في أرجاء العالم.[٢]

وكان باحثا عن الله، وهذا ما دعاه إلى دخول قسم الفلسفة ساعيا وراء أفكاره مما أدى إلى صرف نظره عن حياة الشباب ومستلزماتها، فلم يتزوج حتى بلغ سن الثالثة والأربعين. ولكنه أثناء إعداده لرسالة الماجستير حول فلسفة الجمال مر بأزمة إبداعية إذ وجد نفسه في صراع ما بين الفلسفة والأدب فقرر أن ينتصر للأدب على حساب الفلسفة.[٣] وكتب في مجال القصة، وكان حريصا منذ لحظاته الأولى على الكتابة بالعربية الفصحى في جل أعماله، فعد من أوائل الداعين إلى عدم الفصل بين واقعية الرواية وفصاحة الحوار. ومن السمات البارزة التي اتسم بها أنه كانت علاقته بمصر وطيدة، فهو يناجيها في معظم أعماله كاسرا الحواجز بينها وبين أدبه فهو يستمع إلى نبض مصر في تاريخها وواقعها، ولا يضع حاجزا بينها وبين أدبه. فأعماله انعكاس واضح لتاريخ وأماكن وحوادث مصر.[٤]

ب - مسيرته الروائية: وقد مر بمراحل عديدة في مسيرته الروائية. فمرحلته الأولى هي التاريخية ويتأثر فيها باحتلال بريطانيا لمصر فيكتب عبث الأقدار عام ١٩٣٩، وفي خضم الحرب العالمية الثانية ينشئ رادوبيس عام ١٩٤٣ وكفاح طيبة عام ١٩٤٤، وكل هذه أعمال تاريخية تحمل في ثناياها الروح الفرعونية.[٥] ومرحلته الثانية هي الاجتماعية، ويتحول من التاريخية إليها ليتوغل في تصوير المجتمع المصري وتحوله الاجتماعي بمشكلاته وهمومه، ويبدأ بالقاهرة الجديدة عام ١٩٤٥ ثم ينشئ خان الخليلي عام ١٩٤٦ ثم زقاق المدق عام ١٩٤٧ ثم يتبعها من رؤية نقدية وذاتية لمجتمعه بالسراب عام ١٩٤٨ ثم بداية ونهاية عام ١٩٤٩، ثم يختم هذه المرحلة بإنتاج عمل ضخم يمثل واقع الشعب المصري يعرف بثلاثية القاهرة التي نحن بصدد دراستها من حيث الرؤية الاجتماعية والتحول الاجتماعي.

---

[١] رجاء النقاش، صفحات مذكرات نجيب محفوظ، ص ١٢؛ حسين عيد، نجيب محفوظ سيرة ذاتية وأدبية، ص ٧؛ رجاء النقاش، في حب نجيب محفوظ، ص ٢١

[٢] رجاء النقاش، صفحات من مذكرات نجيب محفوظ، ص ١٤٩

[٣] رجاء النقاش، في حب نجيب محفوظ، ص ٢٥؛ علي شلق، نجيب محفوظ في مجهوله المعلوم، ص ٤٧

[٤] حسن درويش، الاتجاه التعبيري في روايات نجيب محفوظ، ص ١٨؛ محمود فوزي، نجيب زعيم الحرافيش، ص ١٢؛ فاروق شوشة، حوار مع نجيب محفوظ، مجلة الآداب، بيروت، عام ١٩٦٠، العدد الثالث، ص ١٨

[٥] حسن درويش، الاتجاه التعبيري في روايات نجيب محفوظ، ص ٤٧

وقد ركز اهتمامه فيها على الطبقة الوسطى وهي أكثر الطبقات معاناة في مصر.[١] ومرحلته الثالثة هي الواقعية الفلسفية، تبدأ بأولاد حارتنا عام ١٩٥٩ وتمثل الجانب الفلسفي الميتافيزيقي ثم اللص والكلاب عام ١٩٦١، والسمان والخريف عام ١٩٦٢، والطريق عام ١٩٦٤، والشحاذ عام ١٩٦٥، وثرثرة فوق النيل عام ١٩٦٦، وميرامار عام ١٩٦٧.

ج – فكره وفلسفته: وكان بالرغم من ارتباطه الوثيق بمصر لم تكن له علاقة مباشرة بالسياسة فيما عدا حبه الفطري لحزب الوفد.[٢]

وكان متميزا بقدرته الفائقة على اختزان الماضي واستعادته بشكل فني مثير، وكان شموليا ومتنوعا في قراءاته وثقافته. وكانت له علاقات حميمة مع أدباء عصره فقد قابل توفيق الحكيم واستمرت علاقتهما حتى وفاة الحكيم، والتقى بالمازني وأخذ منه نصائح حول زقاق المدق، وكان له علاقة حميمة مع يحيى حقي أيضا.[٣]

وكان له موقف متشدد تجاه الحركات الإسلامية خاصة حركة الإخوان المسلمين، فقد نظر إليهم على أنهم مصدر العنف والتزمت الديني، وعبر عن ارتياحه الكبير مما قام به جمال عبد الناصر في أثناء تصفيتهم عقب حادثة المنشية في مصر. وكان له موقف من عملية السلام مع العدو الصهيوني، فنادى بإمكانية عقد السلام مع العدو على أساس اغتنام الوقت للتنمية وهو يشعر بالفرق الهائل في المستوى الحضاري والتكنالوجي بين العرب والصهاينة.[٤]

وهو كاتب واقعي اجتماعي كبير، لكنه لم يتطرق إلى الكثير من القضايا الخاصة التي شغلت العرب كلهم، فلم نجد له عملا يتحدث فيه عن الأعمال السياسية المهمة في بلاده مصر وجوارها مثل تأميم للقناة أو حرب ١٩٥٦ وحرب ١٩٧٣ وما تبعها من أحداث مؤلمة دكت العالم العربي والإسلامي باحتلال فلسطين. ولعل سبب ابتعاده عنها – ولو جل أعماله الروائية تقترب من الفهم الدقيق للواقع السياسي – يرجع إلى أنه حدد لنفسه دائرة الحركة ضمن الطبقة الوسطى، فيهتم برصد الواقع الاجتماعي والظواهر الاجتماعية والإنسان، ومن خلال هذا الرصد يقدر الغوص في بني المجتمع ويستطيع التعبير عن مشاعره ومواقفه.

ثلاثية القاهرة ومحتوياته:

ثلاثية القاهرة هي عمل روائي ضخم يمثل واقع الشعب المصري عبر ثلاثة أجيال، وقد ختم بها الكاتب مرحلته الاجتماعية. وهي مكوّنة من ثلاث روايات، وهي: بين القصرين (١٩٥٦)، وقصر الشوق (١٩٥٧)، والسكرية (١٩٥٧). وتعتبر أفضل رواية عربية حسب اتحاد كتاب العرب،

[١] حسن درويش، الاتجاه التنعبيري في روايات نجيب محفوظ، ص ٥١

[٢] رجاء النقاش، صفحات من مذكرات نجيب محفوظ، ص ١٢٨

[٣] رجاء النقاش، صفحات من مذكرات نجيب محفوظ، ص ٧١

[٤] رجاء النقاش، صفحات من مذكرات نجيب محفوظ، ص ١٩٥ – ١٩٧

وأخذت أسماءها الثلاث من أسماء شوارع حقيقية بالقاهرة القديمة التي شهدت نشأة وترترع نجيب محفوظ.

وثلاثية نجيب محفوظ هذه كباقي الثلاثيات يمكن أن يقرأ كل جزء منها على حدة، فجزؤها الأول بين القصرين يعرض الكاتب فيه جانبا من حياة الجيل الأول لعائلة السيد أحمد عبد الجواد في حي شعبي من أحياء القاهرة ويبرز الجو العام للأسرة ويركز على بناء نماذج بشرية متنوعة وما يرافقها من حدث ثورة يوليو ١٩١٩ بالإضافة إلى الحال الاجتماعية لأبناء الشعب من انحلال خلقي وميل للهوى وطغيان الهم الاجتماعي.

أما الجزؤ الثاني للثلاثية هو قصر الشوق، ويصور الكاتب فيه حياة الأسرة يعني أسرة السيد أحمد عبد الجواد في منطقة الحسين بعد وفاة ابنه فهمي وأحداث ثورة ١٩١٩ ويعرض ما يحمله هذا الجيل الأوسط من تراكمات الماضي وما يعتريه من تناقضات وملامح نفسية ومحاولات للتخلص من سلطة الأب.

وجزؤها الثالث والنهائي هو السكرية، ويحكي نجيب محفوظ فيه عن الجيل الثالث لأسرة السيد أحمد عبد الجواد ما بعد الثورة ويعرض حارة السكرية وأوضاعها وأحوالها، ويبرز أن هذا الجيل الثالث للأسرة، ويريد به الجيل المصري الجديد، يعتمد على نفسه.[١]

انعكاس الإيديولوجيات المتنوعة:

الإيديولوجية هي من الملامح الفكرية التي تعد ميدانا رحبا للبحث في الدراسات الأدبية، وهي من أوسعها تداخلا مع معظم مجالات الحياة الاجتماعية والثقافية والسياسية والنفسية والتربوية والاقتصادية والإعلامية. وهي مجموعة التصورات التي تعبر عن مواقف محددة تجاه الإنسان والعالم، وهي العقيدة التي تتصل بقيم ثقافية واجتماعية وسياسية.[٢] وهي لا تتكون بقرار ولا تأتي من العدم، إنما هي ضرب من الولادة عبر عملية تاريخية معقدة. وتتميز بأنها نسق للتصور عن العالم، فعلاقتها بالعمل الأدبي الروائي علاقة وثيقة. والمنظور الإيديولوجي هو الجزء الرئيس في خلق تناقضات الرواية. والكاتب لا يكتب من فراغ، بل كتابته جزء من ثقافته وشخصيته وفكره، ومضمون النص مستمد بطبيعة الحال من بيئة الروائي ومحيطه بما يتخللها من إيديولوجيات مسيطرة.

أما ثلاثية القاهرة فهي تظهر وتبرز ثلاثة أطوار فكرية تمثل المجتمع، فالجزء الأول رواية بين القصرين تمثل حقيقة الإيمان بالأشياء والاستسلام لها في ميدان الدين والسياسة والأب

---

[١] محمد عزام، فضاء النص الروائي، دار الحوار للنشر والتوزيع – اللاذقية، الطبعة الأولى، عام ١٩٩٦، ص ٦١

[٢] محمد عزام، فضاء النص الروائي، ص ١٤٧

السيد أحمد عبد الجواد، فهو إيمان مطلق بالله، ثم ولاء وأتباع لسعد زغلول ورفقائه، وطاعة عمياء للسيد أحمد عبد الجواد. أما الجزء الثاني قصر الشوق فهي ميدان الشك والتردد والحيرة بكل القيم والحقائق بالعلم والإيمان والحب والأب. وأما الجزء الثالث السكرية فهي الانتماء والوعي للقيم والمبادئ، والأفكار هو شعارها.[١]

وثلاثية القاهرة هي عمل فني بالدرجة الأولى تصور المجتمع المصري بكل تجلياته الثقافية والفنية والسياسية والأدبية، ولا بد من إدخال هذا الجانب الإيديولوجي المهم في النص الروائي، لأنها جزء من ثقافة المجتمع. ونجد فيها تظهر بعض التوجهات الإيديولوجية بصورة واضحة، نجد فيها شخصية عبد المنعم تمثل جماعة الإخوان المسلمين. وتبدو من خلاله إيديولوجية وفلسفة جماعة الإخوان، فنجد في الرواية: "لكل قوي إيمانه، إنهم يؤمنون بالوطن والمصلحة، أما الإيمان بالله فهو فوق كل شيء وأحرى بالمؤمنين بالله أن يكونوا أقوى من المؤمنين بالحياة الدنيا، فبأيدينا نحن المسلمين ذخيرة مدفونة يجب أن نستخرجها، يجب أن يبعث الإسلام كما بعث أول مرة، هذا هو شعارنا العودة إلى القرآن".[٢]

ونرى شخصية مهمة جدا وهي شخصية أحمد في السكرية، وتبدو من خلاله وحواره إيديولوجية الشيوعية. كما يقول: "تعاليم الإسلام تستند إلى ميتافيزيقية أسطورية تلعب فيها الملائكة دورا خطيرا، لا ينبغي أن نبحث عن حلول مشكلات حاضرنا في الماضي البعيد. الإخوان يصطنعون عملية تزييف هائلة، فهم حيال المثقفين يقدمون الإسلام في ثوب عصري، وهم حيال البسطاء يتحدثون عن الجنة والنار".[٣] وتبدو أيضا أن الشيوعية تعتمد العلم أساسا للحياة على حساب الدين والعقيدة، ويتضح هذا بهذه العبارة: "الدين ملك الناس أما الله فلا علم لنا به.. نعم الإيمان بالعلم به وجاهته.. العلم لغة العقول.. العلم يجمع البشر في نور أفكاره".[٤] وفي موضع: "الشيوعية علم، أما الدين فأسطورة".[٥]

انعكاس الصراع الإيديولوجي والفكري:

ينعكس فيها الخلاف الإيديولوجي والصراع الفكري بين جماعة الإخوان المسلمين والشيوعية، ويظهر هذا الخلاف جليا على لسان كل من أحمد وعبد المنعم، وهما الشخصيتان الهامتان في السكرية الجزء الثالث للثلاثية. ونجد الخلاف يقوم بينهما منذ البداية. وتبدو إيديولوجية كل منهما واالصراع بين منظورهما الإيديولوجي من خلال العرض، فحركة الإخوان

[١] سليمان الشطي، الرمز والرمزية في أدب نجيب محفوظ، الهيئة المصرية للكتاب، الطبعة الأولى، عام ١٩٧٦، ص ٦٨

[٢] نجيب محفوظ، السكرية، مكتبة مصر – القاهرة، الطبعة ١١، عام ١٩٨٤، ص ٨٣ – ٨٥

[٣] نجيب محفوظ، السكرية، ص ٢٦١

[٤] نجيب محفوظ، السكرية، ص ١٠٧

[٥] نجيب محفوظ، السكرية، ص ١٥٢

المسلمين يبرز الكاتب فلسفتها في الرواية خلال عرض أحد أعضائها: "الإنجليز والفرنسيون والألمان والطليان جل اعتمادهم على الحضارة المادية، أما أنتم فاعتمادكم على الإيمان الصادق. إن الإيمان يفلّ الحديد، الإيمان أقوى قوة في العالم، املأوا قلوبكم الطاهرة بالإيمان، تخلص الدنيا لكم".[١] ثم يبرز ويبين أهمية الإيمان كمرتكز إيديولوجي أساسي في دعوة الإخوان: "الإيمان خالق القوة وباعثها، إن القنابل تصنعها أيد كأيدينا، وهي ثمرة القلوب قبل أن تكون من مسبباتها، كيف انتصر النبي – عليه السلام – على أهل الجزيرة...؟".[٢]

ونرى المنوفي شيخ الإخوان في الرواية يحلل العقدة ويوضح أن سبب انتصار الإنجليز هو عدم فقدانهم لعنصر الإيمان فيقول: "لكل قوي إيمانه، إنهم يؤمنون بالوطن والمصلحة، أما الإيمان بالله فهو فوق كل شيء وأحرى بالمؤمنين بالله أن يكونوا أقوى من المؤمنين بالحياة الدنيا، فبأيدينا نحن المسلمين ذخيرة مدفونة يجب أن نستخرجها، يجب أن يبعث الإسلام كما بعث أول مرة، هذا هو شعارنا العودة إلى القرآن".[٣] ويستمر قوله بإيضاح الفكر وأصحابه: "لسنا جمعية للتعليم والتهذيب فحسب، ولكننا نحاول فهم الإسلام كما خلقه الله دينا ودنيا وشريعة ونظام حكم".[٤]

أما طريقة عمل هذه الإيديولوجية فتظهر على لسان عبد المنعم: "ولكننا لا نرجم، وإنما بالموعظة الحسنة، والمثال الطيب نهدي ونرشد، وآية ذلك أن بيتنا يضم أخا مما يستحقون الرجم، وها هو يمرح أمامكم، ويتطاول على خالقه سبحانه".[٥] ولم تكتف هذه الدعوة بتربية الناس وإرشادهم وتطبيق حكم الله، وإنما تتعداه للعمل بحقل السياسة، فهو ميدان واسع للعمل، كما في الرواية: "الدين هو العقيدة والشريعة والسياسة، إن الله أرحم من أن يترك أخطر الأمور الإنسانية دون تشريع وتوجيه".[٦]

وإذا كان عبد المنعم قد تلقى علومه ومبادئه وأفكاره من الشيخ المنوفي شيخ جماعة الإخوان وراح يتردد على مجلسه ليتلقى من فكر ومنابع الدعوة الدينية الجديدة، فإن شقيقه أحمد قد وجد مآله في مجلة الإنسان الجديد تحت وصاية رئيسها عدلي كريم وتلميذته سوسن حماد، فيتلقى ويناقش فكره ومبادئه. وإن كان الشيخ المنوفي صوت الدعوة الدينية، فمجلة الإنسان الجديد هي منبر الدفاع عن الفكر اليساري الشيوعي، فانضم إليها أحمد وهو في المرحلة الثانوية وتربى على يديها من بعيد وقرأ مقالاتها

---

[١] نجيب محفوظ، السكرية، ص ٨٣

[٢] نجيب محفوظ، السكرية، ٨٣

[٣] نجيب محفوظ، السكرية، ٨٣ – ٨٥

[٤] نجيب محفوظ، السكرية، ص ١٣١

[٥] نجيب محفوظ، السكرية، ص ١٣٢

[٦] نجيب محفوظ، السكرية، ص ٨٤

حيث تربى على يد عدلي كريم الذي ربطته به علاقة قوية استطاع من خلالها أن يبث أفكاره إلى أحمد.

ومعطيات هذا الفكر تبرزها الثلاثية عبر الحوار الذي يجري بين عدلي كريم وبين أحمد بعد أن يسأله أحمد عن انتماء الشباب السياسي ليتضح موقف اليساريين من الأحزاب المصرية بجلاء مصر الفتاة، ففي الرواية: "لا وزن لها، فرقة تعد على الأصابع، كان الحزب الوطني حزبا تركيا دينيا رجعيا، أما الوفد فهو مبلور القومية المصرية ومطهرها من الشوائب والخبائث، إنه مدرسة الوطنية والديمقراطية. أما مصر الفتاة فحركة فاشستية رجعية مجرمة، ليست دون الرجعية الدينية خطرا، وهي ليست إلا صدى للعسكرية الألمانية والإيطالية".[١]

ويظهر تبرؤ الشيوعية من الدين ومن كل عقيدة مما يجري من الحوار بين أحمد وأخيه عبد المنعم، يقول أحمد بهدوء: "أعرف أنه دين، وحسبي ذلك، لا أؤمن بالأديان".[٢] وتبدو نظرية الشيوعية لفكر الإخوان والدين من قول أحمد هذا: "تعاليم الإسلام تستند إلى ميتافيزيقية أسطورية تلعب فيها الملائكة دورا خطيرا، لا ينبغي أن نبحث عن حلول مشكلات حاضرنا في الماضي البعيد. الإخوان يصطنعون عملية تزييف هائلة، فهم حيال المثقفين يقدمون الإسلام في ثوب عصري، وهم حيال البسطاء يتحدثون عن الجنة والنار".[٣]

ونجد الشيوعية فيها تعتمد العلم أساسا للحياة على حساب الدين والعقيدة، ويتضح هذا بقول رياض قلدس الفيلسوف الشيوعي في الرواية: "الدين ملك الناس أما الله فلا علم لنا به.. نعم الإيمان بالعلم به وجاهته.. العلم لغة العقول.. العلم يجمع البشر في نور أفكاره".[٤] وفي موضع آخر يتضح الصراع جليا على لسانه: "الشيوعية علم، أما الدين فأسطورة".[٥]

ونرى أحمد في رواية السكرية الجزء الختامي للثلاثية يؤيد فلسفة رياض قلدس فيتابعه ويؤضح فلسفته وإيمانه بالشيوعية والعلم حيث يقول: "لا أؤمن بالأديان.. بإيماني الخالص، إيماني بالعلم والإنسانية والغد وبما التزمه من واجبات".[٦] ونراه يرغب في ذلك القدر من المعرفة والأفكار التي تساند النظم المختلفة في المجتمع السياسي الذي يحاول أن يصل إلى نوع من اتفاق الرأي حول القيم السياسية عن طريق وضع معايير معينة للعملية السياسية.[٧]

وتظهر في الثلاثية أيضا أن الماركسية أصحابها أقل عددا من أنصار حركة الإخوان المسلمين

---

[١] نجيب محفوظ، السكرية، ص ٩٠

[٢] نجيب محفوظ، السكرية، ص ١٣٥

[٣] نجيب محفوظ، السكرية، ص ٢٦١

[٤] نجيب محفوظ، السكرية، ص ١٠٧

[٥] نجيب محفوظ، السكرية، ص ١٥٢

[٦] نجيب محفوظ، السكرية، ص ١٣٥

[٧] عبد الرحمن خليفة، إيديولوجية الصراع السياسي، دار المعرفة الجامعية – الإسكندرية، الطبعة الأولى، عام ١٩٨٨، ص ١٤٧

التي احتلت موقعا كبيرا بين جماهير الطبقات المصرية، ولكن لما منعت الحركة من أن تمارس دورها السياسي بعد الحرب العالمية الثانية ازدادت التبعية للقوى الاشتراكية. وكل هذه العوامل فتحت الباب على مصراعيه لانضمام كثير من أتباع هذه الحركة.

انعكاس العلاقة بين جماعة الإخوان والشيوعية:

أما العلاقة بين حركة الإخوان المسلمين والشيوعية فتظهر في هذه الثلاثية من وجهتين: الأولى نظرية الإخوان تجاه الشيوعية ونظرية الشيوعية تجاه الإخوان المسلمين.

(أ) نظرية الإخوان للشيوعية: أما نظريتهم للشيوعية فهي قائمة على التسامح والموعظة الحسنة والمثال الطيب، ويظهر هذا في خطاب عبد المنعم حيث يقول: "إن الشباب يتهددهم زيغ في العقيدة، وانحلال في الخلق، وليس الرجم بأشد ما يستحقونه، ولكننا لا نرجم، وإنما بالموعظة الحسنة والمثال الطيب نهدي ونرشد. وآية ذلك أن بيتنا يضم أخا مما يستحقون الرجم وها هو يمرح أمامكم ويتطاول على خالقه سبحانه!".[١]

(ب) نظرية الشيوعية للإخوان: أما الشيوعيون فينظرون للإخوان أنهم الخطر المطبق الحاملون لتعاليم الإسلام المنبثقة من عالم الميتافيزيقيا الأسطورية التي تلعب الملائكة فيها دورا كبيرا، وهم الذين يصنعون عملية تزييف هائلة.[٢] ويتبين ذلك مما قالت سوسن حماد تلميذة عدلي كريم: "أعداؤنا كثيرون، الألمان في الخارج، والإخوان والرجعية في الداخل، وكلاهما شيء واحد".[٣]

وهذا من المؤكد أن لكل حزب وفكر سياسي طريقة خاصة، يبرز من خلالها برنامجه ليتدخل بفاعلية في السعي على الحكم وقيادة الناس. ومن خلال استقراء ما قالت سوسن تتضح صورة أخرى في التعامل الإيديولوجي لدى الشيوعية، فعندما تواجه حزبا عاملا آخر تلجأ مباشرة إلى ترتيبه حسب درجة التناقض والتقارب بينها وبينه، وعندما تحدد موقفها بأنه الخصم الرئيس تعطيه محل الصدارة في حقل المواجهة، وتبادر إلى الاهتمام الخاص به. وهكذا يحدث ترتيب محدد للآخرين حول الحزب الساعي إلى السلطة السياسية، وينعكس هذا الترتيب في الصور التي ينتجها عنهم. ويستمر الصراع بين الفكرين.

وتنعكس الشيوعية في الثلاثية قليلة العدد، تعمل بسرية تامة، وتوزع المنشورات ليلا، ولا تجمعهم رابطة قوية كالإخوان.[٤] وهدفهم الأهم

[١] نجيب محفوظ، السكرية، ص ١٣٢

[٢] نجيب محفوظ، السكرية، ص ٢٦١ – ٢٦٦

[٣] نجيب محفوظ، السكرية، ص ٢٦٩

[٤] شفيع السيد، اتجاهات الرواية المصرية، دار المعارف – القاهرة، الطبعة الأولى، عام ١٩٧٨، ص ١١٣

والأعلى هو بيان أهمية التاريخ وإنقاذ الطبقة الكادحة، والهدف الأساس لهم محاربة روح القناعة والخمول والاستسلام، وأما الدين فلن يتأتى القضاء عليه إلا في ظل الحكم الحر.[١]

تصوير و انعكاس أتباع الدين في الثلاثية:

انعكست وبرزت صور أتباع الدين في الثلاثية عبر ثلاثة أنماط. ويتمثل النمط الأول منها في شخصية الشيخ متولي عبد الصمد، الذي يعتمد محبة الناس له وتقربه منهم وقبوله المساعدات المالية والعينية التي تقدم له، كما ورد في رواية بين القصرين الجزء البدائي للثلاثية: "مال الشيخ إلى الوراء.. يا لك من رجل شهم جميل المروءة يا أحمد يا ابن عبد الجواد.. فأشار السيد إلى جميل الحمزاوي ليأتي بهدية الشيخ.. فتناولها الشيخ وهو يقول: رزقك الله رزقا واسعا وغفر لك".[٢] أما أفكاره فلا تعدو أن تكون بعضا من التعاويذ والسور القصيرة وبعض المعلومات الممزوجة بالصحة والخرافات تارة، والأفكار العامية تارة أخرى، كما ورد في نفس الرواية: "اندفع الشيخ إلى المكتب وهو يتمتم الحمد لله رب العالمين، ثم رفع طرف عباءته ومسح بها على وجهه وجلس على الكرسي.. وكان يتلفع بعباءة بالية ناصلة وإن أمكنه أن يستبدل بها خيرا منها بما يجود به المحسنون، ولكنه تمسك بها لأنه فيما يقول رأى الحسين في منامه وهو يباركه فبث فيها خيرا لا يبلى، وكان إلى كراماته في قراءة الغيب والدعوات الشافية وعمل الأحجبة معروفا بالصراحة والظرف".[٣] فالشيخ متولي نراه يتخذ من الدين حرفة ينصح الناس ويعظهم ثم ينال الأجر من السكر والثياب وفاء له.

ثم يقدم الروائي نموذجا آخر متعلقا بأتباع الدين، وهو النمط الثاني يتمثل في تمسك أمينة بالدين وحبها له، فهو جزء لا ينفصل عنها. ونجدها تؤمن إيمانا مطلقا يعتريه الاعتقاد بالموروثات والتقاليد الفاسدة، فنراها تخاطب معاشر الجن قائلة: "ابعد عنا، ليس هذا مقامك، نحن قوم مسلمون موحدون.. ألا تحترم عباد الرحمن! الله بيننا وبينك فاذهب عنا مكرما".[٤] ولا يعدو إيمانها أن يتجاوز تلك الفطرة العامة التي ورثتها من أب شيخ من شيوخ الأزهر دون أي إلمام بعلم أو معرفة، فنراها تدعو ربها قائلة: "اللهم أسألك الرعاية لسيدي وأبنائي وأمي وياسين والناس جميعا مسلمين ونصارى حتى الإنجليز يا ربي وأن تخرجهم من ديارنا إكراما لفهمي الذي لا يحبهم".[٥]

وينعكس في الثلاثية نموذج حي آخر لأتباع الدين وهو النمط الثالث، يتمثل في شخصية عبد

---

[١] نجيب محفوظ، السكرية، ص ٢٩٦

[٢] نجيب محفوظ، بين القصرين، مكتبة مصر، القاهرة، ط ١٢، عام ١٩٨٣، ص ٤٥

[٣] نجيب محفوظ، بين القصرين، ص ٣٨

[٤] نجيب محفوظ، بين القصرين، ص ٨

[٥] نجيب محفوظ، بين القصرين، ص ٣٧

المنعم المنتمي إلى فكر جماعة الإخوان المسلمين، الذي يظهر في الرواية شيخا يتصدى لحل مشكلات الحياة ويعني بتقديم برامج للتغيير في الحياة، فهو ينظر إلى الدين نظرة شمولية بأنه برنامج حياة شاملا فهو ليس جمعية للتعليم والتهذيب فحسب، ولكنه كما خلقه الله دينا ودنيا وشريعة ونظام حكم.[١] فصورة فهمه للدين تنطلق من تعامله معه كحضارة وثقافة وتراث وكتعبير عن الهوية وكمصدر أساسي لفكر يريده أن يكون قادرا اليوم وفي المستقبل على حل مشكلات بلاده ومشكلات العالم من موقع الاندماج في العصر. وعبر استقراء آرائه تظهر مزايا الدين المادية، فهو يشمل جميع نواحي الحياة بمرافقها العامة مع ما يكتنزه من ميزات روحية وتعاليم شاملة لأمور الناس والحياة.

الخاتمة:

لقد تميزت نظرية الرؤية الإيديولوجية وانعكاس الصراع الإيديولوجي في ثلاثية القاهرة بالشمولية حيث صورت أتباع الدين بأنماطهم البشرية الواقعية، فظهرت صورة الشيخ متولي عبد الصمد الذي يتخذ من الدين حرفة ينصح الناس ويعظهم لينال الأجر. ثم قدمت لنا النموذج الآخر ممثلا بالسيدة أمينة التي امتزج إيمانها وحبها للدين ببعض الموروثات والتقاليد الفاسدة. ولم تغفل الثلاثية تصوير الجانب المشرق في النموذج الأخير الممثل بشخصية عبد المنعم الذي يتصدى للتغيير وحل مشكلات الحياة ليظهر بشكل إيجابي مندفعا للعمل والاندماج بالمجتمع.

وتميزت أيضا بعرضها جانبا كبيرا من الحرية في العقيدة والإيمان بالفكر، فتمتعت بتوفير جميع عناصر الحرية من خلال إيجاد مناخ مناسب من حرية الاختيار والقول والفعل والتعبير عن الأفكار بالطريقة والوقت الذي يشاء. وأبرز ما يميزها هو القدرة الواسعة على بسط أفكار كلا الفكرين أمام القارئ دون أدنى تدخل.

[١] نجيب محفوظ، السكرية، ص ١٣١

Kalikoot

Quarterly Arabic Journal
Vol.12 Issue 3, September - December 2022

The Department of Arabic
University of Calicut

Kaalikoot
11201022

Available Online

J. Sci. Res. 14 (1), 289-300 (2022)

JOURNAL OF SCIENTIFIC RESEARCH

www.banglajol.info/index.php/JSR

Identification of Naturally Occurring Carbazole Alkaloids Isolated from *Murraya koenigii* and *Glycosmis pentaphylla* by the Preparation of HPLC Fingerprint

M. Chakraborty*

Government Girls' General Degree College, 7, Mayur Bhanj Road, Kolkata-700023, West Bengal, India

Received 21 May 2021, accepted in final revised form 30 September 2021

Abstract

The plants *Murraya koenigii* and *Glycosmis pentaphylla* are rich sources of different carbazole alkaloids. A number of monomeric carbazole alkaloids with C_{13}, C_{18} and C_{23} carbon frames and a good number of dimeric carbazole alkaloids were isolated from these two plants. Scientists are still working on these two plants in search of more and more novel compounds. Many of these alkaloids have potential biological activities. Scientists have determined the structures of these compounds by detailed analysis of spectral data like UV, IR, Mass, ^{1}H NMR, and ^{13}C NMR (1D and 2D). These procedures require expertise in spectral data analysis and huge time, and also these instruments are very costly. In this paper, I report the preparation of the HPLC fingerprint of some known carbazole alkaloids. These HPLC data will be helpful in quick and unambiguous identification of the natural products.

Keywords: Carbazole alkaloids; *Murraya koenigii*; *Glycosmis pentaphylla*; HPLC fingerprint.

doi: http://dx.doi.org/10.3329/jsr.v14i1.53526 J. Sci. Res. 14 (1), 289-300 (2022)

1. Introduction

Desoky [1] has published his work on isolating several phytosterols from *Murraya exotica* using column chromatography accompanied by HPLC. Similarly, several flavonoids from fruits of *Murraya paniculata* were purified by Ferracin *et al.* [2] using reverse-phase - HPLC. The use of HPLC is limited to the separation and purification of organic molecules. However, the HPLC profile can also be used for the identification and authenticity check of the compounds. In 2021, Chang and the group reported screening of anti-lipase components of *Artemisia Argui* leaves based on spectrum-effect relationship and HPLC-MS/MS [3].

Murraya koenigii, commonly known as curry leaf tree, and Glycosmis pentaphylla, commonly known as 'toothbrush plant,' belongs to the family Rutaceae and are rich sources of carbazole alkaloids [4-6]. The monomeric and dimeric carbazole alkaloids isolated from these plants have important biological activities [7-9]. Many scientists working in this field have also prepared several derivatives of these naturally occurring

* *Corresponding author*: mumu_chak@yahoo.com

Geographical Review of India **84** (1&2) March-June - 2022, 68- 83

Spatio-Temporal Analysis of Crop Combination and Productivity in Purba Barddhaman District, West Bengal

Souvik Kundu[1] and Suradhuni Ghosh[2]

Abstract : *The state of West Bengal has obtained top position in India for the highest quantity of paddy production. Besides, undivided Barddhaman district is known as the "rice bowl" of the state for extensive cultivation of this crop. Since 2017, eastern part of the district is known as East Barddhaman district and is more productive than the West Barddhaman district in terms of agriculture. After Green Revolution in India, modern inputs, the change in crop combination, crop rotation etc. have increased the agricultural productivity of the district but not uniformly. In this context, block level changing scenario obtained from spatio - temporal analysis of crop combination, using Weaver's method and from the analysis of productivity of major crops, using Shafi's technique of Overall Yield Index of the area under present East Barddhaman district, from 2004-05 to 2016-17, is highlighted. It reveals the more improvement of peripheral C. D. blocks than those of core area in the district.*

Key Words: *Crop combination, crop rotation, green revolution, overall yield index, productivity*

Introduction

Agriculture is one of the most important primary sectors of India and is highly dependent on geographical as well as socio- economic factors. Geographical factors most importantly create a foundation for manipulated socio-economic background and affect various aspects of agricultural activity both directly and indirectly (Singh and Dhillon, 1984).

According to De (1990) the district as a whole, has a good geographical background, providing fertile alluvial soil with a complex network of various rain-fed rivers originating from Chotanagpur plateau in the west. Though the impact of a few physical constraints, such as lateritic soil, rugged terrain, scarcity of water in dry season etc. decrease from west to east in the region, the Purba Barddhaman is more engaged in agricultural pursuits than the western part (De, 1990). However, labelling the district by "rice bowl" is good for many aspects but not for all. Too much emphasis on rice production is not healthy crop culture in the long run. So, diversification in crop combination is needed for consideration. This helps for betterment of productivity by providing opportunities

1 UGC JRF. Junior Research Fellow, Department of Geography, University of Kalyani, E-mail: souvik.kgc.2012@gmail.com

2 Assistant Professor, Government Girls' General Degree College, Ekbalpur. E-mail: suradhuni23@yahoo.co.in

GEOGRAPHICAL REVIEW OF INDIA

Volume 84 Numbers 1 & 2 March & June, 2022

CONTENTS

N.B.:– Issue Nos 1&2 have been combined to update the backlog due to Covid-19 Pandemic

GEOGRAPHICAL REVIEW OF INDIA

VOL. 84, NO. 1 & 2

MARCH
&
JUNE, 2022

THE GEOGRAPHICAL SOCIETY OF INDIA
KOLKATA

Eur. Phys. J. D (2022)76:136
https://doi.org/10.1140/epjd/s10053-022-00469-5

THE EUROPEAN PHYSICAL JOURNAL D

Regular Article – Quantum Information

Revealing hidden steering nonlocality in a quantum network

Kaushiki Mukherjee[1,a], Biswajit Paul[2,b], and Soma Mandal[1,c]

[1] Department of Mathematics, Government Girls' General Degree College, Ekbalpore, Kolkata 700023, India
[2] Department of Mathematics, Balagarh Bijoykrishna Mahavidyalaya, Balagarh, Hooghly 712501, India

Received 16 April 2022 / Accepted 25 July 2022

Abstract. By combining two objects with no quantum effect one can get an object with quantum effect. Such a phenomenon, often referred to as *activation*, has been analyzed for the notion of steering nonlocality. Activation of steering nonlocality is observed for different classes of mixed entangled states in linear network scenarios. Characterization of arbitrary two qubit states, in ambit of steering activation in network scenarios has been provided in this context. Using the notion of reduced steering, instances of steerability activation are also observed in nonlinear network. Present analysis involves three measurement settings scenario (for both trusted and untrusted parties) where steering nonlocality is distinguishable from Bell nonlocality.

1 Introduction

Quantum nonlocality is an inherent feature of quantum theory [1,2]. It forms the basis of various information theoretic tasks [3–10]. Presence of entanglement is a necessary condition for generation of nonlocal correlations, though it is not sufficient due to existence of local models of some mixed entangled states [11–13]. Such type of entangled states are often referred to as *local entangled states* [14]. Procedures involving exploitation of nonlocal correlations from local entangled states are often referred to as *activation scenarios.* [15]. Till date, such activation scenarios are classified into three categories: *activation via local filtering* [16–18], *activation by tensoring* [19–23] and *activation in quantum networks.*. Any possible combination of mechanisms involved in these three types is also considered as a valid activation procedure.

In activation by quantum network scenarios, nonlocality is activated by suitable arrangement of states (different or identical copies) in a quantum network [24–28]. Speaking of the role of quantum networks in activation, entanglement swapping networks have emerged as a useful tool for activating nonlocality of states in standard Bell scenario. In present discussion, utility of these networks will be explored in ambit of activating nonlocality beyond Bell scenario.

In an entanglement swapping network, entanglement is created between two distant parties sharing no direct common past [29–31]. Apart from its fundamental importance, it is applicable in various quantum applications. This procedure is also a specific example of quantum teleportation [32].

The key point of quantum nonlocality activation (Bell-CHSH sense) in entanglement swapping scenario is that starting from entangled states (shared between interacting parties) satisfying Bell-CHSH inequality, a Bell-nonlocal state is generated between non-interacting parties at the end of the protocol. In [24,27,28] swapping procedure has been framed as a novel example of nonlocality activation in quantum mechanics. Existing research works have exploited bipartite [24,27,28] and tripartite hidden nonlocality [33] in standard Bell scenario using swapping network. Present work will be exploring the utility(if any) of entanglement swapping network for activation of quantum steering nonlocality. Owing to involvement of sequential measurements in the network scenario, we will refer activation of steering nonlocality as *revealing hidden steering nonlocality* in spirit of Popescu [16].

Motivated by famous EPR argument [1] claiming incompleteness of quantum theory, Schrodinger first gave the concept of *steering* [34,35]. A complete mathematical formalism of such a manifestation of steering was provided in [36] where they characterized *steering correlations*. Several criteria have emerged for detecting steerability of correlations generated from a given quantum state [37–47]. The correlation-based criterion given in [39], often referred to as CJWR inequality, is used here for analyzing activation of steerability. Up to two measurement settings scenario, notions of Bell-CHSH nonlocality and any steering nonlocality are indistinguishable. So, here we consider CJWR inequality for three measurement settings. Violation of this symmetric inequality guarantees steerability of the bipartite

[a] e-mail: kaushiki.wbes@gmail.com (corresponding author)
[b] e-mail: biswajitpaul4@gmail.com
[c] e-mail: soma2778@gmail.com

Published online: 04 August 2022

correlations generated in the corresponding measurement scenario. Such form of steerability is often referred to as F_3 *steerability*. Using such a symmetric inequality as a detection criterion allows interchange of the roles of the trusted and the untrusted parties in the operational interpretation of steering.

Now consider a scenario involving two entangled states (ρ_{AB}, ρ_{BC},say) such that none of them violates CJWR inequality for three settings [39]. Let ρ_{AB} and ρ_{BC} be shared between three distant parties Alice, Bob and Charlie(say) where Alice and Charlie share no direct common past. Let ρ_{AB} be shared between Alice and Bob(say), whereas ρ_{BC} be shared between Bob and Charlie. Let classical communication be allowed between two parties sharing a state. Hence, Alice and Charlie do not interact. In such a scenario, when the parties perform local operations, will it be possible to generate a steerable state between the two non-interacting parties? Affirmative result is obtained when one considers an entanglement swapping network. To be precise, for some outputs of Bob, conditional state shared between the two non-interacting parties (Alice and Charlie) turns out to be F_3 steerable.

After observing hidden steerability for some families of two qubit states in a standard entanglement swapping network (Fig. 1), a characterization of arbitrary two qubits states is given in this context. As already mentioned before, CJWR inequality (for three settings) given in [39] is used as a detection criterion. Instance of genuine activation of steering is also observed in the sense that steerable state is obtained while using unsteerable states in the swapping protocol. Arbitrary two qubit states have also been characterized in perspective of genuine activation. At this junction it should be pointed out that the steerable conditional states resulting at the end of the protocol are Bell-local in corresponding measurement scenario [48].

Exploring hidden steerability in three party entanglement swapping scheme, number of parties is then increased. Results of activation are observed in a star network configuration of entanglement swapping involving nonlinear arrangement of four parties under some suitable measurement contexts.

Rest of our work is organized as follows. In Sect. 2, we provide the motivation underlying present discussion. In Sect. 3, we provide with some mathematical preliminaries. Activation of steerability in three party network scenario is analyzed in Sect. 4. In next section, revelation of hidden steerability is then discussed when number of parties is increased in a nonlinear fashion (in Sect. 5). Phenomenon of genuine activation of steering nonlocality is discussed in Sect. 6 followed by concluding remarks in Sect. 7.

2 Motivation

Steerable correlations are used in various quantum information processing tasks such as cryptography [49–54], randomness certification [55–59], channel discrimination [60,61] and many others. So any steerable quantum state is considered a useful resource. Though pure entangled states are best candidate in this context, but these are hardly available. Consequently, mixed entangled states are used in practical situations all of which are not steerable. From practical perspectives, exploiting steerability from unsteerable entangled states thus warrants attention. In this context revelation of hidden steerability from unsteerable quantum states basically motivates present discussion. Choosing network scenario based on entanglement swapping for the activation purpose is further motivated by the fact that steerable correlations can be generated between two non-interacting parties once the states involved are subjected to suitable LOCC [62]. Such nonclassical correlations in turn may be used as a resource in network-based quantum information and communication protocols [63–65].

3 Preliminaries

3.1 Bloch vector representation

Let ϱ denotes a two qubit state shared between two parties.

$$\varrho = \frac{1}{4}(\mathbb{I}_{2\times 2} + \vec{\mathfrak{u}}.\vec{\sigma} \otimes \mathbb{I}_2 + \mathbb{I}_2 \otimes \vec{\mathfrak{v}}.\vec{\sigma} + \sum_{j_1,j_2=1}^{3} w_{j_1 j_2}\sigma_{j_1} \otimes \sigma_{j_2}), \quad (1)$$

with $\vec{\sigma} = (\sigma_1, \sigma_2, \sigma_3)$, σ_{j_k} denoting Pauli operators along three mutually perpendicular directions($j_k = 1, 2, 3$). $\vec{\mathfrak{u}} = (l_1, l_2, l_3)$ and $\vec{\mathfrak{v}} = (r_1, r_2, r_3)$ stand for the local Bloch vectors($\vec{\mathfrak{u}}, \vec{\mathfrak{v}} \in \mathbb{R}^3$) of party $\mathcal{A}$ and $\mathcal{B}$, respectively, with $|\vec{\mathfrak{u}}|, |\vec{\mathfrak{v}}| \leq 1$ and $(w_{i,j})_{3\times 3}$ denotes the correlation tensor $\mathcal{W}$(a real matrix). The components $w_{j_1 j_2}$ are given by $w_{j_1 j_2} = \mathrm{Tr}[\rho\, \sigma_{j_1} \otimes \sigma_{j_2}]$.

On applying suitable local unitary operations, the correlation tensor becomes diagonalized:

$$\varrho^{'} = \frac{1}{4}(\mathbb{I}_{2\times 2} + \vec{\mathfrak{a}}.\vec{\sigma} \otimes \mathbb{I}_2 + \mathbb{I}_2 \otimes \vec{\mathfrak{b}}.\vec{\sigma} + \sum_{j=1}^{3} \mathfrak{t}_{jj}\sigma_j \otimes \sigma_j), \quad (2)$$

Here, the correlation tensor is $T = \mathrm{diag}(t_{11}, t_{22}, t_{33})$. Under local unitary operations entanglement content of a quantum state remains invariant. Hence, steerability of ϱ and $\varrho^{'}$ remain the same.

3.2 Steering inequality

A linear steering inequality was derived in [39]. Under the assumption that both the parties sharing a bipartite state(ρ_{AB}) perform n dichotomic quantum measurements (on their respective particles), Cavalcanti, Jones, Wiseman, and Reid(CJWR) formulated a series of correlators-based inequalities [39] for checking steerability of ρ_{AB}:

$$\mathcal{F}_n(\rho_{AB},\nu)=\frac{1}{\sqrt{n}}|\sum_{l=1}^{n}\langle A_l\otimes B_l\rangle|\leq 1 \tag{3}$$

Notations used in the above inequality are detailed below:

- $\langle A_l\otimes B_l\rangle=\mathrm{Tr}(\rho_{AB}(A_l\otimes B_l))$
- $\rho_{AB}\in\mathbb{H}_{\mathbb{A}}\otimes\mathbb{H}_{\mathbb{B}}$ is any bipartite quantum state [47].
- $A_l=\hat{a}_l\cdot\overrightarrow{\sigma}$, $B_l=\hat{b}_l\cdot\overrightarrow{\sigma}$, $\hat{a}_l$, $\hat{b}_l\in\mathbb{R}^3$ denote real orthonormal vectors. A_lB_l thus denote inputs of Alice and Bob.
- $\nu=\{\hat{a}_1,\hat{a}_2,\ldots.\hat{a}_n,\hat{b}_1,\hat{b}_2,\ldots,\hat{b}_n\}$ stands for the collection of measurement directions.

In case, dimension of each of local Hilbert spaces $\mathbb{H}_{\mathbb{A}},\mathbb{H}_{\mathbb{B}}$ is 2, ρ_{AB} is given by Eq. (1). Violation of Eq. (3) guarantees both way steerability of ρ_{AB} in the sense that it is steerable from A to B and vice versa.

Steering phenomenon remaining invariant under local unitary transformations, the analytical expressions of the steering inequality remain unaltered if the simplified form [Eq. (2)] of two qubit state ρ_{AB} is considered. The analytical expression of the upper bound of corresponding inequality for 3 settings is given by [47]:

$$\begin{aligned}\mathrm{Max}_{\nu}\mathcal{F}_3(\rho_{AB},\nu)&=\sqrt{\mathrm{t}_{11}^2+\mathrm{t}_{22}^2+\mathrm{t}_{33}^2},\\&=\sqrt{\mathrm{Tr}(T^tT)}\\&=\sqrt{\mathrm{Tr}(W^tW)}\end{aligned}\tag{4}$$

where W and T denote the correlation tensor corresponding to density matrix representation of ρ_{AB} given by Eqs. (1) and (2), respectively. Last equality in Eq. (4) holds as trace of a matrix is unitary equivalent. Hence, by the linear inequality (Eq. 3) (for $n=3$), any two qubit state ρ_{AB}(shared between A and B) is both-way F_3 steerable if:

$$\mathcal{S}_{AB}=Tr[T_{AB}^TT_{AB}]>1. \tag{5}$$

Equation (5) gives only a sufficient condition detecting steerability. So if any state violates Eq. (5), the state may be steerable, but its steerability remains undetected by CJWR inequality [Eq. (3) for $n=3$]. Any state violating Eq. (5) may be referred to as F_3 unsteerable state in the sense that the state is unsteerable up to CJWR inequality for three settings.

3.3 Bell nonlocality in three settings measurement scenario

Consider a bipartite measurement scenario involving three dichotomic measurements settings (on each side). Such a scenario is often referred to as $(3,3,2,2)$ measurement scenario. CHSH is not the only possible facet inequality in $(3,3,2,2)$ scenario [66,67]. A complete list of facet inequalities of Bell polytope (for this measurement scenario) was computed in [67]. There exists only one Bell inequality inequivalent to CHSH inequality. That inequivalent facet inequality is referred to as the I_{3322} inequality [48]. Denoting local measurements of Alice and Bob as A_1,A_2,A_3 and B_1,B_2,B_3, respectively, and the outcomes of each of this measurement as ±1, I_{3322} inequality takes the form [48]:

$$\begin{aligned}&-2P_{B_1}-P_{B_2}-P_{A_1}+P_{A_1B_1}+P_{A_1B_2}+P_{A_1B_3}\\&\quad+P_{A_2B_1}+P_{A_2B_2}-P_{A_2B_3}+P_{A_3B_1}-P_{A_3B_2}\leq 0,\end{aligned}\tag{6}$$

where $\forall\, i,j=1,2,3$, $P_{B_i}=p(1|B_i)$, $P_{A_i}=p(1|A_i)$ denote marginal probabilities and $P_{A_iB_j}=p(11|A_iB_j)$ stands for the joint probability terms. In terms of these probability terms, CHSH inequality [3] takes the form:

$$-(P_{A_1}+P_{B_1}+P_{A_2B_2})+P_{A_1B_1}+P_{A_1B_2}+P_{A_2B_1}\leq 0 \tag{7}$$

There exist quantum states which violate above inequality [Eq. (6)] but satisfy CHSH inequality [Eq. (7)] and vice-versa [48]. Violation of anyone of CHSH [Eq. (7)] or I_{3322} inequality [Eq.(6)] guarantees nonlocality of corresponding correlations in $(3,3,2,2)$ scenario. Conversely, as these two are the only inequivalent facet inequalities of Bell-local polytope, so any correlation satisfying both Eqs. (6, 7) is Bell-local in $(3,3,2,2)$ scenario.

3.4 Reduced steering

Notion of reduced steering has emerged in context of manifesting multipartite steering with the help of bipartite steering [68]. Consider an n-partite quantum state $\varrho_{1,2,\ldots,n}$ shared between n parties $A_1,A_2,\ldots,A_n$ If any one of these parties A_i(say) can steer the particle of another party say $A_j(i\neq j)$ without aid of any of the remaining parties $A_k(k\neq i,j)$, then the n-partite original state $\varrho_{1,2,\ldots,n}$ is said to exhibit reduced steering. So reduced steering is one notion of steerability of $\varrho_{1,2,\ldots,n}$. Technically speaking $\varrho_{1,2,\ldots,n}$ is steerable if at least one of the bipartite reduced states $\varrho_{i,j}$ is steerable.

4 Hidden steerability in linear network

As already mentioned before, we focus on steering activation in quantum network scenario involving qubits such that steerable correlations are generated between two distant parties who do not share any direct common past. We start with an entanglement swapping network involving three parties.

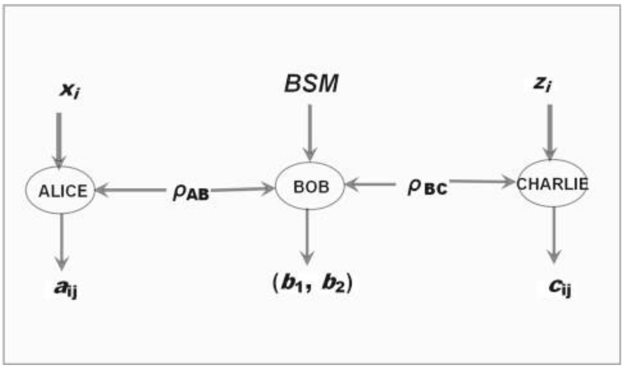

Fig. 1 A network of three parties Alice, Bob and Charlie. Alice and Bob share an entangled state ρ_{AB} and that the state shared between Bob and Charlie is ρ_{BC}. Bob performs Bell basis measurement(BSM) on his two particles and communicates the results to Alice and Charlie who then perform projective measurements on their conditional state

4.1 Linear three party network scenario

Consider a network of three parties Alice, Bob and Charlie arranged in a linear chain (see Fig. 1). Let ρ_{AB} denote the entangled state shared between Alice and Bob, whereas entangled state ρ_{BC} be shared between Bob and Charlie. So initially Alice and Charlie do not share any physical state. Let one way classical communication be allowed between parties sharing a state. To be more specific Bob can communicate to each of Alice and Charlie. Alice and Charlie are thus the two non-interacting parties.

First Bob performs joint measurement on his two qubits in the Bell basis:

$$|\phi^{\pm}\rangle = \frac{|00\rangle \pm |11\rangle}{\sqrt{2}}, |\psi^{\pm}\rangle = \frac{|01\rangle \pm |10\rangle}{\sqrt{2}}. \tag{8}$$

Let $\vec{v} = (b_1 b_2)$ denote the outcome of Bob: $(0,0), (0,1), (1,0), (1,1)$ correspond to $|\phi^+\rangle$, $|\phi^-\rangle$, $|\psi^+\rangle$ and $|\psi^-\rangle$. Bob then communicates the results to Alice and Charlie. Let $\rho_{AC}^{(b_1 b_2)}$ be the conditional state shared between Alice and Charlie when Bob obtains the outcome $\vec{b} = (b_1 b_2)$. Each of Alice and Charlie now performs one of three arbitrary projective measurements on their respective qubits. Let x_i and $z_i (i = 1, 2, 3)$ denote the measurement settings of Alice and Charlie with a_{ij} and $c_{ij} (j = 0, 1)$ denoting the binary outputs corresponding to x_i and z_j, respectively. Bipartite correlations arising from the local measurements of Alice and Charlie are then used to test CJWR inequality for three settings:

$$\frac{1}{\sqrt{3}} |\langle A_1 \otimes C_1\rangle + \langle A_2 \otimes C_2\rangle + \langle A_3 \otimes C_3\rangle| \leq 1 \tag{9}$$

Such a testing of the conditional states is required to check activation of steerability in the network. Idea of steerability activation detection is detailed below.

4.2 Steering activation in network

Phenomenon of steering activation is observed if both the initial states ρ_{AB} and ρ_{BC} are F_3 unsteerable, whereas at least one of the four conditional states $\rho_{AC}^{(00)}, \rho_{AC}^{(01)}, \rho_{AC}^{(10)}, \rho_{AC}^{(11)}$ is F_3 steerable. Precisely speaking, activation occurs if both ρ_{AB} and ρ_{BC} violate Eq. (5), whereas $\rho_{AC}^{b_1 b_2}$ satisfies the same for at least one possible pair (b_1, b_2). Any pure entangled state being F_3 steerable, no activation is possible if one or both of the initial states ρ_{AB} and ρ_{BC} possess pure entanglement. So the periphery of analyzing steerability activation encompasses only mixed entangled states. We next provide with an instance of activation observed in the network.

4.3 An instance of activation

Let us now consider the following families of two qubit states:

$$\gamma_1 = (1-p)|\varphi\rangle\langle\varphi| + p|00\rangle\langle 00| \tag{10}$$
$$\gamma_2 = (1-p)|\varphi\rangle\langle\varphi| + p|11\rangle\langle 11| \tag{11}$$

where $|\varphi\rangle = \sin\alpha|01\rangle + \cos\alpha|10\rangle$, $0 \leq \alpha \leq \frac{\pi}{4}$ and $0 \leq p \leq 1$. These class of states were used for the purpose of increasing maximally entangled fraction in an entanglement swapping network [69]. Each of these families violates Eq. (5) if:

$$2((1-p)\sin 2\alpha)^2 + (2p-1)^2 \leq 1 \tag{12}$$

Now let ρ_{AB} and ρ_{BC} be any member of the family given by γ_1 and γ_2 [Eqs. (10,11)], respectively, such that the state parameters satisfy Eq. (12). When Bob's particles get projected along $|\phi^{\pm}\rangle$, each of the conditional states $\rho_{AC}^{00}, \rho_{AC}^{01}$ is steerable [satisfying Eq. (5)] if:

$$\frac{1}{N_1}(9 - 26p + 25p^2 + 4(3 - 8p + 5p^2)\cos(2\alpha) + 3(-1+p)^2\cos(4\alpha)) > 1 \tag{13}$$

where $N_1 = 2(-1 - p + (-1+p)\cos(2\alpha))^2$. Similarly if Bob's output is $|\psi^{\pm}\rangle$, steerability of each of $\rho_{AC}^{10}, \rho_{AC}^{11}$ is guaranteed if

$$\frac{1}{N_2}(8(-1+p)^4\sin(2\alpha)^4 + N_3) > 1, \tag{14}$$

where $N_2 = (3 - 2p + 3p^2 - 4(-1+p)p\cos(2\alpha) + (-1+p)^2\cos(4\alpha))^2$ and $N_3 = (3 - 10p + 11p^2 + 4(-1+p)p\cos(2\alpha) + (-1+p)^2\cos(4\alpha))^2$. There exist state parameters (p, α) which satisfy Eqs. (12, 13). This in turn indicates that there exist states from the two families [Eqs. (10,11)] for which steerability is activated for Bob obtaining 00 or 01 output (see Fig. 2). For example, activation is observed for all members from these two families characterized by $\alpha = 0.1$, and $p \in (0.001, 0.331)$. However, in case conditional state

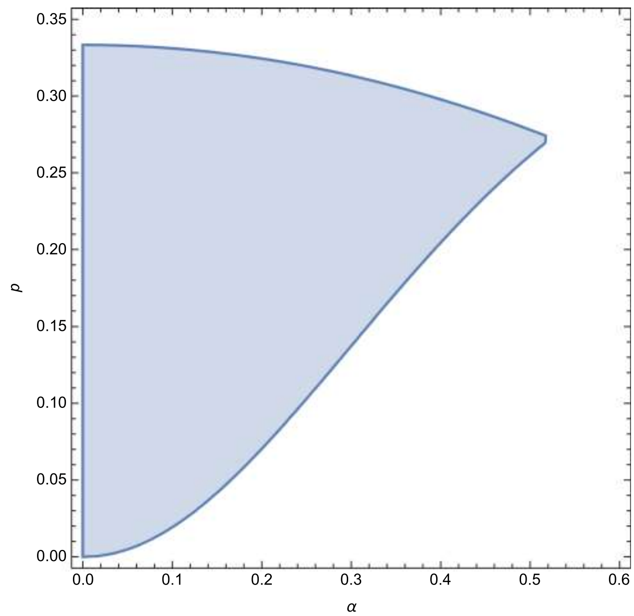

Fig. 2 Shaded region is a subspace in the parameter space (p, α) of the family of states given by Eqs. (10, 11). It indicates region of steering activation [as detected by Eq. (5)] obtained in the entanglement swapping protocol (Fig. 1) when Bob obtains either $|\phi^+\rangle$ or $|\phi^-\rangle$. It should be noted here that none of the conditional states $\rho_{AC}^{(00)}$, $\rho_{AC}^{(01)}$ is Bell nonlocal in three binary measurement settings scenario [48]

$\rho_{AC}^{(10)}$ or $\rho_{AC}^{(11)}$ is obtained, activation of steering is not observed.

To this end one may note that a conditional state satisfying anyone of Eq. (13) or Eq. (14) is Bell-local in $(3, 3, 2, 2,)$ scenario, i.e., it violates neither I_{3322} inequality [Eq. (6)] nor CHSH inequality [Eq. (7)].

4.4 Measurement settings detecting steerability

As already mentioned before, for the purpose of investigating activation, criterion [Eq. (5)] used as a sufficient criterion for detecting steerability of conditional states is a closed form of the upper bound of violation of CJWR inequality for three settings [Eq. (9)[. It may be pointed out that the two parties sharing the conditional state in the network being Alice and Charlie, in Eq. (9), observables C_i considered unlike that of B_i [used in Eq. (3)]. Now, as the closed form involves only state parameters [47], in case any state satisfies the criterion given by Eq. (5), state is steerable. But no information about measurement settings involved in detecting steerability of the state can be obtained. However, from practical view point, it is interesting to know suitable measurement settings which help in steering the states. For that, given a two qubit state, suitable measurement settings are those projective measurements (for each of the two parties) for which the state considered violates Eq. (9). $A_i = \vec{a}_i.\vec{\sigma}$ and $C_i = \vec{c}_i.\vec{\sigma}(i = 1, 2, 3)$ denote projection measurements of Alice and Charlie, respectively. As mentioned in Sect. 3, for violation of CJWR inequality [Eq. (9)], each of Alice and Charlie performs projective measurements in orthogonal directions: $\vec{a_i}.\vec{a_j} = 0 = \vec{c_i}.\vec{c_j}$, $\forall\, i \neq j$. CJWR inequality being symmetric [39], violation of Eq. (9) implies that the corresponding state is steerable from Alice to Charlie and also from Charlie to Alice. Now, for obvious reasons choice of appropriate settings is state specific. For providing some specific examples of suitable measurement settings, we next consider the instance of activation provided in Sect. 4.3.

Consider a particular member from each of the two families [Eqs. (10, 11)] characterized by $(p, \alpha) = (0.214, 0.267)$. None of these two states is steerable [up to Eq. (5)]. So none of these two states violate Eq. (9). Let these two states be used in the linear network. In case Bob gets output $(0, 0)$ or $(0, 1)$, conditional state ρ_{AC}^{00} or ρ_{AC}^{01}, shared between Alice and Charlie, violates Eq. (9) when Alice projects her particle in anyone of the three following orthogonal directions: $(0, 0, 1)$, $(0, -1, 0)$, $(-1, 0, 0)$ and Charlie's projective measurement directions are given by: $(0, 0, 1)$, $(0, 1, 0)$, and $(-1, 0, 0)$. It may be noted here that these are not the only possible directions for which violation of Eq. (9) is observed. Alternate measurement directions may also exist. However, there exists no measurement settings of Alice and Charlie for which the conditional states ρ_{AC}^{10} or ρ_{AC}^{11} violate Eq. (9). So steering activation is possible [up to Eq. (9)] in case Bob obtains output 00 or 01 only.

Getting instances of steering activation in the network, an obvious question arises next: can hidden steerability be observed for arbitrary two qubit states? This however turns out to be impossible in three measurement setting projective measurement scenario(for the non-interacting parties) when one uses Eq. (5) as steerability detection criterion [47]. We now analyze arbitrary two qubit states in this context.

4.5 Characterization of arbitrary two qubit states

Let two arbitrary states be initially considered in the swapping protocol. In density matrix formalism the states are represented as:

$$\rho_{AB} = \frac{1}{4}(\mathbb{I}_{2\times 2} + \vec{\mathfrak{u}_1}.\vec{\sigma} \otimes \mathbb{I}_2 + \mathbb{I}_2 \otimes \vec{\mathfrak{v}_1}.\vec{\sigma} + \sum_{j_1, j_2=1}^{3} w_{1j_1j_2}\sigma_{j_1} \otimes \sigma_{j_2}), \quad (15)$$

$$\rho_{BC} = \frac{1}{4}(\mathbb{I}_{2\times 2} + \vec{\mathfrak{u}_2}.\vec{\sigma} \otimes \mathbb{I}_2 + \mathbb{I}_2 \otimes \vec{\mathfrak{v}_2}.\vec{\sigma} + \sum_{j_1, j_2=1}^{3} w_{2j_1j_2}\sigma_{j_1} \otimes \sigma_{j_2}), \quad (16)$$

Steerability of states remains unhindered under local unitary operations. Let suitable local unitary operations be applied to the initial states for diagonalizing the correlation tensors:

$$\rho'_{AB} = \frac{1}{4}(\mathbb{I}_{2\times 2} + \vec{\mathfrak{a}_1}.\vec{\sigma} \otimes \mathbb{I}_2 + \mathbb{I}_2 \otimes \vec{\mathfrak{b}_1}.\vec{\sigma} + \sum_{j=1}^{3} \mathfrak{t}_{1jj}\sigma_j \otimes \sigma_j), \tag{17}$$

$$\rho'_{BC} = \frac{1}{4}(\mathbb{I}_{2\times 2} + \vec{\mathfrak{a}_2}.\vec{\sigma} \otimes \mathbb{I}_2 + \mathbb{I}_2 \otimes \vec{\mathfrak{b}_2}.\vec{\sigma} + \sum_{j=1}^{3} \mathfrak{t}_{2jj}\sigma_j \otimes \sigma_j), \tag{18}$$

Let both ρ'_{AB} and ρ'_{BC} be F_3 unsteerable, i.e., let both of them violate Eq. (5). Hence $\sum_{j=1}^{3}\sqrt{\mathfrak{t}_{1jj}^2}\leq 1$,$\sqrt{\mathfrak{t}_{2jj}^2}\leq 1$. We next characterize ρ'_{AB} and ρ'_{BC} by analyzing nature of the conditional states $\rho_{AC}^{b_1b_2}$. In this context, we provide three results each of which can be considered as a condition for no steering activation in the network. To be precise, if Bloch parameters of any initial two qubit states satisfy assumptions (see Table 1 for more details) of any of these three results then there will be no activation of F_3 steerability. Of these three results, two are proved analytically, whereas the last one is a numerical observation only. First, we give the two analytic results in form of two theorems.

Theorem 1 *If one or both the initial states [Eqs. (17, 18)] do not have any non-null local Bloch vector (see Table 1) then none of the conditional states $\rho_{AC}^{b_1b_2}$ satisfies Eq. (5).*

Proof See Appendix.A Up to the steering criterion given by Eq. (5), above result implies impossibility of steering activation in swapping network involving two qubit states whose local Bloch vectors(corresponding to both the parties) vanish under suitable local unitary operations. Maximally mixed marginals class of two qubit states has no local Bloch vector. So, activation is not possible in network involving any member from this class. So hidden steerability cannot be exploited in absence of local Bloch vectors corresponding to both the parties of a bipartite quantum state. But can the same be generated if both ρ'_{AB} and ρ'_{BC} has one non-null local Bloch vector? Following theorem provides a negative observation. □

Theorem 2 *If both the initial states ρ'_{AB} and ρ'_{BC} have only one non-null local Bloch vector, i.e., $\vec{\mathfrak{a}_1} = \vec{\mathfrak{a}_2} = \Theta$ or $\vec{\mathfrak{b}_1} = \vec{\mathfrak{b}_2} = \Theta$($\Theta$ denote null vector) then none of the conditional states $\rho_{AC}^{b_1b_2}$ satisfies Eq. (5).*

Proof of Theorem 2 This proof is exactly the same as that for Theorem 1 owing to the fact that here also $\sqrt{\mathrm{Tr}(\mathcal{V}_{b_1b_2}^T\mathcal{V}_{b_1b_2})} = \sqrt{\sum_{k=1}^{3}(t_{1kk}t_{2kk})^2}$ where $\mathcal{V}_{b_1b_2}$ denote correlation tensor of resulting conditional states $\rho_{AC}^{(b_1b_2)}$.

Table 1 Assumptions of three results (analyzed above) are enlisted here. The correlation tensor of each of the two initial states ρ'_{AB} and ρ'_{BC} remain arbitrary. Restrictions are imposed over the local Bloch parameters only

Result	Assumptions	Steerability Activation
Theorem.1	$(\vec{\mathfrak{a}_i}, \vec{\mathfrak{b}_i}) = (\Theta, \Theta)\,\forall\, i$ or $(\vec{\mathfrak{a}_i}, \vec{\mathfrak{b}_i}) = (\Theta, \Theta)$ for $i = 1$ or $(\vec{\mathfrak{a}_i}, \vec{\mathfrak{b}_i}) = (\Theta, \Theta)$ for $i = 2$	No
Theorem.2	$\vec{\mathfrak{a}_1} = \vec{\mathfrak{a}_2} = \Theta$ or $\vec{\mathfrak{b}_1} = \vec{\mathfrak{b}_2} = \Theta$	No
Numerical Observation	$\vec{\mathfrak{a}_1} = \vec{\mathfrak{b}_2} = \Theta$ or $\vec{\mathfrak{b}_1} = \vec{\mathfrak{a}_2} = \Theta$	No

Note that in Theorem 2, $\vec{\mathfrak{a}_1} = \vec{\mathfrak{a}_2} = \Theta$ or $\vec{\mathfrak{b}_1} = \vec{\mathfrak{b}_2} = \Theta$ is considered. But what if $\vec{\mathfrak{a}_1} = \vec{\mathfrak{b}_2} = \Theta$ or $\vec{\mathfrak{b}_1} = \vec{\mathfrak{a}_2} = \Theta$? Does activation occurs in such case? Numerical evidence suggests a negative response to this query:
Numerical Observation: *If $\vec{\mathfrak{a}_1} = \vec{\mathfrak{b}_2} = \Theta$ or $\vec{\mathfrak{b}_1} = \vec{\mathfrak{a}_2} = \Theta$ then none of the conditional states $\rho_{AC}^{b_1b_2}$ satisfies Eq. (5).*

Justification of this observation is based on the fact that numerical maximization of the steerability expression [Eq. (5)] corresponding to each possible conditional state $\rho_{AC}^{b_1b_2}$ gives 1 under the constraints that both the initial quantum states(ρ'_{AB}, ρ'_{BC}). Consequently, none of the conditional states satisfies Eq. (5) if none of ρ'_{AB}, ρ'_{BC} satisfies Eq. (5).

Above analysis points out the fact that for revealing hidden steerability, each of ρ'_{AB} and ρ'_{BC} should have non-null local Bloch vectors corresponding to both the parties. However that condition is also not sufficient for activation. In case, correlation tensor of any one of them is a null matrix, the state is a separable state. When such a state is considered as an initial state in the network, none of the conditional states is entangled and thereby activation of steerability becomes impossible. So, when steerability is activated in the network following are the necessary requirements:

- All of the local Bloch vectors must be non-null: $\vec{\mathfrak{a}_i} \neq \Theta$,$\vec{\mathfrak{b}_i} \neq \Theta\,\forall\, i$ and
- Both the initial states should have non-null correlation tensors.

However, the above conditions are only necessary for activation purpose but are not sufficient for the same. We next provide illustration with specific examples in support of our claim. □

4.5.1 Illustration

Let us now analyze the classes of states given by Eqs. (10, 11) in perspective of above characterization. Both the families of initial states [Eqs. (10, 11)] have local Bloch vectors: $\vec{\mathfrak{a}_1} = (0, 0, p - \cos(2\alpha)(1-p))$, $\vec{\mathfrak{b}_1} = (0, 0, p+\cos(2\alpha)(1-p))$, $\vec{\mathfrak{a}_2} = (0, 0, -p-\cos(2\alpha)(1-p))$, $\vec{\mathfrak{b}_2} = (0, 0, -p + \cos(2\alpha)(1-p))$. Local Bloch vectors are non-null for $\cos(2\alpha) \neq \pm\frac{p}{1-p}$. Correlation tensors of the states from both the families are given by $\mathrm{diag}((1-p)\sin(2\alpha), (1-p)\sin(2\alpha), 2p-1)$. Clearly activation is not observed for all family members having non-null local Blochs as well as non-null correlation tensors. For instance, consider $(p, \alpha) = (0.6, 0.6)$. Bloch parameters of corresponding states are given by:

- $\vec{\mathfrak{a}_1} = (0, 0, 0.455057))$, $\vec{\mathfrak{b}_1} = (0, 0, 0.744943)$,
- $\vec{\mathfrak{a}_2} = (0, 0, -0.455057))$, $\vec{\mathfrak{b}_2} = (0, 0, -0.744943)$,
- $\mathrm{diag}(t_{i11}, t_{i22}, t_{i33}) = \mathrm{diag}(0.372816, 0.372816, 0.2)$, $\forall\, i$

No steering activation is observed when these two states are used in the network. This in turn implies that the criteria given in 4.5 are only necessary but not sufficient to ensure activation in the network. Now, as already discussed in Sect. 4.3, there exist members from these families (see Fig. 2) which when used in the swapping network steering activation is observed.

Network scenario considered so far involved two states shared between three parties. However, will increasing length of the chain, hence increasing number of initial states be useful for the purpose of revealing hidden steerability? Though general response to this query is non-trivial, we consider a star network configuration of four parties to give instances of activation of reduced steering.

5 Nonlinear swapping network involving $n \geq 3$ states

Consider $n+1 (n \geq 3)$ number of parties $A_1, A_2, \ldots, A_n$ and B. Let n bipartite states $\varrho_i (i = 1, 2, \ldots, n)$ be shared between the parties such that ϱ_i is shared between parties B and $A_i (i = 1, 2, \ldots, n)$ (see Fig.3). B performs a joint measurement on his share of qubits from each ϱ_i and communicates outputs to the other parties $A_i (i = 1, 2, \ldots, n)$. Reduced steering of each of the conditional n-partite states is checked. To be precise, it is checked whether at least one possible bipartite reduced state of at least one of the conditional states satisfies Eq. (5). In case at least one of the conditional states has reduced steering when none of $\varrho_i (i = 1.2 \ldots, n)$ satisfies Eq. (5), activation of steerability is obtained. Activation is thus observed when one of the n parties sharing n-partite conditional state can steer the particles of another party without any assistance from remaining $n-2$ parties sharing the same.

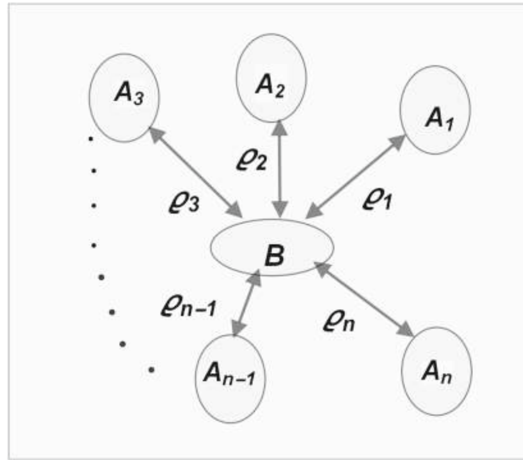

Fig. 3 Schematic Diagram of a star network. For $i = 1, 2, \ldots, n$, bipartite state ϱ_i is shared between parties B and A_i. Party B performs joint measurement on state of his n particles and communicates his output to each of $A_1, A_2, \ldots, A_n$. Reduced steering of corresponding conditional state shared between $A_1, A_2, \ldots, A_n$ is checked

Consider a specific instance of $n = 3$. Let each of $\varrho_1, \varrho_2, \varrho_3$ be a member of the family of states given by Eq.(10) with $p = p_1, p_2, p_3$ for $\varrho_1, \varrho_2, \varrho_3$, respectively. Let B perform joint measurement in the following orthonormal basis:

$$
\begin{aligned}
|\delta_1\rangle &= \frac{1}{\sqrt{3}}(|001\rangle + |100\rangle + |010\rangle)\\
|\delta_2\rangle &= \frac{1}{\sqrt{3}}(|010\rangle - |100\rangle + |000\rangle)\\
|\delta_3\rangle &= \frac{1}{\sqrt{3}}(-|010\rangle + |001\rangle + |000\rangle)\\
|\delta_4\rangle &= \frac{1}{\sqrt{3}}(|100\rangle + |000\rangle - |001\rangle)\\
|\delta_5\rangle &= \frac{1}{\sqrt{3}}(|101\rangle + |110\rangle + |011\rangle)\\
|\delta_6\rangle &= \frac{1}{\sqrt{3}}(|110\rangle - |101\rangle + |111\rangle)\\
|\delta_7\rangle &= \frac{1}{\sqrt{3}}(-|110\rangle + |111\rangle + |011\rangle)\\
|\delta_8\rangle &= \frac{1}{\sqrt{3}}(|111\rangle + |101\rangle - |011\rangle) \qquad (19)
\end{aligned}
$$

When B's particles get projected along δ_j, let $\rho^{(j)} (j = 1, \ldots, 8)$ denote the conditional state shared between A_1, A_2, A_3. Reduced steering of each of the conditional states is checked in terms of the steering inequality given by Eq. (5). Now, let all three initial states $\varrho_1, \varrho_2, \varrho_3$ violate Eq. (5). When B's state gets projected along any one of $\delta_1, \delta_6, \delta_7, \delta_8$ [Eq. (19)], for some state parameters (p, α), each of corresponding condi-

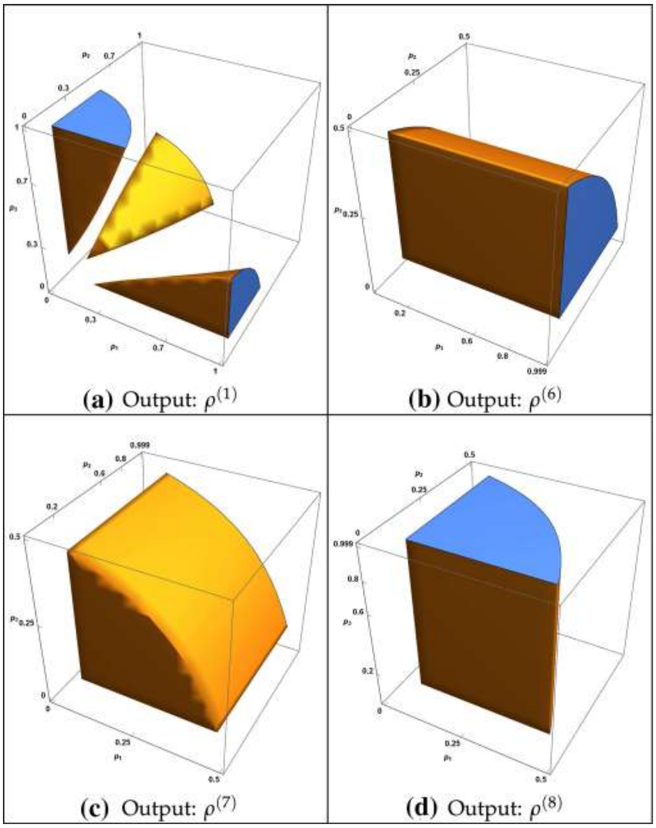

Fig. 4 Shaded region in each of four sub figures in the grid gives the steering activation region obtained stochastically depending on the different possible outputs of party B's measurement in orthonormal basis [Eq. (19)]. Here, the star network scenario (Fig. 3) involves three non-identical states from the class given by Eq. (10) for $\alpha = 0.2$. Starting from the top row and moving from left to right, shaded regions indicates reduced steering activation when B's particles get projected along $\delta_1, \delta_6, \delta_7$ and δ_8, respectively

tional states has reduced steering. Region of activation is thus observed (see Fig. 4). Some particular instances of activation are enlisted in Table 2. At this point it should be pointed out that none of the reduced states corresponding to the conditional states violates neither I_{3322} inequality [Eq. (6)] nor CHSH inequality [Eq. (7)] and hence are Bell local (in $(3, 3, 2, 2)$ scenario).

6 Genuine activation of steerability

Most of the research works in the field of activation scenarios analyze activation of nonclassicality of quantum states with respect to any specific detection criterion of the nonclassical feature considered. To be precise, let $\mathcal{C}$ denote a detection criterion for a specific notion of quantum nonclassicality. Activation is said to be observed in any protocol if using one or more quantum states(or identical copies of the same state), none of which satisfies $\mathcal{C}$, another quantum state is generated(at the end of the protocol) that satisfies $\mathcal{C}$. Using detection criterion of $\mathcal{F}_3$ steerability [39,47], so far we have obtained various cases of steering activation in both linear and nonlinear quantum networks. But quite obviously such a trend of activation analysis is criterion specific and in general can be referred to as *activation of $\mathcal{F}_3$ steerability.* But here we approach to explore activation beyond the periphery of criterion specification. We refer to such activation as *genuine activation of steerability.*

Table 2 Some specific values of state parameters are enlisted here for which stochastic steering activation(in terms of reduced steering) is observed in nonlinear network (Fig. 3)

State	p_1	p_2	Range of p_3
$\rho^{(1)}$	0.08	0.075	$(0.2, 1]$
$\rho^{(6)}$	0.08	0.075	$(0.071, 0.467]$
$\rho^{(7)}$	0.08	0.075	$(0, 071, 0.465]$
$\rho^{(8)}$	0.08	0.075	$(0.2, 1)$

To be more precise, for $\alpha = 0.2$, other parameters p_1, p_2, p_3 are specified for the three non-identical states from the class given by Eq. (10). First column in the table gives the conditional state corresponding to which activation is observed

Let us consider the linear chain of three parties (Fig. 1). For genuine activation we use states which satisfy some criterion of unsteerability and then explore $\mathcal{F}_3$ steerability of the conditional states resulting due to Bell basis measurement(BSM) by the intermediate party(Bob) in the protocol. Genuine activation of steerability occurs in case at least one of $\rho_{AC}^{b_1 b_2}$ satisfies Eq. (5). In [70], the authors proposed an asymmetric sufficient criterion of bipartite unsteerability.

Let ρ_{AB} be any two qubit state shared between Alice and Bob(say). In density matrix formalism ρ_{AB} is then provided by Eq. (1). Consider a positive, invertible linear map Λ, whose action on ρ_{AB} is given by [70]:

$$\mathbb{I}_2 \otimes \Lambda(\rho_{AB}) = \mathbb{I}_2 \otimes \rho_B^{-1} \rho_{AB} \mathbb{I}_2 \otimes \rho_B^{-1}, \qquad (20)$$

where $\mathbb{I}_2$ is 2×2 identity matrix in Hilbert space associated with 1^{st} party and $\rho_B = \mathrm{Tr}_A(\rho_{AB})$. Let $\rho_{AB}^{(1)}$ denote the state density matrix obtained after applying the above map to ρ_{AB}. Local Bloch vector corresponding to 2^{nd} party(Bob) of $\rho_{AB}^{(1)}$ becomes a null vector [70]:

$$\rho_{AB}^{(1)} = \frac{1}{4}(\mathbb{I}_{2\times 2} + \vec{u'}.\vec{\sigma} \otimes \mathbb{I}_2 + \sum_{j_1, j_2 = 1}^{3} w'_{j_1 j_2} \sigma_{j_1} \otimes \sigma_{j_2}), \qquad (21)$$

On further application of local unitary operations to diagonalize correlation tensor, $\rho^{'}_{AB}$ ultimately becomes:

$$\rho^{(2)}_{AB} = \frac{1}{4}(\mathbb{I}_{2\times 2} + \vec{\mathfrak{u}}^{''}.\vec{\sigma}\otimes\mathbb{I}_2 + \sum_{j=1}^{3} w^{''}_{jj}\sigma_j\otimes\sigma_j), \tag{22}$$

$\rho^{(2)}_{AB}$ [Eq. (22)] is referred to as the *canonical form* of ρ_{AB} in [70] where the authors argued that ρ_{AB} will be unsteerable if and only if $\rho^{(2)}_{AB}$ is unsteerable. They showed that ρ_{AB} is unsteerable from Alice to Bob if [70]:

$$\mathrm{Max}_{\hat{x}}((\vec{\mathfrak{a}}.\hat{x})^2 + 2||\mathcal{W}^{''}\hat{x}||) \leq 1 \tag{23}$$

where $\hat{x}$ is any unit vector indicating measurement direction, $\mathcal{W}^{''}$ denotes the correlation tensor of $\rho^{''}_{AB}$ and $||.||$ denotes Euclidean norm.

For our purpose we consider the unsteerability criterion given by Eq. (23). Below, we characterize arbitrary two qubit states in ambit of genuine activation of steerability.

6.1 Characterizing two qubit states

Let ρ_{AB} and ρ_{BC} [Eqs. (15, 16)] denote two arbitrary two qubit states used in the network. It turns out that local Bloch vector corresponding to first party of the initial states play a significant role in determining possibility of genuine activation of steering in the network. Next we give two results. While one of those is provided with an analytical proof, analysis of the other one relies on numerical optimization. We first state the analytical result.

Theorem 3 *If canonical forms of both the initial states ρ_{AB} and ρ_{BC} [Eqs. (15, 16)] satisfy the unsteerability criterion [Eq. (23)], then genuine activation of steerability is impossible if both of them have null local Bloch vector corresponding to first party, i.e., $\vec{u_1}, \vec{u_2} = \Theta$.*

Proof See appendix. Genuine activation being impossible in case both $\vec{u_1}, \vec{u_2}$ are null vectors, an obvious question arises whether it is possible in case at least one of $\vec{u_1}, \vec{u_2} \neq \Theta$. We provide next result in this context. As numerical procedure is involved in corresponding calculations(see Appendix C), our next result will be considered as a numerical observation only.

Numerical Observation: *If canonical forms of both ρ_{AB} and ρ_{BC}* [Eqs. (15, 16)] *satisfy the unsteerability criterion* [Eq. (23)], *then genuine activation of steerability is impossible if any one of ρ_{AB} or ρ_{BC} has null local Bloch vector corresponding to first party, i.e., at least one of $\vec{u_1}, \vec{u_2} = \Theta$.* Justification of this observation is given in Appendix C Clearly, the above two results, combined together provide a necessary criterion for genuine activation of steerability: *When canonical forms of both the initial states satisfy Eq. (23), if steering is genuinely activated in the network then both the initial states must have non-null local Bloch vectors corresponding to first party, i.e., $\vec{u_1} \neq \Theta$, $\vec{u_2} \neq \Theta$.* We next provide with examples in this context. □

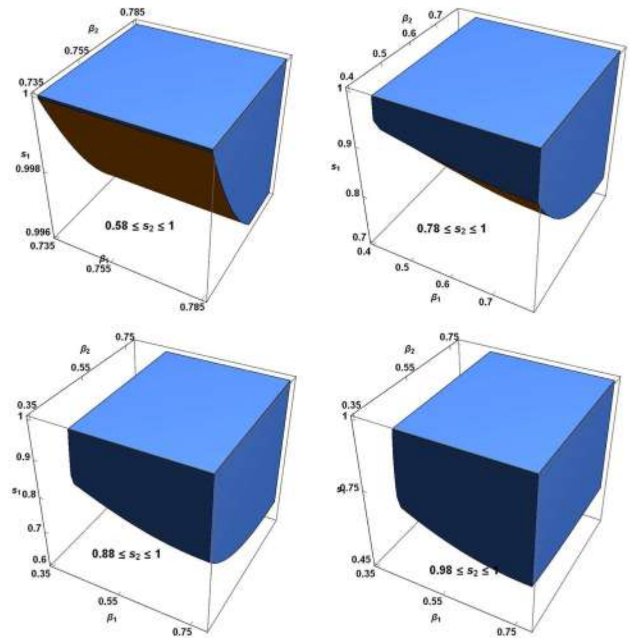

Fig. 5 Shaded regions in the sub figures give region of genuine activation of steerability for different ranges of state parameter s_2. None of the steerable conditional states obtained in the protocol is Bell nonlocal in $(3, 3, 2, 2)$ measurement scenario

6.2 Examples

Consider a family of states [70]:

$$\Omega = s|\chi\rangle\langle\chi| + (1-s)\Omega^1 \otimes \frac{\mathbb{I}_2}{2}, \tag{24}$$

where $|\chi\rangle = \cos(\beta)|00\rangle + \sin(\beta)|11\rangle$, $0 \leq s \leq 1$, $\mathbb{I}_2$ is $2x2$ identity matrix in Hilbert space associated with 2^{nd} party and Ω^1 is the reduced state of first party obtained by tracing out second party from $|\chi\rangle\langle\chi|$, i.e., $\Omega^1 = \cos^2(\beta)|0\rangle\langle 0| + \sin^2(\beta)|1\rangle\langle 1|$. For $\beta \neq \frac{\pi}{4}$, any member from this class has non-null local Bloch vector corresponding to first party:$(0, 0, \cos(2\beta))$. Canonical form [Eq. (22)] of any member of this class satisfies Eq. (23) if [70]:

$$\cos^2(2\beta) \geq \frac{2s-1}{(2-s)s^3}. \tag{25}$$

Let two non-identical members Ω_1 and Ω_2 from this class [Eq. (24)] be used in the entanglement swapping protocol (Fig. 1). Let (β_1, s_1) and (β_2, s_2) be state parameters of Ω_1 and Ω_2, respectively. Let both Ω_1 and Ω_2 be unsteerable. Now, for some values of the state parameters, the conditional states generated in the protocol turn out to be steerable (see Fig. 5) as they satisfy Eq. (5). Range of parameter s_2(for some fixed value of other three parameters (β_1, β_2, s_1)) for which genuine activation occurs, is provided in Table 3.

Now, as discussed above, the criterion of both the initial unsteerable states having non-null local Bloch vector(corresponding to first party) is necessary for

Table 3 For some specific values of parameters (β_1, β_2, s_1), of Ω_1, Ω_2 range of steerability activation other parameter s_2 is specified

State	β_1	β_2	s_1	Range of s_2
ρ_{AC}^{00}	0.75	0.76	0.99	$[0.58, 1]$
ρ_{AC}^{01}	0.65	0.6	0.97	$[0.78, 1]$
ρ_{AC}^{10}	0.55	0.55	0.9	$[0.88, 1]$
ρ_{AC}^{11}	0.6	0.55	0.8	$[0.98, 1]$

First column specifies the conditional state corresponding to which activation is observed

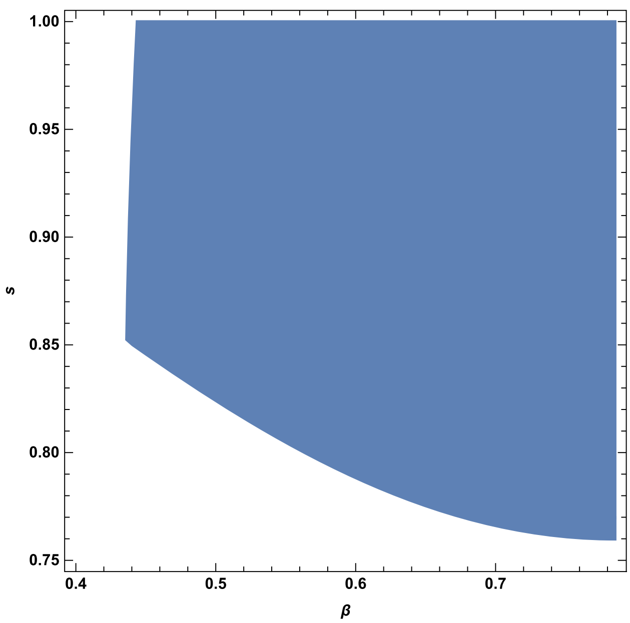

Fig. 6 Genuine activation region obtained for any possible conditional state when two identical copies of a state from Ω class are used in the network

genuine activation. The criterion however turns out to be insufficient for the same. We next provide an example in support of our claim. Consider two distinct members Ω_3, Ω_4 from the family of states given by Eq. (24) corresponding to the parameters: $(\beta_3, s_3) = (0.1, 0.7)$ and $(\beta_4, s_4) = (0.3, 0.59)$. Local Bloch vectors(corresponding to first party) of Ω_3 and Ω_4 are $(0, 0, 0.980067)$ and $(0, 0, 0.825336)$, respectively. Both of Ω_3 and Ω_4 satisfy the unsteerability criterion given by Eq. (25). These two states(in their canonical forms) are now used in the tripartite linear network. Bloch matrix representations of each of the conditional states are enlisted in Table 6(see Appendix D). Unsteerability criterion [Eq. (23)] is then tested for each of these conditional states. The optimal value(obtained numerically) in the maximization problem involved in Eq. (23) turns out to be less than unity for each of the conditional states (Table 6). Hence, all the conditional states are unsteerable. Consequently no genuine activation of steering is observed in the network using Ω_3 and Ω_4.

It may be noted that genuine activation occurs for any possible output of Bob when two identical copies of same state from this class are used in the network (see Fig.6). For instance, when two identical copies of Ω_1 for $\beta_1 = 0.7$ are considered as initial states, steerability is activated genuinely for $s_1 \in (0.77, 1]$.

7 Discussions

In different information processing tasks, involving steerable correlations, better efficiency of the related protocols(compared to their classical counterparts) basically rely upon quantum entanglement. Though pure entanglement is the most suitable candidate, but owing to environmental effects, mixed entanglement is used in practical scenarios. In this context, any steerable mixed entangled state is considered to be useful. In case it fails to generate steerable correlations, it will be interesting to exploit its steerability(if any) by subjecting to suitable sequence of measurements. Entanglement swapping protocol turns out to be an useful tool in this perspective. Let us consider the two families of states given by Eqs. (10, 11). Both of them are noisy versions of pure entangled states φ. To be more specific, these families are obtained via amplitude damping of φ [71]. As already discussed above, steering activation is obtained via entanglement swapping protocol for some members from these two families. This in turn point out that entanglement swapping protocol is useful in exploiting steerability from unsteerable [up to the steering criteria given by Eq. (5)] members from these two families. All such discussions in turn point out the utility of steerability activation in network scenarios from practical viewpoint. Characterization of arbitrary two qubits states will thus be helpful in exploiting utility of any given two qubit state in the ambit of steering activation [up to Eq. (5)]. That steerability of depolarized noisy versions of pure entangled states cannot be activated (in approach considered here) is a direct consequence of such characterization owing to the fact that this class of noisy states has no local Bloch vector. Apart from revealing hidden steerability, it will be interesting to explore whether the activation protocols can be implemented in any information processing task involving network scenario so as to render better results.

In [72], the authors have shown that if a two qubit state is $\mathcal{F}_3$ steerable, i.e., satisfies Eq. (5), then it is useful for teleportation. This in turn points out the utility of the activation networks discussed here in perspective of information theoretic tasks. To be more precise, consider, for example, the tripartite linear network (Fig. 1). Both the initial states ρ_{AB}, ρ_{BC} used in the network violates Eq. (5). So $\rho_{AB}(\rho_{BC})$ cannot be used to teleport qubit from Alice to Bob (from Bob to Charlie). Now, if steerability is activated in the network stochastically, resulting conditional state can be used for the purpose of teleportation. In case, activation occurs for all possible outputs of Bob, any of the four conditional states turns out to be useful in teleportation protocol.

Now our analysis of activation in network scenarios is criterion specific and we have just provided partial characterization of two qubit state space in context of genuine activation of steerability. The unsteerability criterion [70] involves maximization over arbitrary measurement directions [Eq. (23)]. Deriving closed form of this criterion, genuine activation of steerability can be analyzed further. In star network scenario choice of the specific orthonormal basis [Eq. (19)] for joint measurement by the central party(B) served our purpose to show that increasing number of states nonlinearly can yield better results compared to the standard three party network scenario (Fig. 1). Also such activation scenario is significant as hidden steerability is revealed when at least one of the n parties sharing n-partite conditional state can steer the particles of another party without co-operation from remaining $n-2$ parties. Further analysis of such form of steerability activation(via notion of reduced steering) using more general measurement settings of the central party B will be a potential direction of future research. It will also be interesting to analyze a scheme of m copies of bipartite states arranged in a linear chain where activation occurs only after projection on any of $n < m$ copies.

In [73], the authors introduced notion of network steering and network local hidden state (NLHS) models in networks involving independent sources. They have provided with no-go results for network steering in a large class of network scenarios, by explicitly constructing NLHS models. In course of their analysis they have given an instance of both way steering activation using family of Doubly-Erased Werner (DEW) states [73]. Activation phenomenon considered there did not rely on testing any detection criterion in form of steering inequality. So from that perspective, the activation example [73] is comparable with that of genuine steering activation in our work. Characterization of two qubit state space based on genuine activation of steering discussed in Sect. 6.1 thus encompasses a broader class of steering activation results compared to a specific example of activation [73]. To this end one may note that for analysis made there, authors considered not only unsteerability but also separability of the states distributed by the sources. Following that approach, incorporating entanglement content of initial unsteerable states to explore genuine activation of steering will be an interesting direction of future research.

Data Availability Statement This manuscript has no associated data or the data will not be deposited. [Authors comment: The manuscript has no data associated with it].

Appendix A

Proof of Theorem 1 Both ρ'_{AB} [Eq. (17)] and ρ'_{BC} [Eq.(18)] violate Eq. (5). Hence, $\sum_{j=1}^{3}\sqrt{\mathfrak{t}^2_{1jj}}, \sqrt{\mathfrak{t}^2_{2jj}} \leq 1$ which imply that $|\mathfrak{t}_{kjj}| \leq 1, \forall k = 1,2$ and $j = 1,2,3$. Let $\mathcal{V}_{b_1b_2}$ denote the correlation tensor of conditional state $\rho_{AC}^{(b_1b_2)}$. Now, two cases are considered: either one or both the parties have no non-null local Bloch vectors. In both the cases, $\mathrm{Tr}(\mathcal{V}^T_{b_1b_2}\mathcal{V}_{b_1b_2}) = \sum_{k=1}^{3}(t_{1kk}t_{2kk})^2$, $\forall b_1, b_2 = 0,1$. Hence, for each of $\mathcal{V}_{b_1b_2}$, $\sqrt{\mathrm{Tr}(\mathcal{V}^T_{b_1b_2}\mathcal{V}_{b_1b_2})}$ takes the form:

$$\begin{aligned}\sqrt{\mathrm{Tr}(\mathcal{V}^T_{b_1b_2}\mathcal{V}_{b_1b_2})} &= \sqrt{\sum_{k=1}^{3}(t_{1kk}t_{2kk})^2}\\ &\leq \sqrt{\sqrt{\sum_{k=1}^{3}t^4_{1kk}}\cdot\sqrt{\sum_{k=1}^{3}t^4_{2kk}}}\\ &\leq \sqrt{\sqrt{\sum_{k=1}^{3}t^2_{1kk}}\cdot\sqrt{\sum_{k=1}^{3}t^2_{2kk}}}\\ &\leq 1.\end{aligned} \tag{26}$$

The second inequality holds as $|\mathfrak{t}_{kjj}| \leq 1, \forall k = 1,2$ and $j = 1,2,3$ and the last is due to the fact that none of the initial states satisfies Eq. (5). □

Appendix B

Proof of Theorem 3 Here, $\vec{u_1} = \vec{u_2} = \Theta$. ρ_{AB} and ρ_{BC} thus have the form:

$$\rho_{AB} = \frac{1}{4}(\mathbb{I}_{2\times2} + \mathbb{I}_2 \otimes \vec{\mathfrak{v}_1}.\vec{\sigma} + \sum_{j_1,j_2=1}^{3} w_{1j_1j_2}\sigma_{j_1}\otimes\sigma_{j_2}),$$

$$\rho_{BC} = \frac{1}{4}(\mathbb{I}_{2\times2} + \mathbb{I}_2 \otimes \vec{\mathfrak{v}_2}.\vec{\sigma} + \sum_{j_1,j_2=1}^{3} w_{2j_1j_2}\sigma_{j_1}\otimes\sigma_{j_2}),$$

Let Λ [Eq. (20)] be applied on both ρ_{AB} and ρ_{BC} followed by local unitary operations(to diagonalize the correlation tensors). Let $\rho^{(2)}_{AB}$ and $\rho^{(2)}_{BC}$ denote the respective canonical forms [Eq. (22)] of ρ_{AB} and ρ_{BC} [70]:

$$\rho^{(2)}_{AB} = \frac{1}{4}(\mathbb{I}_{2\times2} + \sum_{j=1}^{3} w''_{1jj}\sigma_j\otimes\sigma_j), \tag{27}$$

$$\rho^{(2)}_{BC} = \frac{1}{4}(\mathbb{I}_{2\times2} + \sum_{j=1}^{3} w''_{2jj}\sigma_j\otimes\sigma_j), \tag{28}$$

Now $\rho^{(2)}_{AB}$ and $\rho^{(2)}_{BC}$ both satisfy unsteerability criterion given by Eq. (23). This in turn gives:

$$\mathrm{Max}_{x_1,x_2,x_3}\sqrt{\sum_{j=1}^{3}(x_jw''_{kjj})^2} \leq \frac{1}{2}, \quad k = 1,2 \tag{29}$$

where $\hat{x} = (x_1, x_2, x_3)$ denotes a unit vector. □

We next perform maximization over $\hat{x}$ so as to obtain a closed form of the unsteerability criterion in terms of elements of correlation tensors of the initial states $\rho^{(2)}_{AB}$ and $\rho^{(2)}_{BC}$. *Maximization over unit vector* $\hat{x}$: Taking $\hat{x} = (\sin(\theta)\cos(\phi), \sin(\theta)\sin(\phi), \cos(\theta))$, maximization problem in L.H.S. of Eq. (41) can be posed as:

$$\text{Max}_{\theta,\phi}\sqrt{A(\theta,\phi)} \tag{30}$$

where,

$$A(\theta,\phi) = \sin^2(\theta)(\cos^2(\phi)(w^{''}_{k11})^2 + \sin^2(\phi)(w^{''}_{k22})^2) + \cos^2(\theta)(w^{''}_{k33})^2 \tag{31}$$

Now for any $g_1, g_2 \geq 0$, $\text{Max}_{\kappa}(g_1\cos^2(\kappa) + g_2\sin^2(\kappa))$ is g_1 if $g_1 > g_2$ and g_2 when $g_2 > g_1$. This relation is used for maximizing $A(\theta,\phi)$. In order to consider all possible values of $(w^{''}_{k11})^2$, $(w^{''}_{k22})^2$ and $(w^{''}_{k33})^2$, we consider the following cases:

Case1:$(w^{''}_{k11})^2 > (w^{''}_{k22})^2$: Then $\text{Max}_{\phi}A(\theta,\phi)$ gives:

$$B(\theta) = \sin^2(\theta)(w^{''}_{k11})^2 + \cos^2(\theta)(w^{''}_{k33})^2 \tag{32}$$

Subcase1: $(w^{''}_{k11})^2 > (w^{''}_{k33})^2$, i.e., $(w^{''}_{k11})^2 = \text{Max}_{j=1,2,3}$ $(w^{''}_{kjj})^2$: Then $\text{Max}_{\theta}B(\theta) = (w^{''}_{k11})^2$. Hence,

$$\text{Max}_{\theta,\phi}\sqrt{A(\theta,\phi)} = |w^{''}_{k11}|. \tag{33}$$

Subcase2:$(w^{''}_{k11})^2 < (w^{''}_{k33})^2$, i.e., $(w^{''}_{k22})^2 < (w^{''}_{k11})^2 < (w^{''}_{k33})^2$: Then $\text{Max}_{\theta}B(\theta) = (w^{''}_{k33})^2$. Hence,

$$\text{Max}_{\theta,\phi}\sqrt{A(\theta,\phi)} = |w^{''}_{k33}|. \tag{34}$$

Case2:$(w^{''}_{k11})^2 < (w^{''}_{k22})^2$: Then $\text{Max}_{\phi}A(\theta,\phi)$ gives:

$$B(\theta) = \sin^2(\theta)(w^{''}_{k22})^2 + \cos^2(\theta)(w^{''}_{k33})^2 \tag{35}$$

Subcase1:$(w^{''}_{k22})^2 > (w^{''}_{k33})^2$, i.e., $(w^{''}_{k22})^2 = \text{Max}_{j=1,2,3}$ $(w^{''}_{kjj})^2$: Then $\text{Max}_{\theta}B(\theta) = (w^{''}_{k22})^2$. Hence,

$$\text{Max}_{\theta,\phi}\sqrt{A(\theta,\phi)} = |w^{''}_{k22}|. \tag{36}$$

Subcase2:$(w^{''}_{k22})^2 < (w^{''}_{k33})^2$, i.e., $(w^{''}_{k11})^2 < (w^{''}_{k22})^2 < (w^{''}_{k33})^2$: Then $\text{Max}_{\theta}B(\theta) = (w^{''}_{k33})^2$. Hence,

$$\text{Max}_{\theta,\phi}\sqrt{A(\theta,\phi)} = |w^{''}_{k33}|. \tag{37}$$

So, combining all cases, we get:

$$\text{Max}_{\theta,\phi}\sqrt{A(\theta,\phi)} = \text{Max}^3_{j=1}|w^{''}_{kjj}|,\ k = 1,2. \tag{38}$$

So, the unsteerability criterion [Eq. (41)] turns out to be:

$$\text{Max}_{j=1,2,3}|w^{''}_{kjj}| \leq \frac{1}{2}. \tag{39}$$

Table 4 State parameters of each of the four conditional states are specified here

State	$\vec{X}_1$	$\vec{X}_2$	T
ρ^{00}_{AC}	Θ	Θ	$\text{diag}(w^{''}_{111}w^{''}_{211}, -w^{''}_{122}w^{''}_{222}, w^{''}_{133}w^{''}_{233})$
ρ^{01}_{AC}	Θ	Θ	$\text{diag}(-w^{''}_{111}w^{''}_{211}, w^{''}_{122}w^{''}_{222}, w^{''}_{133}w^{''}_{233})$
ρ^{10}_{AC}	Θ	Θ	$\text{diag}(w^{''}_{111}w^{''}_{211}, w^{''}_{122}w^{''}_{222}, -w^{''}_{133}w^{''}_{233})$
ρ^{11}_{AC}	Θ	Θ	$\text{diag}(-w^{''}_{111}w^{''}_{211}, -w^{''}_{122}w^{''}_{222}, -w^{''}_{133}w^{''}_{233})$

$\vec{X}_1, \vec{X}_2$ denote the local Bloch vectors corresponding to first and second party, respectively, whereas T denote the correlation tensor. $\text{diag}(*,*,*)$ stands for a diagonal matrix. Clearly each of the conditional state is in its canonical form [Eq. (22)]

where $k = 1,2$ correspond to states $\rho^{(2)}_{AB}$ and $\rho^{(2)}_{BC}$, respectively. So $\rho^{(2)}_{AB}$ and $\rho^{(2)}_{BC}$ and therefore ρ_{AB} and ρ_{BC} are unsteerable. Steerability of state remaining invariant under application of linear map [Eq. (20)], considering the canonical forms $\rho^{(2)}_{AB}$ and $\rho^{(2)}_{BC}$ as the initial states used in the network. Depending on the output of BSM obtained by Bob (and result communicated to Alice and Charlie), the conditional states shared between Alice and Charlie are given by ρ^{ij}_{AC}, $i,j = 0,1$ (see Table 4). $\forall i,j$, ρ^{ij}_{AC} has null local Blochs and diagonal correlation tensor.

Hence, for each of the conditional states, L.H.S. of Eq. (23) turns out to be:

$$\text{Max}_{x_1,x_2,x_3}\sqrt{\sum_{j=1}^{3}(x_j w^{''}_{1jj}w^{''}_{2jj})^2} \tag{40}$$

Following the same procedure of maximization as above, the optimal expression of the maximization problem [Eq. (40)] is given by:

$$\text{Max}_{j=1,2,3}|w^{''}_{1jj}w^{''}_{2jj}|$$

Using Eq. (39), the maximum value of Eq. (40) turns out to be $\frac{1}{4}$. Each of the four conditional states thus satisfies the unsteerability criterion [Eq. (23)]. So if both the initial states satisfy Eq. (23) and have null local Bloch vector (corresponding to first party), then none of the conditional states generated in the network is steerable. Hence genuine activation of steering does not occur. States satisfies Eq. (5).

Appendix C

Details of the numerical observation given in Sect. 6: Without loss of any generality, of two initial states, let ρ_{BC} has non-null Bloch vector corresponding to the first party, i.e., $\vec{u_1} = \Theta, \vec{u_2} \neq \Theta$. ρ_{BC} thus has the form:

$$\rho_{BC} = \frac{1}{4}(\mathbb{I}_{2\times 2} + \vec{\mathfrak{u}_2}.\vec{\sigma} \times \mathbb{I}_2 + \mathbb{I}_2 \otimes \vec{\mathfrak{v}_2}.\vec{\sigma} + \sum_{j_1,j_2=1}^{3} w_{2j_1j_2}\sigma_{j_1} \otimes \sigma_{j_2}),$$

After applying Λ [Eq. (20)] followed by local unitary operations, the canonical form $\rho_{AB}^{(2)}$ of ρ_{AB} is given by Eq. (27), whereas that of ρ_{BC} is given by:

$$\rho_{BC}^{(2)} = \frac{1}{4}(\mathbb{I}_{2\times 2} + \vec{\mathfrak{u}_2''}.\vec{\sigma} \times \mathbb{I}_2 + \sum_{j=1}^{3} w_{2jj}''\sigma_j \otimes \sigma_j), \tag{41}$$

Now $\rho_{AB}^{(2)}$ and $\rho_{BC}^{(2)}$ both satisfy unsteerability criterion given by Eq. (23). This in turn gives:

$$\mathrm{Max}_{x_1,x_2,x_3}\sqrt{\sum_{j=1}^{3}(x_j w_{1jj}'')^2} \leq \frac{1}{2} \tag{42}$$

and

$$\mathrm{Max}_{x_1,x_2,x_3}(\vec{\mathfrak{u}_2''}.\hat{x})^2 + 2\sqrt{\sum_{j=1}^{3}(x_j w_{2jj}'')^2} \leq 1 \tag{43}$$

with $\hat{x} = (x_1, x_2, x_3)$ denoting unit vector. While the closed form of Eq. (42) is given by Eq. (39) for $k = 1$, the same for Eq. (43) is hard to derive owing to the complicated form of the maximization problem involved in it. Now as $\rho_{BC}^{(2)}$ satisfies an unsteerability criterion [Eq. (43)] so it is unsteerable and consequently violates Eq. (5):

$$\sum_{j=1}^{3}(w_{2jj}'')^2 \leq 1 \tag{44}$$

As discussed above, the canonical forms $\rho_{AB}^{(2)}$ and $\rho_{BC}^{(2)}$ as the initial states used in the network. Depending on Bob's output, the conditional states shared between Alice and Charlie are given by ρ_{AC}^{ij}, $i, j = 0, 1$ (see Table 5).

Let us consider ρ_{AC}^{00}. Using state parameters (Table 5) of ρ_{AC}^{00}, L.H.S. of Eq. (23) becomes:

$$\mathrm{Max}_{x_1,x_2,x_3}((x_1\mathfrak{u}_{21}''w_{111}'' - x_2\mathfrak{u}_{22}''w_{122}'' + x_3\mathfrak{u}_{23}''w_{133}'')^2 + sqrt\sum_{j=1}^{3}(x_j w_{1jj}''w_{2jj}'')^2), \tag{45}$$

Table 5 State parameters of each of the four conditional states are specified here

State	$\vec{X}_1$	$\vec{X}_2$	T
ρ_{AC}^{00}	$(w_{111}''u_{21}'', -w_{122}''u_{22}'', w_{133}''u_{23}'')$	Θ	$\mathrm{diag}(w_{111}''w_{211}'', -w_{122}''w_{222}'', w_{133}''w_{233}'')$
ρ_{AC}^{01}	$(-w_{111}''u_{21}'', w_{122}''u_{22}'', w_{133}''u_{23}'')$	Θ	$\mathrm{diag}(-w_{111}''w_{211}'', w_{122}''w_{222}'', w_{133}''w_{233}'')$
ρ_{AC}^{10}	$(w_{111}''u_{21}'', w_{122}''u_{22}'', -w_{133}''u_{23}'')$	Θ	$\mathrm{diag}(w_{111}''w_{211}'', w_{122}''w_{222}'', -w_{133}''w_{233}'')$
ρ_{AC}^{11}	$(-w_{111}''u_{21}'', -w_{122}''u_{22}'', -w_{133}''u_{23}'')$	Θ	$\mathrm{diag}(-w_{111}''w_{211}'', -w_{122}''w_{222}'', -w_{133}''w_{233}'')$

$\vec{X}_1, \vec{X}_2$ denote the local Bloch vectors corresponding to first and second party, respectively, whereas T denote the correlation tensor. diag$(*, *, *)$ stands for a diagonal matrix. Clearly each of the conditional state is in its canonical form [Eq. (22)]

where $\mathfrak{u}_{21}'', \mathfrak{u}_{22}'', \mathfrak{u}_{23}''$ are the components of real valued vector Bloch vector $\vec{\mathfrak{u}_2''}$. In Eq. (45), maximization is to be performed over x_1, x_2, x_3, whereas the state parameters are arbitrary. Now the expression in Eq. (45) is numerically maximized over all the state parameters involved and also x_1, x_2, x_3 under the following restrictions:

- $w_{111}'' \leq \frac{1}{2}$
- $w_{122}'' \leq \frac{1}{2}$
- $w_{133}'' \leq \frac{1}{2}$
- $\sum_{j=1}^{3}(w_{2jj}'')^2 \leq 1$.

While the first three restrictions are due to the unsteerability of $\rho_{AB}^{(2)}$, i.e., given by Eq. (39) for $k = 1$, the last restriction is provided by Eq. (44)(a consequence of unsteerability of $\rho_{BC}^{(2)}$). Maximum value of the above maximization problem [Eq. (45)] turns out to be 0.75, corresponding maxima (alternate maxima exists) given by $w_{111}'' = 0.5$, $w_{122}'' = 0.454199$, $w_{133}'' = 0.46353$, $w_{211}'' = -1$, $w_{222}'' = 0$, $w_{233}'' = 0$, $\mathfrak{u}_{21}'' = 1$, $\mathfrak{u}_{22}'' = 0$, $\mathfrak{u}_{23}'' = 0$, $x_1 = 1$, $x_2 = 0$ and $x_3 = 0$. Maximum value less than 1 implies that the original maximization problem [Eq. (45)], where maximization is to be performed only over x_1, x_2, x_3(for arbitrary state parameters) under the above restrictions (resulting from unsteerability of $\rho_{AB}^{(2)}, \rho_{BC}^{(2)}$), cannot render optimal value greater than 1. Consequently conditional state ρ_{AC}^{00} satisfies the unsteerability criterion [Eq. (23)] and is therefore unsteerable. So, in case Bob's particles get projected along $|\phi^+\rangle$, genuine activation of steering does not occur in the linear network. In similar way, considering, other three conditional states, it is checked that the unsteerability criterion [Eq. (23)] is satisfied in each case. Genuine activation of steering is thus impossible for all possible outputs of Bob. Hence when one of the initial states has null local Bloch vector corresponding to first party, genuine activation of steering does not occur.

Appendix D

See Table 6.

Table 6 Bloch matrix parameters of each of the four conditional states generated in the linear swapping network using Ω_3, Ω_4 [Eq. (24)] as initial states are specified here

State	$\vec{U}$	$\vec{V}$	$\mathbf{T}$
ρ_{AC}^{00}	$(0, 0, 0.98107)$	Θ	diag$(0.0729052, -0.0729052, 0.0128697)$
ρ_{AC}^{01}	$(0, 0, 0.98107)$	Θ	diag$(-0.0729052, 00.0729052, 0.0128697)$
ρ_{AC}^{10}	$(0, 0, 0.907448)$	Θ	diag$(0.0729052, 0.0729052, 0 - 0.0128697)$
ρ_{AC}^{11}	$(0, 0, 0.907448)$	Θ	diag$(-0.0729052, -0.0729052, 0 - 0.0128697)$

$\vec{U}, \vec{V}$ denote the local Bloch vectors corresponding to first and second party, respectively, whereas $\mathbf{T}$ denote the correlation tensor. diag$(*, *, *)$ stands for a diagonal matrix. Now, for each conditional state, $\mathbf{T}$ being in diagonal form and $\vec{V} = \Theta$, for all i, j, ρ_{AC}^{ij} is in its canonical form [Eq. (22)]

References

1. A. Einstein, B. Podolsky, N. Rosen, Can quantum-mechanical description of physical reality be considered complete? Phys. Rev. **47**, 777 (1935)
2. J.S. Bell, On the Einstein Podolsky Rosen paradox. Physics **1**, 195 (1964)
3. R. Cleve, H. Buhrman, Substituting quantum entanglement for communication. Phys. Rev. A **56**, 1201 (1997)
4. D. Mayers, A. Yao, Quantum cryptography with imperfect apparatus, in *Proceedings of the 39th IEEE Symposium on Foundations of Computer Science IEEE Computer Society*, pp. 503-509, Los Alamitos (1998)
5. C. Brukner et al., Bell's inequalities and quantum communication complexity. Phys. Rev. Lett. **92**, 127901 (2004)
6. J. Barrett et al., Nonlocal correlations as an information-theoretic resource. Phys. Rev. A **71**, 022101 (2005)
7. A. Acín et al., Device-independent security of quantum cryptography against collective attacks. Phys. Rev. Lett. **98**, 230501 (2007)
8. S. Pironio et al., Random numbers certified by Bell's theorem. Nature **464**, 1021 (2010)
9. R. Colbeck, A. Kent, Private randomness expansion with untrusted devices. J. Phys. A Math. Theor. **44**, 095305 (2011)
10. J.D. Bancal, N. Gisin, Y.C. Liang, S. Pironio, Device-independent witnesses of genuine multipartite entanglement. Phys. Rev. Lett. **106**, 250404 (2011)
11. R.F. Werner, Quantum states with Einstein–Podolsky–Rosen correlations admitting a hidden-variable model. Phys. Rev. A **40**, 4277 (1989)
12. J. Barrett, Nonsequential positive-operator-valued measurements on entangled mixed states do not always violate a Bell inequality. Phys. Rev. A **65**, 042302 (2002)
13. M.L. Almeida et al., Noise robustness of the nonlocality of entangled quantum states. Phys. Rev. Lett. **99**, 040403 (2007)
14. R. Augusiak, M. Demianowicz, A. Acín, Local hidden-variable models for entangled quantum states. J. Phys. A: Math. Theor. **47**, 424002 (2014)
15. A.F. Ducuara, J. Madronero, J.H. Reina, On the activation of quantum nonlocality. Universitas Scientiarum **21**(2), 129–158 (2016)
16. S. Popescu, Bell inequalities and density matrices: Revealing "Hidden" nonlocality. Phys. Rev. Lett. **74**, 2619 (1995)
17. N. Gisin, Hidden quantum nonlocality revealed by local filters. Phys. Lett. A **210**, 151 (1996)
18. C. Palazuelos, Phys. Rev. Lett. **109**, 190401 (2011)
19. M. Navascues, T. Vertesi, Activation of nonlocal quantum resources. Phys. Rev. Lett. **106**, 060403 (2011)
20. A. Peres, Collective tests for quantum nonlocality. Phys. Rev. A **54**, 2685–2689 (1996)
21. L. Masanes, Asymptotic violation of bell inequalities and distillability. Phys. Rev. Lett. **97**, 050503 (2006)
22. L. Masanes, Y.C. Liang, A.C. Doherty, All bipartite entangled states display some hidden nonlocality. Phys. Rev. Lett. **100**, 090403 (2008)
23. Y.C. Liang, L. Masanes, D. Rosset, All entangled states display some hidden nonlocality. Phys. Rev. A **8**(6), 052115 (2012)
24. A. Sen(De), U. Sen, C. Brukner, V. Buzek, M. Zukowski, Entanglement swapping of noisy states: A kind of superadditivity in nonclassicality. Phys. Rev. A **72**, 042310 (2005)
25. D. Cavalcanti, M.L. Almeida, V. Scarani, A. Acín, Quantum networks reveal quantum nonlocality. Nat. Comms **2**, 184 (2011)
26. D. Cavalcanti, R. Rabelo, V. Scarani, Nonlocality tests enhanced by a third observer. Phys. Rev. Lett. **108**, 040402 (2012)
27. A. Wojcik, J. Modlawska, A. Grudka, M. Czechlewski, Violation of Clauser–Horne–Shimony–Holt inequality for states resulting from entanglement swapping. Phys. Lett. A **374**, 4831 (2010)
28. W. Klobus, W. Laskowski, M. Markiewicz, A. Grudka, Nonlocality activation in entanglement-swapping chains. Phys. Rev. A **86**, 020302(R) (2012)
29. M. Zukowski, A. Zeilinger, M.A. Horne, A.K. Ekert, Event-ready-detectors Bell experiment via entanglement swapping. Phys. Rev. Lett. **71**, 4287 (1993)
30. M. Zukowski, A. Zeilinger, H. Weinfurter, Entangling photons radiated by independent pulsed sources. Ann. New York Acad. Sci. **755**, 91 (1995)
31. J.W. Pan, D. Bowmeester, H. Weinfurter, A. Zeilinger, Experimental entanglement swapping: entangling photons that never interacted. Phys. Rev. Lett. **80**, 3891 (1998)

32. C.H. Bennett et al., Teleporting an unknown quantum state via dual classical and Einstein–Podolsky–Rosen channels. Phys. Rev. Lett. **70**, 1895 (1993)
33. B. Paul, K. Mukherjee, D. Sarkar, Revealing hidden genuine tripartite nonlocality. Phys. Rev. A. **94**, 052101 (2016)
34. E. Schrodinger, Discussions on probability relations between separated systems. Proc. Cambridge Philos. Soc. **31**, 555–563 (1935)
35. E. Schrodinger, Probability relations between separated systems. Proc. Camb. Phil. Soc. **32**, 446 (1936)
36. S.J. Jones, H.M. Wiseman, A.C. Doherty, Entanglement, Einstein–Podolsky–Rosen correlations, Bell nonlocality, and steering. Phys. Rev. A **76**, 052116 (2007)
37. M.D. Reid, Demonstration of the Einstein–Podolsky–Rosen paradox using nondegenerate parametric amplification. Phys. Rev. A **40**, 913 (1989)
38. Z.Y. Ou, S.F. Pereira, H.J. Kimble, K.C. Peng, Realization of the Einstein–Podolsky–Rosen paradox for continuous variables. Phys. Rev. Lett. **68**, 3663 (1992)
39. E.G. Cavalcanti, S.J. Jones, H.M. Wiseman, M.D. Reid, Experimental criteria for steering and the Einstein–Podolsky–Rosen paradox. Phys. Rev. A **80**, 032112 (2009)
40. S.P. Walborn et al., Revealing hidden Einstein–Podolsky–Rosen nonlocality. Phys. Rev. Lett. **106**, 130402 (2011)
41. M. Zukowski, A. Dutta, Z. Yin, Geometric Bell-like inequalities for steering. Phys. Rev. A **91**, 032107 (2015)
42. J. Schneeloch et al., Einstein–Podolsky–Rosen steering inequalities from entropic uncertainty relations. Phys. Rev. A **87**, 062103 (2013)
43. S. Jevtic, M.J.W. Hall, M.R. Anderson, M. Zwierz, H.M. Wiseman, Einstein–Podolsky–Rosen steering and the steering ellipsoid. J. Opt. Soc. Am. B **32**, A40 (2015)
44. F. Verstraete , *A study Of Entanglement In Quantum Information Theory*, Ph.D. Thesis, Katholieke universiteit Leuven (2002)
45. S. Jevtic, M. Puesy, D. Jenning, T. Rudolph, Quantum steering ellipsoids. Phys. Rev. Lett. **113**, 020402 (2014)
46. S.J. Jones, H.M. Wiseman, Nonlocality of a single photon: Paths to an Einstein–Podolsky–Rosen-steering experiment. Phys. Rev. A. **84**, 012110 (2011)
47. A.C.S. Costa, R.M. Angelo, Quantification of Einstein–Podolsky–Rosen steering for two-qubit states. Phys. Rev. A **93**, 020103(R) (2016)
48. D. Collins, N. Gisin, A relevant two qubit Bell inequality inequivalent to the CHSH inequality. J. Phys. A: Math. Gen. **37**, 1775–1787 (2004)
49. C. Branciard et al., One-sided device-independent quantum key distribution: Security, feasibility, and the connection with steering. Phys. Rev. A **85**, 010301(R) (2012)
50. X. Ma, N. Lutkenhaus, Improved data post-processing in quantum key distribution and application to loss thresholds in device independent QKD, 2012. Quantum Inf. Comput. **12**, 0203 (2012)
51. Y. Wang et al., Finite-key analysis for one-sided device-independent quantum key distribution. Phys. Rev. A **88**, 052322 (2013)
52. C. Zhou et al., Finite-key bound for semi-device-independent quantum key distribution. Opt. Express **25**, 16971 (2017)
53. E. Kaur, M.M. Wilde, A. Winter, Fundamental limits on key rates in device-independent quantum key distribution. New J. Phys. **22**, 023039 (2020)
54. N. Walk et al., Experimental demonstration of Gaussian protocols for one-sided device-independent quantum key distribution. Optica **3**, 634 (2016)
55. Y.Z. Law, L.P. Thinh, J.D. Bancal, V. Scarani, Quantum randomness extraction for various levels of characterization of the devices. J. Phys. A **47**, 424028 (2014)
56. E. Passaro, E.G. Cavalcanti, P. Skrzypczyk, A. Acín, Optimal randomness certification in the quantum steering and prepare-and-measure scenarios. N. J. Phys. **17**, 113010 (2015)
57. P. Skrzypczyk, D. Cavalcanti, Maximal randomness generation from steering inequality violations using Qudits. Phys. Rev. Lett. **120**, 260401 (2018)
58. F.J. Curchod et al., Unbounded randomness certification using sequences of measurements. Phys. Rev. A **95**, 020102 (2017)
59. B. Coyle, M.J. Hoban, E. Kashefi, One-sided device-independent certification of unbounded random numbers. EPTCS **273**, 14–26 (2018)
60. M. Piani, J. Watrous, Necessary and sufficient quantum information characterization of Einstein–Podolsky–Rosen steering. Phys. Rev. Lett. **114**, 060404 (2015)
61. K. Sun et al., Demonstration of Einstein–Podolsky–Rosen steering with nhanced subchannel discrimination. NPJ Quantum Inf. **4**, 12 (2018)
62. P. Horodecki, M. Horodecki, R. Horodecki, Bound entanglement can be activated. Phys. Rev. Lett. **82**, 1056–1059 (1999)
63. D. Mayers, A. Yao, in *Proceedings of the 39th IEEE Symposiumon Foundations of Computer Science* (IEEE Computer Society, p. 503. Los Alamitos CA, USA (1998)
64. A. Acín, N. Gisin, L.I. Masanes, From Bell's theorem to secure quantum key distribution. Phys. Rev. Lett. **97**, 120405 (2006)
65. N. Brunner, N. Linden, Connection between Bell nonlocality and Bayesian game theory. Nature Commun. **4**, 2057 (2013)
66. A. Garg, N.D. Mermin, Correlation inequalities and hidden variables. Phys. Rev. Lett. **49**, 1220 (1982)
67. I. Pitowsky, K. Svozil, Optimal tests of quantum nonlocality. Phys. Rev. A **64**, 014102 (2001)
68. R. Uola, A.C.S. Costa, H.C. Nguyen, O. Guhne, Quantum steering. Rev. Mod. Phys. **92**, 015001-1-015001–40 (2020)
69. J. Modlawska, A. Grudka, Increasing singlet fraction with entanglement swapping. Phys. Rev. A **78**, 032321 (2008)
70. J. Bowles, F. Hirsch, M.T. Quintino, N. Brunner, Sufficient criterion for guaranteeing that a two-qubit state is unsteerable. Phys. Rev. A **93**, 022121 (2016)
71. W. Song, M. Yang, Z.L. Cao, Sufficient criterion for guaranteeing that a two-qubit state is unsteerable. Phys. Rev. A **89**, 014303 (2014)
72. S.S. Bhattacharya et al., Absolute non-violation of a three-setting steering inequality by two-qubit states. Quantum Inf. Process **17**, 3 (2018)
73. J.D.M. Benjamin et al., Network quantum steering. Phys. Rev. Lett. **127**, 170405 (2021)

74. J.F. Clauser, M.A. Horne, A. Shimony, R.A. Holt, Proposed experiment to test local hidden-variable theories. Phys. Rev. Lett. **23**, 880 (1969)
75. L. Masanes, Y.C. Liang, A.C. Doherty, All Bipartite entangled states display some hidden nonlocality. Phys. Rev. Lett. **100**, 090403 (2008)
76. S.J. Jones, H.M. Wiseman, A.C. Doherty, Entanglement, Einstein–Podolsky–Rosen correlations, Bell nonlocality, and steering. Phys. Rev. A **76**, 052116 (2007)
77. N. Brunner, D. Cavalcanti, A. Salles, P. Skrzypczyk, Bound nonlocality and activation. Phys. Rev. Lett. **106**, 020402 (2011)
78. M. Navascues, T. Vertesi, Activation of nonlocal quantum resources. Phys. Rev. Lett. **106**, 060403 (2011)

Eur. Phys. J. D (2022)76:144
https://doi.org/10.1140/epjd/s10053-022-00478-4

THE EUROPEAN PHYSICAL JOURNAL D

Correction

Correction: Revealing hidden steering nonlocality in a quantum network

Kaushiki Mukherjee[1,a], Biswajit Paul[2,b], and Soma Mandal[3,c]

[1] Department of Mathematics, Government Girls' General Degree College, Ekbalpore, Kolkata 700023, India
[2] Department of Mathematics, Balagarh Bijoykrishna Mahavidyalaya, Balagarh, Hooghly 712501, India
[3] Department of Physics, Government Girls' General Degree College, Ekbalpore, Kolkata 700023, India

Correction:

Eur. Phys. J. D (2022) 76:136
https://doi.org/10.1140/epjd/s10053-022-00469-5

In this article the affiliation details for the author Soma Mandal were incorrectly given as 'Department of Mathematics, Government Girls' General Degree College, Ekbalpore, Kolkata 700023, India' but should have been 'Department of Physics, Government Girls' General Degree College, Ekbalpore, Kolkata 700023, India'.

The original article has been corrected.

The original article can be found online at https://doi.org/10.1140/epjd/s10053-022-00469-5.

[a] e-mail: kaushiki.wbes@gmail.com (corresponding author)
[b] e-mail: biswajitpaul4@gmail.com
[c] e-mail: soma2778@gmail.com

Ilkogretim Online - Elementary Education Online, 2021; Vol 20 (Issue 1): pp. 8827-8837
http://ilkogretim-online.org
doi: 10.17051/ilkonline.2021.01.906

Service Sector, Human Capital Accumulation And Exogenous Growth Model

Dr. Senjuti Gupta Assistant Professor in Economics (W.B.E.S) Department of Economics, Government Girls' General Degree College, Ekbalpore, Kolkata, West Bengal, India.

Abstract: The present paper analyses an external growth model in a two sector economy. The model is constructed with commodity and service sector, with the assumption that the income earned from commodity production is used for consumption and investment purposes. Investment is used here for physical capital accumulation, whereas the service good is totally consumed. The model is formed in such a manner that only skilled labours are employed in the service sector.
In this paper, we have shown that there exists a unique steady state growth path of human capital accumulation which is determined completely by external parameters. The growth rate of consumption is determined by the efficiency of technology parameter of commodity production function and commodity output elasticity of labour.

Key words: Service sector, Exogenous growth model, human capital accumulation, optimal growth path.

Introduction: In introductory part, we will write a short literature review on service sector and growth model. As the basis of increased prosperity of a nation is nothing but economic growth, the accumulation of human and physical capital, both, accelerates the rate of growth. Innovations lead to technical progress. It also plays a major role in economic growth. The accumulation of capital along with innovations raises productivity of inputs and thereby increases the potential level of output. The growth theory, developed in the 1950s and 1960s, showed that the main driving force for economic growth was accumulation of capital via. technical progress which was assumed to be exogenous. The seminal works of Solow (1956) and Swan (1956) formalised the neoclassical one sector growth model where steady-state growth equilibrium of the economy depends on aggregate capital labour ratio that is time invariant. Further, the rate of growth of output is equal to the sum of two exogenous factors: the rate of technological progress and growth rate of labour force. In the transitional phase the rate of growth varies inversely with the capital intensity of the economy leading to globally stable steady state equilibrium. In this model, the monetary and the fiscal policies can not affect rate of growth in long run.

A huge literature exists that modified the simple one sector Solow- Swan growth model and discussed different issues in the theory of economic growth. Studies by Uzawa (1961, 1963, 1965), Hahn (1965), Takayama (1963, 1965), Drandakis (1963), Inada (1963). Tobin(1965) introduces real balance effect in the savings function of the Solow (1956) model where the rate of savings was exogenously given. Cass (1965) and Koopmans (1965), following Ramsey (1928) model introduced household's inter temporal utility maximization behaviour in their model and endogenised the saving rate.

The decade following 1980's experienced the emergence of the endogenous growth theory that determines the growth rate of the economy endogenously. The pioneering literature on endogenous growth theory are mainly contributed by Lucas (1988), Romer (1986, 1990), Arrow (1962), Barro (1990), Grossman and Helpman (1991), Aghion and Howitt (1992) etc. The present dissertation titled "Service sector, skill enhancement and Exogenous Growth" deals with the issues related to service sector in the endogenous growth model along with possible policy issues.

The seminal paper of Lucas (1988) is the first theoretical literature that deals with the role of human capital accumulation on endogenous growth. The growth rate of per capita income in the Lucas (1988) model depends on the rate of growth of human capital accumulation which is determined by the labour time allocation of the individuals to acquire skill. There is effect of human capital on aggregate productivity. Lucas (1988) determined the steady state equilibrium growth rate of a competitive economy and compared it to that of the command economy. It was observed that the economic agents cannot internalize the externality in the competitive economy but the social planner can do so in the planned economy.

Uzawa (1963) constructed a model considering a perishable consumption good sector. This particular feature of the good sector in Uzawa(1963) model is almost same with one of the characteristics of service good. But Uzawa (1963) model did not consider human capital accumulation and it was basically an exogenous growth model with zero rate of growth.

There are number of papers that deal with the issue of human capital in enhancing economic growth. Some of the important papers are mentioned here. The papers by Riley (2012), Mankiw et al.(1992), Fuente and Domenech (2000), Romer(1990), Pistorius (2004), Siggel (2000, 2001), Horwitz(2005), Funke and Strulik (2000), Bundell et al.(1999), Mincer (1995), Fuente and Cicoone (2002) basically deal with the issue of human capital that boosts up economic growth.

The present paper titled 'Service sector, skill enhancement and exogenous growth model' is divided in the following sub-sections :

Section 1 will discuss about the formation of the model. Section 2 will discuss about the growth paths of the economy in this exogenous growth model. Section 3 will deal with the derivation of optimal working hours for skill enhancement.

Section 1: The model:

This section describes the basic model for the functioning of an economy under a command economic regime.

Households, Firms, and Government:

The service and commodity output production functions are as follows:
where 'y_c' and 'y_s' the flow of commodity output and service output respectively.
The commodity production function is $y_c = A_c N_1{}^{\eta} K^{1-\eta}$ 1.
And the service production function $y_s = A_s(N_2 uh)^{\beta}$ 2.
Let η and β be the commodity output elasticity of raw labour and service output elasticity of skilled labour abour respectively.
A_c measures the technological efficiency parameter for commodity production.
A_s measures the technological efficiency parameter for service production.
Following Lucas (1988) model , the accumulation of human capital is assumed to be proportional to the time allocated for education. Hence, human capital accumulation function is given by

$\frac{\dot{h}}{h} = \delta(1-u)$ 3.

Here δbe the productivity parameter in the human capital accumulation function. It is

further assumed that skilled labor allocates 'u' fraction of time to produce commodity

output. Therefore the effective skilled work force in service production is $N_2 uh$.

It is assumed that the number of labor employed in commodity sector is N_1 and number of labour employed in service sector is N_2 respectively and N be the total labour force or working population such that

$N = N_1 + N_2$ 3a.

Population grows at a constant, exogenous rate and more over we assume that each segment of the population is growing at the same rate in the following way:

$\frac{\dot{N}}{N} = \frac{\dot{N}_1}{N_1} = \frac{\dot{N}_2}{N_2} = \lambda$ 3b.

It is assumed that commodity output over aggregate consumption is accumulated as physical capital. The physical capital accumulation function is given by

$\dot{K} = y_c - Nc = y_c - (N_1 + N_2)c$ 4.

(4) can be written as

$\dot{K} = A_c N_1{}^{\eta} K^{1-\eta} - (N_1 + N_2)c$

It is also assumed that the service output is totally consumed

$y_s = sN = s(N_1 + N_2)$ 5.

This paper considers a closed economy model with two sectors namely, commodity sector and service sector. The total labour force is heterogeneous with respect to skill level: skilled labour for service sector and unskilled labour or raw labour for commodity sector. The commodity and the factor markets are characterized by perfect competition. The economy is inhabited by identical rational agents. Production technology is subject to constant returns to scale. Preferences over consumption and service streams are given by the following function where 'c' and 's' denote flow of real per capita consumption of commodity and service respectively:

$u(s,c) = \int_0^{\alpha} \{\frac{(c^{\alpha} s^{1-\alpha})^{1-\sigma} - 1}{(1-\sigma)}\} e^{-\rho t}(N_1 + N_2)dt$ 6.

Here α stands for the intensity of preference for commodity output and σdenotes the elasticity of marginal utility.

Section 2: Derivation of growth path

The objective of the economy is to maximize the value of utility defined by equation (6) subject to the constraints given by (3) and (4) in the above model.

The current value Hamiltonian can be written as,

$H = \frac{(N_1+N_2)}{(1-\sigma)}[(c^{\alpha} s^{1-\alpha})^{1-\sigma} - 1] + \theta_1[A_c N_1{}^{\eta} K^{1-\eta} - (N_1 + N_2)c] + \theta_2[\delta h(1-u)]$
7.

There are two decision variables u and c.

From (5), $y_s = s(N_1 + N_2)$

Or, $s = \frac{A_s (N_2 u h)^{\beta}}{(N_1+N_2)}$ 9.

There are two decision variables u and c.

The first order conditions are

$$\frac{dH}{dc} = 0$$

Or, $\alpha c^{\alpha(1-\sigma)-1} s^{(1-\alpha)(1-\sigma)} = \theta_1$ 8.

$$\frac{dH}{du} = 0$$

Or,

$$\frac{N}{N^{(1-\alpha)(1-\sigma)}}c^{\alpha(1-\sigma)}(A_s)^{(1-\alpha)(1-\sigma)}(N_2h)^{\beta(1-\alpha)(1-\sigma)}(1-\alpha)\beta u^{\beta(1-\alpha)(1-\sigma)-1} = \theta_2\delta h$$

10.

Taking logarithm both sides of equation (9) and differentiating w.r.t time,

$\frac{\dot{A}_s}{A_s} + \beta\frac{\dot{N}_2}{N_2} + \beta\frac{\dot{u}}{u} + \beta\frac{\dot{h}}{h} - \frac{\dot{N}}{N} = \frac{\dot{s}}{s}$ 11.

Two transversality conditions are

$$lim\, e^{-\rho t}\,\theta_1(t)K(t) = lim\, e^{-\rho t}\,\theta_2(t)h(t) = 0$$

The two equations of co-state variables

$\dot{\theta}_1 = \rho\theta_1 - \frac{dH}{dK}$ 12.

$\dot{\theta}_2 = \rho\theta_2 - \frac{dH}{dh}$ 13.

$$H = \frac{(N_1+N_2)}{(1-\sigma)}[(c^\alpha s^{1-\alpha})^{1-\sigma} - 1] + \theta_1[A_c(N_1{}^\eta K^{1-\eta}) - (N_1+N_2)c] + \theta_2[\delta h(1 - u)]$$

$\frac{dH}{dK} = \theta_1 A_c(N_1)^\eta(1-\eta)K^{-\eta}$ 14.

$$H = \frac{(N_1+N_2)}{(1-\sigma)}[c^{\alpha(1-\sigma)}\{\frac{A_s}{(N_1+N_2)}(N_2uh)^\beta\}^{(1-\alpha)(1-\sigma)} - 1] + \theta_1[A_cN_1{}^\eta K^{1-\eta} - (N_1 + N_2)c] + \theta_2\delta(1-u)$$

$\frac{dH}{dh} = (N_1 + N_2)c^{\alpha(1-\sigma)}(\frac{A_s}{N_1+N_2})^{(1-\alpha)(1-\sigma)}(N_2u)^{\beta(1-\alpha)(1-\sigma)}h^{\beta(1-\alpha)(1-\sigma)-1}\beta(1-\alpha) + \theta_2\delta(1-u)$

(15)

Putting the value of $\frac{dH}{dK}$ from (14) into (12)

$\dot{\theta}_1 = \rho\theta_1 - \theta_1 A_c(N_1)^\eta(1-\eta)K^{-\eta}$ (16)

Putting the value of $\frac{dH}{dh}$ from (15) into (13)

$\dot{\theta}_2 = \rho\theta_2 - \frac{N}{N^{(1-\alpha)(1-\sigma)}}c^{\alpha(1-\sigma)}(A_s)^{(1-\sigma)(1-\alpha)}(N_2u)^{\beta(1-\alpha)(1-\sigma)}h^{\beta(1-\alpha)(1-\sigma)-1}\beta(1-\alpha) - \theta_2\delta(1-u)$

(17)

Rewriting equation (8)

$$\alpha c^{\alpha(1-\sigma)-1}s^{(1-\alpha)(1-\sigma)} = \theta_1$$

Taking logarithm both sides and differentiating w.r.t time,

$\{\alpha(1-\sigma)-$
$1\}\frac{\dot{c}}{c}+(1-\alpha)(1-\sigma)\frac{\dot{s}}{s}=\frac{\dot{\theta}_1}{\theta_1}$ (18)

From equation (11)

$\mu_s+\beta\frac{\dot{N}_2}{N_2}+\beta\delta(1-u)-\frac{\dot{N}}{N}=\frac{\dot{s}}{s}$ (11)

or, $\mu_s+(\beta-1)\lambda+\beta\delta(1-u)-\frac{\dot{N}}{N}=\frac{\dot{s}}{s}$

Putting this value from (11) into (18)

$\{\alpha(1-\sigma)-1\}g+(1-\alpha)(1-\sigma)[\mu_s+\beta\delta(1-u)+\lambda(\beta-1)]=\frac{\dot{\theta}_1}{\theta_1}$ (19)

Here g is the growth rate of consumption

Rewriting equation (16),

$\frac{\dot{\theta}_1}{\theta_1}=\rho-A_c(N_1)^{\eta}(1-\eta)K^{-\eta}$ (21)

Substituting the above value into equation (20)

$$\rho-\frac{dy_c}{dK}=\{\alpha(1-\sigma)\}g+(1-\alpha)(1-\sigma)[\mu_s+\beta\delta(1-u)+(\beta-1)\lambda]$$

or, $\frac{dy_c}{dK}=\rho-\{\alpha(1-\sigma)\}g-(1-\alpha)(1-\sigma)[\mu_s+\beta\delta(1-u)+(\beta-1)\lambda]$

In the above equation u , g will grow at a constant rate in steady-state . So

$\frac{dy_c}{dK}$ will also grow at a constant rate in steady-state.

From the production function, $\frac{y_c}{K}=A_cN_1{}^{\eta}K^{-\eta}=\frac{1}{(1-\eta)}\cdot\frac{dy_c}{dK}$ (22)

It is obvious from the above equation that,

$\frac{y_c}{K}$ will also grow at a constant rate in steady-state $y_c=Nc+\dot{K}$

as $\frac{y_c}{K}$ is growing at a constant rate in steady-state

$$y_c=Nc+\dot{K}$$

or, $\frac{y_c}{K}=\frac{Nc}{K}+\frac{\dot{K}}{K}$

$\frac{y_c}{K}$ and $\frac{\dot{K}}{K}$ will grow at a constant rate in steady-state. So, $\frac{Nc}{K}$ must be growing constant in steady-state.

$\frac{Nc}{K}$=constant

Taking logarithm both sides and differentiating with respect to time,

$$\frac{d(\log N)}{dt}+\frac{d(\log c)}{dt}-\frac{d(\log K)}{dt}=0$$

or, $\frac{\dot{N}}{N}+\frac{\dot{c}}{c}=\frac{\dot{K}}{K}$

or, $\lambda+g=k$ (say) (23)

Here λ is the rate of growth of population and g is the growth rate of consumption.

From the production function,

$$\frac{y_c}{K} = A_c N_1{}^{\eta} K^{-\eta}$$

As, $\frac{y_c}{K}$is growing at a constant rate in steady-state, taking logarithm both sides and differentiating w.r.t time we get

$$\frac{\dot{A}_c}{A_c} + \eta\frac{\dot{N}_1}{N_1} + (-\eta)\frac{\dot{K}}{K} = 0$$

Or, $\mu_c + \eta\lambda + (-\eta)(\lambda + g) = 0$ (24)

Rewriting equation (10), $\frac{dH}{du} = 0$

$$\frac{N}{N^{(1-\alpha)(1-\sigma)}} c^{\alpha(1-\sigma)}(A_s)^{(1-\alpha)(1-\sigma)}(N_2h)^{\beta(1-\alpha)(1-\sigma)}(1-\alpha)\beta u^{\beta(1-\alpha)(1-\sigma)-1} = \theta_2\delta h$$

Or, $N^{1-(1-\alpha)(1-\sigma)} c^{\alpha(1-\sigma)}(A_s)^{(1-\alpha)(1-\sigma)}(N_2h)^{\beta(1-\alpha)(1-\sigma)}(1-\alpha)\beta u^{\beta(1-\alpha)(1-\sigma)-1} = \theta_2\delta h$ (25)

Taking logarithm both sides and differentiating w.r.t time,

$$\{1-(1-\alpha)(1-\sigma)\}\frac{\dot{N}}{N} + \alpha(1-\sigma)\frac{\dot{c}}{c} + (1-\alpha)(1-\sigma)\frac{\dot{A}_s}{A_s} + \beta(1-\alpha)(1-\sigma)\frac{\dot{N}_2}{N_2} + \beta(1-\alpha)(1-\sigma)\frac{\dot{h}}{h} + \{\beta(1-\alpha)(1-\sigma)-1\}\frac{\dot{u}}{u} = \frac{\dot{\theta}_2}{\theta_2} + \frac{\dot{h}}{h}$$

Or,

$[1 + (1-\alpha)(1-\sigma)(\beta-1)]\lambda + \alpha(1-\sigma)g + (1-\alpha)(1-\sigma)\mu_s + [\beta(1-\alpha)(1-\sigma)-1][\sigma(1-u)] = \frac{\dot{\theta}_2}{\theta_2}$ (26)

From equation (17)

$$\frac{\dot{\theta}_2}{\theta_2} = \rho - [N^{1-(1-\alpha)(1-\sigma)} c^{\alpha(1-\sigma)}(A_s)^{(1-\sigma)(1-\alpha)}(N_2u)^{\beta(1-\alpha)(1-\sigma)} h^{\beta(1-\alpha)(1-\sigma)-1}\beta(1-\alpha)]\frac{1}{\theta_2} - \delta(1-u) \qquad (27)$$

Putting the value of $\theta_2$from (25) into (27)

$\frac{\dot{\theta}_2}{\theta_2} = \rho - \delta$ (28)

Equating the value of $\frac{\dot{\theta}_2}{\theta_2}$from (26) and (28)

$$[1-(1-\alpha)(1-\sigma)(\beta-1)]\lambda + \alpha(1-\sigma)g + (1-\alpha)(1-\sigma)\mu_s + [\beta(1-\alpha)(1-\sigma)-1][\delta(1-u)] = (\rho-\delta) \qquad (29)$$

From equation (24)

$\mu_c + \eta\lambda - \eta(\lambda + g) = 0$

Or, $g = \frac{\mu_c}{\eta}$

Or, $\frac{\dot{c}}{c} = \frac{\mu_c}{\eta}$

This is the growth rate of the economy.

Thus, the growth rate of the economy is derived here, by using Hamiltonian technique of dynamic optimization.

The growth rate in this model is determined exogenously. Here, the growth rate of the economy is positively influenced by the growth rate of technological progress in commodity sector and negatively affected by commodity output elasticity of raw labour. Commodity output elasticity is the relative responsiveness of commodity output to labour.

Proposition 1: In a command economy, human capital and commodity output have a positive, unique steady-state growth rate.

Proposition 2: The growth rate of technological progress in necessary for the growth
of the economy.

Proposition 3: The growth rate of economy is inversely related with the commodity
output elasticity of labour which implies unskilled labour participation in commodity sector creates retarding influence on growth rate in this exogeneous model.

Section 3:

The number of hours, devoted by labours to acquire skill in commodity sector is derived in the following section:

Substituting the value of g into equation (29) we get

$$(\rho - \delta) = [1 + (1-\alpha)(1-\sigma)(\beta - 1)\lambda] + \alpha(1-\sigma)\frac{\mu_c}{\eta} + (1-\alpha)(1-\sigma)\mu_s + [\beta(1-\alpha)(1-\sigma) - 1]\delta$$
$$-\delta u[\beta(1-\alpha)(1-\sigma) - 1]$$

Or, $u = \frac{[1+(1-\alpha)(1-\sigma)(\beta-1)\lambda]+\alpha(1-\sigma)\frac{\mu_c}{\eta}+(1-\alpha)(1-\sigma)\mu_s+[\beta(1-\alpha)(1-\sigma)-1]\delta}{\delta[\beta(1-\alpha)(1-\sigma)-1]}$

This is the expression of the number of hours that is dedicated for human capital accumulation.

Proposition 4: The number of hours devoted for skill enhancement for commodity sector is positively related to the growth rate of technological progress for both the sectors and is negatively related to the commodity output elasticity of labour. When the relative responsiveness of commodity production to raw labour is low, the number of hours dedicated for skill accumulation increases. It is quite obvious that, as unskilled labours create a retarding influence on growth, the urge for skill generation will be increased maintain a positive growth path.

Therefore, the factors that determine the number of hours which is dedicated to form human capital is derived in the above section. We can make comparative static analysis on the other parameters also.

CONCLUSION:

This paper constructs a two-sector exogenous growth model in a closed economy. Commodity output is produced with only physical capital, whereas skilled labour is the only input used to produce service output. Steady-state growth paths are studied.

This paper simply studies the growth path of human capital accumulation as well as the economy where human capital is used only in services while physical capital is only used as an input to produce final commodities. This paper also finds the factors which will help a labour to decide how many hours to devote for skill development.

Bibliography:

Aghion, P. and Howitt P. W. (1992), "A model of growth through creative destruction", Econometrica, 60(2), 323-351.

Arrow, K. J. (1962), "The economic implications of learning by doing", Review of Economic Studies, 29(3), 155-73.

Barro, R. J, (1990), "Government spending in a simple model of endogenous growth", Journal of Political Economy, 98 (5), S103-S125.

Bundell R., Lorraine D. , Meghir C., Sianesi B. (1999) "Human Capital Investment: The Returns from Education and Training to the Individual, the Firm and the Economy", Fiscal Studies, 20(1), pp. 1-23.

Drandakis E.M.(1963), "Factor substitution in the two-sector growth model", Review of Economic Studies, 30 (2), 217-28.

Fuente D L A, Cicoone A, (2002), "Human capital in a global and knowledge-based economy", Final Report, European Commision.

Fuente D L A, Domenech A.(2000), "A Human capital in growth regressions: how much difference does data quality make? " Economic Department Working Paper No 262, Paris: OECD, 2000 (ECO / WKP (2000) 35.

Funke M., H. Strulik (2000) , "On endogenous growth with physical capital, human capital and product variety", European Economic Review 44 (2000), 491-515;

Hahn, F.H. (1965), "On two-sector growth models", Review of Economic Studies, 32(4), 339-46.

Horwitz, F. (2005) , "HR CAN Competitiveness advance". Executive Business Brief, 10, 50-52.

Inada, K. (1963), "On a two-sector model of economic growth: comments and a generalization", Review of Economic Studies, 30(2),119-127.

Koopmans, T. C. (1965), "On the concept of optimal economic growth", The Econometric Approach to Development Planning, ch 4, 225-87. North-Holland Publishing Co., Amsterdam.

Lucas, R. E (1988), "On the mechanics of economic development", Journal of Monetary Economics, 22 (1), 3-42.

Mincer J, (1995), Economic Development, Growth of Human Capital, and the Dynamics of the Wage Structure, 1994-95 Discussion Paper Series No. 744, (September), Columbia University, p.38

Pistorius, C.(2004) "The Competitiveness and innovation", Vol. 21(3)

Ramsey F.P. (1928), "A mathematical theory of saving", Economic Journal, 38(152), 543-559.

Riley G. (2012) Economic Growth - The Role of Human & Social Capital, Competition & Innovation, http://www.tutor2u.net/economics/revision notes/a2-macro-economic-growth-capital.html, Accessed April 16, 2014;
Mankiw N. G; Romer D, Weil D.N, (1992) Contribution to the Empirics of Economic Growth, The Quarterly Journal of Economics, 107(2), 407-437;

Romer, P (1990) Human capital and growth: theory and evidence, Carnegie Rochester Conference Series on Public Policy 32, 251-286;

Siggel, E. (2000), "Uganda's policy Reforms, Competitiveness and regional integration industry: A comparison with Kenya. African Economic Policy", Discussion paper 24; Washington: United States Agency for International Development: Bureau for Africa.

Siggel E. (2001), India's trade policy Reforms and Competitiveness industry in the 1980s. World Economy, pp.159-183.

Solow, R.M, (1956), “A contribution to the theory of economic growth”, Quarterly Journal of Economics, 70(1), 65-94.

Solow, R.M (2000) “Growth Theory AN EXPOSITION”, Newyork, Oxford, Oxford University Pressolos

Swan, T.W., (1956), “Economic growth and capital accumulation,” Economic Record, 32, 334-61.

Takayama A.(1963), “On a two-sector model of economic growth: A comparative statics analysis”, Review of Economic Studies, 30(2), 95-104.

Takayama, A.(1965), “On a two-sector model of economic growth with technological progress”, Review of Economic Studies, 32(3), 251-62.

Tobin, J. (1965), “Money and economic growth”, Econometrica, 33(4), 671–684.

Uzawa, H. (1961), “On a two-sector model of economic growth”, Review of Economic Studies, 29(1), 117-124.

Uzawa, H. (1963), “On a two-sector model of economic growth: II”, Review of Economic Studies, 30(2), 105-118.

Uzawa, H (1965) “Optimum technical change in an aggregative model of economic growth”, International Economic Review, 6(1), 18-31.

Ilkogretim Online - Elementary Education Online, 2021; Vol 20 (Issue 5): pp. 9282-9292
http://ilkogretim-online.org
doi: 10.17051/ilkonline.2021.05.1013

Endogenous Growth Model In A Two Sector Competitive Economy: Service Good Used As A Factor Input In Commodity Sector

Dr. Senjuti Gupta Assistant Professor in Economics (W.B.E.S) Department of Economics, Government Girls' General Degree College, Ekbalpore, Kolkata, West Bengal, India.

Abstract: This paper considers a closed economy model with two sectors namely, commodity sector and service sector. The service output is exclusively used as an intermediate input in producing commodity output. Here, in this model, an endogenous growth model is considered in which the service output is used as an intermediate good in commodity sector. Accumulation of human capital depends on the government expenditure on education sector. The government levies tax on the commodity output. In this framework, on the basis of the unique steady state growth path, where human capital accumulation works as the source of growth for all other sectors of the economy, a comparative static analysis has been done. In this particular model, we have analysed, how the share of physical capital that is engaged to the service sector is influenced by the commodity output elasticity of physical capital and service output elasticity of skilled labour.

Section 1: Introduction

The last few decades have experienced a rapid growth in the service sector, which has been reflected in an upward trend in the usage of service goods as consumption good, as well as intermediate good. There exists a substantial empirical literature dealing with the issues related to service sector. However, there are very few papers that consider service output as an intermediate good in an endogenous growth model and none of these studies considers any comparative analysis of taxation in command and market economy framework. In this model also, we assume human capital is one of the most important factor in producing service. Most of these services such as education, health, public administration, banks, computer services, recreation, communications, financial services and many others require specialized knowhow. The role of government expenditure on public resources is, to create both, human capital and physical capital, through taxation in endogenous growth models.

The aim of the present paper is to figure out a comparative static analysis on the basis of the optimal growth path in a competitive economy where service sector output is used as an input in the manufacturing sector.

There exists huge literature on intermediate goods. Few of them are mentioned here in below. The papers by **Moro (2007), Sekar et al (2015), Barua and Pant (2013), Imbruno(2012)** have discussed the matters connected to various aspects of intermediate goods in the context of closed or open economies. Seker et al (2015) have tried to develop a general equilibrium model of multi-product firms that explain the relationship between importing intermediate goods, innovation, and firm growth. This paper assumes heterogeneity in firms' efficiency levels as per the model built by Melitz (2003) and following the structural models by **Klette and Kortum (2004) and Seker (2009)**, a stochastic dynamic model of firm on industry evolution is formed. In the paper by Barua and Pant (2013), a theoretical model is built to explain the phenomenon of increasing relative wage inequality between unskilled and skilled wages, in a general equilibrium framework by incorporating intermediate goods. **Imbruno (2011)** attempts to study the impact of trade liberalization in intermediate inputs within a general equilibrium framework built by Melitz (2003), where all firms are assumed to be heterogeneous in productivity and can produce either intermediate goods or final goods under monopolistic competition.

Psarianos I. N (2002) has built an endogenous growth theory and it has been found theoretically and empirically that market economies invest very nominal amount of money in scientific and technical research and the growth rates are found to be lower than socially optimal.

Given the various models on intermediate good, we observe none except **Ishikawa (1991)** has captured service as an intermediate good in the endogenous growth.

The paper by Ishikawa (1991) has considered service as an input to produce manufacturing commodity and in this paper learning by doing in the service sector is the engine of endogenous growth. Following Ishikawa (1991) the present model assumes that service output is used as an input in the manufacturing sector that produces a malleable good used both for consumption and investment in a closed economy. Unlike Ishikawa (1991) we assume that service sector uses human capital, which is accumulated through government expenditure on education sector. Government expenditure is financed by imposing tax on manufacturing sector. We find out growth maximizing tax rate in competitive economy, where the tax is given. One of my papers **written by me and my co-authors,** Gupta et. al (2019), titled "Service good as an intermediate input and optimal government policy in an endogenous growth-model"**,** has left a few comparative static analysis. I have tried to figure out those undone analysis.

The rest of the paper is organised as follows: In section 2, the basic model is presented; In Section 3, a simplified version of the model is built where only human capital is used in service sector. The growth rates are determined in competitive economy along with the comparative static analysis and section 4 concludes.

2. The model:

This section, discusses the basic assumptions of the model and derives the growth path under competitive framework.

Section 2.1: The Households, Firms and Government

This paper considers a closed economy model with two sectors namely, commodity sector and service sector. The service output is exclusively used as an intermediate input in producing commodity output. The total labour force is homogeneous as far as skill is concerned. Identical rational agents inhabit the economy. Production technology is subject to constant returns to scale. The household sector chooses the path of per capita consumption of commodity output by maximising the integral over all future time of discounted instantaneous utility, ρ being the discount rate and σ, the elasticity of marginal utility and inverse of which is known as inter temporal elasticity of substitution. N represents the total labour force or working population.
Preferences over consumption are given by the following function where 'c' denotes flow of real per capita consumption of commodity output:

$$u(c) = \int_0^{\infty} \frac{(c^{1-\sigma} - 1)}{(1-\sigma)} e^{-\rho t} N(t)dt \qquad 1.$$

Here, we assume that the output in the commodity sector can be used for consumption or investment purposes, whereas the output in the service sector is used as a prime factor to produce commodity output.

The commodity output is produced using physical capital and service product. The service output is produced with human capital and physical capital. Both the production functions are Cobb-Douglas type. Here 'K' stands for the level of physical capital. Let α and β be the commodity output elasticity of physical capital and service output elasticity of skilled labour respectively. The commodity and service output production functions can be written as

$$y_c = A\{(1-\varphi)K\}^{\alpha} \; y_s^{1-\alpha} \qquad 2.$$

$$y_s = B(Nh)^{\beta} (\varphi K)^{1-\beta} \qquad 3.$$

Where 'y_c' and 'y_s' are the flow of commodity output and service output respectively. It is obvious that $(1-\alpha)$ measures the commodity output elasticity of service product. Similarly, $(1-\beta)$ measures the service output elasticity of physical capital. The level of population is growing at an exponential rate in the following manner:

$$N(t) = N_0 e^{nt} \qquad 4.$$

Where N_0 is the population size at initial time period. It is assumed that the initial amount of population $N_0 = 1$. Further, we assume that the general skill level of a worker is 'h'. The effective skilled labor input in commodity production is 'Nh'. Let 'φ' be the fraction of physical capital that is dedicated to the service sector. The remaining (1- φ) is engaged in producing commodity output.

It is assumed that Government spends money on working population to create human capital.

The human capital accumulation can be written as

$$\dot{h} = \eta \frac{G}{N} \qquad 5.$$

Here η be the technology parameter of human capital accumulation and G be the government expenditure on education. It is further assumed that only the commodity sector is being taxed. The tax revenue is spent as government expenditure to build human capital. Let the tax rate be τ which is levied on per unit of commodity output. The balanced budget equation can be written

$$G = T = \tau y_c \qquad 6.$$

A part of disposable income is consumed and the rest is invested to form physical capital. Hence, the physical capital accumulation function is given by

$$\dot{K} = (1-\tau) y_c - Nc \qquad 7.$$

In market economy, the households own all capital. The final product is produced by a representative firm that maximises profit. The objective of the economy is to maximize the present discounted value of utility over the infinite time horizon defined by equation (1) subject to the wealth accumulation constraint.

Section 3: Competitive Economy: The comparative static analysis

The objective of an individual consumer is to maximize utility choosing the consumption path. The current value Hamiltonian for this particular problem follows as

$$H = \frac{c^{1-\sigma} - 1}{(1-\sigma)} N(t) + \theta[(1-\tau)(rK + wNh) - cN] \qquad 8.$$

In competitive economy, a representative household chooses c, the flow of consumption. So, c is the decision variable and K is state variable, θ is the shadow price of physical capital. While solving this Hamiltonian function, tax rate τ is considered to be given as per the competitive regime.

The profit of the producers for the commodity sector and service are

$$\pi_c = p_c y_c - r(1-\varphi)K - p_s y_s \qquad 9.$$

$$\pi_s = p_s y_s - (r\varphi K) - (wNh) \qquad 10.$$

Here r is the rate of interest and w is the real wage rate, p_s is the per unit price of service output. It is assumed that the commodity output is numeraire commodity which implies that per unit price of commodity output, i.e., p_c is unity.

The output and the factor markets both are characterized by perfect competition. Hence, equating the value of the marginal product of each factor input to its return and using profit maximisation condition we get the following expressions of r, w and p_s

$$r = A\alpha(1-\varphi)^{\alpha-1}B^{1-\alpha}k^{-\beta(1-\alpha)}\varphi^{(1-\beta)(1-\alpha)} \qquad 11.$$

$$w = Bp_s\beta\varphi^{1-\beta}k^{1-\beta} \qquad 12.$$

$$p_s = A(1-\varphi)^{\alpha}(1-\alpha)B^{-\alpha}k^{\alpha\beta}(\varphi)^{-\alpha(1-\beta)} \qquad 13.$$

Here k is defined as the physical capital per unit of skilled labour, i.e., $k = \frac{K}{hN}$. The value of φ is solved from the above system of equations.

The value of φ is

$$\hat{\varphi} = \frac{(1-\alpha)(1-\beta)}{1-\beta(1-\alpha)} \qquad 14.$$

The steady state growth paths in market economy is defined as the path along which c, h, K grow at constant rate and the value of φ is time independent. The growth rate of human capital accumulation and that of per unit commodity output consumption and the growth rate of physical capital are given by

$$\gamma_h^{comp} = \eta\tau A\{(1-\hat{\varphi})\}^{\alpha}B^{1-\alpha}(\hat{\varphi})^{(1-\beta)(1-\alpha)}k^{1-\beta(1-\alpha)} \qquad 15.$$

$$\gamma_c^{comp} = \frac{(1-\tau)\alpha A(1-\hat{\varphi})^{\alpha}B^{1-\alpha}\hat{\varphi}^{(1-\beta)(1-\alpha)}k^{-\beta(1-\alpha)} - \rho}{\sigma} \qquad 16.$$

$$\gamma_K^{comp} = n + \gamma_h^{comp} \qquad 17.$$

Where γ_x stands for growth rate of the variable x.

Along the steady state, $\gamma_c = \gamma_h$ (See equation (A.28) in Appendix for details). Equating γ_c, γ_h from equation (15) and (16), the following equation is obtained in terms of k, τ and other parameters. τ is considered to be given in competitive economy.

From the steady state $\gamma_c = \gamma_h$ equation, it is can be shown that there exists unique value of k in terms of τ, which is given in competitive economy.

Therefore, there exists positive, unique steady state growth rate for human capital, physical capital and production and consumption of commodity output in competitive economy.

Comparative Static Analysis:

We have done a comparative static analysis on the fraction of physical labor that is devoted to the service sector.

The value of the share of the physical capital

$$\hat{\varphi} = \frac{(1-\alpha)(1-\beta)}{1-\beta(1-\alpha)}$$

In this model, 'φ' be the fraction of physical capital that is dedicated to the service sector. In this model, α and β are the commodity output elasticity of physical capital and service output elasticity of skilled labour respectively.

Differentiating φ with respect to α we get

$$\frac{\partial\varphi}{\partial\alpha} = [\frac{-\{1-\beta(1-\alpha)\}(1-\beta)-(1-\alpha)(1-\beta)\beta}{\{1-\beta(1-\alpha)\}^2}]\beta = \frac{\beta(1-\beta)}{\{1-\beta(1-\alpha)\}^2}$$

Or,

$$\frac{\partial\varphi}{\partial\alpha} = \frac{\beta(1-\beta)}{\{1-\beta(1-\alpha)\}^2} \qquad [$$

Proposition 1: The fraction of physical capital that is dedicated to the service sector increases, when the commodity output elasticity of physical capital rises.

The logic behind the proposition is, when the relative responsiveness of commodity output to the physical capital is positive, the more amount of physical capital will be required. The investment on physical capital will be required by the economy to maintain positive growth.

Differentiating φ with respect to β

$$\frac{\partial\varphi}{\partial\beta} = [\frac{-\{1-\beta(1-\alpha)\}\{(1-\alpha)(-1)-(1-\beta)(1-\alpha)\{-(1-\alpha)\}}{\{1-\beta(1-\alpha)\}^2}][-(1-\alpha)]$$

Or, $\frac{\partial\varphi}{\partial\beta} = [\frac{-\{1-\beta(1-\alpha)\}\{(1-\alpha)(-1)-(1-\beta)(1-\alpha)\{-(1-\alpha)\}}{\{1-\beta(1-\alpha)\}^2}][-(1-\alpha)]$

Or, $\frac{\partial\varphi}{\partial\beta} = \frac{\{1-\beta(1-\alpha)\}\frac{\partial}{\partial\beta}[(1-\alpha)(1-\beta)]-[(1-\alpha)(1-\beta)]\frac{\partial}{\partial\beta}\{1-\beta(1-\alpha)\}}{\{1-\beta(1-\alpha)\}^2}$

Or, $\frac{\partial\varphi}{\partial\beta} = \frac{\{1-\beta(1-\alpha)\}(1-\alpha)(-1)-(1-\alpha)(1-\beta)\{-(1-\alpha)\}}{\{1-\beta(1-\alpha)\}^2}[-(1-\alpha)]$

Or, $\frac{\partial\varphi}{\partial\beta} = \frac{\alpha(1-\alpha)^2}{\{1-\beta(1-\alpha)\}^2}$

Proposition 2: The fraction of physical capital that is dedicated to the service sector increases, if the service output elasticity of skilled labour rises.

The reason behind such result is, when the relative responsiveness of service output to the change in skilled labour increases, the share of physical capital allotted to service sector has to increase, to maintain the capital - labour ratio for the growth of service output production.

Conclusion:

In this paper an endogenous growth model is considered in which the service output is used as an intermediate good in commodity sector. Human capital is used to produce service good. Accumulation of human capital depends on the government expenditure on education sector. The government levies tax on the commodity output. In this framework, on the basis of the unique steady state growth path, where human capital accumulation works as the source of growth for all other sectors of the economy, a comparative static analysis has been done. In this particular model, we have analysed, how the share of physical capital that is dedicated to the service sector is influenced by the commodity output elasticity of physical capital and service output elasticity of skilled labour.

Bibliography:

Barua A.,Pant M.(2014),"Trade and Wage Inequality: A Specific Factor Model with Intermediate Goods", International Review of Economics and Finance, Vol. 33 (2014), pp - 172-185.

Gupta et. al (2019) "Service good as an intermediate input and optimal government policy in an endogenous growth-model", South Asian Journal of Macroeconomics and Public Finance 8(1) 57–91, 2019 SAGE Publication

Imbruno M., (2012), "Trade Liberalization, Intermediate Inputs and Firm Competitiveness: Direct Versus Indirect Modes of Import," University of Nottingham, mimeo.

Ishikawa J.(1992), "Learning by doing, changes in industrial and trade patterns, and growth in a small open economy", Journal of International Economics, 33, 221-244.

Klette, Tor J, and Samuel S. Kortum (2004), "Innovating Firms and Aggregate Innovation," Journal of Political Economy, 112(5): 986-1018.

Moro A. (2007), “Intermediate goods and total factor productivity”. Economic Series (34) Working Paper No. 07-60.

Psarianos I. N (2002)“ Fiscal policy in an endogenous growth model with horizontally differentiated intermediate goods” Spoudai Journal of Economics and Business, 52(4), 1249-1273.

Sekar M & Delgado D R & Ulu M F (2015), “Imported intermediate goods and product innovation: Evidence from India” Working Papers 1537, Reasearch and Monetary Policy Department, Central Bank of the Republic of Turkey.

Appendix 4:

Competitive economy: General Case

The commodity production function can be written as

$$y_c = f(y_s, K) \tag{A.1}$$

Profit function for commodity sector

$$\pi_c = 1.y_c - r(1-\varphi)K - p_s y_s \tag{A.2}$$

The profit maximisation conditions are

$$\frac{d\pi_c}{d\{(1-\varphi)K\}} = 0 \tag{A.3}$$

Or, $A\alpha\{(1-\varphi)K\}^{\alpha-1} y_s{}^{1-\alpha} - r = 0$

Or, $A\alpha\{(1-\varphi)K\}^{\alpha-1} y_s{}^{1-\alpha} = r$ (A.4)

Substituting the value of y_s in equation (A.4)

$$A\alpha\{(1-\varphi)K\}^{\alpha-1}\{B(Nh)^{\beta}(\varphi K)^{1-\beta}\}^{1-\alpha} = r$$

Or, $A\alpha(1-\varphi)^{\alpha-1} K^{(\alpha-1)+(1-\beta)(1-\alpha)} B^{1-\alpha} (Nh)^{\beta(1-\alpha)} \varphi^{(1-\beta)(1-\alpha)} = r$

Or, $A\alpha(1-\varphi)^{\alpha-1} B^{1-\alpha} (\frac{K}{Nh})^{-\beta(1-\alpha)} \varphi^{(1-\beta)(1-\alpha)} = r$

Or, $A\alpha(1-\varphi)^{\alpha-1} B^{1-\alpha} k^{-\beta(1-\alpha)} \varphi^{(1-\beta)(1-\alpha)} = r$ (A.5)

$$\frac{d\pi_c}{dy_s} = 0$$

Or, $A\{(1-\varphi)K\}^{\alpha}(1-\alpha)y_s^{1-\alpha-1} - p_s = 0$

$$A\{(1-\varphi)K\}^{\alpha}(1-\alpha)y_s^{-\alpha} = p_s \qquad (A.6)$$

The service output production function can be written as

$$y_s = f(Nh, K)$$

Profit function for service sector is

$$\pi_s = p_s y_s - (r\varphi K) - (wNh)$$

Or, $\pi_s = p_s B(Nh)^{\beta}(\varphi K)^{1-\beta} - (r\varphi K) - (wNh)$ (A.7)

The profit maximisation conditions are

$$\frac{d\pi_s}{d(\varphi K)} = 0$$

Or, $p_s B(Nh)^{\beta}(1-\beta)(\varphi K)^{-\beta} - r = 0$

Or, $p_s B(Nh)^{\beta}(1-\beta)(\varphi K)^{-\beta} = r$ (A.8)

$$\frac{d\pi_s}{d(Nh)} = 0$$

Or, $p_s B(Nh)^{\beta-1}\beta(\varphi K)^{1-\beta} - w = 0$

Or, $p_s B(Nh)^{\beta-1}\beta(\varphi K)^{1-\beta} = w$ (A.9)

The Hamiltonian function can be formulated as

$$H = \frac{c^{1-\sigma}}{(1-\sigma)}N + \theta[(1-\tau)(rK + wNh) - cN] \qquad (A.10)$$

Here c is the decision variable and K is the state variable.

$$\frac{dH}{dc} = 0$$

Or, $c^{-\sigma} = \theta$ (A.11)

Taking logarithm both sides and differentiating with respect to time

$$-\sigma\frac{\dot{c}}{c}=\frac{\dot{\theta}}{\theta}$$

Or, $-\sigma\gamma_c=\frac{\dot{\theta}}{\theta}$ (A.12)

The co-state equation can be written as

$$\dot{\theta}=\rho\theta-\frac{dH}{dK} \qquad \text{(A.13)}$$

Here $\frac{dH}{dK}=\theta(1-\tau)r$ (A.14)

Substituting this value from (A.14) into (A.13)

$$\dot{\theta}=\rho\theta-\theta(1-\tau)r$$

Or, $\frac{\dot{\theta}}{\theta}=\rho-(1-\tau)r$ (A.15)

Substituting the value from (A.12) we get

$$-\sigma\gamma_c=\rho-(1-\tau)r$$

Or, $\gamma_c=\frac{(1-\tau)r-\rho}{\sigma}$ (A.16)

Substituting the value of r from equation (A.5) in above equation we get

$$\gamma_c=\frac{(1-\tau)A\alpha(1-\varphi)^{\alpha-1}B^{1-\alpha}k^{-\beta(1-\alpha)}\varphi^{(1-\beta)(1-\alpha)}-\rho}{\sigma} \qquad (A.16')$$

From equations (A.5) and (A.8)

$$A\alpha\{(1-\varphi)K\}^{\alpha-1}y_s^{1-\alpha}=p_sB(Nh)^{\beta}(1-\beta)(\varphi K)^{-\beta}$$

Or, $A\alpha\{(1-\varphi)K\}^{\alpha-1}\{B(Nh)^{\beta}(\varphi K)^{1-\beta}\}^{1-\alpha}=p_sB(Nh)^{\beta}(1-\beta)(\varphi K)^{-\beta}$

Or, $A\alpha\{(1-\varphi)K\}^{\alpha-1}B^{-\alpha}(Nh)^{\beta(1-\alpha)-\beta}(\varphi K)^{(1-\beta)(1-\alpha)+\beta}=p_s(1-\beta)$ (A.17)

From equation (A.6) we got

$$A\{(1-\varphi)K\}^{\alpha}(1-\alpha)y_s^{1-\alpha}=p_s$$

And substituting the value of y_s in above expression we have

$$A\{(1-\varphi)K\}^{\alpha}(1-\alpha)\{B(Nh)^{\beta}(\varphi K)^{1-\beta}\}^{-\alpha} = p_s \qquad \text{(A.18)}$$

Or, $A(1-\varphi)^{\alpha}(1-\alpha)B^{-\alpha}(\frac{K}{Nh})^{\beta\alpha}\varphi^{-\alpha(1-\beta)} = p_s$

Or, $A(1-\varphi)^{\alpha}(1-\alpha)B^{-\alpha}k^{\beta\alpha}\varphi^{-\alpha(1-\beta)} = p_s$ (A.19)

Substituting the value of p_s from equation (A.19) into equation (A.17)

$$\frac{(1-\hat{\varphi})}{\hat{\varphi}} = \frac{\alpha}{(1-\alpha)(1-\beta)}$$

Or, $\hat{\varphi} = \dfrac{(1-\alpha)(1-\beta)}{1-\beta(1-\alpha)}$

Now, $\gamma_h^{comp} = \eta\tau A\{(1-\hat{\varphi})\}^{\alpha}B^{1-\alpha}(\hat{\varphi})^{(1-\beta)(1-\alpha)}k^{1-\beta(1-\alpha)}$ (A.20)

$$\gamma_c^{comp} = \frac{(1-\tau)\alpha A(1-\hat{\varphi})^{\alpha}B^{1-\alpha}\hat{\varphi}^{(1-\beta)(1-\alpha)}k^{-\beta(1-\alpha)} - \rho}{\sigma} \qquad \text{(A.21)}$$

Equating equation (A.20) and (A.21) we get

$$\begin{aligned}&\sigma\eta\tau A\{(1-\hat{\varphi})\}^{\alpha}B^{1-\alpha}(\hat{\varphi})^{(1-\beta)(1-\alpha)}k^{1-\beta(1-\alpha)} + \rho = \\ &(1-\tau)\alpha A(1-\hat{\varphi})^{\alpha}B^{1-\alpha}\hat{\varphi}^{(1-\beta)(1-\alpha)}k^{-\beta(1-\alpha)}\end{aligned} \qquad \text{(A.22)}$$

Let $f(k) = L.H.S$ of equation (A.22), where $f' > 0$. $f(k)$

$g(k) = R.H.S$ of equation (A.22), where $g' < 0$. $g(k)$

Diagrammatically, it can be shown that there exists unique value of k in terms of τ and other parameters.

Ilkogretim Online - Elementary Education Online, 2021; Vol 20 (Issue 3): pp. 4980-4991
http://ilkogretim-online.org
doi: 10.17051/ilkonline.2021.03.511

Service Sector And Optimal Taxation In An Endogenous Growth Model

Dr. Senjuti Gupta Assistant Professor in Economics (W.B.E.S) Department of Economics, Government Girls' General Degree College, Ekbalpore, Kolkata, West Bengal, India.

Abstract:
The paper entitled "Service sector and optimal taxation in an endogenous growth model" is formed in a command economy framework. In this model, the commodity output is produced with physical capital only, where the skilled labour is being used for producing the service good. Moreover, in this model, per capita government expenditure is used to create human capital. The model derives the optimal tax rate and steady-state growth path in an endogenous growth framework in a two-sector economy, when the service sector is being taxed only. This paper has done comparative static analysis on optimum service tax. The influence of population growth and the intensity of preference towards commodity consumption on service tax is analysed here.

KEY WORDS: taxation, government policy, endogenous growth, command economy, human capital accumulation.

Introduction: This paper is based on optimal tax policy, in the presence of service sector whose output is fully consumed. The development of endogenous growth theory enabled the policy makers to implement different fiscal policies in the growth model. There exists a huge literature that discusses the effects of various policies in endogenous growth models. The model is based on the assumption that the government spends tax revenue to finance accumulation of human capital.

The study by **Greiner A (2008)** tries to figure out the effects of fiscal policy in an endogenous growth model, giving special emphasis on human capital and heterogeneous agents.

Across the world, the human capital and education sector play a very important role in the development of any economy, a lot of works have been done on the theories of human capital accumulation in growth economics.

Hollanders and Weel (2003) have worked on the role of public expenditure on the human capital accumulation in a Lucas(1988) type growth model. The study by **Greiner (2006)** focuses on an endogenous growth model which is based on the assumption that human capital accumulation results from the investment of the public resources. The investment is financed by imposing income tax and from issuing government bonds.

Following **Heckman (1976) and Rosen (1976)**, the paper by **King and Rebelon (1990)** tries to find optimal accumulation of human capital and the effects of various taxation on optimal accumulation. The basic finding of the model is, the costs of welfare are higher for endogenous growth models than in neoclassical models with exogenously given technical progress.
There exists a huge number of papers that consider the role of government expenditure on public resources by the revenue earned through taxation in endogenous growth models. **Garcia-Castrillo and Sanso (2000) and Gomez (2003)** designed optimal fiscal policies in the **Lucas (1988)** model. The paper by **Gomez (2003)** also finds that the tax financed educational subsidy policy is optimal one. However, in the analysis of Gomez (2003), lump sum tax is never found to be optimal to finance the subsidy.

In the present paper, we assume that there exists a command economy where the service sector uses human capital as one and only input, which is accumulated through government expenditure on education sector. The physical output is used to produce commodity output only. Government expenditure is financed by tax revenue, which is earned through imposing tax on production sectors. In one of my papers, **written by me and my co-authors, Gupta et. al (2019) titled** "Optimal tax policy in an endogenous growth model with a consumable service good", we have derived steady-state growth paths. But , that paper finished out to leave a few comparative static analysis. In this paper, I have tried to figure out those undone derivations using the growth analysis. Therefore, the rest of the paper is organised as follows: In section 2, the basic general model is presented; In Section 3, optimal tax policy and steady-state growth paths are derived when service sector is being taxed only; In section 4, corresponding comparative static analysis is done under command economic regime.

2. The model:

Section 2 first describes the basic model and then shows the functioning of the economy under command economic regime.

The Households, Firms and Government:

A closed economy model is considered with two sectors namely, commodity sector and service sector. The total labour force is homogeneous as far as skill is concerned. The commodity and the factor markets are characterized by perfect competition. Identical rational agents inhabit the economy. Production technology is subject to constant returns to scale. Preferences over the consumption of different combinations of the commodity and service output are given by the following function where 'c' and 's' denote the flow of real per capita consumption of commodity and service output respectively.

$$u(c)=\int_0^{\infty}\frac{(c^{\alpha}s^{1-\alpha})^{1-\sigma}-1}{(1-\sigma)}e^{-\rho t}N(t)dt \qquad 1.$$

Here, we assume that the output of the commodity sector can be used for consumption or investment. The output of the service sector is fully consumed. Let α be the parameter that measures the intensity of preference towards commodity consumption and $(1-\alpha)$ measures the preference for service output consumption. The commodity output is a function of physical capital whereas the service product is produced with human capital only. Let ρ be the discount rate and σ, the elasticity of marginal utility and inverse of which is known as inter temporal elasticity of substitution. Let N represents the total labour force or working population.

The commodity and service output production functions can be written as

$$y_c = AK \qquad 2.$$

$$y_s = B(Nh) \qquad 3.$$

Where y_c and y_s are commodity and service output. K is the aggregate physical capital. It is further assumed that the general skill level of a worker is 'h'. The effective skilled work force in commodity production is 'Nh'. A is a positive constant that reflects the level of technology. B is the index of knowledge available to the workforce.

The level of population is growing at an exponential rate in the following manner:

$$N(t) = N_0 e^{nt} \qquad 4.$$

Here, N_0 stands for the population size at initial time period. For simplicity the initial size of population is normalised, i.e., $N_0 = 1$. According to our assumption, government spends money on education to create human capital.

The human capital accumulation function can be written as

$$\dot{h} = \eta \frac{G}{N} \qquad 5.$$

Here η is the technology parameter of human capital accumulation whose value is always positive and G stands for government expenditure.

While considering the command economy, the objective of the economy is to maximize the value of utility defined by equation (1) subject to the constraint of physical capital and that of human capital.

3. The Command economy: When service sector is being taxed only

In this section, it is assumed that only the service sector is being taxed. The tax revenue is spent as government expenditure to build human capital. Let the tax rate be τ_s which is levied on per unit production of service output. Now the balanced budget equation can be written as

$$G = T = \tau_s y_s \qquad 6.$$

For this particular sector-specific model, the human capital accumulation function is follows as

$$\dot{h} = \eta \frac{G}{N} = \eta \tau_s Bh \qquad 7.$$

After deducting the taxable amount, the service output that is left as disposable service output, is totally consumed by the population. So the market clearing condition is derived as

$$s = (1 - \tau_s) Bh \qquad 8.$$

It is assumed that commodity output over aggregate consumption is accumulated as physical capital. The physical capital accumulation function is given by

$$\dot{K} = y_c - Nc \qquad 9.$$

The Command Economy allocates resources by solving a grand optimization problem **Dasgupta (1999).** The objective of the social planner is to maximize the value of utility defined by equation (1) subject to the constraints given by physical capital and human capital as stated in equation (9) and (7). The value of 's' which denotes per capita consumption of service output in our model, is substituted by equation (8) in the following Hamiltonian function.

The current value Hamiltonian as given in (10) is maximised with respect to the control variables c and τ_s where the state variables are K and h. Here, θ_1 and θ_2 are the shadow prices associated with $\dot{K}$ and $\dot{h}$ which stand for physical capital investment and human capital accumulation.

$$H = N(t)[\frac{[c^{\alpha}\{(1-\tau_s)Bh\}^{1-\alpha}]^{1-\sigma} - 1}{(1-\sigma)}] + \theta_1[AK - cN] + \theta_2 \eta \tau_s Bh \qquad 10.$$

From the first order conditions of the control variables and two co-state equations of state variables, the growth rates of per capita commodity output consumption, human capital accumulation and physical capital are solved (for detailed derivation see Appendix).

Steady-state growth paths when service sector is taxed only:

The growth rate of per capita commodity output is

$$\gamma_c = \frac{(1-\sigma)(1-\alpha)B\eta\tau_s + A - \rho}{\{1-\alpha(1-\sigma)\}} \qquad 11.$$

The growth rate of human capital accumulation is

$$\gamma_h = B\eta\tau_s \qquad 12.$$

Diving both sides of investment function by K in equation (9), the growth rate of physical capital accumulation is found

$$\frac{\dot{K}}{K} = A - c\frac{N}{K}$$

Or, $\gamma_K = A - c\dfrac{N}{K}$ 13.

As γ_K is constant in steady-state $(\dfrac{cN}{K})$ is also constant in steady-state.

Therefore $(\dfrac{cN}{K}) =$ Constant.

Taking logarithm both sides of the above equation and differentiating with respect to time

$$\gamma_K = \gamma_c + n \qquad 14.$$

Thus, the growth rate of human capital accumulation, rate of growth of commodity consumption and that of physical capital are derived from equations (12), (11) and (14) respectively. Let k be the capital to skilled labour ratio or $k = \dfrac{K}{Nh}$.

Taking logarithm both sides of the expression $k = \dfrac{K}{Nh}$, and differentiating with respect to time we get, γ_k.

Now $\gamma_k = \gamma_K - n - \gamma_h$

Or, $\gamma_K = \gamma_k + n + \gamma_h$ 14′.

Equating the value of γ_K from equation (14) and (14’) we get

$$\gamma_c = \gamma_k + \gamma_h \qquad 14''.$$

From the Hamiltonian function using the first order conditions of the control variables and the co-state equations of state variables we get the following equation

$$\rho - B\eta = \alpha(1-\sigma)\gamma_c + \{(1-\alpha)(1-\sigma)-1\}\gamma_h + n \qquad 15.$$

Substituting the expressions of γ_c, γ_h into the above equation we get

$$\rho - B\eta = \alpha(1-\sigma)\frac{\{(1-\sigma)(1-\alpha)B\eta\tau_s - \rho + A\}}{\{1-\alpha(1-\sigma)\}} + \{(1-\alpha)(1-\sigma)-1\}B\eta\tau_s + n \qquad 16.$$

From this equation we can solve the value of optimal tax rate while only the service output is being taxed under command economic regime.

The value of optimal tax rate is

$$\tau_s = \frac{A\alpha(1-\sigma) + \{1-\alpha(1-\sigma)\}(n+B\eta) - \rho}{B\eta\sigma} \qquad 17.$$

Substituting the value of optimal service tax in the growth paths, we can solve the optimal growth rate of the economy. The detail derivation has been done in appendix.

SECTION 4: COMPARATIVE STATIC ANALYSIS:

We have done two comparative static analysis on optimal service tax:

Differentiating service tax, with respect to intensity of preference towards commodity consumption, we get

$$\frac{\partial \tau_s}{\partial \alpha} = \frac{-(1-A)(1-\sigma)}{B\eta\sigma}$$

If σ <1 , which means when the elasticity of marginal utility, the inverse of which is known as inter temporal elasticity of substitution is less than 1, the tax on service commodity will be negatively related to the intensity of preference towards commodity consumption, i.e $\frac{\partial \tau_s}{\partial \alpha}$ <0 and vice versa.

Proposition 1: When σ <1, $\frac{\partial \tau_s}{\partial \alpha}$ < 0 ; the elasticity of marginal utility is less than 1, the tax on service commodity will be inversely related to the intensity of preference towards commodity consumption.

The logic behind such result is quite obvious. If individuals derive more utility from commodity consumption than service consumption it is advised to decrease tax on service output to encourage consumption of service.

Differentiating with respect to population growth,

$$\frac{\partial \tau_s}{\partial n} = \frac{\{1-\alpha(1-\sigma)\}}{B\eta\sigma}$$

If $\alpha < \frac{1}{(1-\sigma)}$, which means when the intensity of preference towards commodity consumption **is sufficiently low,** the tax on service commodity will be positively related to the growth rate of population.

Proposition 2: When $\alpha < \frac{1}{(1-\sigma)}$, $\frac{\partial \tau_s}{\partial n} > 0$**;** the tax on service commodity will be positively related to the growth rate of population.

The logic behind the result is, when population rises, the necessity for human capital accumulation also rises. For the required investment, the service tax has to be raised.

CONCLUSION:

This paper constructs a two-sector endogenous growth model under a command economic regime in order to discover the optimal tax policy. Commodity output is produced with only physical capital, whereas skilled labour is the only input used to produce service output. One tax regime is considered. In this regime, the service sector is taxed only. We first consider the benchmark model where the tax revenue is invested to create human capital through government expenditure. Steady-state growth paths are studied under a command economic regime. The optimal tax rate and steady-state growth path are derived.

Only when the service sector is taxed, along the steady-state balanced growth path the optimal service tax is found to be positive. This paper offers an alternative theory of optimal policy in a simplified model where human capital is used only in final services while physical capital is only used as an input to produce final commodities. This paper has done comparative static analysis on optimum service tax. The influence of population growth and the intensity of preference towards commodity consumption on service tax is analysed here.

Bibliography:

Dasgupta D (1999) "Growth versus welfare in a model of non-rival infrastructure" Journal of Development Economics 58, 359–385.

Garcia-Castrillo, P and Sanso M. (2000), "Human capital and optimal policy in a Lucas-type model", Review of Economic Dynamics, 3(4), 757-770.

Gomez, M. A., (2003), "Optimal fiscal policy in the Uzawa-Lucas model with externalities", Economic Theory, 22(4), 917-925.

Greiner A (2006), “Human capital formation, public debt and economic growth”,Journal of Macroeconomics, 30 (1), 415-427.

Greiner A (2008), “Human capital formation, public debt and economic growth”,Journal of Macroeconomics, 30 (1), 415-427.

Gupta et. al (2019) “Optimal tax policy in an endogenous growth model with a consumable service good”, Economic annals, Volume lxiv, no. 220 / January– march 2019

Heckman J. (1976) "A Life-Cycle Model of Earnings, Learning, and Consumption." J.P.E. 84(4), SII-S44.

Hollanders, H. and B. Weel, (2003), “Skill-biased technical change: On endogenous growth, wage inequality and government intervention”, in: H.Hagemann and S.Seiter (eds.), Growth Theory and Growth Policy, Routledge: London, 156-171.

King, R.G., and Rebelon S. (1990), "Public Policy and Economic Growth: Developing Neoclassical Implications." J.P.E. 98(5), S126-S150.

Lucas, R. E (1988), “On the mechanics of economic development”, Journal of Monetary Economics, 22 (1), 3-42.

Rosen S. (1976) "A Theory of Life Earnings. "J.P.E. 84(4), S45-S67.

Appendix: When tax is levied on service good:

$$u(c,s)=\int \frac{(c^{\alpha}s^{1-\alpha})^{1-\sigma}-1}{(1-\sigma)}e^{-\rho t}N(t)dt \qquad \text{(A.1)}$$

$$y_c = AK \qquad \text{(A.2)}$$

$$y_s = B(hN) \qquad \text{(A.3)}$$

$$\dot{h}=\eta\frac{G}{N} \qquad \text{(A.4)}$$

$$G=T=\tau_s y_s \qquad \text{(A.5)}$$

$$(1-\tau)y_s = sN \qquad \text{(A.6)}$$

$$N(t)=e^{nt} \qquad \text{(A.7)}$$

$$\dot{K} = (1-\tau_s)y_c - cN \qquad \text{(A.8)}$$

Using equation (A.3) into (A.5)

$$G = T = \tau_s y_s \qquad \text{(A.9)}$$

Using equation (A.4) into (A.5)

$$\dot{h} = \eta \frac{\tau_s B(hN)}{N} = \eta \tau B h \qquad \text{(A.10)}$$

Or, $\gamma_h = \eta \tau B$

Substituting the value of y_s into the market clearing equation (A.6) we have

$$(1-\tau_s)B(hN) = sN$$

Or, $s = (1-\tau_s)Bh$ (A.11)

The current value Hamiltonian can be formulated as

$$H = N(t)\{\frac{(c^{\alpha}s^{1-\alpha})^{1-\sigma} - 1}{(1-\sigma)}\} + \theta_1[y_c - cN] + \theta_2 B \tau_s h \eta \qquad \text{(A.12)}$$

Substituting the value of s into the Hamiltonian function

$$H = N(t)\{\frac{(c^{\alpha}\{(1-\tau_s)Bh)^{1-\alpha}]^{1-\sigma} - 1}{(1-\sigma)}\} + \theta_1[y_c - cN] + \theta_2 B \tau_s h \eta \qquad \text{(A.13)}$$

Control variables are c, τ_s. State variables are K, h.

The first order conditions are

$$\frac{dH}{dc} = 0$$

Or, $\alpha c^{\alpha(1-\sigma)-1}(1-\tau_s)^{(1-\alpha)(1-\sigma)} B^{(1-\alpha)(1-\sigma)} h^{(1-\alpha)(1-\sigma)} = \theta_1$ (A.14)

Taking logarithm both sides and differentiating with respect to time we get

$$\frac{\dot{\theta}_1}{\theta_1} = \{\alpha(1-\sigma) - 1\}\gamma_c + (1-\sigma)(1-\alpha)\gamma_h - (1-\alpha)(1-\sigma)\frac{\dot{\tau}_s}{\tau_s}(\frac{\tau_s}{1-\tau_s}) \qquad \text{(A.15)}$$

As τ_s is constant at steady-state, equation (A.15) is written as

$$\frac{\dot{\theta}_1}{\theta_1} = \{\alpha(1-\sigma)-1\}\gamma_c + (1-\sigma)(1-\alpha)B\eta\tau_s \qquad \text{(A.16)}$$

The co-state equation of the state variable K is

$$\dot{\theta}_1 = \rho\theta_1 - \frac{dH}{dK} \qquad \text{(A.17)}$$

Now, $\frac{dH}{dK} = \theta_1 A$

Substituting this value into equation (A.17)

$$\dot{\theta}_1 = \theta_1(\rho - A)$$

Or, $\frac{\dot{\theta}_1}{\theta_1} = (\rho - A)$ (A.18)

Equating the expressions of $\frac{\dot{\theta}_1}{\theta_1}$ from equations (A.16) and (A.18) we get

$$\rho - A = -\{1-\alpha(1-\sigma)\}\gamma_c + (1-\sigma)(1-\alpha)B\eta\tau_s$$

Or, $\gamma_c = \frac{(1-\sigma)(1-\alpha)B\eta\tau_s + A - \rho}{\{1-\alpha(1-\sigma)\}}$ (A.19)

The first order condition for the tax rate is

$$\frac{dH}{d\tau_s} = 0$$

Or, $N(t)c^{\alpha(1-\sigma)}B^{(1-\alpha)(1-\sigma)}h^{(1-\alpha)(1-\sigma)}(1-\alpha)(1-\tau_s)^{(1-\alpha)(1-\sigma)-1} = \theta_2 Bh\eta$ (A.20)Taking logarithm both sides and differentiating with respect to time

$$\{(1-\alpha)(1-\sigma)-1\}\gamma_h + \alpha(1-\sigma)\gamma_c + n = \frac{\dot{\theta}_2}{\theta_2} \qquad \text{(A.21)}$$

The other co-state equation is

$$\dot{\theta}_2 = \rho\theta_2 - \frac{dH}{dh} \qquad \text{(A.22)}$$

The first order condition for the tax rate is

$$\frac{dH}{dh} = N(t)c^{\alpha(1-\sigma)}(1-\tau_s)^{(1-\alpha)(1-\sigma)}B^{(1-\alpha)(1-\sigma)}(1-\alpha)h^{(1-\alpha)(1-\sigma)-1} + \theta_2 B\tau_s\eta$$

Or, $\frac{\dot{\theta}_2}{\theta_2} = \rho - B\eta(1-\tau_s) - B\tau_s\eta = \rho - B\eta$ (A.23)

Equating the expressions of $\frac{\dot{\theta}_2}{\theta_2}$ from (A.21) and (A.23) we get

$$\{(1-\alpha)(1-\sigma)-1\}\gamma_h + \alpha(1-\sigma)\gamma_c + n = \rho - B\eta \quad \text{(A.24)}$$

Substituting the value of γ_h and γ_c

Or, $\{(1-\alpha)(1-\sigma)-1\}\eta\tau_s B + \alpha(1-\sigma)[\frac{(1-\sigma)(1-\alpha)B\eta\tau_s - \rho + A}{\{1-\alpha(1-\sigma)\}}] + n = \rho - B\eta$

Solving τ in terms of parameters.

$$\tau_s = \frac{\{1-\alpha(1-\sigma)\}(n+B\eta) + A\alpha(1-\sigma) - \rho}{B\eta\sigma}$$

Now $\gamma_h = \eta\tau_s B$

Substituting the value of τ_s in growth equation of human capital we get

$$\gamma_h = \frac{\{1-\alpha(1-\sigma)\}(n+B\eta) + A\alpha(1-\sigma) - \rho]}{B\eta\sigma}\eta B$$

Or, $\gamma_h = \frac{\alpha(1-\sigma)[A-n-B\eta] + (n+B\eta-\rho)}{\sigma}$

Substituting the value of τ_s into γ_c expression we get

$$\gamma_c = \frac{(1-\sigma)(1-\alpha)B\eta[\frac{\{1-\alpha(1-\sigma)\}(n+B\eta) + A\alpha(1-\sigma) - \rho}{B\eta\sigma}] + A - \rho}{\{1-\alpha(1-\sigma)\}}$$

Or, $\sigma\{1-\alpha(1-\sigma)\}\gamma_c = [(1-\alpha)(1-\sigma)(n+B\eta) - \rho]\{1-\alpha(1-\sigma)\} + A[\sigma + \alpha(1-\alpha)(1-\sigma)^2]$

Or, $\gamma_c = \frac{[(1-\alpha)(1-\sigma)(n+B\eta) - \rho]}{\sigma} + A\frac{[\sigma + \alpha(1-\alpha)(1-\sigma)^2]}{\sigma\{1-\alpha(1-\sigma)\}}$

Differentiating τ_s with respect to α

$$\frac{\partial \tau_s}{\partial \alpha} = \frac{-(1-A)(1-\sigma)}{B\eta\sigma}$$

Differentiating τ_s with respect to n

$$\frac{\partial \tau_s}{\partial n} = \frac{\{1-\alpha(1-\sigma)\}}{B\eta\sigma}$$

$$\frac{\partial \tau_s}{\partial n} > 0, \text{ if } \{1-\alpha(1-\sigma)\} > 0$$

Now $\{1-\alpha(1-\sigma)\} > 0$

Or, $1 > \alpha(1-\sigma)$

Or, $\alpha(1-\sigma) < 1$

Or, $\alpha < \frac{1}{(1-\sigma)}$

If $\alpha < \frac{1}{(1-\sigma)}$, $\frac{\partial \tau_s}{\partial n} > 0$

The International Journal of Interdisciplinary Organizational Studies
ISSN: 2324-7649 (Print), ISSN: 2324-7657 (Online)
Volume 16, Issue 1, January-March, 2021

CLIMATE CHANGE AND ENDANGERED LIVELIHOOD IN INDIAN SUNDARBANS- A BASELINE APPRAISAL

Dr. Rajashree Dasgupta

Assistant Professor, WBES, Department of Geography, Government Girls' General Degree College, Kolkata-700023 (West Bengal), India

ABSTRACT

The Sundarbans island system in West Bengal India, is facing several natural changes under the situation of climate change . The Island system is undergoing natural threats in the form of relative sea level rise, coastal erosion and inundation, frequent embankment failures, salinity rise and increase in the frequency of high intensity events like cyclones in the last three decades under climate change situation. A tremendous growth of population size (287%) since Independence till 2011 in this fragile island system has further increased the social and economic vulnerability of the coastal communities through over exploitation of natural resources, wide scale reclamation and deforestation practices. The average population density in the region was 897 persons per sq' kms in 2001 which rose to 996 persons per sq. kms. in 2011(11.04% rise). Higher population growth is further anticipated in the coastal blocks of Sagar, Namkhana Patharpratima, Kultali and Gosaba (whose southern boundary is demarcated by Bay of Bengal) compared to the inland blocks.

The population dynamics in the five coastal blocks of Indian Sundarbans with the current livelihood options available to the highly vulnerable and endangered inhabitants of the island system are studied in detail in the present paper . Data analysis has revealed a sharp fall in the number of agriculturists in the region. Furthermore, the expansion of aquaculture farms replacing the agricultural fields for rising salinity problems may invite food insecurity to this poor less educated people of the island system . The present study has tried to asses the local livelihood scenario by household-level information collected from several rounds of surveys conducted over the last two decades in these coastal blocks.

Keywords: Climate Change, Natural Threats, Population Dynamics, Endangered Livelihood

Introduction

Climate scientists working on climate change issues are of the opinion that the coastal areas are the worst affected locales because of climate change phenomenon. This is true for all climatic zones viz. polar, temperate, tropical and arid. However, the problem is much more severe in case of tropical coastal areas where population density is huge. Here in addition to open vulnerability issues the problems of social and economic vulnerability is rising day by day. People are getting increasingly exposed to such natural changes as relative sea level rise, coastal erosion and submergence, frequent embankment failures, rise of salinity in estuarine waters and soil and

increase in the frequency of high intensity events like cyclones. Rise in enormous population size also results in major environmental degradation and wide scale reclamation activities in the coastal zones making the zones extremely fragile. Mostly the coastal communities in tropical zones are poor, less educated, unaware and less skilled for which their coping capacity is also relatively low to face all these climate change natural issues. Therefore, immediate feasible management strategies are required to be designed and implemented to reduce the social and economic vulnerability of these poor coastal masses and to enhance their coping capacity for the future.
Sundarbans is one such vulnerable eco-region lying at the tropical coastal part and spread under both India and Bangladesh which is facing a major environmental degradation at present under the scenario of climate change .This is a unique ecosystem since this is the only mangrove tiger land in the world. This eco-region has also been designated as a World Heritage site by UNESCO because of its huge floral and faunal assemblage. However, at present both the flora and fauna are getting endangered gradually because of the occurrence of several natural changes like relative sea level rise, coastal erosion and submergence, embankment failures, rise in salinity at both estuarine waters and soil, uncertainty of rainfall , reduced sweet water flow and rise in the occurrence of high intensity events like cyclones. The present study is carried out in the Indian Sundarbans part covering a total area of 9630 sq. kms. that includes nineteen community development blocks covered under South and North 24 Parganas district of West Bengal State. Here, the major focus has been given to the coastal blocks facing Bay of Bengal as the southern demarcation and these blocks are Sagar, Namkhana, Patharpratima, Kultali and Gosaba – all included under South 24 Parganas district. The whole of the Indian Sundarbans has experienced a major rise in population size since Independence.

This enormous population size of 4.4 million (2011 Census) has resulted into wide scale reclamation activities, unsustainable resource exploitation practices and deforestation. Interesting to note that the coastal blocks in the Indian part are experiencing a higher population growth compared to the inland blocks in the last two decades inspite of the problems of open vulnerability.

The appraisal made on natural and human induced changes in the Sundarbans currently reveals certain trends which are expected to continue in future under climate change situation and hence make the system further vulnerable to climatogenic impacts. It is evident that temperature is rising over land and sea in Sundarbans and if this same trend continues, the region is expected to experience a rise of 1°C in temperature by 2050. It has been found that the relative mean sea level is rising in this region @ 3.14mm /year- which is much above the global average of 2°C. Considering the present rate of rise only, the sea level might rise to 20 cms. by 2050. This pose a serious threat to flood and inundation in vast areas of Sundarbans and may lead to colossal loss of life and property in the locale.

Study Area Selected

The study area primarily includes the five coastal blocks- Sagar , Namkhana, Patharpratima, Kultali and Gosaba of the Indian Sundarbans located in West Bengal state under South 24 Parganas district. Indian Sundarbans is having a total area of 9630 sq. kms. and includes nineteen community development blocks, thirteen of which lie under South 24 Parganas district and the rest under North 24 Parganas district. The region is delimited in the north by the so-called 'Dampier-Hodges line' demarcating the northern extension of the intertidal zone marked by mangrove forests of 1830 (Chakraborty, P., 1991). The river Hoogly (in the west) and the river Harinbhanga–Raimangal – Ichamati (in the east) demarcate the western and eastern boundaries respectively. The Indian Sundarbans has 4264 sq. kms. of wetland/mangroves covered under the reserve forests and the rest i.e. 5366 sq. kms. is under reclaimed area used for human settlements. A substantial part of Kultali and Gosaba Block comes under the Sundarban reserved forest which is uninhabited. The study area map is provided in Fig.1(below)

Fig.1

LOCATION OF THE STUDY AREA – INDIAN SUNDARBANS

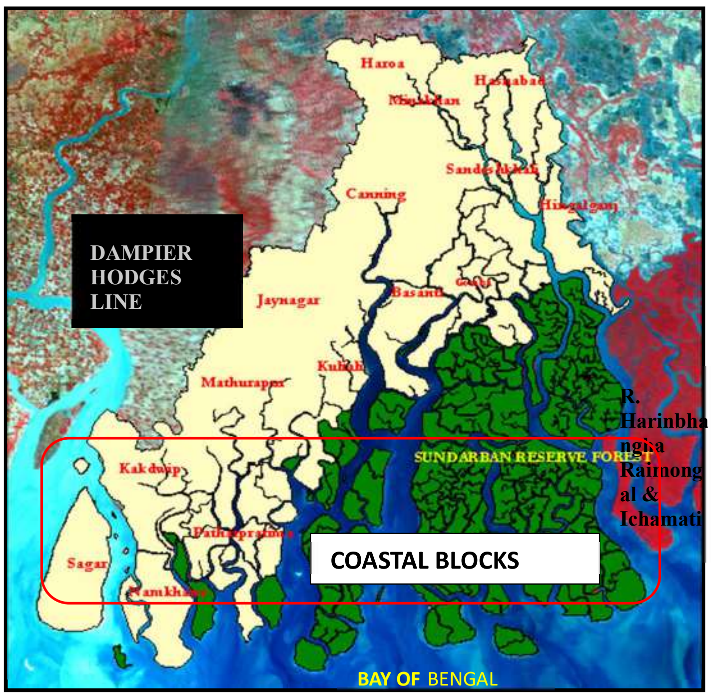

Central Queries Framed

The specific queries in the present study include :

1. To what extent the Indian Sundarbans region has become openly vulnerable to natural changes under climate change scenario?

2. What is the status of population pressure in the study region of the coastal blocks of Indian Sundarbans ?

3. What are the different livelihood options available to to the coastal people in Indian Sundarbans ? To what extent these livelihoods are getting affected by the population dynamics and natural changes in the coastal blocks ?

4. What feasible management strategies may be undertaken to reduce the overall status of vulnerability in the Indian Sundarbans region ?

Methodology Followed

This study relies both on secondary sources and primary information collected from household interviews across different villages of the coastal blocks- Sagar, Namkhana, and Gosaba conducted at several rounds of surveys carried out in 2004, 2006, 2015 and 2019.

Secondary documents include literature and newspaper reports, Census Data and policy documents. In-depth interviews were also conducted over phone with few migrants who have experienced the twin impacts of the cyclone and the lockdown.

Participants were recruited specifically from the Community Development (CD) blocks of Patharpratima, Namkhana ,Sagar, Basanti and Gosaba blocks of South 24 Parganas with the help of a network of key informants from local community-based organisations These blocks were badly affected by storm surge during cyclone *Amphan in 2020* as well as during cyclone *Aila* in May 2009**.**

Results and Findings

- **Observations on natural changes**

The Indian Sundarbans is bearing a very negative inpact of climate change evident in the last three decades. The study performed by the author during her Ph.D research tenure from 2002 to 2007 in the island system has revealed several natural changes that the region is facing under climate change scenario which are listed below.

- Temperature rise over land and sea,
- Marginal increase in rainfall,
- A rise in the frequency of high intensity events (with wind speeds more than 64 knots)
- Salinization of estuarine water and soil
- Loss of forest cover and floral/faunal diversity

It is evident that temperature is rising over this part of Bay of Bengal in Sundarbans @ 0.019 deg.c/year (Fig.2a) . If this same trend continues, the region is expected to experience a rise of 1°C in temperature by 2050. From the analysis of tide gauge data of the Sagar island observatory, it has been found that the relative sea level around this part of the Bay of Bengal is rising @3.14mm/year - significantly higher than the global average of 2.0 mm/year (IPCC, 2019). The study from Satellite data IRS LISS I image of 1961 and IRS LISS III image of 2001 during the Ph.D research tenure has further revealed that from 1969 to 2001, the total land area loss by erosion is estimated to be 163 sq. kms. while the total amount of accretion is almost half i.e. 82.5 sq. kms.

Thus a net loss of 80.5 sq. kms land has occurred from 1969 to 2001 (Fig.3) .It is apprehended that with the present rate of rise, the sea level might reach to 20 cms. by 2050. The sea-facing part of the delta is becoming increasingly vulnerable due to coastal erosion, frequent embankment failures, submergence and flooding. Increased coastal erosion has **completely wiped out some islands like Lohachara, and Bedford** rendering thousands of people homeless. Other densely populated islands like Ghoramara, Sagar & Moushuni are suffering from bulk of erosion.

The trend of change in rainfall pattern over Sundarbans is somewhat ambiguous. A study of 74 years (1930-2004) rainfall pattern over the region (Station Alipore) indicates an increase in the monsoon and post monsoon rainfall which bears some serious consequences over the flood and food security of the region. Hazra et. al. (2003) has estimated that there is a strong probability of rise in relative mean sea level by 50 cm in 2050.

Furthermore, the study of pattern of cyclones over Bay of Bengal coast suggests that though the frequency of depressions and storms (wind velocity 31-50 knots) around Sundarbans have decreased over the years there has been a rise in their intensity (more than 62 knots)shown in Fig.2b . The increase in the number of cyclones/severe cyclones compared to storms and depressions certainly has a strong bearing on coastal flooding, erosion and salinization of the region as has been estimated by Hazra et. al. (2003).

Fig.2a **TEMPERATURE RISE OVER LAND AND SEA**

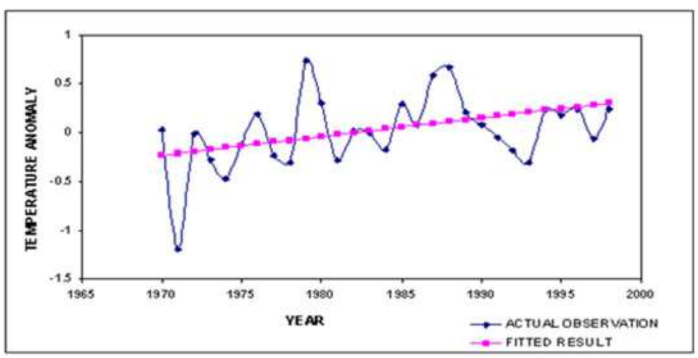

Source Hazra et. al. (2003) .

Fig.2b

RISE IN THE HIGH INTENSITY EVENTS – CYCLONES

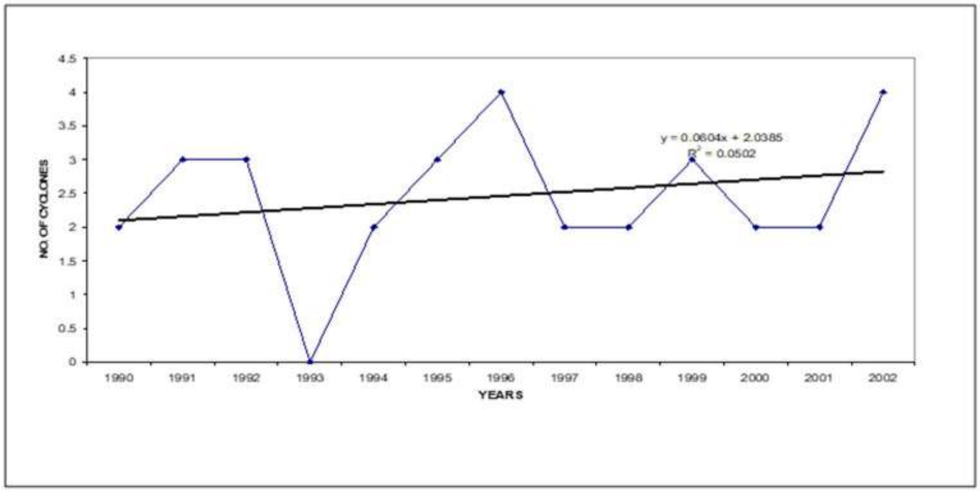

Source : Hazra et. al., 2003

Fig.3

COASTAL EROSION AND ACCRETION IN INDIAN SUNDARBANS

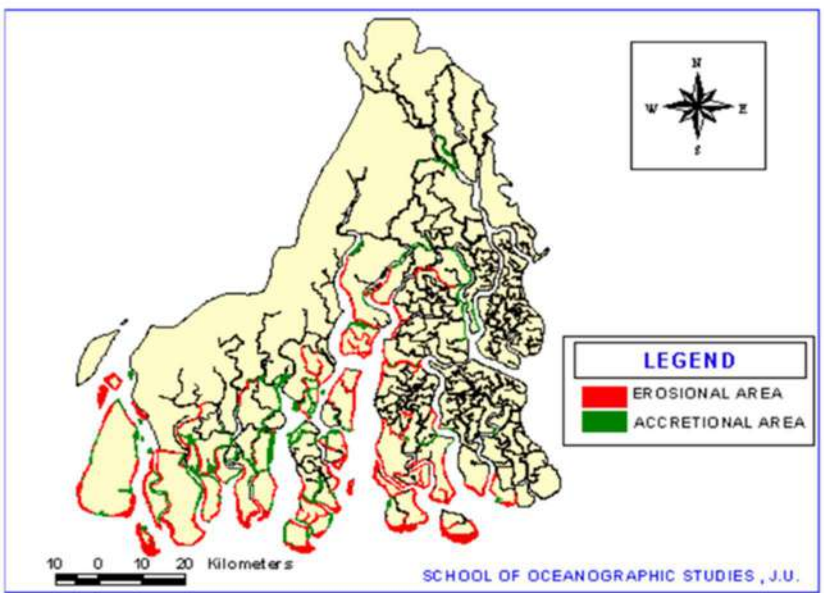

Dakshin Surendranagar (Patharpratima Block), Sagar , namkhana, Moushuni and Ghoramara all islands are suffering a bulk of erosion problems registering a landloss of 15.56%. 4.8%, 4.88%, 14.6% and 41% from 1969 to 2001 displacing a huge number of people compelling them to become *environmental refugees*. The landloss of few islands from 1969 to 1999 are provided below (Fig. 4a, 4b, 4c and 4d)

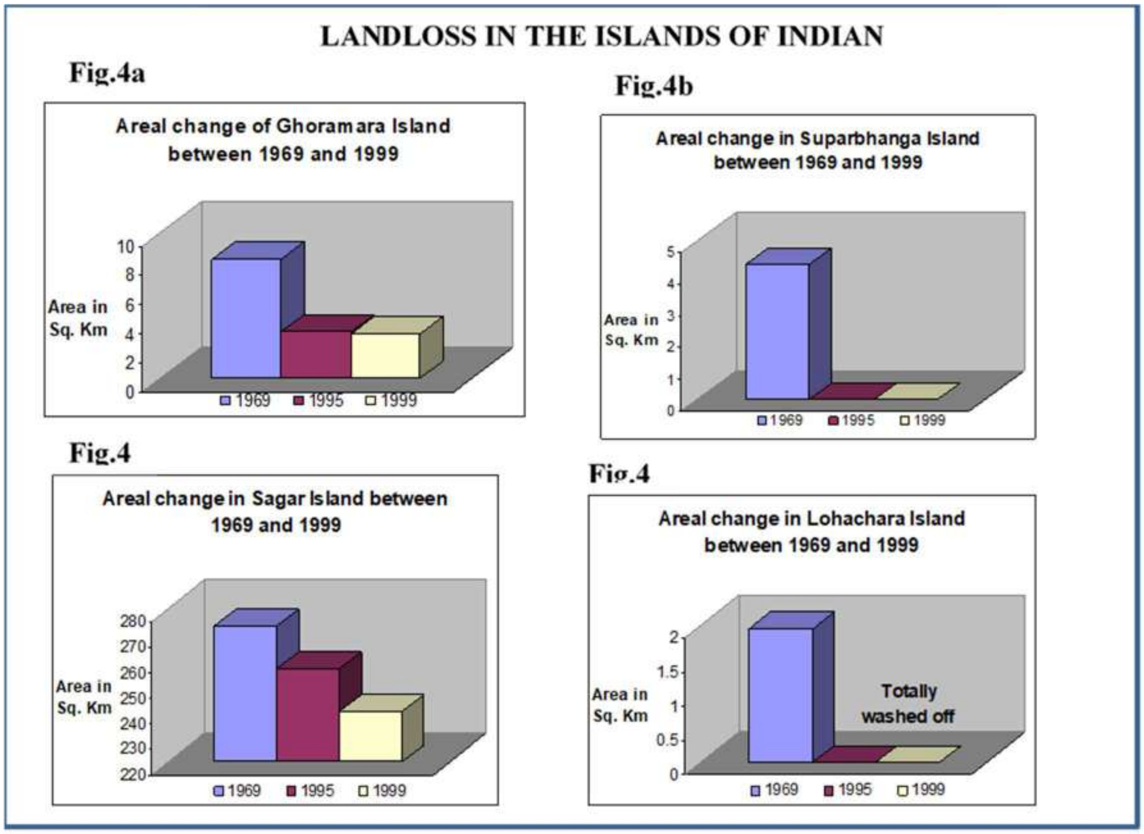

Source : Hazra et. al., 2003

Infact, the rise in the mean sea level by 50 cm, rise in wind velocity during high intensity cyclones and rise in the surge height which may be more than 3.5 meter during once in a 50 year storm pose a serious threat to flood and inundation in vast areas of Sundarbans. This may lead to colossal loss of life and property.

- **Population explosion in Indian Sundarbans and change in Occupational Pattern**

Census data reveal that Sundarbans has experienced a rise of 281.72% in population size since independence from (1,15,9559 in 1951 to 4,42,6259 in 2011). This spectacular rise in population has resulted to wide scale reclamation, deforestation together with unsustainable resource exploitation practices. In 2001, the population density in Indian Sundarbans was 897 persons per sq. km. and in 2011 the population density figure is 996 persons per sq. km. which indicates a sharp rise of 11.04%.

The population density for the coastal blocks (Sagar, Namkhana, Pathrapratima, Kultali and Gosaba combined) stands to be 645 persons per sq. km. in 2011 and this has also risen from the figure of 2001 which was 561 persons per sq. km (Data Source Census Data 1991, 2001 and 2011).

The population projection of Sundarbans for the year 2021 done in absence of published data indicates that the region might have experienced a population explosion with nearly more than 60 lakhs of inhabitants (Fig.5) . Based on previous Census data of 1981, 1991, 2001 and 2011 it is further anticipated that the coastal blocks (5 in number) might have experienced a growth of 105.68% in population size from 2001 to 2021 while for inland blocks the corresponding figure will be 96.80%.

POPULATION PROJECTION IN INDIAN SUNDARBANS

Fig.5

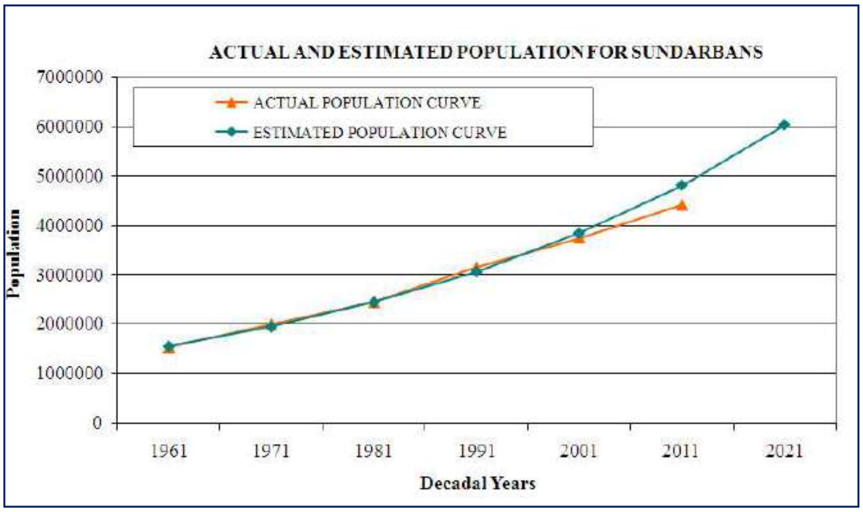

The analysis of workers for all community development blocks of Indian Sundarbans based on Census data further indicates that the percentage of cultivators over has declined significantly while the proportion of landless agricultural labourers has increased (Fig5a).

This may be due to loss in cultivable land by coastal erosion. The rise in the proportion of agricultural labourers further adds to the poverty level resulting in more social vulnerability.

For coastal blocks - Percentage of cultivators and agricultural labourers is relatively less compared to the average Sundarban figs (Fig.5b). On the other hand, the Proportion of household industry workers and other workers (engaged in business, transport or hotel) are more in coastal blocks than the average Sundarban figs (Fig.5b) .

There has also been a marked decrease in the percentage of cultivators in the last decade in coastal blocks. While proportion of agricultural labourers have increased pushing the vulnerability level of these coastal locales to a higher side (Fig5c).

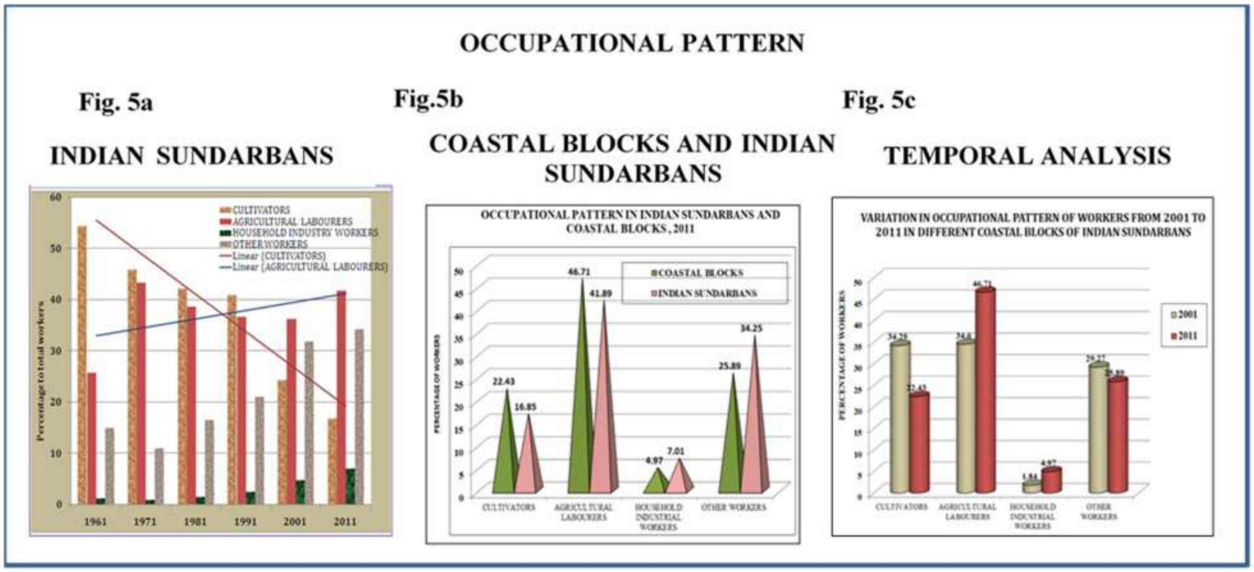

- **Impact of Climate Change on Different Production systems**

Agriculture : Since the British period (last 200 years) the Sundarbans ecoregion is considered as a very fertile detail part of the coastal West Bengal where paddy is the major crop grown in every season year after year. More than 45% of the total workers are still today engaged in the agricultural sector either as cultivators or agricultural labourers. The region is primarily dependent on rainfed aman paddy though Boro paddy is also cultivated in different locales of the island system. The agricultural diversification is very less in Indian Sundarbans. The crop combination maps prepared in the years 1992 -93 and 199-2000 further reveals that even in the early 90s the region used to produce wheat along with paddy. However with a decade the scenario changed and the region turned into a monocrop area producing chiefly the rain fed aman paddy.

Another interesting point to note regarding the relation between the aman paddy productivity with both monsoon and post monsoon rains is provided below :

➢ There is a rising trend in the both monsoon and post monsoon rains for the whole of South 24 Parganas district of West Bengal from 1980 to 2015 (Centre –Alipore, IMD data) shown in Fig. 6.

➢ However, the productivity of Aman paddy is showing a declining trend with rise in the monsoon and post monsoon rainfall when regressed (Fig. 7a and 7b).

This observation is really striking under climate change situation because if this trend continues ten surely it is going to increase the vulnerability of the farmers in the region.

Fig.7a

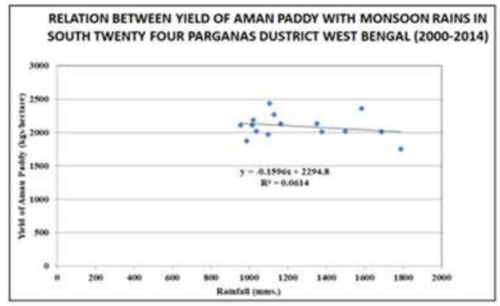

Fig.6

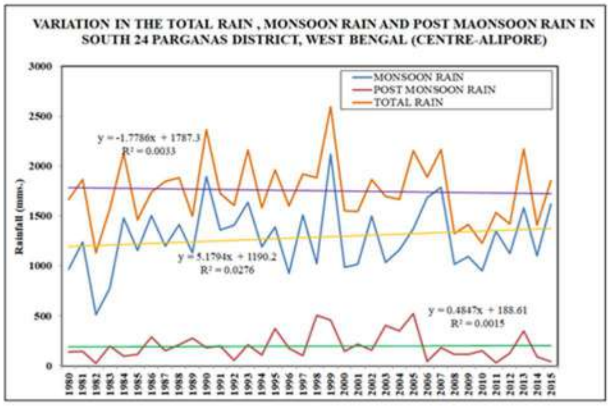

Fig.7b

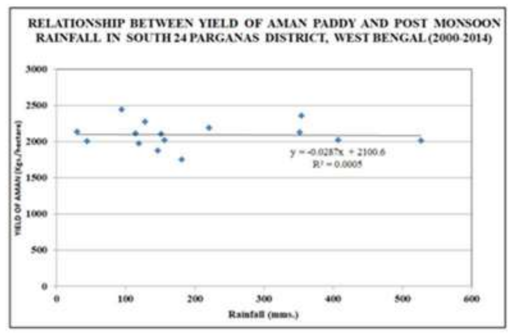

The net sown area under both paddy and Boro has also fallen in the period from 2000-`01 to 2014-`15` in Indian Sundarbans though there has been a slight increase in the cropping intensity and productivity of both Aman and Boro paddy within the same time frame .

Different rounds of surveys conducted in different coastal villagers of Gosaba, Sagar and Namkhana in 2004, 2006, 2015 and 2019 have revealed that rise of salinity and uncertainty in the rainfall conditions have led to major problems for crop growth in the Indian Sundarbans. Fragmented small size of landholdings also pose major problems for agriculture development and expansion . The villagers have also opined the problem of very less crop diversification to be another reason for declining agricultural production in these locales.

Fisheries: In Indian Sundarbans, within the 15 years time span i.e. from 1984-`85 to 2002`-03, the catch per unit effort is found to be declining. This has occurred mainly due to over fishing. Under this situation, if warming continues in the region under climate change scenario, the plankton production may get adversely affected in future and may lead to further reduction in fish stock. This will endanger the livelihood and sustenance of the ecological community of Sundarbans.

The Hilsa catch that constitutes a major share in the overall fish catch has declined from 1981-`82 to 1999-2000. This may be perhaps due to decline in hatcheries ground of Hilsa at the downstream part

Forestry: In addition to agriculture and fisheries the forestry sector is also bearing a negative impact due to climate change. Quite a large number of villagers in Gosaba and Kultali block still earn their family income by collection of forest products like honey, timber etc from the buffer zone of the Sundarban Reserve forest. However, the Indian Sundarbans region has experienced a substantial loss of 116.843 sq. kms. in the forest area cover as has been observed from 1969 to 2001 from satellite data (IRS LISS I image of 1969 and IRS LISS III image of 2001). This is due to coastal erosion as well as from natural degradation and anthropogenic intervention. A trend in the degradation of mangrove forest cover has also been observed along with changes in the existing species combination due to unavailability of sweet water. Some fresh water species like *Heritiera* (Sundari), *Nypa* (Golpata) or *Zylocurpus* (Dhundul & Passur) are already showing a trend of migrating northward, but might not get enough space due to the advancing human habitation front and may thus get extinct unless appropriate adaptation strategies are taken.

- **Change in Landuse Pattern in different islands of Indian Sundarbans**

Throughout the Indian Sundarbans a large scale change in the landuse pattern is taking place presently due to rise in salinity in the soil and estuarine waters. In coastal blocks there has occurred a marked increase (164.65% rise) in aquaculture area from 1986 to 2004 **(40.76 sq. kms. in 1986 to 107.87 sq. kms. in 2004)** compared to the inland blocks of where there has only been **42.87%** rise. This may be due to saline water ingression in the agricultural fields making the fields infertile especially after the cyclone events that have become very frequent in recent years under the climate change situation. The change in the landuse pattern at the expense of agricultural lands as found from satellite data in different islands of the coastal blocks of Indian Sundarbans is shown in Fig. 8 (below). It is apprehended that if this massive change of landuse continues in the region in future then the problem of food insecurity may get initiated at any time under climate change scenario

CHANGE IN THE LANDUSE PATTERN OF DIFFERENT ISLANDS OF COASTAL BLOCKS IN INDIAN SUNDARBANS (1986-2004)

Fig.8

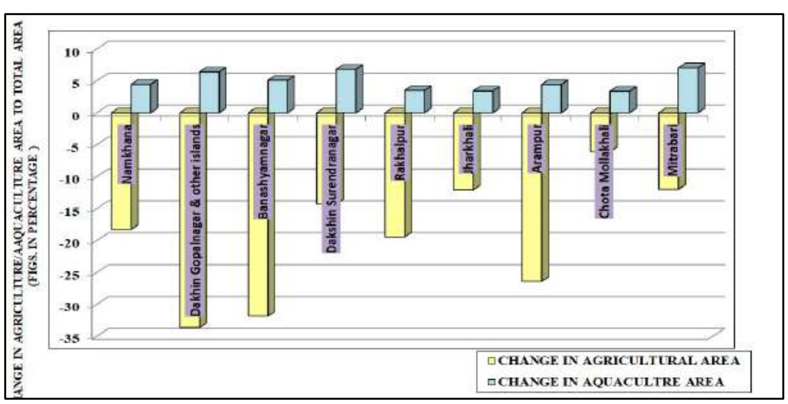

Economic Condition and Human Development Status of the Inhabitants

Indian Sundarbans is an economically depressed zone where more than 90% people live in rural areas. The people are mostly unskilled and under-educated to get absorbed in secondary or tertiary activities. So till date their livelihood is dependent on agriculture and fishing mostly in the coastal blocks. However the sustainability of these production systems are getting threatened day by day due to climate change issues. Hence the social vulnerability is rsing in the region and the coping capacity of the people is reducing fast.

The Rural Households Survey conducted by Development and Planning Department, Govt. Of West Bengal in 2005 revealed that the percentage of households below poverty line in Indian Sundarbans was 44% . For blocks located in the inland parts near to Kolkata metropolis, the economic condition is relatively better since the job opportunities for the male workers are more compared to the coastal blocks lying far away from the metropolis. Infact for all the coastal blocks like Sagar, Namkhana, Patharpratma, Kultali and Goaba the percentage of households below poverty line is above the average figure of Sundarbans.In the inland blocks ,the landless agricultural labourers with average per capita per month income of Rs. 300 to 400/- are the most vulnerable groups in terms of their income while in the coastal blocks the meen seed collectors is the most vulnerable economic group with per capita per month income ranging from Rs. 300 to Rs. 500/- . This is less than the landless agricultural labourers in the coastal locations. The aqua-culturists group with average per capita per month income of Rs. 15000 to 16000/- owing to export earnings holds much better position than other occupational groups in Sundarbans.

The Human Development Index value for the whole Sundarbans region (as obtained from individual block level data) is **0.549 i.e. 0.55**. This is much low compared to the State's average HDI figure of 0.61. (Source : Human Development Report, North and South 24 Parganas, West Bengal 2009). Interesting to find that the average HDI for coastal blocks stands to be **0.56** while for inland blocks, the figure is **0.52**. This HDI scenario indicates that the people's well being in Sundarbans is much lagging behind compared to other parts of the state. If proper developmental and adaptive measures are not taken the human development status may further worsen in future under climate change scenario

Sundarbans do not have any industrial development to offer jobs for the people. Hence in absence of suitable job opportunities many youths from the Indian Sundarbans are now migrating to other nearby states and to Kolkata metropolis for offering themselves as casual labourers in construction activities or as delivery boys mostly in the unorganized sector having no proper terms and conditions for their jobs . They are subjected to different kinds of exploitation by their employers. Again since they leave their elderly family members with children and females in their native villages the physical coping capacity of these masses during calamities gets further reduced.

Feasible Management Strategies

At this backdrop therefore, some fruitful adaptation strategies and mitigation measures are suggested to increase the coping capacity of the vulnerable coastal community . These are listed below

- ❖ To boost up the agricultural production in the region under the scenario of rising salinity many researchers working in the similar fields have opined that it will be more viable to revert to salt-tolerant varieties of rice**.** Hamilton and Malta varieties of paddy may be introduced in the Sundarbans.
- ❖ The role of village administration is very crucial in facilitating, monitoring and accessing the schemes of National and State Governments that will enhance the coping capacity of the vulnerable communities. This will enable the households to build resilience to natural hazards events and other weather-related shocks.
- ❖ To ensure no poverty, good well-being and zero hunger the village administration has to play a fundamental role in the identification of the vulnerable sections of the community and their needs. These exercises would ensure that families are covered and included in the Public Distribution System.
- ❖ For imparting Quality Education and to ensure gender equity the village administration can plan for more residential schools for children, both boys and girls. It can also ease access to scholarships, textbooks, uniforms, and meals. The village council can also facilitate vocational evening courses for both school children and school dropouts.
- ❖ To ensure decent work and economic growth the local village administration may take major initiatives to provide assistance and training to youths both male and female, to start small and medium businesses.

Concluding Remarks

High intensity events under climate change situation often result in irreparable losses and impede long-term development prospects in climate volatile hotspots like Sundarbans . The local village administration here can play a crucial role to facilitate awareness about climate change and climate variability on the lives and livelihoods of people in the community. Micro level vulnerability assessments are required to be conducted by the village administration.. Community-based management of forest areas through the Joint Forest management scheme is operational in the region which may prove to be fruitful for restoring the degraded mangrove forests. These should be further linked with Mahatma Gandhi National Rural Employment Guarantee Scheme where local species of mangroves and other tree and plant species should be promoted. Further awareness on conservation of forests should be developed, especially given the uncertainties of weather and extreme weather events. Community participation is the key word for ensuring developmental activities in Indian Sundarbans in a sustainable way to manage climate change and climate volatility effectively by empowering local people to become active agents in creating resilience. Finally, decentralization and coordination in the planning process together with the assurance of huge technical assistance and hence huge fund from both within and outside the nation is very much needed to save our beloved Sundarbans from getting extinct in the near future.

References :

1. Census of India, 1961. District Census Handbook, Village and Town-wise Primary Census Abstract, Series 23. 24 Parganas. West Bengal

2. Census of India, 1971. District Census Handbook, Village and Town-wise Primary Census Abstract, Series 23. 24 Parganas . West Bengal

3. Census of India, 1981. District Census Handbook, Village and Town-wise Primary Census Abstract, Series 23. Part XIII B, 24 Parganas . West Bengal

4. Census Report. 1991. District Census Handbook. 24 Parganas, Part XII-B.

5. Census of India 2001, Primary Census Abstract, Orissa and West Bengal in CD. Published by Office of the Register General, India, New Delhi.

6. Census of India 2011, Primary Census Abstract, Orissa and West Bengal in CD. Published by Office of the Register General, India, New Delhi

7. Chakraborti, P. 1991. Morphostratigraphy of Coastal Quaternaries of West Bengal and Subarnarekha Delta, Orissa. Indian Jour.Earth.Scs.vol.18, No 3-4, pp.219-225.

8. Human Development Report, North 24 Parganas, 2009. Published by Development & Planning Department, Govt. of West Bengal.

9. Human Development Report, South 24 Parganas, 2009. Published by Development & Planning Department, Govt. of West Bengal.

10. Hazra S., Sen G., Samanta K., Bhattachraya S., Dasgupta R., 2003. NATCOM Report on Vulnerability Assessment in a Climate Change Scenario: A Pilot Study on Ecologically Sensitive Sundarban Island System, West Bengal, March 2003. Prepared by School of Oceanographic Studies, Jadavpur University. Submitted to Ministry of Environment & Forests, Govt. of India

11. IPCC, 2019: Summary for Policymakers. In: IPCC Special Report on the Ocean and Cryosphere in a Changing Climate [H.-O. Pörtner, D.C. Roberts, V. Masson-Delmotte, P. Zhai, M. Tignor, E. Poloczanska, K. Mintenbeck, A. Alegría, M. Nicolai, A. Okem, J. Petzold, B. Rama, N.M. Weyer (eds.)]. Cambridge University Press, Cambridge, UK and New York, NY, US. https://doi.org/10.1017/9781009157964.001.

KOLKATA CITY AND ITS DETERIORATING SLUM ENVIRONMENT IN TERMS OF HEALTH AND NUTRITION STATUS - ISSUES IN PERSPECTIVE

DR. RAJASHREE DASGUPTA
Assistant Professor of Geography (WBES)
Government Girls' General Degree College, Kolkata

Abstract
Kolkata city is one of the largest urban agglomerations in India having 144 Wards . It is experiencing the emergence of slums in large numbers to accommodate the huge number of people migrating from surrounding regions. The emergence of slums has started since the colonial period when the city was considered as the financial hub of the East India Company. Similar to other third world cities, urban inequality in terms of the access of resources is the prime reason behind the origin of slums in Kolkata. Kundu (2003) also opined that the inequality of resource distribution is the major factor behind the deterioration of a section of urban dwellers. The total slum population in Kolkata as per 2011 Census was 1,409,721 where a considerable volume of urban poor face a diverse deprivation and insecurity of housing and livelihood. As estimated by Kundu (2003), the entire slum population of Kolkata live in about 2011 registered and 3500 unregistered slums in the KMC, containing about 13 million hutments or 338,000 rooms. The easy availability of jobs in the city has attracted huge numbers of migrant population in addition to social and political history of the city. This in turn has led to a number of authorised and unauthorised slums in Kolkata which are identified as Hot spots of poverty having substandard living.

At this backdrop, the present paper has tried to make an overview of the status of slums in terms of health and nutrition profile of slum dwellers in Narkeldanga slum locale of Kolkata city falling under ward number 29 of Kolkata Municipal Corporation. As observed during the study, the continuous deterioration of health and nutrition status of the dwellers in the shanty and unhygienic environment of the slums has resulted to increased number of morbidity cases in the recent years. The paper has relied primarily on a variety of literatures, Government and Non-Government reports related to the origin of slums and its growth since Independence in the city. Data on slum population of Kolkata city has been collected from Census of India report of Government of India, 2001. Primary household surveys on Health and nutrition status have also been conducted in few slums along Narkeldanga Main Road in Ward No. 29 in Kolkata to conduct a preliminary assessment of the livelihood conditions of slum dwellers.

***Key words** : Migration , Growth of Slums, Deprivation, Poverty, Health, Nutrition, Diseases.*

INTRODUCTION :

There has been an extraordinary rise in the process of urbanization throughout the word in the last fifty years. The fastest urban growth is observed in the fringes of cities, resulting to mega-agglomerations of mostly illegal squatter settlements. Growth of cities has led to major rise of urban poverty. However, the process of urbanization has invited a number of problems that include acute shortage of dwelling units, infringement of public land and extension of unauthorized residential colonies. People from rural areas mostly migrate to towns and cities in search of suitable jobs. But in absence of proper place to reside, the migrants usually encroach public land and the sites earmarked for various developmental projects. This results in the rise of unauthorized colonies building tremendous pressure on civic services and may create hindrances in the proper development of cities.

According to Fry, Cousins, and Olivola, (2002) India's urban population has increased by 31.2% between 1991 and 2001—nearly doubling the increase of 17.9% in rural population within the same period. India has experienced 2.32 % rise in urban population from 2021 to 2022. Thirty-five million plus cities are there in India and the three UAs i.e. Urban agglomerations with more than 10 million people knows as mega cities include Greater Mumbai, Delhi and Kolkata, where around 30% to 40% of urban dwellers live in utter poverty. Majority of the urban poor reside in shanty squatter colonies (slums) or on the pavement . Slums have emerged as the end products of failed policies, bad governance, corruption and inappropriate regulations. Each of the failed policies has further contributed to the deterioration of the condition of people and lowering the immense potential of human development that an urban locale may offer. Comprehensive information on the slums is therefore needed for the formulation of effective and coordinated policy for their improvement. The Census of India, a Central Government Organization took initiatives to prepare a systematic data on demography of slum dwellers residing in urban and rural areas from 2001 based on actual count. This has enabled to compile and prepare special tables for slums.

Health is an asset to a person in all the stages of life. However for urban dwellers living in slums, the health problems multiply due to their living conditions, lack of proper sanitation and sewerage, use of contaminated water, improper ventilation, acute shortage of space, crowding and dampness in the homes (Basu, 2006). Besides the environmental hazards, poor nutrition also contributes to the lowering of the resistance of the aged slum dwellers, making them susceptible to infection and chronic diseases finally accounting for the high mortality rate.

Under this backdrop, the present paper intends to perform a baseline assessment of the health and nutrition status of different age group people (infants, children , adults and old) residing in slum areas of an urban area in West Bengal, India. The urban area selected for the assessment is Kolkata, the state capital of West Bengal and a megacity in India hosting a total population of 4,580,544 (as per 2001 Census) with a slum population of 1490811 comprising of 32.54 % of the total population). As per 2011 Census, 31.35% of the total population (4.5 millions) live in slums majority of whom belong to poverty line group. These people serve as domestic workers, daily wage labourers, factory workers, rickshaw pullers, hawkers and security guards. According to Institute of Local Government and Urban Studies (2001), there are 2,011 registered (authorized slums called bustees), and 3,500 unregistered slums (squatter slums) in Kolkata (Kundu, 2003). These slums provide housing to more than 1.5 million people. The living conditions of the people living in these slums along the side of canals, large drains garbage dumps, railway tracks and roads are the worst. The slums do not have proper access to any basic amenities like sanitation and basic drinking water facilities. Majority of the slum dwellers are rag pickers with garbage dumped outside their houses adds to environmental pollution factor. Furthermore the awful living conditions of bustees and squatter settlements make them unfit for human habitation which results in large number of water borne and vector borne diseases like diarrhea, cholera , malaria, typhoid, dengue and tuberculosis among the slum dwellers.

Study Area Selected:

The study area of the present paper is Kolkata City – the State capital of West Bengal consisting of 144 Municipal wards at present. Latitudinally, the region extends from 22^{0} 45`N to $22^{0}$65`N and longitudinally from 88^{0}25`E to $88^{0}$45`E (Fig. 1). The total area covered by Kolkata Municipal Corporation is 187.33 sq. kms. Apart from Kolkata , there is no major urban unit within hundred kilometers of distance The other cities in the Eastern Region of India serve as provincial centres with small populations having limited economic and employment prospects. This has caused an overwhelming attraction of Kolkata in the eastern part of the country. Though the study area includes the whole of Kolkata Municipal Corporation area and secondary information have been collected for the entire region, but for a detailed household survey, a specific ward (Ward no. Ward no. 29 in North Kolkata) has been selected out of 141 wards. Presently the city has 144 wards. However when the study was carried out Kolkata was having 141 wards. So all the maps have been prepared showing 141 wards.

Fig.1

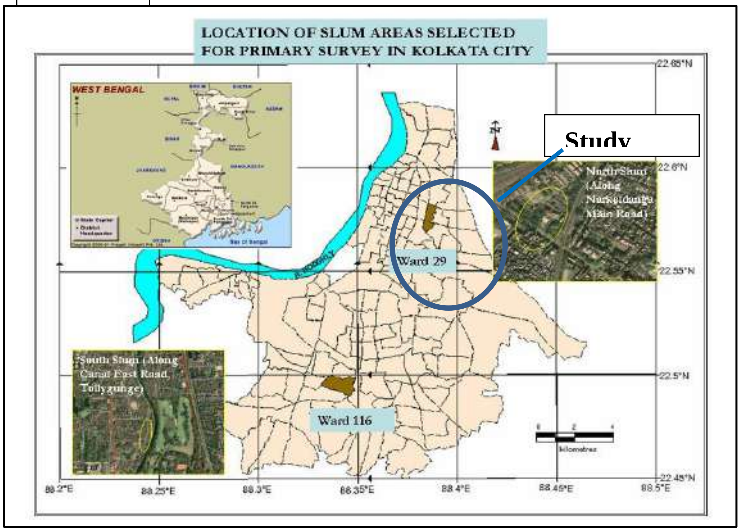

Source : District Planning Map of Kolkata published by National Atlas and Thematic Mapping Organization, Govt. India) .

Central Queries:

The major queries of the present paper include the following

1. What are the general health hazards the Kolkata people are exposed to in different locales? What are the infrastructural facilities (especially govt. and Non-Government Hospitals) at recent times available to Kolkata dwellers?
2. What is the concentration of slum population in different localities of Kolkata city? What infrastructural facilities are available to slum dwellers in different localities within the City?
3. What are the common ailments that strike the different age group people (infants, children, adults and old persons) in the slums of Kolkata? What is the disease profile of slum dwellers in the engaged in different types of activities?
4. What is the nutrition status of different category workers in the slums? Is there any recognizable difference in the disease profile and nutrition status among different category workers in the slums?

METHODOLOGY

For the present study both primary and secondary information have been used. Primary data have been obtained by field visit and stakeholder analysis. The Government organizations from where the secondary information have been collected for the study include Census of India ,Kolkata Municipal Corporation ,Swastha Bhavan , Govt. of West Bengal , Bureau of Applied Economics and Statistics, Govt. of West Bengal

To strengthen, and support the secondary database, primary data have been collected from the slum (under Ward 29 in North Kolkata along Narkeldanga) running a structured questionnaire at the household level. For the household survey in the slum, sample houses were selected following Random Sampling without Replacement method (Source: Mahmood A, 1997) .Here sample size was selected as 5% of the total slum households (2000 households) along the main road of Narkeldanga locality which amounts to a total of 100 households . To carry out the household survey in the slum, the sample houses were selected following Random Sampling Procedure (without Replacement). GIS tools have been used to prepare different thematic maps. Here the maps have been prepared using Arc View GIS Software 3.1 V.

RESULTS AND DISCUSSION :

♣ ***Disease Profile of Kolkata People (In general)***

Kolkata residents mostly suffer from Acute respiratory infection, Acute Diarrheal Diseases, Malaria, Enteric Fever, Chicken pox, PUO(Fever of Unknown Origin), Unusual syndrome and Measles. Variation in the percentage of people affected by different diseases in different boroughs for the year 2009 has been shown in Fig. 2. (Based on the information available from Kolkata Municipal Corporation, the boroughs have been arranged in decreasing order under each of the diseases in table1 (below).

Fig.2

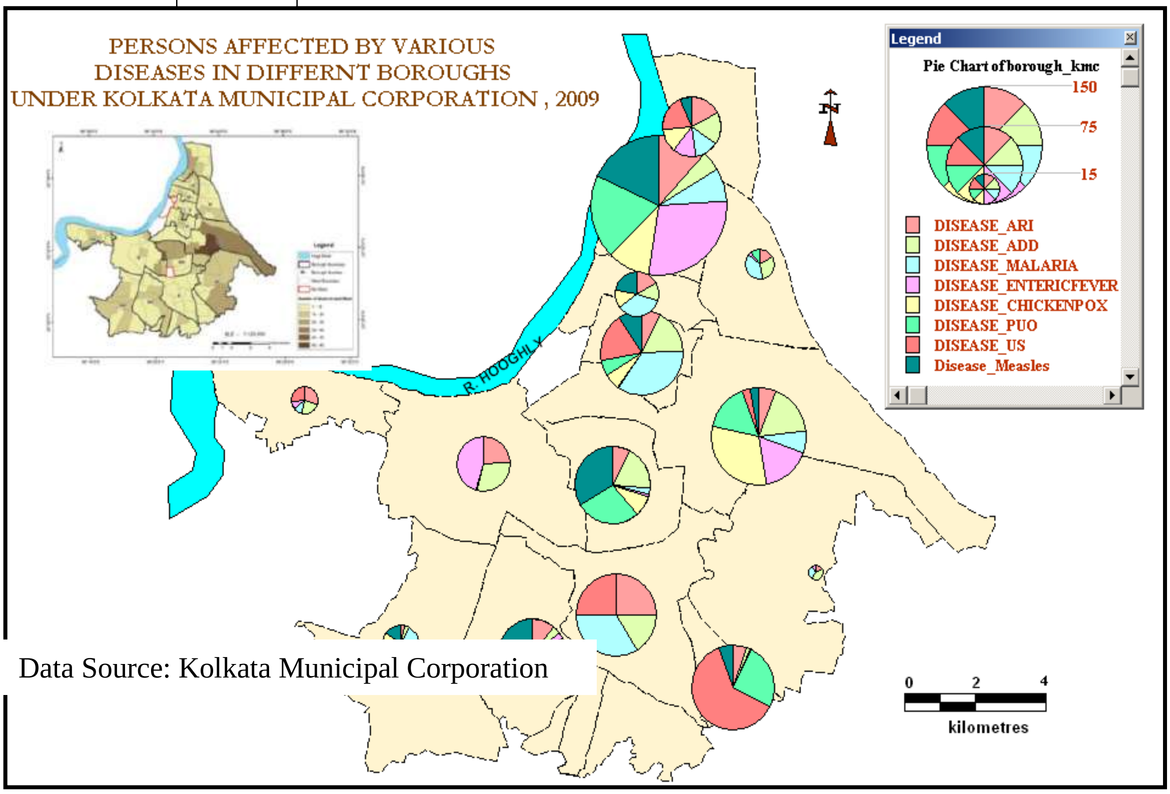

Data Source: Kolkata Municipal Corporation

The above fig. 2 shows that Borough VII located in eastern part of Kolkata Municipal Corporation area is exposed to maximum risks of Acute Diarrheal Diseases and Chicken Pox. The maximum number of people affected by Acute Respiratory Infection (ARI) , Enteric Fever, PUO & Measles is under Borough III (located in northern portion of KMC area). While unusual syndrome is mostly found among the residents of Borough XV located in the southern part of Kolkata city. It has been observed in general that Kolkata residents are affected mostly by Acute Diarrheal diseases (water- borne) , Acute Respiratory Infection (air-borne) and by the viral disease Malaria. Borough III being located near to Baranagar Area (in the extreme northern portion of KMC) where a number of factories are located, there the number of people suffering from Acute Respiratory Infection is relatively high. Moreover, a substantial portion of Borough VII (in the Topsia, Tangra locality in the Eastern Suburban portion) a number of tanneries are located. The wastes from these tanneries gets discharged in the local water bodies thus contaminating the water quality and hence results increased number of acute diarrheal cases in the particular locale.

A vulnerability map (Fig 3) was prepared based on intensity of diseases affecting the Kolkata residents borough wise considering eight diseases frequent in the city limits viz. acute diarrhoeal diseases (ADD), acute respiratory diseases (ARI), malaria, enteric fever, chicken pox, P.U.O , unusual syndromes and measles. Categorization of boroughs has been done on the basis of three vulnerable classes – High medium and low on the basis of total composite scores so obtained by assigning individual ranks to each boroughs under eight different diseases. Under a particular disease, Rank 1 was assigned to that borough where maximum number of people were affected by that disease. After assigning ranks under individual diseases to each borough the ranks were summed up to get a composite value for each of the boroughs (Note: no data was available from KMC for Borough IV). Finally on the basis of composite scores so obtained three classes were categorized viz. Highly Vulnerable (with values ranging from 42 to 57) , Moderately Vulnerable (with values ranging from 26 – 41) and Less Vulnerable (with values ranging from 10-25).

Fig. 3

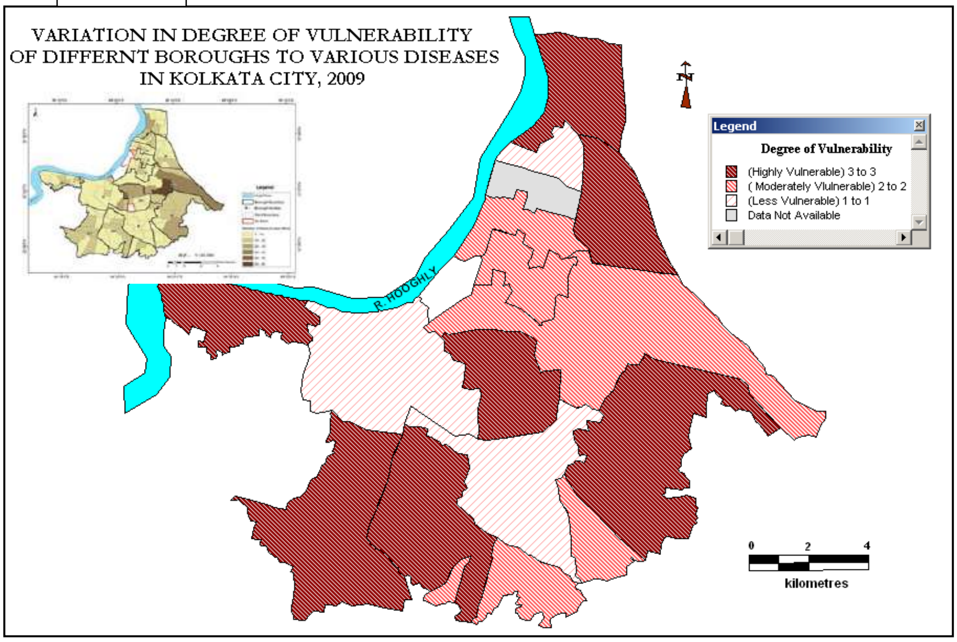

Note : Borough map of Kolkata in the inset provided from the source Mukherjee et. al. 2021

It was observed that highly vulnerable boroughs were distributed randomly in different portions of Kolkata (found in extreme northern parts, south eastern parts, south western part and extreme western parts /port area). Moderately vulnerable boroughs were found in central and southern portions while less vulnerable boroughs occupy south central part of the city.

Concentration of Slum Population & Health Infrastructural Facilities Available to Slum Population

The prime goal of the present study was a preliminary assessment of health and nutrition status of slum dwellers in Kolkata city. For the purpose efforts were taken to prepare a map showing the slum distribution of population in different wards of the city (Fig. 4). To prepare the map LQ figs. have been calculated taking into consideration the total population and the slum population figs. of each of the 141 wards. The distribution of the Kolkata wards under each of the LQ categories is shown in Table 1, wherefrom it is found that excepting few wards (34 in number) all other wards are having slum population. The high concentration of slum dwellers was found mainly in the extreme western part (port area). In North Kolkata, Ward 29 (Narkeldanga area) was having high concentration of slum population while in eastern suburban part ward 58 (in the Topsia, Tangra locality), slum concentration was significant.

(It may be mentioned here that Ward 29 having high concentration of slums was selected in the present study for the household survey)

Fig. 4

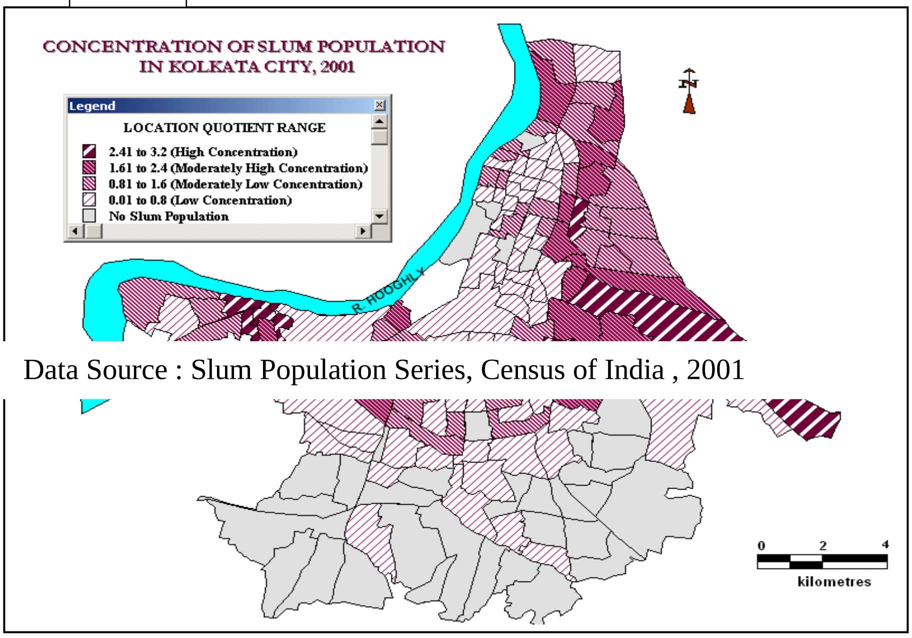

Data Source : Slum Population Series, Census of India , 2001

Table 1 : Distribution Of Wards Under Different LQ Ranges

LQ Range Categories	Ward Nos.	Total
High Concentration	29,58,65,134,135,136,137	7
Moderately High Concentration	6,3,13,14,28,30, 36,56,57,59,66,67,75,79,133	15
Moderately Low Concentration	1,4,5,7,9,15,19,21,24,31,32,33,34,35,37,38,39,44,64,74,76,77,78, 81, 85, 88, 90, 138,139,141	30
Low Concentration	2,10,11,12,16,17,18,20,22,23,25,26,27,40,41,43,46,48,49,51,52,53,54, 55,60,61,62,63,68,69,70,71,72,73,80, 82,83,84,86,89,91,92,93,94,97,98,100, 108, 117,118,120,123,131,132,140	55
No Slum Concentration	8,42,45,47,50,87,95,96,99,101,102,103,104,105,106,107,109,110,111,112, 113,114,115,116,119,121,122,124,125,126,127,128,129,130	34

Source : Computed by the author from Fig. 4 above

Further, to assess the health infrastructural facilities available to the huge number of slum dwellers (as per 2001 Census data), attempts were taken to estimate the beds available per lakh slum population in different wards of Kolkata city. From the respective fig.5 (below) it was observed that majority of the wards have beds varying between 1 to 100 per lakh slum population.

Fig. 5

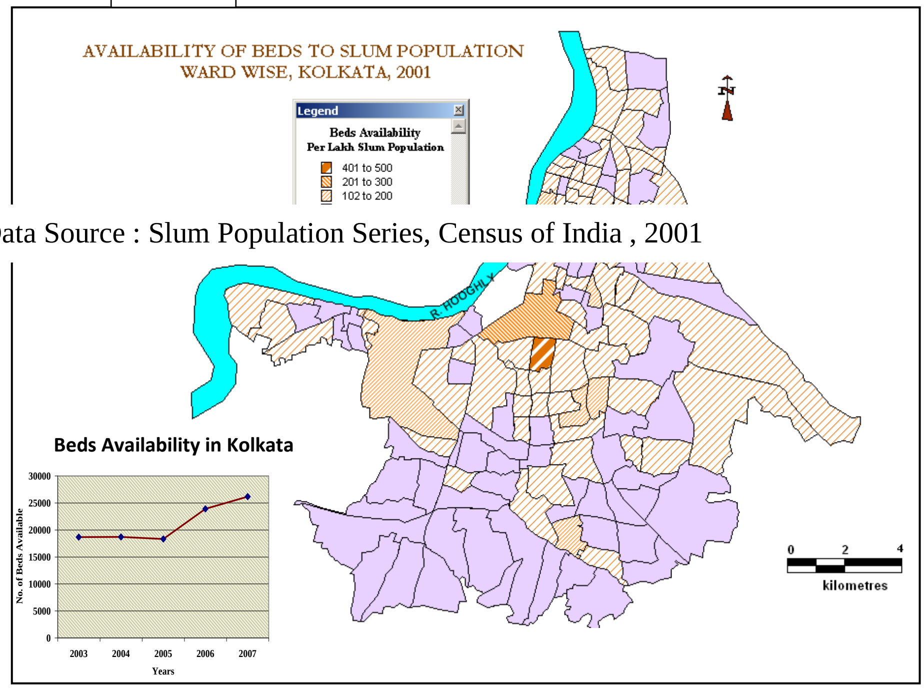

Data Source : Slum Population Series, Census of India , 2001

The wards having bed facilities ranging from 102 to 200 were few in number (only four).The number of beds available to per lakh slum dwellers above 200 was almost negligible. However, in absolute terms the number of beds in different health units increased markedly after 2003.

Health Hazards Among the Slum Dwellers in the Slums Surveyed

The slum where the major primary survey was carried out for the present study , all age group people (0-1 years, 1-12 years, 12-18 years, 18-45 years; 45-60 years and above 60 years) were considered to assess the health and nutrition status. The sex ratio was very high in the North Kolkata slum located in ward 29. Compared to south Kolkata slum that is located in Ward 116 (surveyed earlier in the year 2008) having sex ratio 932, this north slum had a higher sex ratio. The work participation rate was however found to be higher in south Kolkata slum compared to North Kolkata. This has resulted to higher dependency ratio in the North Kolkata slum compared to south Kolkata. The majority of the slum dwellers in Ward 29 were engaged as craftsman, drivers, shopkeepers, domestic maids and cobblers besides casual labourers .

The incidences of such diseases like malaria (vector borne), tuberculosis (air-borne), jaundice (water borne), bronchitis (also air-borne) were found to be high among the working age group belonging to 18-45 years. However, it was observed among the infants (with age varying between 0-1 years) and children (1-12 years) that they mostly suffer from fever; while the aged persons (with age above 60 years) mostly suffer due to Gastritis and ill digestion problem. Earlier study conducted at a South Kolkata slum in ward 116 revealed that the adult persons (with age 18-45 years) were also suffering from thyroid problem which was not found in case of north slum along the Narkeldanga main road.
A significant percentage of drivers suffer mostly by gastritis, malaria, diabetes, heart diseases, high blood pressure, tuberculosis and bronchitis. The high incidences of tuberculosis and bronchitis are likely to be high among the drivers because of the nature of their jobs. The drivers are constantly exposed to the risks of vehicular air pollution. The incidences of gastritis are relatively more common among business men and cobblers. A significant percentage of cobblers also suffer from malaria, diabetes, sinusitis and bronchitis problems. Under diarrhoea, the percentages of people who are mostly affected are engaged in construction works. These people also do suffer largely from sinusitis problem. Business man, attendants and domestic maids (primarily females) mostly suffer from

gastritis problems and high blood pressure. The incidences of cases being affected by high blood pressure are also high among the craftsmen (engaged in handicrafts).
The probable reasons of the presence of such high incidences of tuberculosis and bronchitis in the north slum may be due to vehicular congestion and hence automobile pollution (being situated along Narkeldanga Main road) Moreover the frequent uses of chullas by the dwellers in the houses and in the commercial food-stalls (which the dwellers run to earn income) might have worsened the air quality status of the locality. A number of small size factories are also located near this north slum, whose wastes get discharged in the nearby water-bodies deteriorating the water quality. This results in large number of cases under cholera – the disease which is not frequently found in South Kolkata slums.

Nutrition status of the Slum Dwellers

The *Food Insecurity Atlas of Urban India* (MSSRF 2002) has estimated that Urban India has approximately 38 per cent of children below the age of three years in suffering from underweight problems and more than 35 per cent short for their age. The nutrition norms laid down by the Indian Council of Medical Research (ICMR) has become very difficult for the urban poor to meet. According to Ghosh and Shah, 2004, nutritional problems like protein energy malnutrition (PEM), anemia and vitamin A deficiency are much more common among the urban slum children compared to the rural children. The same source has inferred that poor maternal nutrition arises because of low birth weight, inadequate breastfeeding, delayed and insufficient complementary feeding. This may be due to inadequacy in the access to food, health, environmental and caring resources among the slums. Added to this issue is the lack of awareness and knowledge among the slum dwellers regarding the food requirements and lack of responsible adult care giver also results in high prevalence of malnutrition among young children.
In the north slum area, among the male residents, the proportion of underweight persons under different age groups viz. infants (0-1 years), children (1-12 years), adolescence (12-18 years), adults (18-45 years) and aged (above 60 years) were all high excepting the adults whose age vary between 45-60 years. Among the females, the percentage of underweights of infants (0-1 years), adolescence (12-18 years), adults (18-45 years) and aged persons (above 60 years) were also high compared to healthy, overweight and obese persons. Unlike the north slum, the situation in the south slum (survey done in the previous year-2008) is such that among the males, the percentages of healthy persons under different age groups like infants, children, adolescence, adults and old persons are all high compared to underweight persons. Similar to the male category, among the females also, excepting the children and the old persons, the percentage of slum dwellers was high among the healthy category than the underweight.The observation of greater number of people falling in the underweight category under the adult age group (among both males and females) in the north Kolkata slum is really striking because this group comprises the working force on whom the children and old persons depend. Therefore, if majority of the persons in the adult age group are underweight, the chances of people's physical ability to cope with different social and economic problems fall.

Among different category workers in the slum, it was observed that in the north Kolkata slum, the percentage of underweight is relatively high among the cobblers than other category workers. The earlier study of the south slum revealed higher percentages of underweight among the craftsmen, company workers, domestic maids and cobblers than other category workers.

Status of Basic Facilities in the slums

Urban Squatter locales do not have adequate water supply and sanitation facilities. Some settlements have community toilets that are generally unacceptable. Hence in recent times also people in large numbers defecate in pits or in the open or in ditches, canals, or rivers creating a very polluted environment. The public health consequences are severe, especially for young children. (Fry, Cousins & Olivia, 2002). Regular collection of solid waste from the households seldom takes place in these localities. Accumulated waste creates huge amount of garbage which serve as work sites of

scavengers, (mostly children). Garbage dumps also act as breeding sites for rodents and insects, like mosquitoes, which carry dengue and malaria. According to Fry, Cousins & Olivia (2002), biomedical waste poses a special threat to the health of the urban poor.
Furthermore Kolkata suffers from the air pollution problems. The level of air pollution is much more that the maximum tolerance level as defined by World Health Organization. The increasing number of motor vehicles on road together with unregulated industrial activities that emits smoke and particles result in rising number of lung diseases among the city's residents. Having relatively poor means, the slum dwellers often do not get an easy access to adequate medical treatment and hence these disease become chronic among the poor slum residents.

Whether a group lives in urban poverty or not is influenced by such factors like marginalization, unawareness, illiteracy, class or caste status, and gender. Cities have "relative inequality," where poverty is not absolute but measured by the opportunities and resource differences between "haves" and "have-nots". This regional disparity in terms of opportunities and resource access was also observed when two consecutive studies were made in Kolkata – one in South Kolkata (in ward 116) in 2008 and another in Ward 29 along Narkeldanga main road in north Kolkata in 2009. The average family income in the north slum ranges between Rs. 700 to Rs. 18000/- while in the south slum the range varies from Rs. 1000/- to Rs. 16000. Depending on the income categories the proportion of medical expenses also vary from one income group to another. The lowest medical expenses was found among those who belong to below poverty level (Below Rs. 1000/- per family per month) while the highest medical expenses was observed among the income group with more than Rs. 10000/- per family per month income. Social and economic disparities weakens urban poor communities. A majority of urban poor households headed by women are compelled to earn a living for the family. This state has major consequences on the health status and mental development of small children. Small children are often engaged in the workforce who mostly works in the informal economic sector at the lowest paying.
Through primary household investigation, it was revealed that though the slum residents in both localities rely primarily on allopathic medicine, due to expensive allopathic treatment, a significant number of dwellers at present (10 to 15%) are presently relying on homeopathy medication. For emergencies the residents of North Kolkata slum mostly approach Nilratan Sarcar Medical College (NRS) located within a distance of seven-eight kms. from the locality. The slum dwellers consult the physicians occasionally (when the need arises). None of the dwellers go for regular health treatment. Further it was revealed from field survey that the awareness among the slum dwellers regarding the courses of vaccination (like BCG, TT, Polio & DPT) was quite impressive and almost 100% infants and children (among the households surveyed) were vaccinated depending on their respective ages. In the slum, the major sources of drinking water is tubewells (with depths varying from 400 to 500 ft.) and water supply by Municipal corporation at definite hours per day (three times – two hours in the morning, one hour at afternoon and 30 minutes at evening) through pipe lines. Due to inadequate number of public latrines in the slum till date a significant number of slum dwellers (around 70%) depend on open air defecation thus polluting the local environment.. The private latrine use among the slum dwellers is almost negligible.

Governmental Measures to tackle Health Problems in General

For the eradication of poverty the State Government so far has proposed and implemented a number of policies. In most of the cases the programmes are targeted at the slum dwellers. Infectious diseases like diarrhea, ARI and measles results into malnutrition problems among the children. overcrowded housing in the cities has lead to major deterioration of the health condition among the urban poor. Thus improvement of environmental sanitation, provision of safe drinking water and modification of personal hygiene and health seeking behaviors are the basic requirements to improve health and nutritional status of urban poor. Infact, any nutritional program may fail under the in absence of proper sanitation, proper health care and proper personal hygiene.
The standard of living of the slum dwellers was a concern even during colonial rule. However, only after the formation of the Calcutta Improvement Trust in 1913 some initiatives were taken for 'area

development' and slum clearance, which is absolutely needed to offer the urban slums a healthy environment to live in.

In the north Kolkata slum surveyed during the present study, the benefits of Kolkata Slum Improvement Project (SIP) was noticed where a good number of community latrines were constructed to tackle the environment pollution problem in the slums A small number of slum dwellers (with age above) in both the localities were getting some financial benefits under the National Old Age Pension Scheme. The percentage of these category people is around 3% in the north slum and around 2% in the south slum. 2% of the pregnant women in the south slum has also get financial benefits under the National Maternity Benefit Scheme (NMBS). Moreover under the universal immunization programme in both the slums 100% infants and children have been covered for vaccination at their different ages.

Inspite of so many programmes initiated by the State Government for the Slum Improvement, ***Kolkata Slum Improvement Project (SIP); the EIUS (Environment Improvement In Urban Sector)*** ; ***Neheru Rozgar Yojana (NRY)*** in 1989 ; ***Prime Minister's Integrated Urban Poverty Eradication Programme (PMIUPEP)in 1994*** ; these the ***National Slum Development Programme (NSDP), National Old Age Pension Scheme (NOPS); the National Maternity Benefit Scheme (NMBS); the Family Benefit Programme (***aimed at Below the Poverty Line category) due to absence of proper institutional arrangements and lack of convergence efforts of different departments of Kolkata Municipal Corporation (KMC), the progress of all these schemes are not very impressive. .

CONCLUDING REMARKS

The present micro level study has tried to assess the status of slum environment in terms of health hazards and health care facilities available to slum dwellers in the Kolkata city based on a sample study of a north Kolkata Slum located in Ward 29 along Narkeldanga main road . Comparisons regarding health and nutrition status of this slum dwellers were made with a South Kolkata slum (located in ward 116). It was observed that marked differences lie across the slums in terms of income, provisional facilities of drinking water, sanitation and living conditions. In general however, the stressful living conditions in slums pose a direct bearing on the strength of body and mind. The unacceptable environmental and economic conditions result in malnutrition problems among different age group people in the localities. Due to poor hygiene conditions the incidences of such diseases as diarrhea, jaundice, and cholera are relatively high in slums compared to non-slum areas. The observations from the slums in Kolkata even in the last five years from 2015 onwards is that the overall conditions for living has not improved much in the last two decades and the slum residents are increasingly getting affected by such respiratory diseases as bronchitis, asthma, acute respiratory infection, tuberculosis, lung and heart diseases owing to rising levels of air pollution in the city. The number of vector borne diseases like Dengue is also found frequently among these dwellers. Due to absence of open spaces in the slum locales (because of overpopulation and congestion) majority of the children suffer from developmental complexes and physical imbalance.

The preliminary observation on the status of institutional medical facilities available to the slum dwellers in Kolkata city is still very inadequate. Hospitals, health care centres and charitable dispensaries offer meager assistance and the slum residents have to remain satisfied with such kind of scanty services. The growing dependence on western medicines (under allopathic medication) also compels the poor dwellers to shift to other types of medication like homeopathic and ayurvedic. However, from self medication to a full fledged disease care, the familial support plays the most vital role as an informal care-giving unit.

In recent years (last 15 to 20 years), the Central and the State Governments have undertaken a number of programmes for the improvement of the urban poor. However, due to lack of institutional arrangements and coordination among different departments of the Kolkata Municipal Corporation the performance and the progress of these schemes is not very impressive. Promotion of private-public partnerships along with self help group activities are expected to solve the local problems especially in slums to some extent.

ACKNOWLEDGEMENT

I extend my thanks to one of my former post graduate student Ms. Manti Sarkar from Dept. of Geography, Krishnagar Government College, Krishnagra, Nadia for helping me to collect a large volume of household data from the two slums (both from north Kolkata and south Kolkata) for the present study

REFERENCES

[1] **Kundu, N, 2003.** *The case of Kolkata, India. Published in the Journal of* UNDERSTANDING SLUMS: Case Studies for the Global Report on Human Settlements

a. (Site Reference : www.ucl.ac.uk/dpu-projects/Global_Report/pdfs/Kolkata.pdf)

[2] **Fry, S., Cousins, B. and Olivola, K., (2002).** Activity Report 109 on Health of Children Living in Urban Slums in Asia and the Near East : Review of Existing Literature and Data. Prepared for the Asia and Near East Bureau of USAID under EHP Project.

[3] (Site Reference : www.ehproject.org/.../Activity_Reports/AR109ANEUrbHlthweb.pdf)

[4] **Basu, S., 2006. Health and Health Care IN Twilight Years-Reflection from Kolkata Slums. Published in Book entitled** Environment Drinking Water and Public Health: Problems and Future Goais. (Ed.)Arnab Ghosh. Publishede by Daya Publishers.

[5] Available at www.infibeam.com/Books/info/...**health**.../9788170354819.html

[6] Slum Population (India) Series –1.Census Of India 2001, Published by Census of India Organization, Govt.. of India

[7] Census Of India 2011, Published by Census of India Organization, Govt.. of India

[8] **Mahmood , A, 1977.** "Statistical Methods In Geographical Studies. Published by Rajesh Publications, New Delhi.

[9] **Ghosh, S and Shah D(2004).** Nutritional Problems in Urban Slum Children. A Special Article Series. Published in Journal of Indian Pediatrics – Environment Health Project . Volume 41, 2004

[10] **Mukherjee S, Sikdar, P.K., Pal S., and Schutt B. March 2021 . Article on "**Assessment of Environmental Water Security of an Asian Deltaic Megacity and Its Peri-Urban Wetland Areas**"**. Published in Sustainability Journal. Vo-13 3(2772):2772

[11] Kolkata District Statistical Handbook, 2007. Published By Bureau Of Applied Economics and Statistics, Govt. Of West Bengal

[12] Project summary on Kolkata Environmental Improvement Project (Supplementary Loan) : India. Prepared By Asian Development Bank

[13] (Site Reference : Http://Www.Adb.Org/Projects/Project.Asp?Id=29466)

[14] "Struggling for survival: slums. May, 2010. An article published in Express India. Available at Site : http://www.expressindia.com/latest-news/Struggling-for-survival-slums/314573/

[15] West Bengal Human Development Report, 2004. Published by Development and Planning Department, Govt. of West Bengal .

[16] Site Reference :

[17] http://59.160.153.188/library/node/275

[18] https://www.ucl.ac.uk/dpu-projects/Global_Report/home.htm

Regular Article - Quantum Information | Published: 17 February 2021

Any two-qubit state has nonzero quantum discord under global unitary operations

Kaushiki Mukherjee, Biswajit Paul & Sumana Karmakar

The European Physical Journal D **75**, Article number: 65 (2021)

Abstract

Quantum discord is significant in analyzing quantum nonclassicality beyond the paradigm of entanglement. Presently, we have explored the effectiveness of global unitary operations in manifesting quantum discord from a general two-qubit zero discord state. Apart from the emergence of some obvious concepts such as absolute classical-quantum and absolute quantum-classical states, more interestingly, it is observed that set of states characterized by absoluteness contains only maximally mixed state. Consequently, this marks the peak of effectiveness of global unitary operations in purview of manifesting nonclassicality from arbitrary two-qubit state when other standard methods fail to do so. A set of effective global unitaries has been provided in this context. Our observations have direct implications in remote state preparation task.

Graphic Abstract

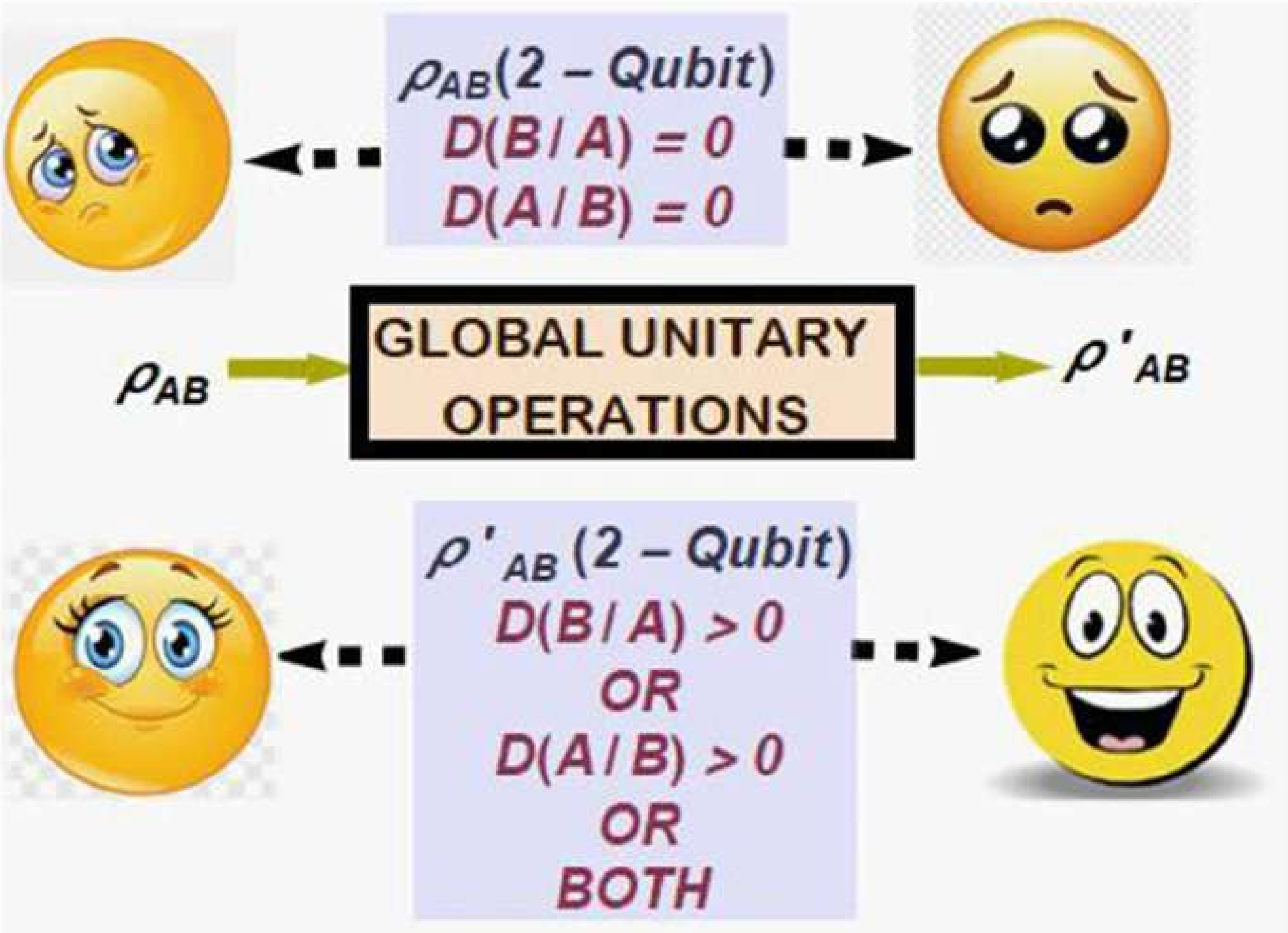

Data Availability Statement

This manuscript has associated data in a data repository. [Authors' comment: This manuscript has associated data in arxiv.org(quant-ph). Arxiv number is: arXiv:2004.12991(quant-ph).]

References

1. 1.
   R. Horodecki, P. Horodecki, M. Horodecki, K. Horodecki, Rev. Mod. Phys. **81**, 865–942 (2009)

2. 2.
   S. Sazim, I. Chakrabarty, Eur. Phys. J. D **67**, 174 (2013)

3. 3.
   M. Hillery, V. Buzek, A. Berthiaume, Phys. Rev. A **59**, 1829 (1999)

4. 4.
   S. Adhikari, I. Chakrabarty, P. Agrawal, Quantum Info. Comp. **12**, 0253 (2012)

5. 5.
   S. Sazim et al., Quantum. Info. Process. **14**, 4651 (2015)

6. 6.
   C.H. Bennett, S.J. Wiesner, Phys. Rev. Lett. **69**, 2881 (1992)

7. 7.

I. Chakrabarty, P. Agrawal, A.K. Pati, Quantum Inf. Comput. **12**, 0271 (2012)

8. 8.
C.H. Bennett et al., Phys. Rev. Lett. **70**, 1895 (1993)

9. 9.
R. Horodecki, M. Horodecki, P. Horodecki, Phys. Lett. A **222**, 21 (1996)

10. 10.
A.K. Ekert, Quantum cryptography based on Bell's theorem. Phys. Rev. Lett. **67**, 661–665 (1991)

11. 11.
C. Brukner, M. Zukowski, J.-W. Pan, A. Zeilinger, Bell's inequalities and quantum communication complexity. Phys. Rev. Lett. **92**, 127901–127905 (2004)

12. 12.
H. Buhrman, R. Cleve, S. Massar, R. de Wolf, Nonlocality and communication complexity. Rev. Mod. Phys. **82**, 665–698 (2010)

13. 13.
G. Passante, O. Moussa, D.A. Trottier, R. Laflamme, Experimental detection of nonclassical correlations in mixed-state quantum computation. Phys. Rev. A **84**, 044302–044306 (2011)

14. 14.

E. Knill, R. Laflamme, Power of one bit of quantum information. Phys. Rev. Lett. **81**, 5672–5675 (1998)

15. 15.
C.A. Ryan, J. Emerson, D. Poulin, C. Negrevergne, R. Laflamme, Characterization of complex quantum dynamics with a scalable NMR information processor. Phys. Rev. Lett. **95**, 250502–250507 (2005)

16. 16.
D.A. Meyer, Sophisticated quantum search without entanglement. Phys. Rev. Lett. **85**, 2014–2017 (2000)

17. 17.
B.P. Lanyon, M. Barbieri, M.P. Almeida, A.G. White, Experimental quantum computing without entanglement. Phys. Rev. Lett. **101**, 200501–200505 (2008)

18. 18.
K. Modi, A. Brodutch, H. Cable, T. Paterek, V. Vedral, Rev. Mod. Phys. **84**, 1655–1707 (2012)

19. 19.
H. Ollivier, W.H. Zurek, Phys. Rev. Lett. **88**, 017901 (2001)

20. 20.
L. Henderson, V. Vedral, J. Phys. A Math. Gen. **34**, 35 (2001)

21. 21.

A. Datta, A. Shaji, C.M. Caves, Phys. Rev. Lett. **100**, 050502 (2008)

22. 22.
Borivoje Dakic, Vlatko Vedral, Caslav Brukner, Phys. Rev. Lett. **105**, 190502 (2010)

23. 23.
A. Datta, Phys. Rev. A **80**, 052304 (2009)

24. 24.
M.D. Lang, C.M. Caves, A. Shaji, Int. J. Quantum Inform. **09**, 1553–1586 (2011)

25. 25.
A. Ferraro et al., Phys. Rev. A **81**, 052318 (2010)

26. 26.
B. Bylicka, D. Chruscinski, Phys. Rev. A **81**, 062102 (2010)

27. 27.
J. Maziero, R.M. Serra, Int. J. Quantum Inf. **10**, 1250028 (2012)

28. 28.
D. Girolami, G. Adesso, Phys. Rev. A **83**, 052108 (2011)

29. 29.
K. Mukherjee, S. Karmakar, B. Paul, D. Sarkar, Detecting two qubit both-way positive discord states. Eur. Phys. J. D **73**, 188 (2019)

30. 30.

L. Roa, J.C. Retamal, M. Alid-Vaccarezza, Dissonance is required for assisted optimal state discrimination. Phys. Rev. Lett. **107**, 080401–080405 (2011)

31. 31.
D. Cavalcanti et al., Operational interpretations of quantum discord. Phys. Rev. A **83**, 032324–032329 (2011)

32. 32.
M. Piani, P. Horodecki, R. Horodecki, No-local-broadcasting theorem for multipartite quantum correlations. Phys. Rev. Lett. **100**, 090502–090507 (2008)

33. 33.
V. Madhok, A. Datta, Role of quantum discord in quantum communication. Preprint at arXiv:1107.0994 (2011)

34. 34.
V. Madhok, A. Datta, Interpreting quantum discord through quantum state merging. Phys. Rev. A **83**, 032323–032327 (2011)

35. 35.
A. Datta, A. Shaji, C.M. Caves, Quantum discord and the power of one qubit. Phys. Rev. Lett. **100**, 050502–050507 (2008)

36. 36.
D.A. Meyer, Sophisticated quantum search without entanglement. Phys. Rev. Lett. **85**, 2014 (2000)

37. 37.
E. Knill, R. Laflamme, Power of one bit of quantum information. Phys. Rev. Lett. **81**, 5672 (1998)

38. 38.
S.L. Braunstein et al., Separability of very noisy mixed states and implications for NMR quantum computing. Phys. Rev. Lett. **83**, 1054 (1999)

39. 39.
A. Datta, S.T. Flammia, C.M. Caves, Entanglement and the power of one qubit. Phys. Rev. A **72**, 042316 (2005)

40. 40.
J.M. Matera, D. Egloff, N. Killoran, M.B. Plenio, Coherent control of quantum systems as a resource theory. Quantum Sci. Technol. **1**, 1 (2016)

41. 41.
B. Dakic et al., Nat. Phys. **8**, 666 (2012)

42. 42.
L.G. Giorgi, Quantum discord and remote state preparation. Phys. Rev. A **88**, 022315 (2013)

43. 43.
O. Gamel, Entangled Bloch spheres: Bloch matrix and two-qubit state space. Phys. Rev. A **93**, 062320 (2016)

44. 44.

K. Zyczkowski, P. Horodecki, A. Sanpera, M. Lewenstein, Volume of the set of separable states. Phys. Rev. A **58**, 883 (1998)

45. 45.
N. Johnston, Separability from spectrum for qubit-qudit states. Phys. Rev. A **88**, 062330 (2013)

46. 46.
F. Verstraete, K. Audenaert, B. De Moor, Maximally entangled mixed states of two qubits. Phys. Rev. A **64**, 012316 (2001)

47. 47.
N. Ganguly et al., Bell-CHSH violation under global unitary operations: necessary and sufficient conditions. Int. J. Quantum Inf. **16**(4), 1850040 (2018)

48. 48.
S.S. Bhattacharya et al., Absolute non-violation of a three-setting steering inequality by two-qubit states. Quantum Inf. Process. **17**, 3 (2018)

49. 49.
S. Patro, I. Chakrabarty, N. Ganguly, Phys. Rev. A **96**, 062102 (2017)

50. 50.
C.H. Bennett et al., Remote state preparation. Phys. Rev. Lett. **87**, 077902 (2001)

51. 51.

A.K. Pati, Minimum classical bit for remote preparation and measurement of a qubit. Phys. Rev. A **63**, 014302 (2000)

52. 52.
A. Brodutch, D.R. Terno, Phys. Rev. A **83**, 010301 (2011)

53. 53.
V. Giovannetti, S. Lloyd, L. Maccone, Phys. Rev. Lett. **96**, 010401 (2006)

54. 54.
S. Sachdev, *Quantum Phase Transitions* (Cambridge University Press, Cambridge, 2000)

55. 55.
L. Amico et al., Rev. Mod. Phys. **80**, 517 (2008)

56. 56.
C. Bennett, P. Hayden, D. Leung, P. Shor, A. Winter, Remote preparation of quantum states. Inf. Theory IEEE Trans. **51**, 56 (2005)

Author information

Affiliations

1. Department of Mathematics, Government Girls' General Degree College, Ekbalpore, Kolkata, 700023, India

Kaushiki Mukherjee

2. Department of Mathematics, Balagarh Bijoykrishna Mahavidyalaya, Balagarh, Dist. - Hooghly, 712501, India

Biswajit Paul

3. Department of Mathematics, The Heritage College, Anandapur, Kolkata, 700107, India

Sumana Karmakar

Contributions

K. Mukherjee developed main idea of the work, performed the analysis and wrote the paper. S. Karmakar and B. Paul cross checked the findings and also assisted K. Mukherjee in writing the paper. All the authors have read and approved the final manuscript.

Corresponding author

Correspondence to Kaushiki Mukherjee.

Appendices

Appendix A

Proof of Theorem.1

Let $\rho_{AB} \in CQ$. Let it be subjected to an arbitrary general (global) unitary operation $\mathcal{U}$. It has already been discussed before that application of a general (global) unitary $\mathcal{U}$ over any two-qubit state can be interpreted as that of applying local unitary operations (on subsystems) followed by nonlocal unitary operations on the whole system and then again followed by local unitary operations. Let $\rho^{(1)}_{\mathcal{AB}}$, $\rho^{(2)}_{\mathcal{AB}}$, $\rho^{(3)}_{\mathcal{AB}}$ denote the transformed states in subsequent stages of transformation $\rho_{\mathcal{AB}} \to \rho^{'}_{\mathcal{AB}}$:

$$\begin{aligned}
\rho^{(1)}_{\mathcal{AB}} &= \mathcal{U}^1_{\mathcal{A}} \otimes \mathcal{U}^1_{\mathcal{B}} \rho_{\mathcal{AB}} (\mathcal{U}^1_{\mathcal{A}} \otimes \mathcal{U}^1_{\mathcal{B}})^{\dagger} \\
\rho^{(2)}_{\mathcal{AB}} &= \widehat{\mathcal{U}} \rho^{(1)}_{\mathcal{AB}} (\widehat{\mathcal{U}})^{\dagger} \\
\rho^{(3)}_{\mathcal{AB}} &= \rho^{'}_{\mathcal{AB}} = \mathcal{U}^2_{\mathcal{A}} \otimes \mathcal{U}^2_{\mathcal{B}} \rho^{(2)}_{\mathcal{AB}} (\mathcal{U}^2_{\mathcal{A}} \otimes \mathcal{U}^2_{\mathcal{B}})^{\dagger}
\end{aligned}$$
(23)

Now, applying local unitaries has no effect on quantum discord of a two-qubit state [18]. So if $\rho_{\mathcal{AB}} \in CQ$, then $\rho^{(1)}_{\mathcal{AB}} \in CQ$. Now, as $\rho^{(1)}_{\mathcal{AB}}$ is a classical-quantum state (Eq. 12), all possible forms (Bloch vector representation [29]) of $\rho^{(1)}_{\mathcal{AB}}$ are given in Table 1. Nonlocal unitary operation $\widehat{\mathcal{U}}$ is now applied on $\rho^{(1)}_{\mathcal{AB}}$. The detailed analysis of applying $\widehat{\mathcal{U}}$ on all possible forms of $\rho^{(1)}_{\mathcal{AB}}$ (to be discussed below) shows that for every possible form of $\rho^{(1)}_{\mathcal{AB}}$ except $\frac{1}{4}\mathbb{I}_{2\times 2}$, there exists a nonlocal unitary operation (see Table 2 for suitable values of parameters ϕ_1, ϕ_2, ϕ_3) such that resulting state $\rho^{(2)}_{\mathcal{AB}}$ is not a classical-quantum state. Now, $\mathbb{D}(\mathcal{B}/\mathcal{A}) \neq 0$ if and only if $\rho^{(2)}_{\mathcal{AB}}$ is not a classical-quantum state [18]. Hence, every $\rho^{(2)}_{\mathcal{AB}}$ except $\frac{1}{4}\mathbb{I}_{2\times 2}$ has nonzero 'one-way' discord ($\mathbb{D}(\mathcal{B}/\mathcal{A}) \neq 0$. Lastly, local unitary operation $\mathcal{U}^2_{\mathcal{A}} \otimes \mathcal{U}^2_{\mathcal{B}}$ is applied resulting in state $\rho^{(3)}_{\mathcal{AB}}$. $\mathbb{D}(\mathcal{B}/\mathcal{A})$ remaining invariant under local unitaries, and any possible form of $\rho^{(3)}_{\mathcal{AB}}$ except $\frac{1}{4}\mathbb{I}_{2\times 2}$ has nonzero 'one-way' discord. $Hence$, excepting the maximally mixed state ($\frac{1}{4}\mathbb{I}_{2\times 2}$), any member $\rho_{\mathcal{AB}}$ from the set of classical-quantum states (CQ) gets transformed into a ‘one-way’ nonzero discord state $\rho'_{\mathcal{AB}}$. Consequently, $ACQ = \{\frac{\mathbb{I}_{2\times 2}}{4}\}$ □

Analysis of the effect of nonlocal unitary operations $\widehat{\mathcal{U}}$ *on state* $\rho^{(1)}_{\mathcal{AB}}$ (Eq. 23): This part of the discussion is based on the necessary and sufficient condition that $\mathbb{D}_{\rho^{(2)}_{\mathcal{AB}}}(\mathcal{B}/\mathcal{A})$ vanishes if and only if it can be expressed as a classical-quantum state (Eq. 12). As indicated in the main text, every possible form of $\rho^{(1)}_{\mathcal{AB}}$ as a classical-quantum state is given in Table 1. Now, for each of those forms, if possible, let us assume that $\rho^{(2)}_{\mathcal{AB}}$ (Eq. 23) can be expressed as a classical-quantum state (Eq. 12). To be precise, we assume existence of unit vector $\mathbf{u} = (u_1, u_2, u_3)$ giving direction of projector ($\Pi^{\mathcal{A}}_i$) corresponding to classical part of $\rho^2_{\mathcal{AB}}$. Now, under this assumption, $\forall i, k, j, l \in \{0, 1\}$ coefficient of $|ik\rangle\langle jl|$ of $\rho^{(2)}_{\mathcal{AB}}$, C_{ikjl}(say) should be equal to that of coefficient of $|ik\rangle\langle jl|$ corresponding to classical-quantum state form of $\rho^{(2)}_{\mathcal{AB}}$, C^{CQ}_{ikjl} (say). Given a $\rho^{(2)}_{\mathcal{AB}}$, failing to obtain equality ($C_{ikjl} = C^{CQ}_{ikjl}$) for at least one (i, k, j, l) indicates that such a comparison is impossible which in turn proves that our assumption is wrong: $\rho^{(2)}_{\mathcal{AB}}$ is not a classical-quantum state. Consequently, $\mathbb{D}_{\rho^{(2)}_{\mathcal{AB}}}(\mathcal{B}/\mathcal{A})$ turns out to be nonzero.

Now, Table 1 indicates two possible forms of classical quantum states (Eq. 12).

$$\rho^{(1)}_{\mathcal{AB}} = \frac{1}{4}(\mathbb{I}_{2\times 2} + \mathfrak{m}.\sigma \otimes \mathbb{I}_2 + \mathbb{I}_2 \otimes \mathfrak{n}.\sigma)$$
(24)

and

$$\rho^{(1)}_{\mathcal{AB}} = \frac{1}{4}(\mathbb{I}_{2\times 2} + \mathfrak{m}_i\sigma_i \otimes \mathbb{I}_2 + \mathbb{I}_2 \otimes \mathfrak{n}.\sigma + \mathfrak{s}_{ii}\sigma_i \otimes \sigma_i)$$
(25)

where $\mathfrak{m} = (\mathfrak{m}_1, \mathfrak{m}_2, \mathfrak{m}_3)$ and $\mathfrak{n} = (\mathfrak{n}_1, \mathfrak{n}_2, \mathfrak{n}_3)$ are real vectors. In Eq. (25), the index $i \in \{1, 2, 3\}$. Corresponding possible cases are as follows:

1. 1.
   $\mathfrak{m} = (m_1, 0, 0), \mathcal{S} = diag(s_{11}, 0, 0)$, $\mathfrak{n}$ arbitrary

2. 2.
   $\mathfrak{m} = (0, m_2, 0), \mathcal{S} = diag(0, s_{22}, 0)$, $\mathfrak{n}$ arbitrary

3. 3.
   $\mathfrak{m} = (0, 0, m_3), \mathcal{S} = diag(0, 0, s_{33})$, $\mathfrak{n}$ arbitrary

We now start with the first form (Eq. 24). For arbitrary $\mathfrak{n}$, depending on $\mathfrak{m}$ in Eq. (24) following cases are possible:

1. 1.
   $\mathfrak{m} = \boldsymbol{\Theta}$

2. 2.
   $\mathfrak{m} = (0, 0, m_3)$

3. 3.
   $\mathfrak{m} = (0, m_2, 0)$

4. 4.
   $\mathfrak{m} = (m_1, 0, 0)$

5. 5.
   $\mathfrak{m} = (m_1, 0, m_3)$

6. 6.

$\mathfrak{m} = (m_1, m_2, 0)$

7. 7.
$\mathfrak{m} = (0, m_2, m_3)$

8. 8.
$\mathfrak{m} = (m_1, m_2, m_3)$

Firstly, let us consider the trivial subcase of Case.1 where both $\mathfrak{m}$ and $\mathfrak{n} = \Theta$. This corresponds to the maximally mixed state:$\rho^{(1)}_{\mathcal{AB}} = \frac{1}{4}\mathbb{I}_{2\times 2}$. Clearly, after application of any nonlocal unitary operation, $\rho^{(1)}_{\mathcal{AB}}$ remains unchanged. Consequently, $\rho^{(2)}_{\mathcal{AB}}$ in this case is a classical-quantum state, thereby having vanishing discord.

We now approach with all possible nontrivial subcases related to each of the above cases starting with that of Case.1.

Case1: $\mathfrak{m} = \boldsymbol{\Theta}$ and $vec\mathfrak{n}$ is arbitrary. Possible subcases of Case.1 are:

- $\mathfrak{n} = (n_1, 0, 0)$
- $\mathfrak{n} = (0, n_2, 0)$
- $\mathfrak{n} = (n_1, n_2, 0)$
- $\mathfrak{n} = (n_1, n_2, n_3)$ with $n_3 \neq 0$ whereas n_1 and n_2 are arbitrary.

Subcase 1: Let nonlocal unitary operation $\widehat{\mathcal{U}} = \widehat{\mathcal{U}}(\phi_1, \phi_2, \phi_3)$ characterized by $\phi_1 = \frac{\pi}{2}$, $\phi_2 = \phi_3 = \frac{\pi}{4}$ be applied on $\rho^{(1)}_{\mathcal{AB}}$. As stated above, let us now consider coefficient of term $|01\rangle\langle 00|$ of $\rho^{(2)}_{\mathcal{AB}}(C_{0100})$ and that of coefficient of term $|01\rangle\langle 00|$ appearing in assumed classical-quantum state form of $\rho^{(2)}_{\mathcal{AB}}(C^{CQ}_{0100})$. Equality $C_{0100} = C^{CQ}_{0100}$ demands:

$$n_1(1-u_3^2) = 0$$
(26)

As $n_1 \neq 0$ and $u_1^2 + u_2^2 + u_3^2 = 1$, $u_3 = \pm 1$, $u_2 = u_1 = 0$. Again $C_{1000} = C^{CQ}_{1000}$ demands:

$$n_1(-1 + u_1 u_2 + u_2^2) = 0$$
(27)

Using $u_2 = u_1 = 0$ in Eq. (27) demands $n_1 = 0$ leading to a contradiction. Hence, $C_{0100} = C^{CQ}_{0100}$ and $C_{1000} = C^{CQ}_{1000}$ do not hold simultaneously. Consequently, for this subcase, $\rho^{(2)}_{\mathcal{AB}}$ obtained from classical-quantum state $\rho^{(1)}_{\mathcal{AB}}$ after applying nonlocal unitary operation $\widehat{\mathcal{U}}(\frac{\pi}{2}, \frac{\pi}{4}, \frac{\pi}{4})$ is not a classical-quantum state. So under application of $\widehat{\mathcal{U}}(\frac{\pi}{2}, \frac{\pi}{4}, \frac{\pi}{4})$, the classical-quantum state $\rho^{(1)}_{\mathcal{AB}}$ (Eq. 24), characterized by $\mathfrak{n} = (n_1, 0, 0)$ and $\mathfrak{m} = \Theta$, gets converted to a 'one-way' discord nonzero state.

Subcase 2: Let nonlocal unitary operation $\widehat{\mathcal{U}}(\frac{\pi}{4}, 0, \frac{\pi}{2})$ be applied. $C_{0100} = C^{CQ}_{0100}$ demands:

$$n_2(1-u_3^2) = 0$$
(28)

Hence, $C_{0100} = C^{CQ}_{0100}$ demands $u_3 = \pm 1$, $u_2 = u_1 = 0$. But $C_{1101} = C^{CQ}_{1101}$ demands:

$$n_2(1-u_2^2) = 0$$
(29)

which requires $n_2 = 0$ as u_2 must be 0 if $C_{0100} = C^{CQ}_{0100}$ (Eq. 28). This again leads to a contradiction as for this subcase, $n_2 \neq 0$.

Subcase 3: $\mathfrak{n} = (n_1, n_2, 0)$

Let nonlocal unitary operation $\widehat{\mathcal{U}}(\frac{\pi}{4}, 0, \frac{\pi}{2})$ be applied. $C_{1000} = C_{1000}^{CQ}$ demands:

$$n_2(1 - u_2^2) = 0$$
(30)

Hence, $C_{1000} = C_{1000}^{CQ}$ demands $u_2 = \pm 1$, $u_3 = u_1 = 0$. But $C_{0100} = C_{0100}^{CQ}$ demands:

$$n_1(1 - u_3^2) = 0$$
(31)

which requires $n_1 = 0$ as u_3 must be 0 which leads to a contradiction as for this subcase, $n_1 \neq 0$.

Subcase 4: $\mathfrak{n} = (n_1, n_2, n_3)$ with $n_3 \neq 0$ whereas n_1 and n_2 are arbitrary.

Let nonlocal unitary operation $\widehat{\mathcal{U}}(\frac{\pi}{4}, \frac{\pi}{4}, 0)$ be applied. $C_{0100} = C_{0100}^{CQ}$ demands:

$$u_3 u_1 n_3 = 0 \, and \, u_3 u_2 n_3 = 0$$
(32)

For the above relation to be true, if possible let $u_3 = 0$. But for $u_3 = 0$, $C_{0000} = C_{0000}^{CQ}$ demands $n_3 = 0$ which is a contradiction. So $u_3 \neq 0$. Consequently, Eq. (32) requires $u_1 = u_2 = 0$. But then $C_{1001} = C_{1001}^{CQ}$ demands $n_3 = 0$ which is impossible and so again contradiction obtained as for this subcase, $n_3 \neq 0$.

Case 2: $\mathfrak{m} = (0, 0, m_3)$.

Possible subcases are as follows:

Subcase 1: $\mathfrak{n} = (n_1, n_2, n_3)$ where $n_1 \neq 0$ and n_2, n_3 are arbitrary

Here, $\widehat{\mathcal{U}}(0, \frac{\pi}{2}, 0)$ is applied. $C_{1000} = C^{CQ}_{1000}$ demands:

$$n_1(1 - u_2^2) = 0$$

(33)

So, $u_3 = u_1 = 0$ and $u_2 = \pm 1$. But using these in relation $C_{1100} = C^{CQ}_{1100}$ gives $m_3 = 0$ which is impossible.

Subcase 2: $\mathfrak{n} = (0, n_2, n_3)$ where $n_2 \neq 0$ and n_3 is arbitrary. Here, $\widehat{\mathcal{U}}(0, \frac{\pi}{2}, \frac{\pi}{2})$ is applied. $C_{1100} = C^{CQ}_{1100}$ and $C_{1001} = C^{CQ}_{1001}$ demand:

$$m_3(u_3^2 + u_2^2) = 0$$

(34)

As $m_3 \neq 0$, $u_3 = u_2 = 0$ and $u_1 = \pm 1$. But using these in relation $C_{0100} = C^{CQ}_{0100}$ gives $n_2 = 0$ which leads to contradiction.

Subcase 3: $\mathfrak{n} = (0, 0, n_3)$ where n_3 is arbitrary $\widehat{\mathcal{U}}(0, \frac{\pi}{4}, \frac{\pi}{4})$ is applied. $C_{0000} = C^{CQ}_{0000}$ requires:

$$m_3(1 - u_3^2) = 0$$

(35)

So, $u_1 = u_2 = 0$ and $u_3 = \pm 1$. But using these in relations $C_{1001} = C^{CQ}_{1001}$ gives

$$n_3 - m_3 = 0$$

(36)

and in $C_{1100} = C^{CQ}_{1100}$ gives

$$n_3 + m_3 = 0$$

(37)
Above two relations require $m_3 = n_3 = 0$ which is impossible.

Case3: $\mathfrak{m} = (0, m_2, 0)$. Possible subcases are as follows:

Subcase 1:$\mathfrak{n} = (n_1, n_2, n_3)$ where $n_1 \neq 0$ and n_2, n_3 are arbitrary. Here, $\widehat{\mathcal{U}}(0, 0, \frac{\pi}{2})$ is applied.
$C_{0100} = C_{0100}^{CQ}$ demands:

$$n_1(1 - u_3^2) = 0$$
(38)
So, $u_2 = u_1 = 0$ and $u_3 = \pm 1$. But using these in relation $C_{1000} = C_{1000}^{CQ}$ gives $m_2 = 0$ which is impossible as $m_2 \neq 0$.

Subcase 2: $\mathfrak{n} = (0, n_2, n_3)$ where $n_2 \neq 0$ and n_3 is arbitrary. $\widehat{\mathcal{U}}(0, \frac{\pi}{2}, \frac{\pi}{4})$ is applied.

$C_{0000} = C_{0000}^{CQ}$ demands:

$$m_2 u_3 (u_1 + u_2) = 0$$
(39)
As $m_2 \neq 0$, above relation implies either $u_3 = 0$ or $u_1 + u_2 = 0$. If possible, let $u_3 = 0$. Then, $C_{0100} = C_{0100}^{CQ}$ implies $n_2 = 0$ which is impossible. Hence, $u_3 \neq 0$. Consequently, $u_1 + u_2 = 0$. Now, using $u_3 \neq 0$ in $C_{0101} = C_{0101}^{CQ}$ gives $u_1 - u_2 = 0$.

Now, $u_1 \pm u_2 = 0$ implies $u_1 = u_2 = 0$. Now, this relation when used in $C_{0010} = C_{0010}^{CQ}$ gives $m_2 = 0$ which is impossible. Hence, Eq. (39) is impossible.

Subcase 3: $\mathfrak{n} = (0, 0, n_3)$ where n_3 is arbitrary. $\widehat{\mathcal{U}}(\frac{\pi}{4}, 0, \frac{\pi}{4})$ is applied. $C_{0100} = C_{0100}^{CQ}$ requires:

$$m_2(1 - u_3^2) = 0$$
(40)

So $u_2 = u_1 = 0$ and $u_3 = \pm 1$. But using these in relation $C_{1000} = C_{1000}^{CQ}$ gives $m_2 = 0$ which is impossible.

Case 4: $\mathfrak{m} = (m_1, 0, 0)$. Possible subcases are as follows:

Subcase 1: $\mathfrak{n} = (n_1, n_2, n_3)$ where $n_1 \neq 0$ and n_2, n_3 are arbitrary. Here, $\widehat{\mathcal{U}}(0, \frac{\pi}{2}, 0)$ is applied. $C_{0100} = C_{0100}^{CQ}$ demands:

$$m_1(1 - u_3^2) = 0$$
(41)

As $m_1 \neq 0$, $u_2 = u_1 = 0$ and $u_3 = \pm 1$. But using these in relation $C_{1000} = C_{1000}^{CQ}$ gives $n_1 = 0$ which is impossible as $n_1 \neq 0$.

Subcase 2: $\mathfrak{n} = (0, n_2, n_3)$ where $n_2 \neq 0$ and n_3 is arbitrary. $\widehat{\mathcal{U}}(\frac{\pi}{4}, \frac{\pi}{2}, 0)$ is applied.

$C_{0100} = C_{0100}^{CQ}$ demands relation given by Eq. (41). So $u_2 = u_1 = 0$ and $u_3 = \pm 1$. But using these in relation $C_{1000} = C_{1000}^{CQ}$ gives $n_2 = 0$ which is impossible as $n_2 \neq 0$.

Subcase 3: $\mathfrak{n} = (0, 0, n_3)$ where n_3 is arbitrary. $\widehat{\mathcal{U}}(0, \frac{\pi}{4}, \frac{\pi}{4})$ is applied.

$C_{0100} = C_{0100}^{CQ}$ demands relation given by Eq. (41) and hence $u_2 = u_1 = 0$ and $u_3 = \pm 1$. But using these in relation $C_{1000} = C_{1000}^{CQ}$ gives $m_1 = 0$ which is impossible.

Case 5: $\mathfrak{m} = (m_1, 0, m_3)$ and $\mathfrak{n}$ is arbitrary.
$\widehat{\mathcal{U}}(0, 0, \frac{\pi}{2})$ is applied.

$C_{0000} = C_{0000}^{CQ}$ and $C_{0101} = C_{0101}^{CQ}$ together demand:

$$m_3(1 - u_3^2) = 0$$
(42)

As $m_3 \neq 0$, $u_2 = u_1 = 0$ and $u_3 = \pm 1$. But using these in relation $C_{1000} = C_{1000}^{CQ}$ gives $m_1 = 0$ which is impossible as $m_1 \neq 0$.

Case 6: $\mathfrak{m} = (m_1, m_2, 0)$ and $\mathfrak{n}$ is arbitrary.
$\widehat{\mathcal{U}}(0, \frac{\pi}{2}, 0)$ is applied.

$C_{1011} = C_{1011}^{CQ}$ demands relation given by Eq. (41). As $m_1 \neq 0$, $u_2 = u_1 = 0$ and $u_3 = \pm 1$. But using these in relation $C_{0111} = C_{0111}^{CQ}$ gives $m_2 - n_1 = 0$ and in relation $C_{0010} = C_{0010}^{CQ}$ gives $m_2 + n_1 = 0$. This in turn implies $m_2 = n_1 = 0$ which is impossible as $m_2 \neq 0$.

Case 7: $\mathfrak{m} = (0, m_2, m_3)$ and $\mathfrak{n}$ is arbitrary.
$\widehat{\mathcal{U}}(\pi, \pi, \frac{\pi}{2})$ is applied.

$C_{0000} = C_{0000}^{CQ}$ and $C_{0101} = C_{0101}^{CQ}$ together demand relation given by Eq. (42). As $m_3 \neq 0$, $u_2 = u_1 = 0$ and $u_3 = \pm 1$. But using these in relation $C_{1101} = C_{1101}^{CQ}$ gives $m_2 = 0$ which is impossible as $m_2 \neq 0$.

Case 8: $\mathfrak{m} = (m_1, m_2, m_3)$ and $\mathfrak{n}$ is arbitrary.
Clearly, this case can be proved by anyone of above

three cases (5–7).

Now, we consider the possible cases of states given by Eq. (25).

Case 1.: $\mathfrak{m} = (m_1, 0, 0)$, $\mathcal{S} = diag(s_{11}, 0, 0)$ and $\mathfrak{n}$ arbitrary. $\widehat{\mathcal{U}}(0, 0, \frac{\pi}{2})$ is applied. $C_{0111} = C^{CQ}_{0111}$ requires:

$$m_1(1 - u_2^2) = 0$$

(43)

So $u_3 = u_1 = 0$ and $u_2 = \pm 1$. But using these in relation $C_{0011} = C^{CQ}_{0011}$ gives $s_{11} = 0$ which is impossible.

Case 2.: $\mathfrak{m} = (0, m_2, 0)$, $\mathcal{S} = diag(0, s_{22}, 0)$, $\mathfrak{n}$ arbitrary. $\widehat{\mathcal{U}}(\frac{\pi}{2}, \frac{\pi}{2}, 0)$ is applied. $C_{1011} = C^{CQ}_{1011}$ requires relation given by Eq. (40) and hence $u_2 = u_1 = 0$ and $u_3 = \pm 1$. But using these in relation $C_{0011} = C^{CQ}_{0011}$ gives $s_{22} = 0$ which is impossible.

Case 3.: $\mathfrak{m} = (0, 0, m_3)$, $\mathcal{S} = diag(0, 0, s_{33})$, $\mathfrak{n}$ arbitrary. $\widehat{\mathcal{U}}(\pi, \frac{\pi}{2}, \pi)$ is applied. $C_{0011} = C^{CQ}_{0011}$ and $C_{0110} = C^{CQ}_{0110}$ together require relation given by Eq. (34) and hence $u_3 = u_1 = 0$ and $u_1 = \pm 1$. But using these in relation $C_{1111} = C^{CQ}_{1111}$ gives $s_{33} = 0$ which is impossible. So in each of the possible cases of $\rho^{(1)}_{\mathcal{AB}}$, it is shown that after applying suitable nonlocal unitary operation, the transformed state $\rho^{(2)}_{\mathcal{AB}}$ no longer remains a classical-quantum state. Consequently, $\mathbb{D}_{\rho^{(2)}_{\mathcal{AB}}}(\mathcal{B}/\mathcal{A}) \neq 0$. We enlist the suitable required nonlocal unitary operations for all possible subcases of individual cases corresponding to first possible form of $\rho^{(1)}_{\mathcal{AB}}$ (Eq. 24) and also for second possible form given by Eq. (25).

Appendix B

Here, we discuss the effect of nonlocal unitary operations over all possible forms of quantum-classical states [29]. As discussed in 'Appendix A,' here also we enlist those nonlocal unitaries which are effective in generating states having nonvanishing $\mathbb{D}_{\rho'_{\mathcal{AB}}}(\mathcal{A}/\mathcal{B})$ starting from quantum-classical states $\rho_{\mathcal{AB}}$. One of the forms of quantum-classical state (after application of suitable local unitaries) is given by Eq. (24), while the other is given by:

$$\rho^{(1)}_{\mathcal{AB}} = \frac{1}{4}(\mathbb{I}_{2\times 2} + \mathfrak{m}.\sigma \otimes \mathbb{I}_2 + \mathbb{I}_2 \otimes \mathfrak{n}_i\sigma_i + \mathfrak{s}_{ii}\sigma_i \otimes \sigma_i)(i = 1, 2, 3)$$

(44)

With eight possible forms (as listed in 'Appendix A') of quantum-classical states corresponding to Eq. (24), the possible cases as given by Eq. (44) are:

1. 1. $\mathfrak{n} = (n_1, 0, 0)$, $\mathcal{S} = diag(s_{11}, 0, 0)$, $\mathfrak{m}$ arbitrary

2. 2. $\mathfrak{n} = (0, n_2, 0)$, $\mathcal{S} = diag(0, s_{22}, 0)$, $\mathfrak{m}$ arbitrary

3. 3. $\mathfrak{n} = (0, 0, n_3)$, $\mathcal{S} = diag(0, 0, s_{33})$, $\mathfrak{m}$ arbitrary

We now enlist the effective nonlocal unitaries for all possible cases in Table 3.

Appendix C

Discussing effectiveness of global unitary operations to convert zero discord state to nonzero discord state in main text, here we discuss the mechanism of this conversion in detail.

Application of Global Unitary Operations: Given an arbitrary two-qubit state $\rho_{\mathcal{AB}}$, with correlation tensor $\mathcal{T}$, singular value decomposition of $\mathcal{T}$ may be obtained by performing suitable local unitary operations $\mathcal{U}_{\mathcal{A}}^{1} \otimes \mathcal{U}_{\mathcal{B}}^{1}$ over $\rho_{\mathcal{AB}}$ [43]. Let $\rho_{\mathcal{AB}}$ be a classical-quantum state. Let $\kappa_i^L (i = 1, 2, 3)$ and , $\kappa_i^R (i = 1, 2, 3)$ denote orthonormalized left and right singular vectors of $\mathcal{T}$, respectively. $\forall i$, denoting $\kappa_i^{L(R)} \in \mathbb{R}^3$ as $(\kappa_{i1}^{L(R)}, \kappa_{i2}^{L(R)}, \kappa_{i3}^{L(R)})$, local unitary matrices $\mathcal{U}_{\mathcal{A}}^{1}, \mathcal{U}_{\mathcal{B}}^{1}$ are given by:

$$\mathcal{U}_{\mathcal{A}}^{1} = \begin{pmatrix} \kappa_{11}^L & \kappa_{12}^L & \kappa_{13}^L \\ \kappa_{21}^L & \kappa_{22}^L & \kappa_{23}^L \\ \kappa_{31}^L & \kappa_{32}^L & \kappa_{33}^L \end{pmatrix}$$
$$\mathcal{U}_{\mathcal{B}}^{1} = \begin{pmatrix} \kappa_{11}^R & \kappa_{12}^R & \kappa_{13}^R \\ \kappa_{21}^R & \kappa_{22}^R & \kappa_{23}^R \\ \kappa_{31}^R & \kappa_{32}^R & \kappa_{33}^R \end{pmatrix}$$
(45)

$\rho_{\mathcal{AB}}$, being a classical-quantum state, after application of the local unitary operations $\mathcal{U}_{\mathcal{A}}^{1} \otimes \mathcal{U}_{\mathcal{B}}^{1}$ (Eq. 45), $\rho_{\mathcal{AB}}^{(1)}$ (Eq. 23) corresponds to one of the possible forms prescribed in Table 1. Then, observing the exact form of $\rho_{\mathcal{AB}}^{(1)}$ the suitable nonlocal unitary operation $\widehat{\mathcal{U}}(\phi_1, \phi_2, \phi_3)$ to be applied is chosen from Table 2 (which enlists required nonlocal unitary for every possible form of classical-quantum state given in Table 1).

Table 2 Details of nonlocal unitary operations to be applied on any possible classical-quantum state having forms given by Eqs. (24) and (25) so that resulting state has nonzero $\mathbb{D}_{\rho'_{\mathcal{AB}}}(\mathcal{B}/\mathcal{A})$

Table 3 List of suitable nonlocal unitary operations application of which converts any possible quantum-classical state (forms given by Eqs. (24), (44)) to $\rho'_{\mathcal{AB}}$ such that $\mathbb{D}_{\rho'_{\mathcal{AB}}}(\mathcal{A}/\mathcal{B})$

Now, to obtain 'one-way' zero discord state starting from an arbitrary quantum-classical state $\rho_{\mathcal{AB}}$, analogous treatment is to be made with now considering Table 3 instead of for obvious reasons.

An Example: Consider a two-qubit product state:

$$\rho_{prod} = \frac{1}{4}(\mathbb{I}_2 + \mathbf{r}^a.\sigma) \otimes (\mathbb{I}_2 + \mathbf{r}^b.\sigma)$$
(46)

where $\mathbf{r}^{a(b)} = (r_1^{a(b)}, r_2^{a(b)}, r_3^{a(b)})$.
$\mathbb{D}_{\rho_{prod}}(\mathcal{B}/\mathcal{A}) = \mathbb{D}_{\rho_{prod}}(\mathcal{A}/\mathcal{B}) = 0$ [29]. So ρ_{prod} is a zero discord state. Correlation tensor is given by:

$$\mathcal{T}_{prod} = \begin{pmatrix} r_1^a r_1^b & r_1^a r_2^b & r_1^a r_3^b \\ r_2^a r_1^b & r_2^a r_2^b & r_2^a r_3^b \\ r_3^a r_1^b & r_3^a r_2^b & r_3^a r_3^b \end{pmatrix}$$
(47)

The suitable local unitary operations are:

$$\mathcal{U}^1_{\mathcal{A}(\mathcal{B})} = \begin{pmatrix} -\frac{r_3^{a(b)}}{r_1^{a(b)} n_1^{a(b)}} & 0 & \frac{1}{n_1^{a(b)}} \\ -\frac{r_2^{a(b)}}{r_1^{a(b)} n_2^{a(b)}} & \frac{1}{n_2^{a(b)}} & 0 \\ \frac{r_1^{a(b)}}{r_3^{a(b)} n_3^{a(b)}} & \frac{r_2^{a(b)}}{r_3^{a(b)} n_3^{a(b)}} & \frac{1}{n_3^{a(b)}} \end{pmatrix}$$

where $n_1^{a(b)} = \sqrt{1 + (\frac{r_3^{a(b)}}{r_1^{a(b)}})^2}$, $n_2^{a(b)} = \sqrt{1 + (\frac{r_2^{a(b)}}{r_1^{a(b)}})^2}$ and $n_3^{a(b)} = \sqrt{\frac{(r_1^{a(b)})^2 + (r_2^{a(b)})^2 + (r_3^{a(b)})^2}{(r_3^{a(b)})^2}}$. After application of these local unitary operations, $\rho^{(1)}_{prod}$ is given by:

$$\begin{aligned} \rho^{(1)}_{prod} =& \frac{1}{4}(\mathbb{I}_{2\times 2} + \mathfrak{a}^{(1)}.\sigma \otimes \mathbb{I}_2 + \mathbb{I}_2 \otimes \mathfrak{b}^{(1)}.\sigma \\ & + \sum_{j_1,j_2=1}^{3} \mathfrak{t}^{(1)}_{j_1 j_2} \sigma_{j_1} \otimes \sigma_{j_2}), \end{aligned}$$

(48)

where $\mathfrak{a}^{(1)} = (0, 0, n_3^a r_3^a)$, $\mathfrak{b}^{(1)} = (0, 0, n_3^b r_3^b)$ and correlation tensor $\mathcal{T}^{(1)}_{prod}$ is a diagonal matrix $diag(0, 0, r_3^a r_3^b n_3^a n_3^b)$. Clearly, $\rho^{(1)}_{prod}$ (Eq. 48) corresponds to a form in Table 1 and is also a quantum-classical state [29]. Observing the particular form in Table 1, on application of nonlocal unitary operation $\widehat{\mathcal{U}}(\pi, \frac{\pi}{2}, \pi)$(as prescribed by Table 2), resulting state $\rho^{(2)}_{prod}$ is no longer a classical-quantum state ($\mathbb{D}_{\rho^{(2)}_{prod}}(\mathcal{B}/\mathcal{A}) > 0$). Again treating $\rho^{(1)}_{prod}$ as a quantum-classical state, $\widehat{\mathcal{U}}(\pi, \frac{\pi}{2}, 0)$ is the suitable nonlocal unitary operation (Table 3) application of which gives $\mathbb{D}_{\rho^{(2)}_{prod}}(\mathcal{A}/\mathcal{B}) > 0$. So $\rho^{(2)}_{prod}$ turns out to be a nonzero discord state. Lastly, suitable local unitaries $\mathcal{U}^2_{\mathcal{A}}, \mathcal{U}^2_{\mathcal{B}}$ may again be applied so as to obtain a simplified version of the state.

Alternatively, given any $\rho_{\mathcal{AB}}$ one may directly apply suitable nonlocal unitary operation $\widehat{\mathcal{U}}(\phi_1, \phi_2, \phi_3)$ considering $\mathcal{U}^1_{\mathcal{A}} = \mathcal{U}^1_{\mathcal{B}} = \frac{\mathbb{I}}{2}$. One such instance is cited in next section.

Rights and permissions

About this article

Cite this article

Mukherjee, K., Paul, B. & Karmakar, S. Any two-qubit state has nonzero quantum discord under global unitary operations. *Eur. Phys. J. D* **75,** 65 (2021). https://doi.org/10.1140/epjd/s10053-021-00055-1

- Received03 October 2020
- Accepted18 January 2021
- Published17 February 2021
- DOIhttps://doi.org/10.1140/epjd/s10053-021-00055-1

Indian Journal of Chemistry
Vol. 59B, June 2020, pp. 837-841

Reactions of the carbazole alkaloid Mahanimbine with mineral acid, Lewis acid and *m*-chloroperbenzoic acid

Mumu Chakraborty
Department of Chemistry, Government Girls' General Degree College
7, Mayurbhanj Road, Kolkata 700 023, India
E-mail: mumu_chak@yahoo.com

Received 9 September 2019; accepted (revised) 22 May 2020

Mahanimbine, a C_{23} carbazole alkaloid, has been isolated from the leaves of *Murraya koenigii* Spreng. This carbazole alkaloid, with a C_5H_9 ring residue, on reaction with different acids shows some interesting results. Structures of the naturally occurring compound as well as the synthetic products have been ascertained on the basis of 1D and 2D NMR spectroscopic data. In this paper is discuss isolation, structure elucidation and some chemical transformations of mahanimbine on reaction with mineral acid, Lewis acid and *m*-chloroperbenzioc acid.

Keywords: *Murraya koenigii*, carbazole alkaloids, mahanimbine, Lewis acid, mineral acid

The plant *Murraya koenigii* (L.) Spreng. belonging to the family Rutaceae is native to India and now distributed in most of southern Asia. The leaves of this plant are well-known as curry leaves and have been used as one of the important herbs of south Indian cooking. Various parts of the plant have been used in traditional medicine for the treatment of headache, toothache and stomachaches, influenza, rheumatism, traumatic injury, and insect and snake bites, and as an antidysentric as well as an astringent. Intake of the leaves can increase digestive secretions and relieve nausea, indigestion and vomiting[1]. The leaves and bark are used in analgesia and local anesthesia and for the treatment of eczema and dropsy[2]. Chloroform extract of the root bark of *M. koenigii* displayed significant cytotoxic activity against cultured KB cell.

Murrayanine is the first carbazole alkaloid isolated from the stem bark of *M. koenigii*. After that a number of carbazole alkaloids have been isolated from this plant, possessing C_{13}, C_{18} and C_{23} skeletons[3-6]. A number of derivatives of these carbazole alkaloids were also prepared, many of which showed potent biological activities[7-9].

Mahanimbine[10] was isolated from the leaves of *Murraya koenigii* Spreng, popularly known as curry leaves tree. Spectroscopic studies revealed that the compound is a pyranocarbazole alkaloid with a C_{23} skeleton. The compound also has a C_5H_9 side chain. Application of the Lewis acid BF_3-etherate on mahanimbine **1** resulted in the cyclisation of its side chain furnishing a penta-cyclic compound **2** (Scheme I), whereas in presence of mineral acid mahanimbine was converted into cyclomahanimbine **3** (Scheme II). Compound **2** was later proved to be an isomer of cyclomahanimbine **3**. On the other hand, reaction of mahanimbine **1** with *m*-chloroperbenzioc acid resulted in the formation of an interesting product **4** containing both an epoxy ring as well as two hydroxyl functionalities (Scheme III).

Results and Discussion

Reaction of mahanimbine **1** with BF_3-etherate resulted in the cyclisation of its C_5H_9 side chain and a penta-cyclic product **2** was formed. The ^{1}H NMR spectrum of the product showed signals for five aromatic protons at δ 7.44 (H-4), 7.63(H-5), 7.34(H-6), 7.89(H-7) and 7.14(H-8). It also showed signals for one benzylic methine at δ 4.26 (H-1'), one aromatic methyl at δ 2.13 (H-10) and one gem-dimethyl group at δ 1.43(H-8' and H-9'). The product displayed 23 signals in the ^{13}C NMR spectrum (five aromatic doublets, one aromatic methyl, one gem-dimethyl, one oxygen-bearing quaternary carbon, seven aromatic singlets, three characteristic aliphatic triplets, one C-C double bond, one benzylic methine and one aliphatic methyl). The product has close structural resemblance with cyclomahanimbine **3**. The major distinguishing factor between **2** and cyclomahanimbine **3** is the number of

66

Available Online

JOURNAL OF SCIENTIFIC RESEARCH

J. Sci. Res. 12 (4), 665-672 (2020)

www.banglajol.info/index.php/JSR

Mumunine - A New Carbazole Alkaloid from *Murraya koenigii* (Linn.) Spreng

M. Chakraborty*

Government Girls' General Degree College, 7, Mayurbhanj Road, Kolkata – 700023, West Bengal, India

Received 14 February 2020, accepted in final revised form 26 May 2020

Abstract

The plant *Murraya koenigii*, commonly known as curry leaf tree is a rich source of carbazole alkaloids. A number of monomeric as well as dimeric carbazoles with C_{13}, C_{18} and C_{23} skeleton have been isolated from the plant. In my present work, a new carbazole alkaloid, designated as mumunine, was isolated from the bark of *Murraya koenigii* (Linn) Spreng, along with a known carbazole alkaloid, viz. mahanimbine. The structure of the new alkaloid **1** was elucidated on the basis of 1D and 2D NMR spectral data analysis. In this paper, the isolation and structure elucidation of the new compound will be discussed in detail.

Keywords: *Murraya koenigii*; Rutaceae; Carbazole alkaloids; Mumunine; 2D NMR.

doi: http://dx.doi.org/10.3329/jsr.v12i4.45499 J. Sci. Res. 12 (4), 665-672 (2020)

1. Introduction

Many of the medicinally important plant-derived pharmaceuticals have been essential in the era of modern medicine and some of these substances, such as morphine have attained the official status of strategic materials. However, despite these many important past contributions from the plant kingdom, a great number of many plant species have never been described and remain unknown to science and relatively few have been surveyed systematically to any extent for biologically active chemical constituents. Thus, it is reasonable to expect that new plant sources of pharmaceutically interesting materials remain to be discovered and developed.

India and neighbouring countries like Sri Lanka, China, Bangladesh etc. are very rich sources of medicinal plants. Many researchers from these countries are working hard in search of bioactive organic substances from their natural resources. Penu *et al.* have recently published a paper on investigation of the phytochemicals and their antioxidant, antimicrobial and thrombolytic activities and also estimated total phenolic and flavonoid contents of *Pandanus odoratissimus* (*P. odoratissimus*) leaves of methanol extract [1].

* *Corresponding author*: mumu_chak@yahoo.com

NJC

ROYAL SOCIETY OF CHEMISTRY

PAPER

Check for updates

Cite this: New J. Chem., 2020, 44, 4898

An unorthodox metal-free synthesis of dihydro-6*H*-quinoline-5-ones in ethanol/water using a non-nucleophilic base and their cytotoxic studies on human cancer cell line†

Arijit Kundu,[a] Bhaswati Bhattacharyya,[b] Kaliprasanna Dhara,*[c] Subhabrata Paul,[d] Indira Majumder[e] and Rita Kundu[e]

A DBU-catalysed metal-free domino reaction strategy has been developed for the facile synthesis of dihydro-6*H*-quinoline-5-ones. This protocol employs a very expedient route to the synthesis of pyridine frameworks using β-chloro-α,β-unsaturated aldehydes, 1,3-diketones, and ammonium acetate in ethanol : water (1 : 1) solvent under eco-friendly conditions. Diverse types of acyclic and cyclic β-chloro-α,β-unsaturated aldehydes were used to obtain a variety of dihydro-6*H*-quinoline-5-ones. The mechanism of the domino reaction was established by isolating the intermediate compound, which was subjected to the next step of the reaction to obtain the target product. The structure of the intermediate was established from spectral and single crystal XRD studies. Most of the synthesized dihydro-6*H*-quinoline-5-one derivatives were found to be cytotoxic to the HeLa cell lines, showing profound cytotoxicity in MTT assays. The DNA fragmentation assay showed no fragmented DNA in the treated sets, which indicated that the compounds did not induce apoptosis of the HeLa cells. In most of the cases, autophagic cell death was evident from fluorescence microscopy studies, though necrosis was also observed in some cases.

Received 23rd December 2019, Accepted 17th February 2020

DOI: 10.1039/c9nj06346c

rsc.li/njc

Introduction

In the recent eon of research, the discovery of small molecules with the efficiency to work in complex biological processes to prevent diseases has been one of the major challenges facing researchers.[1] This trend has clearly indicated a paradigm shift of the spotlight from natural product chemistry to combinatorial chemistry.[2] Among numerous nitrogen heterocycles, quinoline is a scaffold of crucial importance with respect to biomedical use. Several quinoline derivatives, isolated from natural resources or prepared synthetically, show a wide variety of biological activities.[3] One such type of important quinoline moiety is dihydroquinoline, which exhibits interesting biological and pharmaceutical activities including antitubercular (1), anti-HIV (2), anticancer (3), apical sodium-dependent bile acid transporter (ASBT) inhibition (4), (Fig. 1) *etc.* Compounds, streptonigrin (5), ascidiathiazones and lavendamycin, (Fig. 1) showed antibiotic, anticancer, and antiproliferative activities, respectively.[3]

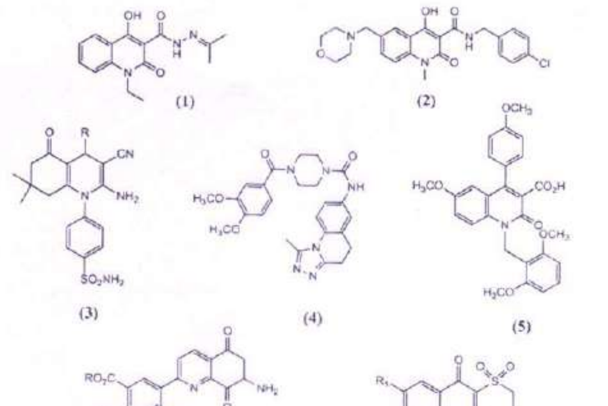

Fig. 1 Some naturally occurring quinoline derivatives.

Numerous skeletal analogues incorporating these crucial moieties have been prepared using synthetic approaches to

[a] Department of Chemistry, Maulana Azad College, Kolkata-700013, India
[b] Department of Chemistry, Government Girls General Degree College, Ekbalpur, Kolkata-700023, India
[c] Department of Chemistry, University College of Science and Technology, University of Calcutta, Kolkata-700009, India. E-mail: chemkpd@gmail.com
[d] Department of Botany, Presidency University, Kolkata-700019, India
[e] Department of Botany, University of Calcutta, Kolkata-700019, India

† Electronic supplementary information (ESI) available. CCDC 1542885 and 1542887. For ESI and crystallographic data in CIF or other electronic format see DOI: 10.1039/c9nj06346c

Characterizing quantum correlations in a fixed-input n-local network scenario

Kaushiki Mukherjee,[1,*] Biswajit Paul,[2,†] and Arup Roy[3,‡]
[1]*Department of Mathematics, Government Girls' General Degree College, Ekbalpore, Kolkata-700023, India*
[2]*Department of Mathematics, Balagarh Bijoykrishna Mahavidyalaya, Balagarh, Dist.-Hooghly-712501, India*
[3]*S. N. Bose National Centre for Basic Sciences, Salt Lake, Kolkata 700 106, India*

(Received 18 November 2019; accepted 28 February 2020; published 19 March 2020)

Contrary to the Bell scenario, quantum nonlocality can be exploited even when all the parties do not have freedom to select inputs randomly. Such manifestation of nonlocality is possible in networks involving independent sources. One can utilize such a feature of quantum networks for purpose of entanglement detection of bipartite quantum states. In this context, we characterize correlations simulated in networks involving a finite number of sources generating quantum states when some parties perform fixed measurement. Beyond bipartite entanglement, we inquire the same for networks involving sources now generating pure tripartite quantum states. Interestingly, here also randomness in input selection is not necessary for every party to generate nonlocal correlation.

DOI: 10.1103/PhysRevA.101.032328

I. INTRODUCTION

Entanglement of multipartite quantum systems [1] plays a pragmatic role in manifesting deviation of quantum theory (QT) from the classical world. Bell used this intrinsic feature of the theory to abandon the possibility of existence of any local realistic interpretation of QT [2,3] which, however, respects the no-signaling principle. Bell's theorem provides an empirical methodology to detect nonlocal behavior of quantum correlations (often referred to as Bell nonlocality), an experimental demonstration of which has already been provided [4,5].

Speaking of tests demonstrating Bell nonlocality, the most simple test was proposed by Clauser *et al.* [6]. Such a test involves two distant observers (Alice and Bob, say) such that each of them performs one binary measurement choosing randomly from a set of two measurements. To be precise, Alice randomly chooses one input from a set of two inputs ($\{\mathcal{A}_0, \mathcal{A}_1\}$, say) and similarly Bob randomly chooses input from another set, say $\{\mathcal{B}_0, \mathcal{B}_1\}$. Moreover, the choice of inputs of Alice does not depend on that of Bob and vice versa (measurement independence). Bipartite correlations generated after measurements are used in testing correlator-based inequality, more commonly referred to as CHSH inequality. Violation of CHSH inequality indicates nonlocal nature of corresponding correlations. To date, analogous to CHSH inequality [6], different correlator-based inequalities (referred to as Bell inequalities) have been derived. Detecting quantum nonlocality by any of these tests requires randomness in the choice of inputs of both the observers present in the corresponding measurement scenario. However, random selection of inputs by all observers is not a necessity to exploit nonclassicality of quantum correlations simulated in network scenarios [7–12] characterized by source independence (often referred to as n-local networks).

n-local quantum networks [13–19] basically refer to a network of n sources, independent of each other, such that each of these sources generates an m-partite quantum state ($m \geqslant 2$) shared between m distinct parties. Nonlocality of correlations generated in such networks was first observed in a bilocal ($n, m = 2$) network [13,14] where entanglement was distributed from two independent sources. Such type of nonlocality is referred to as nonbilocality [13,14]. Nonbilocality, or more general non-n-locality, differs from the usual sense of Bell nonlocality (standard nonlocality) where entanglement is distributed from a common source. Some of the measurement scenarios involved in n-local networks have been proposed where some (P_{14} or P_{13} measurement scenarios [13]) or all [8,9] of the observers perform a single measurement (referred to as "fixed measurement" [9]). All of these studies basically analyzed some specific instances of quantum non-n-locality in such measurement scenarios where not all observers [13] can randomly select inputs, thereby manifesting instances of "quantum nonlocality without inputs" [9]. Now, observation of quantum nonlocality in networks can be used for the purpose of detection of quantum entanglement in the same. In this context, we first intend to exploit quantum nonlocality in networks, characterized by source independence and fixed input criterion (for at least one of the observers). Quantum networks witnessing non-n-locality can then be used for detection of entanglement resources.

For our purpose, we first characterize quantum correlations, thereby analyzing the non-n-local nature of the correlations as detected via violation of existing non-n-local inequality [16] when each of the sources generates an arbitrary two-qubit state. In this context, one may note that such a study of quantum violation was recently initiated in [7] where only two entangled sources ($n = 2$) were considered (bilocal network).

As a direct consequence of our findings in practical ground, we propose a scheme of detecting entanglement (if any) using

*kaushiki_mukherjee@rediffmail.com
†biswajitpaul4@gmail.com
‡arup145.roy@gmail.com

networks involving independent sources where not all parties have access to random choice of inputs. Such a protocol, relying on n-local correlations generated in "fixed input" measurement scenario [16], serves the purpose of bipartite entanglement detection. Fixing measurements of some of the parties makes implementation of our protocol easier compared to the simplest standard Bell scenario of measurements. However, it must be pointed out that more easier implementation of protocols (compared to the scenario to be considered presently) may be possible if parties are allowed to randomly select from some suitable measurement settings which are more easily implementable. But, we do not consider those easily implementable measurement setting scenarios with a motivation to detect entanglement in absence of random input selections.

Recently, n-local networks involving sources distributing multipartite entanglement have been designed in [17]. However, in such a measurement scenario, all the parties had access to random choice of measurements. To verify quantum nonlocality even in absence of randomness in input selection (by some of the parties), we consider a measurement scenario where now three independent sources generate tripartite quantum states. In this context, we have designed a set of nonlinear Bell inequalities, a violation of which suffices to detect non-n-locality. The nonlinear trilocal network scenario is then used for the purpose of tripartite entanglement detection. Our protocol (characterized by fixed measurement setting by two parties) can detect both biseparable and genuine entanglement (some members of GGHZ and W classes) of pure tripartite quantum states. Interestingly, it can be used to distinguish between genuine entanglement and biseparable entanglement of pure states and can even specify the exact nature of biseparable entanglement. Finally, we conjecture generalization of our protocol for detecting entanglement of multipartite ($m \geqslant 4$) pure states. Apart from entanglement detection, the study of analyzing quantumness of network correlations may be contributory in the study of various information processing tasks such as distribution of quantum key (QKD) [20–23], generation of private randomness [24,25], Bayesian game theoretic applications [26], etc.

The rest of our work is organized as follows. We start with discussing the motivation behind our work in Sec. II followed by some basic preliminaries in Sec. III. In Sec. IV first we analyze the nature of quantum correlations generated in n-local linear network [16] using n number of bipartite quantum states followed by proposal of the scheme for bipartite entanglement detection. In Sec. V, first we derive the set of Bell inequalities for the nonlinear trilocal network scenario, then study violation of corresponding inequalities by pure tripartite quantum states, and then design tripartite entanglement detection scheme for some pure tripartite states. In Sec. VI, we generalize the nonlinear trilocal network to a nonlinear n-local network scenario when each of n independent sources generates an m-partite ($m \geqslant 4$) state. Finally, we end with some concluding remarks in Sec. VII.

II. MOTIVATION

Nonlocal behavior (Bell nonlocality) of correlations acts as a signature of presence of entanglement distributed (by a common source) among the parties who perform local measurements on their respective particles forming the entangled state. In a network scenario, specifically for a bilocal network, Gisin *et al.* proved that all bipartite entangled states violate the bilocal inequality (see Sec. III) indicating nonbilocality of corresponding network correlations [13]. Their findings [7] generate the idea of using a bilocal network to detect entanglement of the states distributed by the sources. This idea basically motivates this work. We exploit the nonclassical nature of quantum correlations generated in a network (involving n independent sources) where all the parties do not have access to random input selection. Subsequently, we use the observations for detecting entanglement of bipartite states involved in the network. We not only confine within the scope of bipartite entanglement, but consider tripartite entanglement also.

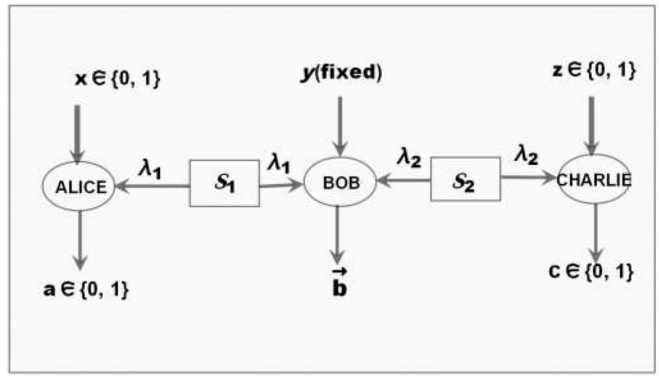

FIG. 1. Schematic diagram of bilocal network [13,14]. In the P_{14} scenario, y denotes fixed measurement of Bob together with $\vec{b}$ referring to four outputs $b_0b_1 = 00,\ 01,\ 10,\ 11$.

III. PRELIMINARIES

A. Bilocal scenario

A bilocal network (Fig. 1) was framed in [13,14]. It is a network of three parties, say, Alice (A), Bob (B), and Charlie (C), and two sources $\mathbf{S}_1$ and $\mathbf{S}_2$ arranged linearly. Sources $\mathbf{S}_1$ and $\mathbf{S}_2$ are independent to each other (*bilocal assumption*). Each of $\mathbf{S}_1$ and $\mathbf{S}_2$ sends a physical system characterized by variables λ_1 and λ_2, respectively. Intermediate party Bob gets two particles (one from each source). In P^{14} scenario [13,14], each of Alice and Charlie performs any one of two binary output measurements on their respective subsystems: $x,\ z \in \{0, 1\}$ denote respective input sets for Alice and Charlie whereas their outputs are labeled as $a,\ c \in \{0, 1\}$. Bob performs a single (fixed) measurement (y) having four outcomes: $b = \overrightarrow{\mathbf{b}} = b_0b_1 = 00, 01, 10, 11$ on the joint state of the two subsystems received from $\mathbf{S}_1$ and $\mathbf{S}_2$.

Correlations generated in the network are local if these can be decomposed as $P_{14}(a, b, c|x, y, z) = \iint d\lambda_1 d\lambda_2 \rho(\lambda_1, \lambda_2) V$

$$\text{with } V = P_{14}(a|x, \lambda_1) P_{14}(b|y, \lambda_1, \lambda_2) P_{14}(c|z, \lambda_2). \quad (1)$$

Tripartite correlations $P_{14}(a, b, c|x, y, z)$ are bilocal if these can be written in the above form [Eq. (1)] along with the constraint (referred to as *bilocal constraint*)

$$\rho(\lambda_1, \lambda_2) = \rho_1(\lambda_1)\rho_2(\lambda_2) \quad (2)$$

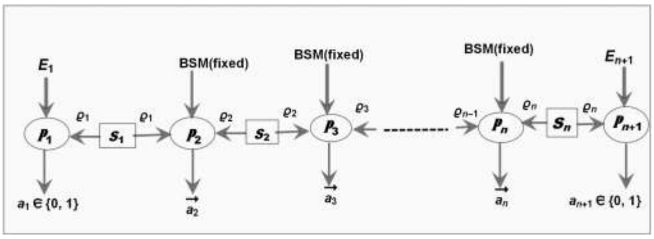

FIG. 2. Schematic diagram of quantum n-local linear network. E_1 and E_{n+1} stand for observables corresponding to binary inputs x_1 and x_{n+1} of $\mathcal{P}_1$ and $\mathcal{P}_{n+1}$, respectively. Here, each of $\mathcal{P}_i$ $(i = 2, ..., n)$ performs asingle measurement denoted by BSM, which stands for complete Bell basis measurement with $\vec{a}_i$ referring to four outputs $a_{i0}a_{i1} = 00,\ 01,\ 10,\ 11$.

imposed on the probability distributions of the hidden variables λ_1, λ_2. A linear extension of this model involving n independent sources and $n+1$ parties was made in [16].

Nonbilocality of tripartite correlations is guaranteed if these violate the inequality $\sqrt{|I|} + \sqrt{|J|} \leqslant 1$ (for details, see [13]). Quantum violation of the bilocal inequality was pointed out in [7]. Based on their findings it can be said that any bipartite two-qubit entangled state violates the bilocal inequality. Linear extension of bilocal network, referred to as *n-local linear network*, was given in [16] where the number of independent sources is n. n-local quantum linear network is considered for our purpose (see Fig. 2).

B. Complete Bell basis and GHZ basis measurement

Both of these measurements are instances of quantum entangled (joint) measurements. The operator of complete Bell basis measurement [7], often referred to as "Bell state measurement" (BSM), is represented in terms of its four eigenvectors (Bell states):

$$|\phi^{\pm}\rangle = \frac{|00\rangle \pm |11\rangle}{\sqrt{2}}, \tag{3}$$

$$|\psi^{\pm}\rangle = \frac{|01\rangle \pm |10\rangle}{\sqrt{2}}. \tag{4}$$

Analogous to the bipartite entangled measurement of BSM, the operator corresponding to tripartite entangled measurement of complete GHZ basis measurement (GSM) is given in terms of the GHZ basis [15]:

$$|\phi_{mnk}\rangle_{\text{GHZ}} = \frac{1}{\sqrt{2}} \sum_{r=0}^{1} (-1)^{m*r} |r\rangle |r \oplus n\rangle |r \oplus k\rangle,\ m, n, k \in \{0, 1\}. \tag{5}$$

IV. QUANTUM VIOLATION OF LINEAR n-LOCAL INEQUALITY

Here, we consider an n-local linear network [16] involving quantum states (see Fig. 2). Let each of n independent sources generate a two-qubit state: source $\mathbf{S}_i$ generating state ϱ_i $(i = 1, 2, \ldots, n)$. Two qubits of state ϱ_i are sent to parties $\mathcal{P}_i$ and $\mathcal{P}_{i+1}$ $(i = 1, 2, \ldots, n)$. The overall joint quantum system involved in the network is $\otimes_{i=1}^{n} \varrho_i$. After receiving qubits, each of the extreme two parties $\mathcal{P}_1$ and $\mathcal{P}_{n+1}$ performs projective measurements in any of two arbitrary directions locally on their respective particles: $\mathcal{P}_1$ chooses any one of directions $\vec{\alpha}_0$ and $\vec{\alpha}_1$ (say) whereas for $\mathcal{P}_{n+1}$ let the directions be along any one $\vec{\beta}_0$ and $\vec{\beta}_1$. Each of remaining $n-1$ intermediate parties $\mathcal{P}_i$ $(i = 2, \ldots, n-1)$ performs a complete Bell-basis measurement (fixed setting) on the joint state of their respective two particles received from adjoining sources $\mathbf{S}_i$ and $\mathbf{S}_{i+1}$ (see Fig. 2). $(n+1)$-partite correlations generated in the network are then used to test the n-local inequality [16]

$$\sqrt{|I_{14}|} + \sqrt{|J_{14}|} \leqslant 1. \tag{6}$$

Terms appearing in the above equation are detailed in Table I.

Clearly, excepting the extreme two parties A_1 and A_{n+1}, none of the remaining $n-1$ parties have access to random choice of measurements. Under such circumstances, we consider two separate cases.

Network involving pure states. Let each of the n sources generate a pure two-qubit state. To be precise, say $\mathbf{S}_i$ emits

$$\varrho_i = \gamma_{0i}|00\rangle + \gamma_{1i}|11\rangle, \tag{7}$$

where γ_{0i} and γ_{1i} $(i = 1, \ldots, n)$ are positive real Schmidt coefficients [27] satisfying normalization condition $\gamma_{oi}^2 + \gamma_{1i}^2 = 1$. ϱ_i is entangled for any nonzero value of both γ_{0i} and γ_{i1} $(i = 1, 2, \ldots, n)$, i.e., $\gamma_{0i}\gamma_{1i} > 0$. Maximizing over all possible projective measurement directions of extreme two parties A_1 and A_{n+1}, the upper bound of violation ($\mathcal{B}_{14}$, say) of Eq. (6) turns out to be

$$\mathcal{B}_{14} = \mathcal{B}_{14}^{(\text{pure})} = \sqrt{1 + 2^n \Pi_{i=1}^{n} \gamma_{oi}\gamma_{1i}}. \tag{8}$$

$\mathcal{B}_{14} > 1$ implies that all the pure states involved in the network are entangled. Hence, up to the existing sufficient criterion

TABLE I. Details of the terms appearing in Eq. (6). E_1 and E_{n+1} denote respective observables corresponding to binary inputs x_1 and x_{n+1} of parties $\mathcal{P}_1$ and $\mathcal{P}_{n+1}$. $a_1, a_{n+1} \in \{0, 1\}$ stand for corresponding outputs.

I_{14} and J_{14}	Correlators	Measurement and outputs of $\mathcal{P}_i$ $(i = 2, \ldots, n)$
$I_{14} = \frac{1}{4}\sum_{x_1, x_{n+1}=0,1} \langle E_1 E_2^0 \ldots E_n^0 E_{n+1} \rangle$	$\langle E_1 E_2^y \ldots E_n^y E_{n+1}\rangle = \sum_U (-1)^{a_1 + a_{2y} + \ldots + a_{ny} + a_{n+1}} V_{14}$	E_i^y:observable of $\mathcal{P}_i$
	$U = \{a_1, a_{20}, a_{21}, \ldots, a_{n0}, a_{n1}, a_{n+1}\}$	Corresponding to a single input
$J_{14} = \frac{1}{4}\sum_{x_1, x_{n+1}=0,1} (-1)^{x_1 + x_{n+1}} \langle E_1 E_2^1 \ldots E_n^1 E_{n+1} \rangle$	$V_{14} = P(a_1, \overrightarrow{a_2}, \ldots, \overrightarrow{a_n}, a_{n+1} \vert x_1, x_{n+1})$	having 4 outputs:
		$\overrightarrow{a_i} = a_{i0}a_{i1} = 00,\ 01,\ 10,\ 11$

given by Eq. (6) for detecting nonbilocality, nonbilocal correlations are generated in a network only if all pure states involved in the network are entangled.

Network involving mixed bipartite states. Let us now consider the case when each of $\mathbf{S}_j$ emits a mixed bipartite state (density matrix formalism)

$$\varrho_j = \frac{1}{2^2}\sum_{i_1,i_2=0}^{3} t^{(j)}_{i_1 i_2}\sigma^1_{i_1}\bigotimes\sigma^2_{i_2}, \tag{9}$$

where σ^q_0 stands for the identity operator of the Hilbert space which is associated with qubit q and $\sigma^q_{i_q}$, denote the Pauli operators along three mutually perpendicular directions, $i_q = 1, 2, 3$. $t^{(j)}_{i_1 i_2}$ $(i, j = 1, 2, 3)$ denote the elements of the correlation tensor $T^{(j)}$ (say) of the bipartite state ϱ_j. Polar value decomposition of correlation tensor $(T^{(j)})$ for each of ϱ_j generates the matrix $U^{(j)}M^{(j)} = T^{(j)}$ where $U^{(j)}$ denotes a unitary matrix and $M^{(j)} = \sqrt{(T^{(j)})^{\dagger}T^{(j)}}$ having eigenvalues $\lambda^{(j)}_1 \geqslant \lambda^{(j)}_2 \geqslant \lambda^{(j)}_3$. The polar decomposition of $\varrho^{(j)}$ and $\varrho^{(j+1)}$ characterize the fixed measurement (BSM) of A_j $(j = 2,\dots,n)$ who performs suitable local unitaries over subsystems received from sources $\mathbf{S}_j$ and $\mathbf{S}_{j+1}$ (for detailed discussion on the methodology used here, see [7]). The upper bound of violation $(\mathcal{B}_{14})$ now turns out to be

$$\mathcal{B}_{14} = \mathcal{B}^{(\text{mixed})}_{14} = \sqrt{\Pi^n_{j=1}\lambda^{(j)}_1 + \Pi^n_{j=1}\lambda^{(j)}_2}. \tag{10}$$

Now, let none of ϱ_j $(j = 1,\dots,n)$ violate standard Bell-CHSH inequality, i.e., by Horodecki criterion [28]

$$\mathcal{B}^{(j)}_{\text{CHSH}} = \sqrt{\left(\lambda^{(j)}_1\right)^2 + \left(\lambda^{(j)}_2\right)^2} \leqslant 1, \tag{11}$$

where $\mathcal{B}^{(j)}_{\text{CHSH}}$ denotes the upper bound of violation of Bell-CHSH inequality by ϱ_j. This in turn indicates that for each of ϱ_j $(j = 1,\dots,n)$, $\lambda^{(j)}_i$ $(i = 1, 2, 3) < 1$. Under such circumstances, Eq. (10) gives

$$\begin{aligned}\mathcal{B}_{14} &< \max_{k\neq l}\sqrt{\lambda^{(k)}_1\lambda^{(l)}_1 + \lambda^{(k)}_2\lambda^{(l)}_2}, \quad k, l = 1,\dots,n\\ &\leqslant \sqrt{\left(\lambda^{(k)}_1\right)^2 + \left(\lambda^{(k)}_2\right)^2}\sqrt{\left(\lambda^{(l)}_1\right)^2 + \left(\lambda^{(l)}_2\right)^2}\\ &= \mathcal{B}^{(k)}_{\text{CHSH}}\mathcal{B}^{(l)}_{\text{CHSH}}\\ &\leqslant 1.\end{aligned} \tag{12}$$

Hence, $\mathcal{B}_{14} > 1$ implies that at least one of the states ϱ_j generated by $\mathbf{S}_j$ is Bell-CHSH nonlocal.

A. Bipartite entanglement detection

Let there be n unknown bipartite quantum states Φ_i generated by n distinct sources $\mathbf{S}_i$ $(i = 1,\dots,n)$. All these n sources being spatially separated, they are independent of each other. In order to detect whether at least one of Φ_i is entangled or not, let the sources be arranged linearly and the states be distributed among $n+1$ parties $\mathcal{P}_i$ $(i = 1,\dots,n+1)$ so as to form a n-local network (Fig. 2). Let each of $\mathcal{P}_1$ and $\mathcal{P}_{n+1}$ perform projective measurements in any one of two arbitrary directions whereas intermediate $n-1$ parties (receiving two particles each) perform complete Bell basis measurement (BSM). Practical implementation of this protocol, where only some of the parties $(\mathcal{P}_1, \mathcal{P}_{n+1})$ have to choose randomly from a set of two measurements, is easier compared to any protocol where none of the parties involved perform fixed measurement. $(n+1)$-partite correlations generated therein are used to test the n-local inequality [Eq. (6)]. Observation of violation of the inequality guarantees that at least one of Φ_i is entangled. Utility of the violation of Eq. (6) is already justified in the previous subsection. Clearly, this protocol detects entanglement of all the states involved in a device-dependent manner (as each of the intermediate parties have to perform BSM thereby making the scheme depending on inner working of the device) in case all Φ_i $(i = 1,\dots,n)$ are identical copies of an unknown quantum state.

Having used a n-local linear network for the purpose of bipartite entanglement detection, we now proceed to do the same for some families of pure tripartite entangled states. For that, we first analyze trilocal nonlinear network scenario.

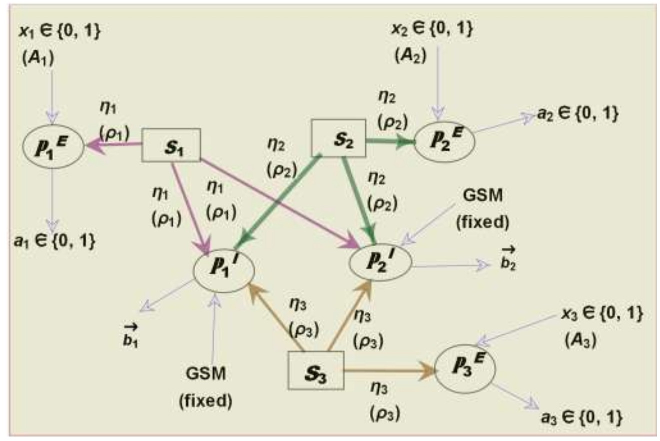

FIG. 3. Trilocal nonlinear network. Source $\mathbf{S}_i$ is characterized by hidden variable η_i $(i = 1, 2, 3)$. In case of quantum network $\mathbf{S}_i$ generates tripartite quantum state ρ_i. A_i denotes observables corresponding to binary inputs x_i of $\mathcal{P}_i$ $(= 1, 2, 3)$, respectively. Here, each of $\mathcal{P}^I_1$, $\mathcal{P}^I_2$ performs single measurement (GHZ basis measurement) denoted by "GSM" with three-dimensional vector $\vec{b}_i$ now referring to eight outputs $b_{i0}b_{i1}b_{i2}$= 000, 001, 010, 100, 101, 110, 011, 111.

V. TRILOCAL NONLINEAR NETWORK SCENARIO

The scenario is based on a five-party $(\mathcal{P}^E_1, \mathcal{P}^E_2, \mathcal{P}^E_3, \mathcal{P}^I_1, \mathcal{P}^I_2)$ network involving three independent sources $\mathbf{S}_1$, $\mathbf{S}_2$, and $\mathbf{S}_3$ (see Fig. 3). Source $\mathbf{S}_i$ is characterized by hidden variable η_i $(i = 1, 2, 3)$. Source independence implies existence of independent probability distributions

$$\Lambda(\eta_1, \eta_2, \eta_3) = \Lambda_1(\eta_1)\Lambda_2(\eta_2)\Lambda_3(\eta_3), \tag{13}$$

where $\int d\eta_i\Lambda_i(\eta_i) = 1\ \forall\ i$. Source $\mathbf{S}_i$ sends particles to parties $\mathcal{P}^I_1$, $\mathcal{P}^I_2$, $\mathcal{P}^E_i$ $(i = 1, 2, 3)$. Parties $\mathcal{P}^I_1$ and $\mathcal{P}^I_2$ receiving three particles (one from each source) are referred to as *intermediate* parties and the remaining three parties $\mathcal{P}^E_1, \mathcal{P}^E_2, \mathcal{P}^E_3$, each receiving a single particle, are referred to as *extreme* parties. Let x_1, x_2, $x_3(\in \{0, 1\})$ stand for binary inputs of parties $\mathcal{P}^E_1$, $\mathcal{P}^E_2$, $\mathcal{P}^E_3$, respectively, whereas a_1, a_2, $a_3(\in \{0, 1\})$ correspond to the respective outputs. Each of $\mathcal{P}^I_1$ and $\mathcal{P}^I_2$ has access to single input giving eight

TABLE II. Detailing of the terms used in Eq. (15). A_i denote the observable for input x_i of $\mathcal{P}_i^E$ ($i = 1, 2, 3$) whereas B_1, B_2 denote observable corresponding to single input of $\mathcal{P}_1^I$ and $\mathcal{P}_2^I$, respectively.

Correlators
$I^{(18)}_{m_1(n_1),m_2(n_2),i} = \frac{1}{8}\sum_{x_1,x_2,x_3=0,1}(-1)^{i*(x_1+x_2+x_3)}\langle A_{1,x_1}A_2^{m_1(n_1)}A_3^{m_2(n_2)}A_{4,x_2}A_{5,x_3}\rangle,\ i,\ m_1,\ m_2,\ n_1,\ n_2\ \in\{0,1\}$
$\langle A_{1,x_1}B_1^{m_1(n_1)}B_2^{m_2(n_2)}A_{2,x_2}A_{3,x_3}\rangle = \sum_{\mathcal{C}}(-1)^h P_{18}(a_1,\vec{b}_1,\vec{b}_2,a_2,a_3\vert x_1,x_2,x_3)$
where $\mathcal{C} = \{a_1,a_2,a_3,b_{10},b_{11},b_{12},b_{20},b_{21},b_{22}\}$ and $h = a_1+a_2+a_3+s_{m_1(n_1)}(b_{10},b_{11},b_{12})+s_{m_2(n_2)}(b_{20},b_{21},b_{22})$
with functions $s_i(x,y,z)$ being defined as $s_0(x,y,z) = x+y+z+1$ and $s_1(x,y,z) = x*y+y*z+x*z$

outputs $\vec{b}_1 = (b_{10}, b_{11}, b_{12})$ and $\vec{b}_2 = (b_{20}, b_{21}, b_{22})$ ($b_{ij} \in \{0,1\}\ \forall\ i = 1,2$ and $j \in \{0,1,2\}$) denote the outputs of parties $\mathcal{P}_1^I$ and $\mathcal{P}_2^I$, respectively. Parties are not allowed to communicate between themselves. Correlations generated in this network scenario are *trilocal* if they can be factorized as follows:

$$P_{18}(a_1,\vec{b}_1,\vec{b}_2,a_2,a_3|x_1,x_2,x_3) = \iiint d\eta_1 d\eta_2 d\eta_3 \Lambda(\eta_1,\eta_2,\eta_3)W,$$

$$\text{where } W = P_{18}(a_1|x_1,\eta_1)P_{18}(\vec{b}_1|\eta_1,\eta_2,\eta_3)P_{18}(\vec{b}_2|\eta_1,\eta_2,\eta_3) \times P_{18}(a_2|x_2,\eta_2)P_{18}(a_3|x_3,\eta_3) \quad (14)$$

along with the restriction imposed by Eq. (13). Under source independence restriction [Eq. (13)], correlations which cannot be decomposed as above [Eq. (23)] are said to be *nontrilocal* in nature. It may be noted that the network scenario introduced here is in some extent similar to that of the scenario discussed in [17] where each of the parties involved has the freedom to choose from a set of two measurements. So, the scenario in the present discussion and that introduced in [17] differ on the basis of whether the intermediate parties perform a single measurement or not. Correspondingly, the correlations characterizing the measurement scenarios and the inequalities involved therein are different from those discussed in [17]. We now derive a set of sufficient criteria in the form of nonlinear Bell-type inequalities sufficient to detect nontrilocal correlations.

Theorem 1. For any trilocal five-partite correlation, each of the following inequalities necessarily holds:

$$\sqrt[3]{\left|I^{(18)}_{m_1,m_2,0}\right|} + \sqrt[3]{\left|I^{(18)}_{n_1,n_2,1}\right|} \leqslant 1\,\forall\, m_1,\ m_2,\ n_1,\ n_2\ \in\{0,1\}. \quad (15)$$

For details of the correlators used in Eq. (15), see Table II.

Proof. For proof, see Appendix A.

The set of 16 inequalities given by Eq. (15) being only necessary criteria of trilocality, there may exist nontrilocal correlations satisfying all of them. However, violation of at least one of these inequalities guarantees nontrilocality of the correlations. Violation of Eq. (15) for at least one possible (m_1, m_2, n_1, n_2) is thus sufficient for detecting nontrilocality of corresponding correlations.

A. Quantum violation

Consider a network involving three independent sources $\mathbf{S}_1$, $\mathbf{S}_2$, and $\mathbf{S}_3$, each generating a three-qubit state $\rho^{(i)}$ (see Fig. 3). The overall quantum state involved in the network becomes

$$\rho_{12345} = \rho^{(1)}\otimes\rho^{(2)}\otimes\rho^{(3)}. \quad (16)$$

After the qubits are distributed from the sources, no communication takes place between the parties who now perform measurements on their respective subsystems. Each of $\mathcal{P}_1^I$ and $\mathcal{P}_2^I$ performs complete GHZ basis measurement (GSM) on the joint state of the three qubits that each of them receives from the three sources. Each of $\mathcal{P}_1^E$, $\mathcal{P}_2^E$, and $\mathcal{P}_3^E$ performs projective measurements on their single qubit in any of two arbitrary directions: $\mathcal{P}_i^I$ ($i = 1, 2, 3$) measures in any one of $\vec{\gamma}_{i0}$ and $\vec{\gamma}_{i1}$ directions.

Interestingly, if each of the sources $\mathbf{S}_i$ generates arbitrary tripartite product state

$$\rho_i = \otimes_{j=1}^3(v_{0ij}|0\rangle + v_{1ij}|1\rangle)(|v_{0ij}|^2 + |v_{1ij}|^2 = 1), \quad (17)$$

none of the inequalities given by Eq. (15) are violated. We now proceed to discuss some possible cases of quantum violation of inequalities given by Eq. (15). For our purpose, we consider tripartite pure states.

Let each of the sources generate an arbitrary biseparable (in 12/3 cut) entangled state

$$\left|\varphi^i_{(12/3)}\right\rangle = (c_{0i}|00\rangle_{12} + c_{1i}|11\rangle_{12})\otimes(v_{0i}|0\rangle_3 + v_{1i}|1\rangle_3) \quad (18)$$

with $v_{0i}^2 + v_{1i}^2 = 1$ and $c_{0i}^2 + c_{1i}^2 = 1$ (v_{ij}, c_{ij} are the Schmidt coefficients) [27]. Now, compatible with the arrangement of the sources and parties in this network, let the first qubit of each $\rho_i = |\varphi^i_{(12|3)}\rangle\langle\varphi^i_{(12|3)}|$ ($i = 1, 2, 3$) is sent to the extreme parties: $\mathcal{P}_1^E$, $\mathcal{P}_2^E$, and $\mathcal{P}_3^E$ receiving the first qubit of ρ_1, ρ_2, and ρ_3, respectively, whereas the second and third qubits of each ρ_i are sent to the intermediate parties: $\mathcal{P}_1^I$ receives the second qubit of ρ_1, ρ_2, ρ_3 and $\mathcal{P}_3^I$ receives the third qubit of these states. Violation of Eq. (15) is observed for some members of this family [Eq. (18)]. Violation is also observed if each of $\mathbf{S}_i$ generates some states having biseparable entanglement in 13/2 cut:

$$\left|\varphi^i_{(13/2)}\right\rangle = (c_{0i}|00\rangle_{13} + c_{1i}|11\rangle_{13})\otimes(v_{0i}|0\rangle_2 + v_{1i}|1\rangle_2). \quad (19)$$

However, violation is impossible if $\mathbf{S}_i$ generates any member from the family of biseparable entangled states having entanglement among its second and third qubits:

$$\left|\varphi^i_{(23/1)}\right\rangle = (c_{0i}|00\rangle_{23} + c_{1i}|11\rangle_{23})\otimes(v_{0i}|0\rangle_1 + v_{1i}|1\rangle_1). \quad (20)$$

At this junction, it should be noted that violation of Eq. (15) depends on the order of distribution of qubits of each ρ_i ($i = 1, 2, 3$) among the parties. Compatible with the network scenario (Fig. 3), when first qubit of each ρ_i ($i = 1, 2, 3$) is sent to the extreme parties and remaining two qubits of each ρ_i are

TABLE III. Exploring some specific instances of nontrilocal nature of correlations observed when some tripartite pure quantum states are used in the nonlinear trilocal network under the assumption that each of $\mathcal{P}_1^E$, $\mathcal{P}_2^E$, and $\mathcal{P}_3^E$ receives the first qubit of ρ_1, ρ_2, and ρ_3, respectively, whereas the remaining two qubits of each ρ_i are received by the intermediate parties. No violation of trilocal inequalities (at least one) is, however, obtained when tripartite state has entangled second and third qubits [Eq. (20)] as $\mathcal{B}_{18} \leqslant 1$.

State (ρ_i generated by $\mathbf{S}_i$)	State parameters giving violation
$\lvert\varphi_{\mathrm{GHZ}}^{(i)}\rangle$ [Eq. (21)]	$\beta_1 = 0.72, \beta_2 = 0.75, \beta_3 = 0.7$
$\lvert\varphi_{W}^{(i)}\rangle$ [Eq. (22)]	$\omega_{1i} = 0.558327, \omega_{2i} = 1.5708,\ \forall\, i \in \{1,2,3\}$
$\lvert\varphi_{(12\vert3)}^{i}\rangle$ [Eq.(18)]	$c_{0i} = 0.592368,\ v_{0i} = 1,\ \forall\, i \in \{1,2,3\}$
$\lvert\varphi_{(13\vert2)}^{i}\rangle$ [Eq. (19)]	$c_{0i} = 1.5708 - \imath\, 0.15776,\ v_{0i} = 1,\ \forall\, i \in \{1,2,3\}$
$\lvert\varphi_{(23\vert1)}^{i}\rangle$ [Eq.(20)]	No violation is obtained. Upper bound ($\mathcal{B}_{18}$, say)
	of trilocal inequalities [Eq. (15)]
	for identical copies $\mathcal{B}_{18} = \mathrm{Max}[2^{\frac{2}{3}}\lvert c_{01}c_{11}\rvert, (c_{01}^4 + 4c_{01}^3c_{11}^3 + c_{11}^4)^{\frac{1}{3}}]$
	where $c_{k1} = c_{k2} = c_{k3},\ k = 0, 1$

received by the intermediate parties (as discussed), violation is observed in networks involving biseparable entanglement in $13/2$ [Eq. (19)] or $12/3$ [Eq. (18)] cuts only. But, violation is not observed if ρ_i have biseparable entanglement in $23/1$ cut [Eq. (20)]. But, networks involving biseparable entanglement in $23/1$ [Eq. (20)] cut also gives violation if the second qubit of each ρ_i ($i = 1, 2, 3$) is sent to the extreme parties and the remaining two qubits of each ρ_i are received by the intermediate parties. However, violation of any one of the trilocal inequalities given by Eq. (15) is not always arrangement (of qubits) specific. We consider genuine entanglement in support of our claim.

Let each of $\mathbf{S}_i$ in the nonlinear trilocal network now generate a generalized GHZ (GGHZ) state ([29]) $\rho_i = \lvert\varphi_{\mathrm{GHZ}}^{(i)}\rangle\langle\varphi_{\mathrm{GHZ}}^{(i)}\rvert$ where

$$\left|\varphi_{\mathrm{GHZ}}^{(i)}\right\rangle = \cos(\beta_i)|000\rangle + \sin(\beta_i)|111\rangle, \quad \beta_i \in \left[0, \frac{\pi}{4}\right]. \tag{21}$$

Contrary to biseparable entanglement, nontrilocal correlations are obtained in the network (see Table. III) for some states from the GGHZ family [Eq. (21)] irrespective of distribution of qubits of each of the states (ρ_i). Analogous observation is obtained when W states [30] are involved in the network:

$$\left|\varphi_{W}^{(i)}\right\rangle = \cos\omega_{2i}\sin\omega_{1i}|001\rangle + \sin\omega_{2i}\sin\omega_{1i}|010\rangle + \cos\omega_{1i}|100\rangle,\ \omega_{1i}, \quad \omega_{2i} \in \left[0, \frac{\pi}{4}\right]. \tag{22}$$

Now, if both biseparable and genuine entanglement of the W state [Eq. (22)] are used in the network, violation again depends on arrangement of qubits. Here, it should be pointed out that if one of the three tripartite pure states generated by the sources is a product state, then violation of trilocal inequalities cannot be observed even if the remaining two states are entangled.

Based on the above analysis of quantum violation and the fact that such violation is sufficient to detect nontrilocal nature of network correlations, we now design a scheme to detect both biseparable and genuine entanglement of tripartite pure states. But, it may be pointed out that this scheme may fail to detect presence of entanglement in some cases as violation is not possible for all tripartite pure entangled states.

B. Tripartite pure entanglement detection

Consider a nonlinear trilocal network. The three unknown pure tripartite states κ_1, κ_2, and κ_3 are generated by $\mathbf{S}_1$, $\mathbf{S}_2$, and $\mathbf{S}_3$ in the network. Distribution of qubits among the parties plays a significant role in violation of trilocal inequalities. Consequently, for designing a scheme of entanglement detection, we consider all the possible arrangement of qubits. The protocol breaks up into 27 phases: $t_{i,j,k}$ ($i, j, k \in \{1, 2, 3\}$). In phase $t_{i,j,k}$, for every possible value of $i, j, k \in \{1, 2, 3\}$, ith, jth, kth qubits of $\kappa_1, \kappa_2, \kappa_3$, respectively, are sent to extreme parties. Hence, $\mathcal{P}_1^E$, $\mathcal{P}_2^E$, and $\mathcal{P}_3^E$ receive ith, jth, kth qubits of $\kappa_1, \kappa_2, \kappa_3$, respectively (for more details see Table VI in Appendix B). The remaining qubits of each of the unknown states are distributed among the intermediate parties in any pattern compatible with the nonlinear trilocal network scenario (Fig. 3). One may note that ordering of the phases is not essential. After receiving the particles, in each of these phases, the parties perform measurements on their respective subsystems. Correlated statistics are then used to test the trilocal inequalities [Eq. (15)]. If violation of at least one of the inequalities is observed in at least one phase, then each of κ_1, κ_2, and κ_3 is a tripartite entangled state whereas violation in all the phases ensures genuine entanglement of all the three unknown states. In the protocol, either violation occurs in no phase or in specific number of phases (see Table IV).

Interestingly, comparison of the possible nature of biseparable entanglement of $\kappa_1, \kappa_2, \kappa_3$ from Table VI ensures the nature of entanglement of each of the unknown states. To be more precise, at the end of the protocol, one can detect which of the three unknown states is genuinely entangled and which one is biseparable. Also, the specific nature of biseparable entanglement can be detected.

As already discussed, the total count of phases in which violation may be encountered is not arbitrary (see Table IV). Leaving aside the implications in the last two cases

TABLE IV. Total count of phases for which violation can be observed in the protocol is enlisted here. Implications are obvious from observations discussed in Sec. V A. In case of no violation in any of the phases, the protocol fails to detect entanglement.

Total number of phases	Implication
0	No definite conclusion
8	All are biseparable
12	Any two of the unknown states are biseparable and the remaining is genuinely entangled other than GGHZ [Eq. (21)] or W [Eq. (22)] classes
18	Only one of three unknown states is biseparable with the other two being genuinely entangled but does not belong to GGHZ or W families
$\geqslant$19 but $<$27	Each κ_i has genuine entanglement but is neither a member of GGHZ family [Eq. (21)] nor W state [Eq. (22)]
27	Each of κ_i is genuinely entangled

(corresponding to last two rows of Table IV), let us consider the remaining cases individually:

(i) Let violation be obtained in 18 phases. Then, definitely two of three unknown states are genuinely entangled but are neither a GGHZ nor W state and the remaining one is a biseparable entangled state. For instance, violation in only first 18 phases of the protocol $(t_{1,j,k}, t_{2,j,k}, j, k \in \{1, 2, 3\})$ ensures that only κ_1 is a biseparable entangled state having entanglement in 12/3 cut. This implication is obvious if one notes that the 12/3 cut biseparable entanglement is the only possible nature of entanglement of κ_1 if violation is obtained in first 18 phases (Table VI).

(ii) Violation in only 12 phases ensures that two of three unknown states are biseparable entangled and other one is genuinely entangled (other than GGHZ or W state). Consider a specific instance. Let violation be obtained in $t_{1,2,k}, t_{3,2,k}, t_{1,3,k}, t_{3,3,k}, \ \forall\, k \in \{1, 2, 3\}$. Then, κ_1, κ_2 are biseparable entangled states in 13/2 and 23/1 cuts, respectively, and κ_3 is genuinely entangled.

(iii) Violation in only 8 phases ensures that all three unknown states are biseparable entangled. The nature of biseparable entanglement of each κ_i is also detected. Consider the instance where violation is obtained in phases $t_{1,2,k}, t_{3,2,k}, t_{1,3,k}, t_{3,3,k}, \ \forall\, k \in \{1, 2\}$. Then, $\kappa_1, \kappa_2, \kappa_3$ are biseparable entangled states in 13/2, 23/1, and 12/3 cuts, respectively.

All these implications are direct consequences of the fact that violation of trilocal inequalities is not distribution (of qubits) specific in networks involving only genuine entanglement of GGHZ or W states whereas the same is crucial if at least one of the sources generates biseparable entanglement or genuine entanglement other than GGHZ [Eq. (21)] and W [Eq. (22)] classes.

VI. *n*-LOCAL NONLINEAR NETWORK SCENARIO

A trilocal nonlinear network can be extended to a network involving $2n-1$ parties and n independent sources, each generating an n-partite state. Each of n number of parties $\mathcal{P}_i^E$ $(i = 1, 2, \dots, n)$ (say) receives only one particle and are referred to as *extreme* parties whereas each of remaining $n-1$ parties $\mathcal{P}_i^I$ $(i = 1, 2, \dots, n-1)$, referred to as *intermediate* party, receives n particles (each from one source). Let $x_i \in \{0, 1\}$ and $a_i \in \{0, 1\}$ denote the binary input and output, respectively, of $\mathcal{A}_i$ $(i = 1, 2, \dots, n)$. Each of $\mathcal{B}_i$ $(i = 1, 2, \dots, n-1)$ performs a fixed measurement having 2^n outputs labeled as a n-dimensional vector $\vec{b}_i = (b_{i0}, \dots, b_{in-1})$.

After receiving qubits from the sources, parties do not communicate. $(2n-1)$-partite correlations are n-local if they can be decomposed as

$$P_{12^n}(a_1, \vec{b}_1, \dots, \vec{b}_{n-1}, a_2, \dots, a_n|x_1, \dots, x_n) = \int \dots \int d\eta_1 \dots d\eta_n \Lambda(\eta_1, \dots, \eta_n) W_n$$
$$\text{where } W_n = \Pi_{i=1}^{n} P_{12^n}(a_i|x_i, \eta_i) \Pi_{i=1}^{n-1} P_{12^n}(\vec{b}_i|\eta_1, \dots, \eta_n) \quad (23)$$

together with the constraint

$$\Lambda(\eta_1, \eta_2, \dots, \eta_n) = \Pi_{i=1}^{n} \Lambda_i(\eta_i), \quad (24)$$

where η_i characterizes source $\mathbf{S}_i$ and $\int d\eta_i \Lambda_i(\eta_i) = 1\ \forall\, i \in \{1, \dots, n\}$. Correlations inexplicable in the above form are non-n-local. The n-local inequalities are given by the following theorem.

Theorem 2. Any n-local $(2n-1)$-partite correlation term necessarily satisfies

$$\sqrt[n]{\left|I_{f_1,\dots,f_{n-1},0}^{(12^n)}\right|} + \sqrt[n]{\left|I_{g_1,\dots,g_{n-1},1}^{(12^n)}\right|} \leqslant 1 \quad (25)$$

where $f_1, \dots, f_{n-1}, g_1, \dots, g_{n-1} \in \{0, 1\}$.

Correlators used in Eq. (25) are detailed in Table V.

TABLE V. Detailing of the terms used in Eq. (25).

Correlators related to n-local nonlinear inequalities [Eq. (25)]
$I_{f_1(g_1),\dots,f_{n-1}(g_{n-1}),i}^{(12^n)} = \frac{1}{2^n} \sum_{x_1,\dots,x_n=0,1} (-1)^{i*(x_1+\dots+x_n)} \langle A_{1,x_1} B_1^{f_1(g_1)} \dots B_{n-1}^{f_{n-1}(g_{n-1})} \dots A_{n,x_n} \rangle$, with $i, f_1, \dots, f_{n-1}, g_1, \dots, g_{n-1} \in \{0, 1\}$
$\langle A_{1,x_1} B_1^{f_1(g_1)} \dots B_{n-1}^{f_{n-1}(g_{n-1})} \dots A_{n,x_n} \rangle = \sum_{\mathcal{Y}} (-1)^h P_{12^n}(a_1, \vec{b}_1, \dots, \vec{b}_{n-1}, \dots, a_n|x_1, \dots, x_n)$ where $\mathcal{Y} = \{a_1, \dots, a_n, b_{10}, \dots, b_{1n-1}, \dots, b_{n-10}, \dots, b_{n-1n-1}\}$ and $h = a_1 + \dots + a_n + s_{f_1(g_1)}(b_{20}, \dots, b_{2n-1}) + \dots + s_{f_{n-1}(g_{n-1})}(b_{n-10}, \dots, b_{n-1n-1})$ with functions $s_{i-1}(k_1, \dots, k_n)$ being defined as the sum of all possible product terms of $k_1, \dots, k_n$ taking i k_j's at a time $(i = 1, \dots, n-1)$.

Proof. The proof is based on the same technique as adopted for proving Theorem 1. As mentioned in Appendix A, for proving Theorem 1 we need to relate the correlators (used in present scenario) with that introduced for designing another trilocal network scenario in [17]. Analogously, Theorem 2 can be proved following the same line of argument (as that in Theorem 1). For that one should relate correlators (Table V) introduced for the n-local nonlinear scenario here with that of n-local network developed in [17]. ■

Violation of inequalities [Eq. (25)] for at least one possible $(f_1, \ldots, f_{n-1}, g_1, \ldots, g_{n-1})$ ensures non n-locality of corresponding correlations.

In the quantum scenario, let each source generate an n-qubit state. Each of the intermediate parties $\mathcal{P}_1^I, \ldots, \mathcal{P}_{n-1}^I$ performs complete n-dimensional GHZ basis measurement on the joint of n qubits (jth qubit coming from $\mathbf{S}_i$) whereas each of the extreme $\mathcal{P}_i^E$ $(i = 1, \ldots, n)$ performs projective measurement on its respective qubit. We conjecture that quantum violation of Eq. (25) can be obtained. In support of our conjecture we provide a numerical observation for $n = 4, 5$.

Let each of n independent sources $\mathbf{S}_i$ generate n-dimensional GHZ state

$$\vartheta_n = \frac{|0, 0, \ldots, 0\rangle + |1, 1, \ldots, 1\rangle}{\sqrt{2}}. \tag{26}$$

Violation of at least one n-local inequality [Eq. (25)] is obtained. This ensures generation of non-n-local correlations are generated in the network for $n = 4, 5$.

VII. DISCUSSIONS

In the recent past, nonlocality of quantum network correlations under circumstances that some of the parties perform a fixed measurement has been studied extensively. The topic of our paper evolves in this direction. We analyze the nonlocal feature of quantum correlations in networks involving uncorrelated sources when some of the parties do not have the freedom to choose their inputs randomly. Deriving quantum bounds of preexisting [16] n-local inequalities [Eq. (6)] turned

TABLE VI. Detailed distribution of qubits among the extreme parties in phases of the protocol. $\forall\ j, k \in \{1, 2, 3\}$, Q_j^k denotes the kth qubit of κ_j. For each $i = 1, 2, 3$, $(i+4)^{\text{th}}$ column of the table denotes the possible nature of entanglement of unknown state κ_i other than genuine entanglement when violation of at least one trilocal inequality is obtained in the corresponding phase.

Phase	$\mathcal{P}_1^E$	$\mathcal{P}_2^E$	$\mathcal{P}_3^E$	κ_1	κ_2	κ_3
$t_{1,1,1}$	$Q_1^{(1)}$	$Q_2^{(1)}$	$Q_3^{(1)}$	12/3 or 13/2 cut	12/3 or 13/2 cut	12/3 or 13/2 cut
$t_{1,1,2}$	$Q_1^{(1)}$	$Q_2^{(1)}$	$Q_3^{(1)}$	12/3 or 13/2 cut	12/3 or 13/2 cut	12/3 or 23/1 cut
$t_{1,1,3}$	$Q_1^{(1)}$	$Q_2^{(1)}$	$Q_3^{(1)}$	12/3 or 13/2 cut	12/3 or 13/2 cut	23/1 or 13/2 cut
$t_{1,2,1}$	$Q_1^{(1)}$	$Q_2^{(2)}$	$Q_3^{(1)}$	12/3 or 13/2 cut	12/3 or 23/1 cut	12/3 or 13/2 cut
$t_{1,2,2}$	$Q_1^{(1)}$	$Q_2^{(2)}$	$Q_3^{(1)}$	12/3 or 13/2 cut	12/3 or 23/1 cut	12/3 or 23/1 cut
$t_{1,2,3}$	$Q_1^{(1)}$	$Q_2^{(2)}$	$Q_3^{(1)}$	12/3 or 13/2 cut	12/3 or 23/1 cut	23/1 or 13/2 cut
$t_{1,3,1}$	$Q_1^{(1)}$	$Q_2^{(3)}$	$Q_3^{(1)}$	12/3 or 13/2 cut	23/1 or 13/2 cut	12/3 or 13/2 cut
$t_{1,3,2}$	$Q_1^{(1)}$	$Q_2^{(3)}$	$Q_3^{(1)}$	12/3 or 13/2 cut	23/1 or 13/2 cut	12/3 or 23/1 cut
$t_{1,3,3}$	$Q_1^{(1)}$	$Q_2^{(3)}$	$Q_3^{(1)}$	12/3 or 13/2 cut	23/1 or 13/2 cut	23/1 or 13/2 cut
$t_{2,1,1}$	$Q_1^{(2)}$	$Q_2^{(1)}$	$Q_3^{(1)}$	12/3 or 13/2 cut	12/3 or 13/2 cut	12/3 or 13/2 cut
$t_{2,1,2}$	$Q_1^{(2)}$	$Q_2^{(1)}$	$Q_3^{(1)}$	12/3 or 13/2 cut	12/3 or 13/2 cut	12/3 or 23/1 cut
$t_{2,1,3}$	$Q_1^{(2)}$	$Q_2^{(1)}$	$Q_3^{(1)}$	12/3 or 13/2 cut	12/3 or 13/2 cut	23/1 or 13/2 cut
$t_{2,2,1}$	$Q_1^{(2)}$	$Q_2^{(2)}$	$Q_3^{(1)}$	12/3 or 13/2 cut	12/3 or 23/1 cut	12/3 or 13/2 cut
$t_{2,2,2}$	$Q_1^{(2)}$	$Q_2^{(2)}$	$Q_3^{(1)}$	12/3 or 13/2 cut	12/3 or 23/1 cut	12/3 or 23/1 cut
$t_{2,2,3}$	$Q_1^{(2)}$	$Q_2^{(2)}$	$Q_3^{(1)}$	12/3 or 13/2 cut	12/3 or 23/1 cut	23/1 or 13/2 cut
$t_{2,3,1}$	$Q_1^{(2)}$	$Q_2^{(3)}$	$Q_3^{(1)}$	12/3 or 13/2 cut	23/1 or 13/2 cut	12/3 or 13/2 cut
$t_{2,3,2}$	$Q_1^{(2)}$	$Q_2^{(3)}$	$Q_3^{(1)}$	12/3 or 13/2 cut	23/1 or 13/2 cut	12/3 or 23/1 cut
$t_{2,3,3}$	$Q_1^{(2)}$	$Q_2^{(3)}$	$Q_3^{(1)}$	12/3 or 13/2 cut	23/1 or 13/2 cut	23/1 or 13/2 cut
$t_{3,1,1}$	$Q_1^{(3)}$	$Q_2^{(1)}$	$Q_3^{(1)}$	12/3 or 13/2 cut	12/3 or 13/2 cut	12/3 or 13/2 cut
$t_{3,1,2}$	$Q_1^{(3)}$	$Q_2^{(1)}$	$Q_3^{(1)}$	12/3 or 13/2 cut	12/3 or 13/2 cut	12/3 or 23/1 cut
$t_{3,1,3}$	$Q_1^{(3)}$	$Q_2^{(1)}$	$Q_3^{(1)}$	12/3 or 13/2 cut	12/3 or 13/2 cut	23/1 or 13/2 cut
$t_{3,2,1}$	$Q_1^{(3)}$	$Q_2^{(2)}$	$Q_3^{(1)}$	12/3 or 13/2 cut	12/3 or 23/1 cut	12/3 or 13/2 cut
$t_{3,2,2}$	$Q_1^{(3)}$	$Q_2^{(2)}$	$Q_3^{(1)}$	12/3 or 13/2 cut	12/3 or 23/1 cut	12/3 or 23/1 cut
$t_{3,2,3}$	$Q_1^{(3)}$	$Q_2^{(2)}$	$Q_3^{(1)}$	12/3 or 13/2 cut	12/3 or 23/1 cut	23/1 or 13/2 cut
$t_{3,3,1}$	$Q_1^{(3)}$	$Q_2^{(3)}$	$Q_3^{(1)}$	12/3 or 13/2 cut	23/1 or 13/2 cut	12/3 or 13/2 cut
$t_{3,3,2}$	$Q_1^{(3)}$	$Q_2^{(3)}$	$Q_3^{(1)}$	12/3 or 13/2 cut	23/1 or 13/2 cut	12/3 or 23/1 cut
$t_{3,3,3}$	$Q_1^{(3)}$	$Q_2^{(3)}$	$Q_3^{(1)}$	12/3 or 13/2 cut	23/1 or 13/2 cut	23/1 or 13/2 cut

out to be useful for designing a protocol capable of detecting bipartite resource of entanglement distributed in the network.

Analyzing network scenarios involving bipartite entanglement sources, we have then designed networks where sources now generate tripartite quantum states. In this context, we have framed a set of trilocal inequalities [Eq. (15)], violation of which (at least one) is sufficient to guarantee nontrilocality of corresponding correlations. Discussions in Sec. V ensure that randomness in choice of inputs for every party involved is not necessary to generate nonlocal (in sense of nontrilocality) correlations even when tripartite entanglement resources are distributed in the network. Based on numerical evidence we conjecture the same for exploiting non-n-locality ($n \geqslant 4$) also. Consequently, even when all the observers cannot randomly select their respective inputs in network scenarios involving m-partite ($m \geqslant 4$) entanglement (generated by sources), nonlocal (non-n-local) correlations can be obtained.

Apart from theoretical perspectives, these trilocal network scenarios turned out to be useful on practical grounds for detection of tripartite entanglement of pure states. More interestingly, protocols designed here can discriminate between some genuinely entangled states and biseparable entanglement existing in any possible grouping of two qubits constituting the three-qubit state. In this context, it will be interesting to enhance the capability of this protocol to discriminate between arbitrary genuine entanglement and biseparable entanglement of any tripartite state. n-local nonlinear network scenario introduced here may be explored further with an objective to detect entanglement of m-partite ($m \geqslant 4$) states and also to discriminate between genuine entanglement from any other form of m-partite entanglement.

APPENDIX A

In [17], another trilocal network scenario was introduced where each of the five parties, involved in the network, performs one of two dichotomic measurements, i.e., unlike the measurement scenario introduced here, none of the parties has fixed input (for details, see [17]). Correlations generated in such a network [17] are trilocal if they satisfy

$$\sqrt[3]{|\mathcal{I}_{u_1,u_2,0}|} + \sqrt[3]{|\mathcal{I}_{v_1,v_2,1}|} \leqslant 1 \ \forall\ u_1,\ u_2,\ v_1,\ v_2\ \in \{0,1\} \text{ with} \tag{A1}$$

$$\mathcal{I}_{u_1(v_1),u_2(v_2),t} = \frac{1}{8}\sum_{x_1,x_2,x_3=0,1}(-1)^{t*q}\langle \mathcal{A}_{1,x_1}\mathcal{B}_{1,y_1=u_1(v_1)}\mathcal{B}_{2,x_2=u_2(v_2)}\mathcal{A}_{2,x_2}\mathcal{A}_{3,x_3}\rangle, \quad t\in\{0,1\}, \quad q = x_1+x_2+x_3, \tag{A2}$$

where

$$\langle \mathcal{A}_{1,x_1}\mathcal{B}_{1,y_1}\mathcal{B}_{2,y_2}\mathcal{A}_{2,x_2}\mathcal{A}_{3,x_3}\rangle = \sum_{a_1,b_1,b_2,a_2,a_3}(-1)^m P(a_1,b_1,b_2,a_2,a_3|x_1,y_1,y_2,x_2,x_3), \quad \text{with } m = a_1+b_1+b_2+a_2+a_3, \tag{A3}$$

where $x_i \in \{0,1\}$ denote the input whereas $a_i \in \{0,1\}$ denote the corresponding output of extreme party $\mathcal{P}_i^E$ ($i = 1,2,3$). Similarly, y_1, y_2 denote input and b_1, b_2 denote output of intermediate party $\mathcal{P}_1^I, \mathcal{P}_2^I$, respectively. $\mathcal{A}_1, \mathcal{A}_2, \mathcal{A}_3, \mathcal{B}_1, \mathcal{B}_2$ denote the corresponding observables. We now proceed to prove Theorem 1.

Proof. For simplicity, we use the notations $s_{y_i}(b_{i0}, b_{i1}, b_{i2}) = s_{y_i}$ ($i = 1,2$). Now comparison of the correlation terms related to these two scenarios gives

$$\begin{aligned} P(a_1,b_1,b_2,a_2,a_3|x_1,y_1,y_2,x_2,x_3) &= P_{18}(a_1, s_{y_1}=b_1, s_{y_2}=b_2, a_2, a_3|x_1,x_2,x_3) \\ &= \sum_{\mathcal{D}}\delta_{b_1,s_{y_1}}\delta_{b_2,s_{y_2}}P_{18}(a_1,b_{10},b_{11},b_{12},b_{20},b_{21},b_{22},a_2,a_3|x_1,x_2,x_3), \end{aligned} \tag{A4}$$

where $\mathcal{D} = \{b_{10},b_{11},b_{12},b_{20},b_{21},b_{22}\}$. By Eq. (A3),

$$\begin{aligned} \langle \mathcal{A}_{1,x_1}\mathcal{B}_{1,y_1}\mathcal{B}_{2,y_2}\mathcal{A}_{2,x_2}\mathcal{A}_{3,x_3}\rangle = \sum_{a_1,a_2,a_3}(-1)^{a_1+a_2+a_3}[&P(a_1,0,0,a_2,a_3|x_1,y_1,y_2,x_2,x_3) + P(a_1,1,1,a_2,a_3|x_1,y_1,y_2,x_2,x_3) \\ &-P(a_1,0,1,a_2,a_3|x_1,y_1,y_2,x_2,x_3) - P(a_1,1,0,a_2,a_3|x_1,y_1,y_2,x_2,x_3)]. \end{aligned} \tag{A5}$$

Now, Eq. (A4) implies

$$P(a_1,i,j,a_2,a_3|x_1,y_1,y_2,x_2,x_3) = \sum_{\mathcal{D}}\delta_{i,s_{y_1}}\delta_{j,s_{y_2}}P_{18}(b_{10},b_{11},b_{12},b_{20},b_{21},b_{22},a_2,a_3|x_1,x_2,x_3), \quad \forall\ i,j\in\{0,1\}.$$

Using the above relations, in Eq. (A5) and $\mathcal{C} = \{a_1,a_2,a_3,b_{10},b_{11},b_{12},b_{20},b_{21},b_{22}\}$ we get

$$\begin{aligned} \langle \mathcal{A}_{1,x_1}\mathcal{B}_{1,y_1}\mathcal{B}_{2,y_2}\mathcal{A}_{2,x_2}\mathcal{A}_{3,x_3}\rangle &= \sum_{\mathcal{C}}(-1)^{a_1+a_2+a_3}\sum_{i,j=0,1}(-1)^{i+j}\delta_{i,s_{y_1}}\delta_{j,s_{y_2}}P_{18}(a_1,b_{10},b_{11},b_{12},b_{20},b_{21},b_{22},a_2,a_3|x_1,x_2,x_3) \\ &= \sum_{\mathcal{C}}(-1)^{a_1+a_2+a_3+s_{y_1}+s_{y_2}}P_{18}(a_1,b_{10},b_{11},b_{12},b_{20},b_{21},b_{22},a_2,a_3|x_1,x_2,x_3). \end{aligned}$$

Hence,

$$\langle \mathcal{A}_{1,x_1}\mathcal{B}_{1,y_1}\mathcal{B}_{2,y_2}\mathcal{A}_{2,x_2}\mathcal{A}_{3,x_3}\rangle = \langle A_{1,x_1}B_1^{y_1}B_2^{y_2}A_{2,x_2}A_{3,x_3}\rangle. \tag{A6}$$

By Eqs. (A1), (A2), (A3), and(A6), we get the required criteria given by Eq. (15).

APPENDIX B

As already mentioned in the main text that distribution of qubits among the extreme parties is crucial in the context of obtaining violation by biseparable entanglement. So, for designing the protocol for purpose of detecting tripartite entanglement, all possible arrangements of qubits among the extreme parties are considered. At this junction, one may recall that in the nonlinear trilocal network scenario (Fig. 3), for a fixed source, the pattern of arranging qubits among the intermediate parties does not contribute in detecting the nature of biseparable entanglement. So, distribution of qubits only among the extreme parties $\mathcal{P}_1^E$, $\mathcal{P}_2^E$, and $\mathcal{P}_3^E$ is enlisted in Table VI. The last three columns of Table VI indicate the possible nature of biseparable entanglement of the unknown state under the circumstance that violation of at least one trilocal inequality [Eq. (15)] is obtained in the corresponding phase. For instance, consider the phase $t_{1,2,3}$. If violation is obtained in this phase of the protocol, then following are the possible natures of the three unknown quantum states:

(i) κ_1 is either genuinely entangled or have biseparable entanglement content in $12/3$ or $13/2$ cut.

(ii) κ_2 is either genuinely entangled or have biseparable entanglement content in $12/3$ or $23/1$ cut.

(iii) κ_3 is either genuinely entangled or have biseparable entanglement content in $23/1$ or $13/2$ cut.

[1] R. Horodecki, P. Horodecki, M. Horodecki, and K. Horodecki, Quantum entanglement, Rev. Mod. Phys. **81**, 865 (2009).

[2] J. S. Bell, On the Einstein Podolsky Rosen paradox, Physics **1**, 195 (1964).

[3] J. S. Bell, *Speakable and Unspeakable in Quantum Mechanics* (Cambridge University Press, Cambridge, England, 1987).

[4] S. Groblacher, T. Paterek, R. Kaltenbaek, C. Brukner, M. Zukowski, M. Aspelmeyer, and A. Zeilinger, An experimental test of non-local realism, Nature (London) **446**, 871 (2007).

[5] A. Aspect, J. Dalibard, and G. Roger, Experimental Test of Bell's Inequalities Using Time-Varying Analyzers, Phys. Rev. Lett. **49**, 1804 (1982).

[6] J. F. Clauser, M. A. Horne, A. Shimony, and R. A. Holt, Proposed Experiment to Test Local Hidden-Variable Theories, Phys. Rev. Lett. **23**, 880 (1969).

[7] N. Gisin, Q. Mei, A. Tavakoli, M. O. Renou, and N. Brunner, All entangled pure quantum states violate the bilocality inequality, Phys. Rev. A **96**, 020304(R) (2017).

[8] N. Gisin, The elegant joint quantum measurement and some conjectures about N-locality in the triangle and other configurations, arXiv:1708.05556.

[9] M. R. Renou, E. Bäumer, S. Boreiri, N. Brunner, and N. Gisi, Genuine Quantum Nonlocality in the Triangle Network, Phys. Rev. Lett. **123**, 140401 (2019).

[10] T. Fraser and E. Wolfe, Causal compatibility inequalities admitting quantum violations in the triangle structure, Phys. Rev. A **98**, 022113 (2018).

[11] M. O. Renou, Y. Wang, S. Boreiri, S. Beigi, N. Gisin, and N. Brunner, Limits on Correlations in Networks for Quantum and No-Signaling Resources, Phys. Rev. Lett. **123**, 070403 (2019).

[12] N. Gisin, Entanglement 25 years after quantum teleportation: testing joint measurements in quantum networks, Entropy **21**, 325 (2019).

[13] C. Branciard, D. Rosset, N. Gisin, and S. Pironio, Bilocal versus nonbilocal correlations in entanglement-swapping experiments, Phys. Rev. A **85**, 032119 (2012).

[14] C. Branciard, N. Gisin, and S. Pironio, Characterizing the Nonlocal Correlations Created via Entanglement Swapping, Phys. Rev. Lett. **104**, 170401 (2010).

[15] A. Tavakoli, P. Skrzypczyk, D. Cavalcanti, and A. Acín, Nonlocal correlations in the star-network configuration, Phys. Rev. A **90**, 062109 (2014).

[16] K. Mukherjee, B. Paul, and D. Sarkar, Correlations In n-local scenario, Quantum Inf. Process. **14**, 2025 (2015).

[17] K. Mukherjee, B. Paul, and D. Sarkar, Nontrilocality: Exploiting nonlocality from three-particle systems, Phys. Rev. A **96**, 022103 (2017).

[18] K. Mukherjee, B. Paul, and D. Sarkar, Revealing advantage in a quantum network, Quantum Inf. Process. **15**, 2895 (2016).

[19] K. Mukherjee, B. Paul, and D. Sarkar, Restricted distribution of quantum correlations in bilocal network, Quantum Inf. Process. **18**, 212 (2019).

[20] J. Barrett, L. Hardy, and A. Kent, No Signaling and Quantum Key Distribution, Phys. Rev. Lett. **95**, 010503 (2005).

[21] D. Mayers and A. Yao, Quantum cryptography with imperfect apparatus, in *Proceedings of the 39th IEEE Symposiumon Foundations of Computer Science* (IEEE Computer Society, Los Alamitos, CA, 1998), p. 503.

[22] A. Acín, N. Brunner, N. Gisin, S. Massar, S. Pironio, and V. Scarani, Device-Independent Security of Quantum Cryptography against Collective Attacks, Phys. Rev. Lett. **98**, 230501 (2007).

[23] A. Acín, N. Gisin, and L. Masanes, From Bell's Theorem to Secure Quantum Key Distribution, Phys. Rev. Lett. **97**, 120405 (2006).

[24] R. Colbeck and A. Kent, Private randomness expansion with untrusted device, J. Phys. A: Math. Theor. **44**, 095305 (2011).

[25] S. Pironio, A. Acín, S. Massar, A. B. de la Giroday, D. N. Matsukevich, P. Maunz, S. Olmschenk, D. Hayes, L. Luo, T. A. Manning, and C. Monroe, Random numbers certified by Bell's theorem, Nature (London) **464**, 1021 (2010).

[26] N. Brunner and N. Linden, Connection between Bell nonlocality and Bayesian game theory, Nat. Commun. **4**, 2057 (2013).

[27] J. Preskill, *Lecture Notes for Physics: Quantum Information and Computation* (California Institute of Technology, Pasadena, CA, 1998).

[28] R. Horodecki, P. Horodecki, and M. Horodecki, Violating Bell inequality by mixed spin $-\frac{1}{2}$ states: necessary and sufficient condition, Phys. Lett. A **200**, 340 (1995).

[29] K. Mukherjee, B. Paul, D. Sarkar, Efficient test to demonstrate genuine three particle nonlocality, J. Phys. A: Math. Theor. **48**, 2025 (2015).

[30] A. Acín, Generalized Schmidt Decomposition and Classification of Three-Quantum-Bit States, Phys. Rev. Lett. **85**, 1560 (2000).

Quantum Information Processing (2019) 18:212
https://doi.org/10.1007/s11128-019-2328-0

Restricted distribution of quantum correlations in bilocal network

Kaushiki Mukherjee[1] **· Biswajit Paul**[2] **· Debasis Sarkar**[3]

Received: 9 November 2018 / Accepted: 12 May 2019 / Published online: 18 May 2019

Abstract
Analyzing shareability of correlations arising in any physical theory may be considered as a fruitful technique of studying the theory. Our present topic of discussion involves an analogous approach of studying quantum theory. For our purpose, we have deviated from the usual procedure of assessing monogamous nature of quantum correlations in the standard Bell-CHSH scenario. We have considered correlations arising in a quantum network involving independent sources. Precisely speaking, we have analyzed monogamy of nonbilocal correlations by deriving a relation restricting marginals. Interestingly, restrictions constraining distribution of nonbilocal correlations remain same irrespective of whether inputs of the nodal observers are kept fixed (in different bilocal networks) while studying nonbilocal nature of marginal correlations.

Keywords Quantum correlations · Monogamy · Bell locality · Quantum network · Bilocality

1 Introduction

Entanglement and nonlocality, the two most intrinsic features of quantum theory, play ubiquitous role in analyzing departure of the theory from the classical world. While the former is a property of quantum states [1], the latter mainly characterizes nature of

✉ Debasis Sarkar
dsarkar1x@gmail.com, dsappmath@caluniv.ac.in

Kaushiki Mukherjee
kaushiki_mukherjee@rediffmail.com

Biswajit Paul
biswajitpaul4@gmail.com

1 Department of Mathematics, Government Girls' General Degree College, Ekbalpore, Kolkata 700023, India

2 Department of Mathematics, South Malda College, Malda, West Bengal, India

3 Department of Applied Mathematics, University of Calcutta, 92, A.P.C. Road, Kolkata 700009, India

correlations arising due to measurements on quantum systems [2–4]. Considered to be two inequivalent resources in general, both of these features form the basis of various information processing tasks such as device-independent entanglement witnesses [5], quantum key distribution (QKD) [6–9], Bayesian game theoretic applications [10], private randomness generation [11,12], etc, which cannot be performed by any classical resource. One of the inherent features responsible for strengthening efficiency of quantum resources over classical ones is the existence of restrictions over shareability of quantum particles or quantum correlations in multiparty scenario [13–24].

Research activities conducted so far clearly point out the existence of limitations over shareability of both quantum nonlocality [13,15] and entanglement [14,20–24]. Such sort of limitations is frequently referred to as monogamy of nonlocality and entanglement, respectively. Precisely speaking, let a tripartite state be shared between three parties, say, Alice, Bob and Charlie. If Alice's qubit is maximally entangled with that of Bob, then neither the state shared between Alice and Charlie nor that between Bob and Charlie is entangled. Now consider the tripartite correlations generated due to measurements on a quantum system shared between Alice, Bob and Charlie. If the marginal correlations shared between any two parties, say Alice and Bob violate Bell-CHSH inequality [25] maximally then neither marginal shared between Alice and Charlie nor that shared between Bob and Charlie can show Bell-CHSH violation. However, no such restriction exists over shareability of classical correlations. Over years, different trade-off relations have been designed to capture monogamous nature of not only quantum correlations but also of correlations abiding by no signaling principle [26]. Our present topic of discussion is contributory in this direction. To be precise, we have explored shareability of correlations characterizing quantum *bilocal network*.

Over past few years, there has been a trend of studying quantum networks involving independent sources [27,28]. Network involving two independent sources is referred to as 'bilocal' network (see Fig. 1). It was first introduced in [27]. Since then study of quantum networks characterized with source independence has been subject matter of thorough investigations [29–38] due to multi-faceted utility of the source independence assumption both from theoretical and experimental perspectives such as lowering down restrictions for detecting quantumness (nonclassical feature) in a network via some notions of quantum nonlocality (different from the standard Bell nonlocality) [30,33]. Besides, it is found to be important to study detection loophole in some local models [39,40]. From experimental perspectives, source independent networks form basis of various experiments related to quantum information and communication such as various device-independent quantum information processing tasks [5,8–10], some communication networks dealing with entanglement percolation [41], *quantum repeaters* [42] and *quantum memories* [43], etc. Owing to the significance of these networks, study of correlations generated in such networks has gained immense importance. In this context, one obvious direction of investigation evolves around manifesting shareability of correlations in such networks. Our discussions will channelize in that direction.

To the best of authors' knowledge, research activities on monogamy of quantum correlations, conducted so far, basically consider the standard Bell scenario [13,15]. Here, we have shifted from that usual notion of Bell-CHSH nonlocality thereby exploring shareability of quantum correlations in spirit of nonbilocality [27,28]. Precisely speaking, we have considered quantum network involving two independent sources with an urge to investigate whether nonclassical feature of quantum correlations generated in such networks exhibit monogamy or not. We have obtained affirmative answer to this query which in turn points out the indifference between the two notions of nonlocality: Bell-CHSH nonlocality and nonbilocality in context of characterizing shareability of quantum correlations.

One may note that for studying monogamy in the standard Bell-CHSH scenario, it is assumed that the nodal party (for instance Alice in the example discussed before) has fixed measurement settings. For instance, to analyze Bell violation by each of two sets of bipartite correlations: $P(a, b|x, y)$, shared between Alice, Bob and $P(a, c|x, z)$, shared between Alice, Charlie (a, b, c and x, y, z denoting binary outputs and inputs of Alice, Bob and Charlie, respectively), Alice's measurement settings are assumed to be fixed. However, recently, in [44], a trade-off relation has been suggested giving restriction over upper bound of Bell-CHSH violation by all the possible bipartite marginals where the measurement settings of nodal party were not assumed to be fixed. Here, we have firstly derived a monogamy relation for nonbilocal correlations. Then, we have relaxed the assumption of fixed setting by nodal party, thereby designing a trade-off relation restricting the nonbilocal nature of the marginal correlations. Interestingly, nature of restrictions to exhibit nonbilocality by the marginals remains invariant irrespective of the assumption of fixed measurement settings of nodal party. Throughout the manuscript we have considered that each party has a two-dimensional quantum system under its control.

Rest of the article is organized as follows. First, we discuss some ideas motivating our work in Sect. 2. Next in Sect. 3, we give a brief review of the bilocal network scenarios and some results related to these scenarios which in turn will facilitate our further discussions. In Sect. 4, we first sketch the network scenario(s) in details. Depending on inputs and also outputs of some of the parties (involved in the scenario), we basically consider two scenarios. Then, we derive the monogamy relation in Sect. 4 followed by a trade-off relation in Sect. 5 restricting the correlations generated therein. Some practical implications of our findings have been discussed in Sect. 6. Finally, we have concluded in Sect. 7 discussing possible future directions of research activities.

2 Motivation

As already pointed out before, in recent times, study of quantum networks (with independent sources) has gained paramount interest [29–36]. So, in context of analyzing nonclassicality of quantum correlations in such networks, assessment of monogamous nature (if any) of the correlations is crucial for developing a better insight in related fundamental issues. Interestingly, from practical view point, existence of restrictions over shareability of quantum correlations is utilized to design quantum secret sharing protocol secure against eavesdropping [45–47]. To be specific, it is this nonclassical feature of quantum correlations that plays a vital role to provide security against external attack better than any classical protocol. So, if monogamous nature of correlations arising in quantum networks involving independent sources can be guaranteed then that will be definitely helpful for security analysis in secret sharing protocols involving such networks. So possible issues related with restricted shareability of quantum correlations in network scenario deserve detailed investigations. This basically motivates our current topic.

3 Preliminaries

3.1 Bilocal scenario

Bilocal network as designed in [27,28] is shown in Fig. 1. Out of three scenarios described in [28], here we consider two scenarios, namely P^{14} and P^{22} scenarios involving bilocal network. The network involves three parties Alice(A), Bob(B) and Charlie(C) and two sources $\mathbf{S}_1$ and $\mathbf{S}_2$. All the parties and sources are arranged in a linear fashion. A source is shared between any pair of adjacent parties. Sources $\mathbf{S}_1$ and $\mathbf{S}_2$ are independent to each other (*bilocal assumption*). A physical system represented by variables λ_1 and λ_2 is send by $\mathbf{S}_1$ and $\mathbf{S}_2$, respectively. Bob receives two particles (one from each of $\mathbf{S}_1$ and $\mathbf{S}_2$). Independence of λ_1 and λ_2 is ensured by that of $\mathbf{S}_1$ and $\mathbf{S}_2$. In both P^{14} and P^{22} scenarios, each of Alice and Charlie can perform dichotomic measurements on their systems. The binary inputs are denoted by $x, z \in \{0, 1\}$ for Alice and Charlie, and their outputs are labeled as $a, c \in \{0, 1\}$, respectively. Bob performs measurement on the joint state of the two systems that he receives from $\mathbf{S}_1$ and $\mathbf{S}_2$. In P^{22} scenario, Bob performs two dichotomic measurements $y \in \{0, 1\}$ having outputs $b \in \{0, 1\}$.

In P^{14} scenario, Bob performs single measurement y having 4 outputs $b = \overrightarrow{\mathbf{b}} = b_0b_1 = 00, 01, 10, 11$.

In both scenarios, the correlations obtained in the network are local if they take the form: $P(a, b, c|x, y, z) = \iint d\lambda_1 d\lambda_2 \rho(\lambda_1, \lambda_2)U$

$$\text{where } U = P(a|x, \lambda_1)P(b|y, \lambda_1, \lambda_2)P(c|z, \lambda_2) \tag{1}$$

where λ_1 characterizes the state of the bipartite system produced by the source S_1 and λ_2 for the system S_2. Tripartite correlations $P(a, b, c|x, y, z)$ are bilocal if they can be decomposed in above form (Eq. (1)) together with the restriction:

$$\rho(\lambda_1, \lambda_2) = \rho_1(\lambda_1)\rho_2(\lambda_2) \tag{2}$$

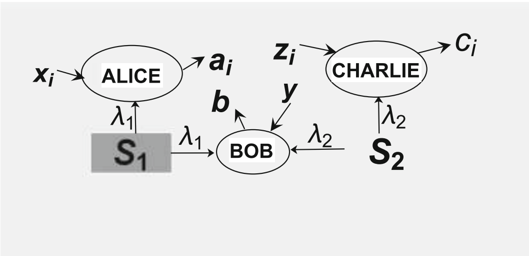

Fig. 1 Schematic diagram of a bilocal network [27,28]. In P^{22} scenario, y corresponds to two inputs of Bob y_0 and y_1 and b corresponds to two outputs b_0 and b_1. In P^{14} scenario, y corresponds to single input of Bob and b corresponds to 4 outputs $b_0b_1 = 00, 01, 10, 11$

imposed on the probability distributions of the hidden variables λ_1, λ_2. Eq. (2) refers to the *bilocal constraint*. Tripartite correlations of the form (Eq. (1)) and (Eq. (2)) are bilocal if they satisfy the inequality [28]:

$$\sqrt{|I|} + \sqrt{|J|} \leq 1 \tag{3}$$

Terms appearing in above equation are discussed in Table 1. Denoting $\sqrt{|I|} + \sqrt{|J|}$ as $\mathbf{B}$, Eq. (3) becomes:

$$\mathbf{B} \leq 1 \tag{4}$$

Clearly, violation of Eq. (4) acts as a sufficient criterion for detecting nonbilocality of corresponding correlations. In [36,37], referring $\mathbf{B}$ as *bilocality parameter*, an upper bound of quantum violation of the bilocal inequality (Eq. (4)) has been derived for both P^{22} scenario [36] and P^{14} scenario [37]. We next briefly review scenarios considered in [36,37] along with some of the related findings which will be used later in course of our work.

3.2 Bilocal quantum network [27,28]

Let each of $\mathbf{S}_1$ and $\mathbf{S}_2$ sends a two qubit quantum state. Let $\mathbf{S}_1$ sends ρ_{AB} to Alice and Bob, whereas $\mathbf{S}_2$ sends ρ_{BC} to Bob and Charlie. In general, any bipartite state density matrix representing a quantum state (ρ, say) can be defined as:

$$\rho = \frac{1}{2^2} \sum_{i_1, i_2 = 0}^{3} T_{i_1 i_2} \sigma_{i_1}^1 \bigotimes \sigma_{i_2}^2 \tag{5}$$

with σ_0^k, denoting the identity operator in the Hilbert space of k^{th} qubit and $\sigma_{i_k}^k$, denote the Pauli operators along three mutually perpendicular directions, $i_k = 1, 2, 3$. The entries of the correlation matrix T_ρ of ρ denoted by $T_{i_1 i_2}$ are real and given by:

$$T_{i_1 i_2} = \text{Tr}[\rho \sigma_{i_1}^1 \bigotimes \sigma_{i_2}^2],\ i_1, i_2 \in \{1, 2, 3\}. \tag{6}$$

Let T_{AB} and T_{BC} denote correlation tensor of state ρ_{AB} and ρ_{BC}, respectively, and let upper bound of violation of the bilocal inequality (Eq. (4)) be given by $\mathbf{B}_{\text{Max}}$. Recently, $\mathbf{B}_{\text{Max}}$ has been derived for both the scenarios [36,37]. Interestingly, irrespective of variation in measurement settings of Bob (see Table 2), closed form of $\mathbf{B}_{\text{Max}}$ turns out to be same:

$$\mathbf{B}_{\text{Max}} = \sqrt{\sum_{i=1}^{2} \sqrt{\omega_i^A * \omega_i^C}},\quad \omega_1^{A(C)} > \omega_2^{A(C)}, \tag{7}$$

with ω_1^A and ω_2^A (ω_1^C and ω_2^C) are the larger two eigenvalues of $T_{\text{AB}}^T T_{\text{AB}} (T_{BC}^T T_{BC})$.

Table 1 Details of the terms appearing in Eq. (3) in both the scenarios [27,28]. A_x and C_z stand for the observables corresponding to binary inputs x and z of Alice and Charlie, respectively. $a, c \in \{0, 1\}$ denote the corresponding outputs

Scenario	I and J	Expressions of correlators	Observables and outputs of Bob
P^{22}	$I = \frac{1}{4} \sum_{x,z=0,1} \langle A_x B_0 C_z \rangle$	$\langle A_x B_y C_z \rangle = \sum_{a,b,c} (-1)^{a+b+c} P(a, b, c\|x, y, z)$	B_y:observable corresponding to binary inputs y of Bob with outputs $b \in \{0, 1\}$.
	$J = \frac{1}{4} \sum_{x,z=0,1} (-1)^{x+z} \langle A_x B_1 C_z \rangle$		
P^{14}	$I = \frac{1}{4} \sum_{x,z=0,1} \langle A_x B^0 C_z \rangle$	$\langle A_x B^y C_z \rangle = \sum_{a,b_0 b_1,c} (-1)^{a+b_y+c} P(a, b_0 b_1, c\|x, z)$	B^y:observable corresponding to a single input 4 outputs: $\overrightarrow{\mathbf{b}} = b_0 b_1 =$ 00, 01, 10, 11.
	$J = \frac{1}{4} \sum_{x,z=0,1} (-1)^{x+z} \langle A_x B^1 C_z \rangle$		

Table 2 The table provides the measurement settings of Bob for both the scenarios. $\mathbf{fi_i}^A$ denotes the direction along which Bob performs projective measurement on the particle that it receives from source S_1 and $\mathbf{fi_i}^D$ denotes the direction along which Bob performs projective measurement on the particle that it receives from source S_2. Alice and Charlie perform projective measurements in two arbitrary directions: $_\mathbf{i}$.œ and $_\mathbf{i}$.œ$(i = 0, 1)$, respectively [36,37]

Scenario	Bob's measurement settings
P^{22} [36]	$\mathbf{fi_i}^A$.œ $\otimes$ $\mathbf{fi_i}^D$.œ$(i = 0, 1)$ i.e., Bob performs separable measurements on joint state of two qubits (received from $\mathbf{S}_1$ and $\mathbf{S}_2$)
P^{14} [37]	Bob performs full Bell-state measurements, i.e., he measures joint state of two qubits in Bell-basis. Projection of the joint state in a Bell state thereby corresponding to an output (total 4)

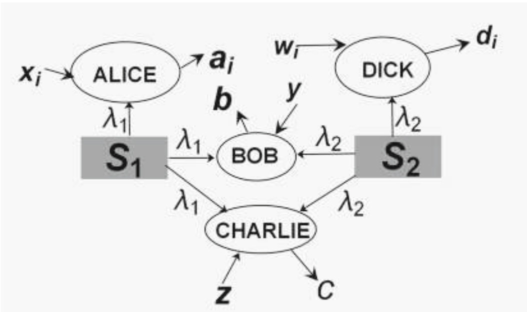

Fig. 2 Schematic diagram of network $\mathcal{N}$. In P^{22} scenario y, z corresponds to two inputs of Bob y_0 and y_1 and two inputs of Charlie z_0 and z_1, respectively. b corresponds to two outputs b_0 and b_1 of Bob, and likewise c denotes two outputs of Charlie c_0, and c_1. In P^{14} scenario y, z corresponds to Bell-state measurement (single input) of Bob and Charlie, respectively. b corresponds to 4 outputs: $b_0b_1 = 00,\ 01,\ 10,\ 11$ according to projection of the joint state of two qubits in Bob's control in Bell state $|\phi^+\rangle$, $|\phi^-\rangle$, $|\psi^+\rangle$ and $|\psi^-\rangle$, respectively. Analogously 4 outputs of Charlie are denoted by $c_0c_1 = 00,\ 01,\ 10,\ 11$

After discussing the mathematical pre-requisites, we proceed to present our findings.

4 Nonbilocal monogamy

For our purpose, we have considered P^{22} scenario and P^{14} scenario under the assumption that Bob performs Bell-state measurement (as stated in Table 2). For exploring restriction(if any) over shareability of nonbilocal correlations, first we define the network (Fig. 2) which will encompass both the scenarios.

4.1 Quantum network scenario

Consider a network ($\mathcal{N}$) involving four parties Alice, Bob, Charlie, Dick and two independent sources $\mathbf{S}_1$ and $\mathbf{S}_2$. Each of the two sources generates a tripartite quantum state. Let $\mathbf{S}_1$ generates ρ_{ABC}, sending a qubit to each of Alice, Bob and Charlie. Analogously, $\mathbf{S}_2$ generates ρ_{BCD}, sending a qubit to each of Bob, Charlie and Dick. So, each of Bob and Charlie receives two qubits, whereas remaining two parties receives one qubit each. Let Bob and Charlie be referred to as *intermediate parties*, whereas Alice and Dick be referred to as *extreme parties*. The extreme parties perform arbitrary projective measurements locally on their qubits. Inputs of Alice and Dick are labeled as $x, w \in \{0, 1\}$ and outputs as $a, d \in \{0, 1\}$, respectively. Each of two intermediate parties Bob and Charlie performs measurements on joint state of its two qubits. In P^{22} scenario, each of Bob and Charlie performs dichotomic measurements, i.e., $y, z \in \{0, 1\}$ with corresponding outputs $b, c \in \{0, 1\}$, whereas in P^{14} scenario each of them can perform a single measurement having four outputs (as discussed in Sect. 3). We consider some specific forms of measurements for Bob and Charlie in both the scenarios. While in P^{22} scenario, each of Bob and Charlie can perform separable measurements [36], in P^{14} scenario each of them performs Bell-state measurement (BSM) [37] on the joint state of the two qubits sent by the sources. In both these scenarios, four partite correlation terms $P(a, b, c, d|x, y, z, w)$, arising due to measurements by the parties on their respective qubits characterize the network ($\mathcal{N}$). Let W_B and W_C denote the set of tripartite marginals $P(a, b, d|x, y, w)$ and $P(a, c, d|x, z, w)$, respectively. Now W_B can be interpreted as the set of tripartite correlations arising due to binary measurements by each of three parties Alice, Bob and Dick in a network involving two independent sources $\mathbf{S}_1$ and $\mathbf{S}_2$. Hence, correlations from W_B characterize the bilocal network ($\mathcal{N}_B$, say) involving Alice, Bob and Dick. Analogously, W_C characterizes bilocal network ($\mathcal{N}_C$, say) involving parties Alice, Charlie and Dick. Each of the two bilocal networks $\mathcal{N}_B$ and $\mathcal{N}_C$ may be referred to as a *reduced network* obtained from the original bilocal network $\mathcal{N}$. Clearly, extreme parties of $\mathcal{N}$ are common in both the reduced networks ($\mathcal{N}_B$, $\mathcal{N}_C$) and may be referred to as the *nodal parties*. In Fig. 3, we give a flowchart to design the scenario involved herein.

Now, we put forward the monogamy relation restricting nonbilocality of the tripartite marginals $P(a, b, d|x, y, w)$ and $P(a, c, d|x, z, w)$ in both the scenarios.

4.2 Restrictions over quantum correlations

Theorem 1 *Under the assumption that each of the extreme parties performs separable measurements or Bell-state measurements, if* $\mathbf{B}^B_{\text{Max}}$ *and* $\mathbf{B}^C_{\text{Max}}$ *denote the upper bound of violations of bilocal inequality (Eq. (4)) by correlations* $P(a, b, d|x, y, w)$ *and* $P(a, c, d|x, z, w)$*, respectively, then,*

$$(\mathbf{B}^B_{\text{Max}})^2 + (\mathbf{B}^C_{\text{Max}})^2 \leq 2. \tag{8}$$

Proof This theorem basically follows from the proof of Theorem 2 which will be discussed shortly.

Compared to a single nodal (common) party in standard Bell scenario, here, measurement settings of both the nodal parties (Alice and Dick) are kept fixed in order to sketch the monogamy relation (Eq. (8)). Alice and Dick's fixed measurement settings mainly refer to the fact each of their measurement settings remain unchanged

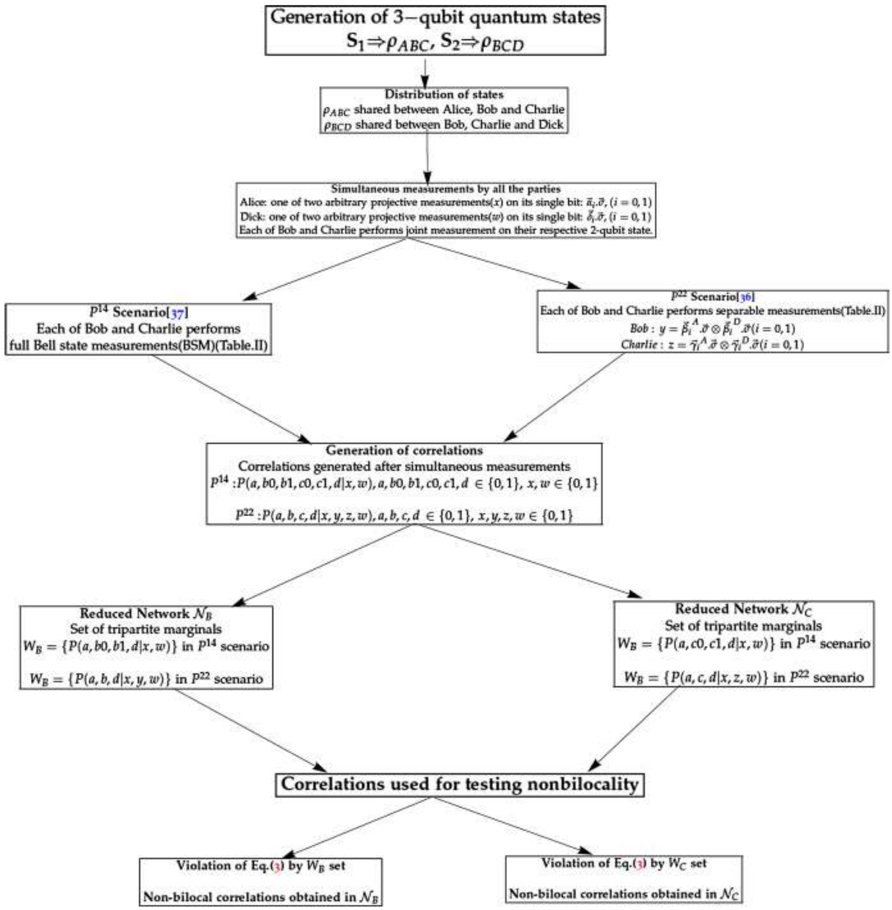

Fig. 3 A flowchart underlying our scheme of testing correlations is provided thereby listing all the steps involved therein. Due to nonbilocal monogamy (or trade-off relation) given by Eq. (8), any one of the two observations given in the two blocks at the end of the chart occurs. For deriving monogamy relation, Alice and Dick's measurement settings are kept fixed while collecting correlations in W_B and W_C. For sketching trade-off relation, no such restriction is imposed over their settings

in both the reduced networks $\mathcal{N}_B$, $\mathcal{N}_C$. To be precise, if Alice(Dick) performs measurement $M_A(M_D)$ in network $\mathcal{N}_B$, then in network $\mathcal{N}_C$ also measurement setting of Alice(Dick) is $M_A(M_D)$. As $\mathbf{B}_{\text{Max}}$ has the same form(Eq. (7)) in both P^{14} and P^{22} scenarios, so the inequality imposing restrictions on correlations in the two scenarios remains invariant.

Tightness of the constraint: By tightness of the monogamy relation given by Eq. (8), we interpret the existence of quantum correlations reaching the upper bound 2. For a particular instance, let each of the two sources $\mathbf{S}_1$ and $\mathbf{S}_2$ generates identical copy of a W state [48]:

$$|\Psi\rangle = \cos\mu_0|001\rangle + \sin\mu_1 \sin\mu_0|010\rangle + \sin\mu_0 \cos\mu_1|100\rangle \tag{9}$$

where $\mu_i(i = 0, 1) \in [0, \frac{\pi}{2}]$. Let, for $\mu_0 = \frac{\pi}{2}$, identical copies of the corresponding state($|\Psi\rangle\langle\Psi|$) are used in the network ($\mathcal{N}$). Let 1st, 2nd and 3rd qubit of one copy are sent to Alice, Bob and Charlie, respectively, whereas 1st, 2nd and 3rd qubit of second copy are sent to Dick, Bob and Charlie, respectively. Using the upper bound of violation given by Eq. (7) we get $(\mathbf{B}^B_{\text{Max}})^2 + (\mathbf{B}^C_{\text{Max}})^2 = \sqrt{(\text{Max}[0, \cos^2(2\mu_1)])^2} + \sqrt{(\text{Max}[1, \sin^2(2\mu_1)])^2} + \sqrt{(\text{Min}[0, \cos^2(2\mu_1)])^2} + \sqrt{(\text{Min}[1, \sin^2(2\mu_1)])^2}$. Clearly on simplification, $(\mathbf{B}^B_{\text{Max}})^2 + (\mathbf{B}^C_{\text{Max}})^2 = 2$.

Before discussing any further observation, we first put forward a lemma. □

Lemma *Under the assumption that Bob performs separable measurements in P^{22} scenario [36] and Bell-state measurement (BSM) in P^{14} scenario [37], maximal violation of the bilocal inequality (Eq. 4) is $\sqrt{2}$, maximum being taken over all possible quantum states .*

Proof From upper bound of violation of bilocal inequality (Eq. (4)) given by Eq. (7),

$$\mathbf{B}^2_{\text{Max}} = \sum_{i=1}^{2} \sqrt{\omega^A_i * \omega^C_i}. \tag{10}$$

By Cauchy–Schwarz's inequality, we get

$$\mathbf{B}^2_{\text{Max}} \leq \sqrt{\omega^A_1 + \omega^A_2}\sqrt{\omega^C_1 + \omega^C_2} \tag{11}$$

Now $\sqrt{\omega^A_1 + \omega^A_2} = M(\rho_{\text{AB}})$ and likewise $\sqrt{\omega^C_1 + \omega^C_2} = M(\rho_{\text{BC}})$ where $2M(\rho)$ denote maximal violation of Bell-CHSH inequality by a quantum state ρ [49]. Again, maximal possible quantum violation of Bell-CHSH is given by $2\sqrt{2}$, referred to as Tsirelson's bound [50]. Hence, maximal possible quantum violation of the bilocal inequality (Eq. (4)) turns out to be $\sqrt{2}$. □

The monogamy relation (Eq. (8)) puts restrictions over distribution of nonbilocal correlations among the two networks $\mathcal{N}_B$ and $\mathcal{N}_C$ in both P^{14} and P^{22} scenarios. To be precise, maximal violation of bilocal inequality (Eq. (4)), being $\sqrt{2}$, both of $(B^B_{\text{Max}})^2$ and $(B^C_{\text{Max}})^2$ could have been 2. But, this becomes impossible due to the restriction imposed by Eq. (8). Moreover, if any one set of tripartite marginals, say $P(a, b, d|x, y, w)$ (W_B set) shows violation of the bilocal inequality, the others set (W_C) of marginals does not violate the bilocal inequality. So, generation of nonbilocal correlations in one reduced network ($\mathcal{N}_B$, say) guarantees (considering generation of nonbilocal correlations up to detection by the sufficient criterion provided by violation of the bilocal inequality (Eq. (4))) the absence of any such nonclassical feature (nonbilocality) of quantum correlations in the other reduced network system ($\mathcal{N}_C$). Hence, if maximal violation of bilocal inequality is observed in one reduced network ($\mathcal{N}_B$, say), then correlations from $\mathcal{N}_C$ cannot violate the bilocal inequality (Eq. (4))) and hence may not be nonbilocal. Such an observation is analogous to existing results related to monogamy of quantum entanglement and nonlocality (standard Bell-CHSH sense).

5 Nonbilocal trade-off relation

Monogamy relation (Eq. (8)) guarantees existence of restrictions over distribution of nonbilocal correlations in reduced bilocal network systems. As already mentioned in the previous section, analogous to monogamy of nonlocal correlations in standard Bell-CHSH sense, measurement settings of nodal parties are kept fixed (in both the scenarios) for assessing monogamy of nonbilocal correlations. However, in [44], it was pointed out that comparison of monogamy and trade-off relations of nonlocal correlations guarantees relaxation of restrictions over shareability of nonlocal correlations among bipartite reduced states. Such an observation is quite intuitive owing to the fact that in contrast to fixed measurement settings of the nodal party (considering nature of the bipartite marginals for sketching monogamy relation), for giving trade-off relation (connecting amount of Bell-CHSH violation by the bipartite marginals), the measurement settings for the nodal parties are not considered to be invariant. Hence, optimization over parameters characterizing inputs of the nodal parties is possibly separate while considering Bell-CHSH violation by each of the reduced states. For instance, it may so happen that Bell-CHSH violation by reduced state ϱ_{AB} (obtained from state ϱ_{ABC}), is optimized for one measurement direction ($\mathbf{x_0}$, say) of Alice while the same by reduced state ϱ_{AC} is optimized for some other measurement direction ($\mathbf{x_1} \neq \mathbf{x_0}$, say) of Alice.

In this context, one may expect to encounter analogous observations in case of characterizing shareability of nonbilocal correlations. However, our findings guarantee somewhat counterintuitive feature. To be precise, relaxation of the restriction over nodal parties to have fixed measurement settings in both reduced networks fails to relax restrictions over shareability of nonbilocal correlations (up to existing sufficient criterion of detection of nonbilocality, i.e., violation of Eq. (3)). Also, proof of Theorem.1 turns out to be a special case of the proof of the following theorem.

Theorem 2 *In both P^{14} (Bob and Charlie performing Bell-state measurement) and P^{22} scenario (Bob and Charlie performing separable measurements), trade-off relation satisfied by upper bound of violation of bilocal inequality (Eq. (4)) by tripartite marginals in reduced networks $\mathcal{N}_B$ and $\mathcal{N}_C$ is same as the monogamy relation given by Eq.* (8).

Proof Each of Bob and Charlie performs separable measurements in P^{22} scenario, whereas perform Bell-state measurement in P^{14} scenario. In either of these scenarios, measurement settings of the nodal parties Alice and Dick may vary while considering violation of bilocal inequality in each of the two reduced networks ($\mathcal{N}_B$ and $\mathcal{N}_C$). Hence, by Eq. (11), we get:

$$(\mathbf{B}^B_{\mathrm{Max}})^2 + (\mathbf{B}^C_{\mathrm{Max}})^2 \leq \sqrt{\iota^B_1 + \iota^B_2}\sqrt{\Lambda^B_1 + \Lambda^B_2} + \sqrt{\iota^C_1 + \iota^C_2}\sqrt{\Lambda^C_1 + \Lambda^C_2} \quad (12)$$

where $\Lambda^B_1 \geq \Lambda^B_2 \geq \Lambda^B_3$, $\Lambda^C_1 \geq \Lambda^C_2 \geq \Lambda^C_3$, $\iota^B_1 \geq \iota^B_2 \geq \iota^B_3$ and $\iota^C_1 \geq \iota^C_2 \geq \iota^C_3$ are the eigen values of $T^T_{\mathrm{AB}}T_{\mathrm{AB}}$, $T^T_{\mathrm{AC}}T_{\mathrm{AC}}$, $T^T_{\mathrm{BD}}T_{\mathrm{BD}}$ and $T^T_{\mathrm{CD}}T_{\mathrm{CD}}$, respectively. Applying

A.M. $\geq$ G.M. over the positive terms $\iota_1^B + \iota_2^B$, $\Lambda_1^B + \Lambda_2^B$; $\iota_1^C + \iota_2^C$, and $\Lambda_1^C + \Lambda_2^C$, we get,

$$\frac{\iota_1^B + \iota_2^B + \Lambda_1^B + \Lambda_2^B + \iota_1^C + \iota_2^C + \Lambda_1^C + \Lambda_2^C}{2}.$$

Now for the state ρ_{ABC}(generated by the source $\mathbf{S}_1$) which is shared between Alice, Bob and Charlie [51],

$$\Lambda_1^B + \Lambda_2^B + \Lambda_1^C + \Lambda_2^C \leq 2, \tag{13}$$

Analogously, for the state ρ_{BCD}(generated by the source $\mathbf{S}_2$), we get,

$$\iota_1^B + \iota_2^B + \iota_1^C + \iota_2^C \leq 2, \tag{14}$$

Using, Eqs.(13,14), in Eq. (12), we get the required relation(Eq. (8)). □

Proof of Theorem 1 from that of Theorem 2 As has already been pointed out in the proof of Theorem 2, nodal parties are free to choose different measurement settings in the two reduced networks $\mathcal{N}_B$ and $\mathcal{N}_C$. Let M_A^B and M_A^C denote measurement settings of Alice in reduced network $\mathcal{N}_B$ and $\mathcal{N}_C$, respectively. Likewise, let M_D^B and M_D^C denote measurement settings of the other nodal party Dick in reduced network $\mathcal{N}_B$ and $\mathcal{N}_C$, respectively. So, quite obviously, $M_A^B = M_A^C$ and $M_D^B = M_D^C$ came as a special case of all possible measurement settings of Alice (M_A^B, M_A^C) and Dick (M_D^B and M_D^C). But this special case corresponds to the restriction of fixed measurement settings of nodal observers that is usually imposed for deriving monogamy relations and hence corresponds to the assumptions of Theorem 1. This in turn guarantees assumptions involving nodal observers' inputs in Theorem 1 as a subcase of the assumptions over nodal observers' inputs in Theorem 2. Consequently, proof of Theorem 1 is following from that of Theorem 2 and hence, monogamy relation and trade-off relation restricting shareability of nonbilocal correlations are the same (Eq. (8)). □

Tightness of trade-off relation: Assumptions over nodal observers' inputs in Theorem.1 being a sub case of that in Theorem 2, tightness of trade-off relation follows immediately from tightness of monogamy relation (Eq. (8)).

The trade-off relation, being of the same form as that of the monogamy relation, restriction over shareability of nonclassical feature of quantum correlations (in terms of nonbilocality) is the same irrespective of whether measurement settings of the nodal parties remain fixed or not. Recent study on Bell-CHSH nonlocality reveals analogous findings regarding the fact that restrictions over distribution of nonclassical quantum correlations are independent of the fact whether nodal party's inputs are fixed or not. To be specific in [51], a trade-off relation restriction shareability of nonlocal quantum correlations (Bell-CHSH) has been given which has the same form as that of a monogamy relation of Bell-CHSH nonlocality which was previously given in [44].

As has already been mentioned before, one should note that all our observations are applicable for qubits. This is a consequence of the fact that the network (see Fig. 2) involves sources which generate three qubit states. Whether our observations hold for higher dimensional quantum systems is an area of open research work.

After ensuring existence of restriction over shareability of nonclassical correlations in quantum network scenario (characterized by source independence), we now discuss below practical significance of monogamy of nonbilocal correlations.

6 Practical implication

Establishing existence of restrictions over shareability of correlations in bilocal networks involving quantum systems, we now proceed to justify that such monogamous nature of nonbilocal correlations may be used to provide security in quantum secret key sharing protocol (actual design of any such protocol is however yet to be accomplished). Before starting the analysis, we briefly review an existing result involving the use of monogamy of the standard Bell nonlocality in such a protocol.

In [46], Barrett et.al. proved a connection between the possibility of existence of a protocol secure against postquantum eavesdropping and quantum violation of Bell-CHSH inequality under nosignaling assumption. To be precise, they designed a protocol involving two parties (Alice and Bob, say). Alice and Bob share identical copies of entangled states. At the end of the protocol, a secret bit is generated in between Alice and Bob although the source, generating the entangled states, is controlled by eavesdropper. Security of such a protocol is based on monogamy of Bell-CHSH violation by quantum correlations. Though unable to design any such protocol involving bilocal network, we only give justification in support of our claim that nonbilocal monogamy can provide security analogously.

Consider a secret key sharing protocol based on a quantum network involving three parties Alice, Bob and Dick and two independent sources $\mathbf{S}_1$ and $\mathbf{S}_2$ each of which generates an entangled state. Alice, Bob and Dick are referred to as trusted parties. Let the parties perform simultaneous measurements on their respective quantum particles that they receive from the sources (analogous to Fig. 1). Entangled state being generated by each of the two sources, correlations obtained after simultaneous measurements of the parties (Bob performing separable measurements) are nonbilocal in nature [36]. Now, it may happen that the two sources $\mathbf{S}_1$ and $\mathbf{S}_2$ are under the control of an eavesdropper (untrusted party). Such a situation may be interpreted in the form of the sources generating tripartite quantum state where one bit from each source is under the control of the eavesdropper (schematic diagram involved herein is analogous to that of our scenario, Fig. 2, where Charlie may be considered as the eavesdropper). Now, the eavesdropper also performs measurement on his qubits. Depending on his control over the sources, the eavesdropper will get access to the key generated in the protocol. If he can get information about the secret key then the correlations shared between Alice, Dick and the eavesdropper will be nonbilocal (can be interpreted as correlations in reduced network $\mathcal{N}_C$ in our scenario). But in such a case, due to monogamous nature of nonbilocal correlations, the correlations shared between Alice, Bob and Dick (analogous to correlations in reduced network $\mathcal{N}_B$) will be bilocal (up to testing of bilocal inequality (Eq. (3))). Based on this observation, the trusted parties can detect the presence of the eavesdropper and thereby discard the protocol. On the contrary, if eavesdropper cannot gain any information about the key then the correlations shared between Alice, Dick and Charlie will no longer be nonbilocal and consequently nonbilocal correlations will be generated between the trusted parties. On getting nonbilocal correlations, they are assured that secrecy of the protocol is maintained. So monogamy of nonbilocality can be applied to design a secret bit sharing protocol involving quantum network secured against attacks of eavesdropper. Below, we give justification in support of our claim.

Now in our network scenario (Fig. 2), monogamy of nonbilocal correlations involves Bell violation by reduced states ρ_{AB}, ρ_{AC}, ρ_{BD} and ρ_{CD}. So, restrictions over distribution of nonbilocal correlations(due to sufficient criterion of nonbilocality given by violation of bilocal inequality given by Eq. (3)) in reduced networks $\mathcal{N}_B$ and $\mathcal{N}_C$ involve restrictions over shareability of nonlocal correlations (in sense of Bell-CHSH violation) among the reduced states. Framing of the secret key sharing protocol, being based on our network scenario, security of the protocol thus ultimately rests upon monogamous nature of the standard Bell-CHSH nonlocal correlations. Now, as already discussed before, there exists secret quantum key sharing protocol where security is guaranteed by monogamy of Bell-CHSH nonlocality [46]. This gives an indication about the possibility of designing a protocol, secured against eavesdropper's attack, via which secret bit can be generated in bilocal network scenario involving Alice, Bob (performing separable measurements or Bell-state measurement) and Dick even if any eavesdropper (Charlie) who is capable of performing any separable measurement or Bell-state measurement have control over both the independent sources $\mathbf{S}_1$ and $\mathbf{S}_2$.

7 Discussions

Over years, there has been thorough investigation of monogamous nature of quantum entanglement and quantum nonlocality in the standard Bell-CHSH scenario. In this paper, we have considered bilocal quantum network to investigate the same for some weaker form of quantum nonlocality (nonbilocality). Exploitation of our observations ensures monogamous nature of nonbilocal quantum correlations (up to existing detection criterion for nonbilocality (Eq. (4)))). For our purpose, we have considered P^{22} and P^{14} scenarios. Interestingly, restrictions over shareability of distribution of nonbilocal correlations among reduced networks ($\mathcal{N}_B$ and $\mathcal{N}_C$) are the same irrespective of the inputs of the nodal parties (Alice and Dick) remaining fixed or not for observing violation of bilocal inequality in the reduced networks individually. From our discussions so far, it can be safely concluded that under the assumption of Bob and Charlie performing separable measurements or Bell-state measurement (BSM), if quantum correlations in one reduced network ($\mathcal{N}_B$, say) exhibit nonbilocality, then the correlations from the other one ($\mathcal{N}_C$) cannot violate the bilocal inequality (Eq. (4)) and hence may be bilocal. As we have already discussed, such monogamous nature of nonbilocal correlations can be utilized to design a secret sharing protocol secure against eavesdropper's attack. However, we have not been able to explicitly design any such protocol. One may find interest to develop one such protocol involving bilocal network. Also, the assumption that an eavesdropper can perform only separable measurements or Bell-state measurement is a weaker assumption as there may be cases where an eavesdropper can perform more general measurements. For those cases, one may try to design monogamy relation of nonbilocal correlations under the assumption that Bob and Charlie can perform more general measurements. One may try to explore the utility of bilocal monogamy in quantum dialog protocols [52,53]. However, in [52,53], continuous variable systems are involved in quantum dialog protocol but till date the bilocal scenarios involve only discrete quantum systems. So, in order to utilize restrictions over shareability of nonbilocal correlations in such protocols, criterion to detect nonbilocal correlations must be established following which one may explore application (if any) of monogamous nature of nonbilocality in all such protocols. Also, study investigating inter-relation between monogamy of nonbilocality and other nonclassical aspects of quantum theory is a potential source of research activities.

References

1. Horodecki, R., Horodecki, P., Horodecki, M., Horodecki, K.: Quantum entanglement. Rev. Mod. Phys. **81**, 865 (2009)
2. Bell, J.S.: On the Einstein Podolsky Rosen Paradox. Physics **1**, 195 (1964)
3. Bell, J.: Speakable and Unspeakable in Quantum Mechanics, 2nd edn. Cambridge University Press, Cambridge (2004)
4. Brunner, N., Cavalcanti, D., Pironio, S., Scarani, V., Wehner, S.: Bell nonlocality. Rev. Mod. Phys. **86**, 419 (2014)
5. Bancal, J.-D., Gisin, N., Liang, Y.-C., Pironio, S.: Device-independent witnesses of genuine multipartite entanglement. Phys. Rev. Lett. **106**, 250404 (2011)
6. Acín, A., Brunner, N., Gisin, N., Massar, S., Pironio, S., Scarani, V.: Device-independent security of quantum cryptography against collective attacks. Phys. Rev. Lett. **98**, 230501 (2007)
7. Barrett, J., Hardy, L., Kent, A.: No signaling and quantum key distribution. Phys. Rev. Lett. **95**, 010503 (2005)
8. Mayers, D., Yao, A.: Proceedings of the 39th IEEE Symposiumon Foundations of Computer Science (IEEE Computer Society, p. 503. Los Alamitos CA, USA (1998p)
9. Acín, A., Gisin, N., Masanes, L.: From Bell's theorem to secure quantum key distribution. Phys. Rev. Lett. **97**, 120405 (2006)
10. Brunner, N., Linden, N.: Connection between Bell nonlocality and Bayesian game theory. Nat. Commun. **4**, 2057 (2013)
11. Pironio, S., Acín, A., Massar, S., de la Giroday, A.B., Matsukevich, D.N., Maunz, P., Olmschenk, S., Hayes, D., Luo, L., Manning, T.A., Monroe, C.: Random numbers certified by Bell's theorem. Nature **464**, 1021 (2010)
12. Colbeck, R., Kent, A.: Private randomness expansion with untrusted devices. J. Phys. A Math. Theor. **44**, 095305 (2011)
13. Toner, B.: Monogamy of non-local quantum correlations. Proc. R. Soc. A **465**, 59–69 (2009)
14. Coffman, V., Kundu, J., Wootters, W.K.: Distributed entanglement. Phys. Rev. A **61**, 052306 (2000)
15. Sadhukhan, D., Roy, S.S., Rakshit, D., Sen, A., Sen, U.: Beating no-go theorems by engineering defects in quantum spin models. New J. Phys. **17**, 043013 (2015)
16. Toner, B., Verstraete, F.: Monogamy of Bell correlations and Tsirelson's bound, arXiv:quant-ph/0611001
17. Kurzynski, P., Paterek, T., Ramanathan, R., Laskowski, W., Kaszlikowski, D.: Correlation complementarity yields Bell monogamy relations. Phys. Rev. Lett. **106**, 180402 (2011)
18. Kay, A., Kaszlikowski, D., Ramanathan, R.: Optimal cloning and singlet monogamy. Phys. Rev. Lett. **103**, 050501 (2009)
19. de Oliveira, T.R., Saguia, A., Sarandy, M.S.: Nonviolation of Bell's inequality in translation invariant systems. Eur. Phys. Lett. **100**(6), 60004 (2013)
20. Osborne, T.J., Verstraete, F.: General monogamy inequality for bipartite qubit entanglement. Phys. Rev. Lett. **96**, 220503 (2006)

21. Seevinck, M.: Classification and monogamy of three-qubit biseparable Bell correlations. Phys. Rev. A **76**, 012106 (2007)
22. Ou, Y.C., Fan, H.: Monogamy inequality in terms of negativity for three-qubit states. Phys. Rev. A **75**, 062308 (2007)
23. Adesso, G., Serafini, A., Illuminati, F.: Multipartite entanglement in three-mode Gaussian states of continuous-variable systems: quantification, sharing structure, and decoherence. Phys. Rev. A **73**, 032345 (2006)
24. Lee, S., Park, J.: Monogamy of entanglement and teleportation capability. Phys. Rev. A **79**, 054309 (2009)
25. Clauser, J.F., Horne, M.A., Shimony, A., Holt, R.A.: Proposed experiment to test local hidden-variable theories. Phys. Rev. Lett. **23**, 880 (1969)
26. Masanes, L., Acin, A., Gisin, N.: General properties of nonsignaling theories. Phys. Rev. A **73**, 012112 (2006)
27. Branciard, C., Gisin, N., Pironio, S.: Characterizing the nonlocal correlations created via entanglement swapping. Phys. Rev. Lett. **104**, 170401 (2010)
28. Branciard, C., Rosset, D., Gisin, N., Pironio, S.: Bilocal versus nonbilocal correlations in entanglement-swapping experiments. Phys. Rev. A **85**, 032119 (2012)
29. Tavakoli, A., Skrzypczyk, P., Cavalcanti, D., Acín, A.: Nonlocal correlations in the star-network configuration. Phys. Rev. A **90**, 062109 (2014)
30. Mukherjee, K., Paul, B., Sarkar, D.: Correlations in n-local scenario. Quantum Inf. Process. **14**, 2025 (2015)
31. Chaves, R.: Polynomial Bell inequalities. Phys. Rev. Lett. **116**, 010402 (2016)
32. Rosset, D., Branciard, C., Barnea, T.J., Putz, G., Brunner, N., Gisin, N.: Nonlinear Bell inequalities tailored for quantum networks. Phys. Rev. Lett. **116**, 010403 (2016)
33. Mukherjee, K., Paul, B., Sarkar, D.: Revealing advantage in a quantum network. Quantum Inf. Process. **15**(7), 2895–2921 (2016)
34. Mukherjee, K., Paul, B., Sarkar, D.: Nontrilocality: exploiting nonlocality from three-particle systems. Phys. Rev. A **96**, 022103 (2017)
35. Tavakoli, A., Renou, M.O., Gisin, N., Brunner, N.: Correlations in star networks: from Bell inequalities to network inequalities. New J. Phys. **119**, 073003 (2017)
36. Andreoli, F., Carvacho, G., Santodonato, L., Chaves, R., Sciarrino, F.: Maximal qubit violation of n-locality inequalities in a star-shaped quantum network. New J. Phys. **19**, 113020 (2017)
37. Gisin, N., Mei, Q., Tavakoli, A., Renou, M.O., Brunner, N.: All entangled pure quantum states violate the bilocality inequality. Phys. Rev. A **96**, 020304 (2017)
38. Marc-Olivier R.Y., Wang, S., Boreiri, S., Beigi, N., Gisin, N.: Limits on Correlations in Networks for Quantum and No-Signaling Resources. Brunner arXiv:1901.08287 [quantph] (2019)
39. Gisin, N., Gisin, B.: A local variable model for entanglement swapping exploiting the detection loophole. Phys. Lett. A **297**, 279 (2002)
40. Greenberger, D.M., Horne, M., Zeilinger, A., Żukowski, M.: Bell theorem without inequalities for two particles. II. Inefficient detectors. Phys. Rev. A **78**, 022111 (2008)
41. Aćin, A., Cirac, J.I., Lewenstein, M.: Entanglement percolation in quantum networks. Nat. Phys. **3**, 256–259 (2007)
42. Sangouard, N., Simon, C., de Riedmatten, H., Gisin, N.: Quantum repeaters based on atomic ensembles and linear optics. Rev. Mod. Phys. **83**, 33 (2011)
43. Hammerer, K., Sorensen, A.S., Polzik, E.S.: Quantum interface between light and atomic ensembles. Rev. Mod. Phys. **82**, 1041 (2010)
44. Qin, H.H., Fei, S.M., Jost, X.L.: Trade-off relations of Bell violations among pairwise qubit systems. Phys. Rev. A **92**, 062339 (2015)
45. Ekert, A.K.: Quantum cryptography based on Bell's theorem. Phys. Rev. Lett. **67**, 661 (1991)
46. Barrett, J., Hardy, L., Kent, A.: No signaling and quantum key distribution. Phys. Rev. Lett. **95**, 010503 (2005)
47. Acin, A., Gisin, N., Masanes, L.: From Bell's theorem to secure quantum key distribution. Phys. Rev. Lett. **97**, 120405 (2006)
48. Ajoy, A., Rungta, P.: Svetlichny's inequality and genuine tripartite nonlocality in three-qubit pure states. Phys. Rev. A **81**, 052334 (2010)
49. Horodecki, R., Horodecki, P., Horodecki, M.: Violating Bell inequality by mixed states: necessary and sufficient condition. Phys. Lett. A **200**, 340 (1995)

50. Cirelson, B.S.: Quantum generalizations of Bell's inequality. Lett. Math. Phys. **4**, 93 (1980)
51. Cheng, S., Hall, M.J.W.: Anisotropic invariance and the distribution of quantum correlations. Phys. Rev. Lett. **118**, 010401 (2017)
52. Gong, L.H., Li, J.F., Zhou, N.R.: Continuous variable quantum network dialogue protocol based on single-mode squeezed states. Laser Phys. Lett. **15**, 105204 (2018)
53. Gong, L., Tian, C., Li, J., Zou, X.: Quantum network dialogue protocol based on continuous-variable GHZ states. Quantum Inf. Process. **17**, 331 (2018)

Publisher's Note Springer Nature remains neutral with regard to jurisdictional claims in published maps and institutional affiliations.

Ilkogretim Online - Elementary Education Online, 2019; Vol 18 (Issue 4): pp. 2572-2582
http://ilkogretim-online.org
doi: 10.17051/ilkonline.2019.641252

Human Capital Accumulation In Two Sector Endogenous Growth Model: Special Emphasis On Service Good – A Comparative Static Analysis

Dr. Senjuti Gupta Assistant Professor in Economics (W.B.E.S) Department of Economics, Government Girls' General Degree College, Ekbalpore, Kolkata, West Bengal, India.

Abstract: The present paper considers endogenous growth model with commodity sector and service sector. This extension of Lucas model shows that there exists unique steady state growth rate of human capital accumulation which works as the main driving force for the economy as a whole. On the base of an endogenous growth model, a few the comparative static analysis has been done in this paper. It shows how the share of unskilled labor force, devoted into the commodity sector is influenced by the two factors: the intensity of preference for commodity output and the service output elasticity of skilled labour.

Section 1: Introduction

The paper tries to extend the paper written by Lucas (1988), by incorporating service sector in the model where the households consume the service good. In last few decades, growth of this sector as well as that of the entire economy depends on the accumulation of human capital. There exists a number of papers that deal with the problems of service sector. A huge literature exists that modified the simple one sector Solow-Swan growth model and discussed different issues in the theory of economic growth. Studies by Uzawa (1961, 1963, 1965), Hahn (1965), Takayama (1963, 1965), Drandakis (1963), Inada (1963) introduced real balance effect in the savings function of the Solow (1956) model where the rate of savings was exogenously given. Cass (1965) and Koopmans (1965), following Ramsey (1928) model introduced household's inter temporal utility maximization behaviour in their model and endogenized the saving rate.

Empirical work includes the papers by Chand (1983), Lorence (1991), Lee and Wolpin (2006), Kirn (1987), Wood (1990), Marks (2006). Eswaran and Kotwal (2002), Sasaki (2007), Konan and Maskus (2006), Baumol et al. (1989), Pugno (2006), Zhang (2013) have done a few theoretical works on service sector. But none of these papers consider the issue of service sector and endogenous growth with Lucas (1988) type human capital accumulation function which is the main issue of the present analysis.
In a paper titled "Service Sector, Human Capital Accumulation and Endogenous Growth" written by me and my co-authors, Chakraborty et. al (2015), an endogenous growth model was formed with commodity and service sector. It derived that there exists a

unique steady state growth rate of human capital accumulation which worked as the source of growth for all other sectors of the economy. On the base of the growth paths derived before, this paper tries to figure out a few comparative static analysis.The paper is organised as follows: In section 2, the basic model is presented, section 3 describes the growth rates along with the steady state equilibrium conditions and comparative static analysis and finally section 4 concludes.

2. The model:

This paper considers a closed economy model with two sectors namely, commodity sector and service sector. The total labour force is heterogeneous with respect to skill level: skilled labour and unskilled labour or raw labour. The commodity and the factor markets are characterized by perfect competition. The economy is inhabited by identical rational agents. Production technology is subject to constant returns to scale. Preferences over consumption and service streams are given by the following function where 'c' and 's' denote flow of real per capita consumption of commodity and service respectively:

$$U(c,s)=\frac{(c^{\alpha}s^{1-\alpha})^{1-\sigma}-1}{(1-\sigma)} \qquad 1.$$

Here α stands for the intensity of preference for commodity output and σ denotes the elasticity of marginal utility.

In our model, it is assumed that the output in the commodity sector can be used for consumption or investment. However, the output in the service sector is fully consumed as services cannot be stored for future uses. The commodity output is a function of human capital, raw labor and physical capital. The services are produced with human capital and raw labor only. Both the production functions are Cobb-Douglas type. Skilled labour allocates 'u' fraction of time to produce commodity output, 'v' fraction of time to produce service output and (1-u-v) fraction of time for human capital accumulation. Let 'K' be the level of physical capital in commodity sector. Let α_1 and β be commodity output elasticity of skilled labour and the service output elasticity of skilled labour respectively and α_2 be the commodity output elasticity of physical capital.The service and commodity output production functions are as follows where 'y_s' and 'y_c' be the flow of commodity output and service output respectively.

$$y_s=(N_1vh)^{\beta}((1-\phi)N_2)^{1-\beta} \qquad 2.$$

$$y_c=(N_1uh)^{\alpha_1}K^{\alpha_2}(\phi N_2)^{1-\alpha_1-\alpha_2} \qquad 3.$$

It is assumed that the number of skilled labor and unskilled labor be N_1 and N_2 respectively and N be the total labour force or working population such that

$$\mathrm{N} = \mathrm{N}_1 + \mathrm{N}_2 \qquad 4.$$

Population grows at a constant, exogenous rate and more over we assume that each segment of the population is growing at the same rate in the following way:

$$\frac{\dot{\mathrm{N}}}{\mathrm{N}} = \frac{\dot{\mathrm{N}}_1}{\mathrm{N}_1} = \frac{\dot{\mathrm{N}}_2}{\mathrm{N}_2} = \mathrm{n} \geq 0 \qquad 5.$$

It is further assumed that the general skill level of a worker is 'h'. The effective skilled work force in commodity production is '$\mathrm{N}_1\mathrm{uh}$' and that in service production is '$N_1 vh$'. These are skill-weighted man-hours devoted to current commodity and service output production respectively. Let 'ϕ' be the fraction of total unskilled labor force that is devoted in the commodity sector. The remaining (1- ϕ) fraction is engaged in producing service output.

Following Lucas (1988), the accumulation of human capital is assumed to be proportional to the time allocated for education. Hence, human capital accumulation function is given by

$$\gamma_{\mathrm{h}} = \dot{\mathrm{h}}/\mathrm{h} = \delta(1-\mathrm{u}-\mathrm{v}) \qquad 6.$$

Here δ be the productivity parameter in the human capital accumulation function. It is assumed that commodity output over aggregate consumption is accumulated as physical capital. The physical capital accumulation function is given by

$$\dot{K} = y_c - Nc \qquad 7.$$

Service output is totally consumed. So the market clearing condition is

$$y_s = Ns \qquad 8.$$

The objective of the economy is to maximize the value of utility defined by equation (1) subject to the constraints given by (2), (3), (6), (7) and (8).

The current value Hamiltonian of this dynamic optimization problem can be formulated as

$$H = \frac{N}{(1-\sigma)}[(c^{\alpha}s^{1-\alpha})^{1-\sigma} - 1] + \theta_1[(N_1uh)^{\alpha_1}K^{\alpha_2}(\phi N_2)^{1-\alpha_1-\alpha_2} - Nc]$$
$$+\theta_2[\delta h(1-u-v)] + \lambda[(N_1vh)^{\beta}((1-\phi)N_2)^{1-\beta} - Ns] \qquad 9.$$

Where θ_1 and θ_2 are shadow prices associated with $\dot{K}$ and $\dot{h}$ respectively and λ be the Lagrange multiplier as the market clearing condition given by equation (9) is a static constraint. There are five control variables c, s, u, v, ϕ in this model. The state variables are K and h.

3. Steady state Growth path

The model results show that along the steady state growth path c, s, K grow at constant rate and u, v, φ are time independent. In the steady state the growth path of human capital is given in equation (10a).

$$\gamma_h = \delta(1-u-v) = \frac{A}{B} \qquad \text{10a.}$$

Here $A = n + \delta - \rho$ 10.b

$B = 1 - x$ 10.c

Where $x = (1-\sigma)\{\beta(1-\alpha) + \frac{\alpha\alpha_1}{(1-\alpha_2)}\}$ 10d.

Let γ_i denotes the growth rate of ith variable where i= c, s, and K . Equilibrium growth path for these variables are given as follows:

$$\gamma_c = \left(\frac{\alpha_1}{1-\alpha_2}\right)\gamma_h \qquad \text{11a.}$$

$$\gamma_s = \beta\gamma_h \qquad \text{11b.}$$

$$n + \gamma_c = \gamma_K \qquad \text{11c.}$$

We observe that growth rate of human capital is the source of growth for other three sectors. Thus, this model with service sector where entire service output is consumed confirms the findings of Lucas model that human capital accumulation is the engine of growth.

From the first order conditions of optimization we obtain the values of u, v and ϕ defined as follows:

$$u = (\delta B - A)/\delta B(1+D) \qquad \text{12a.}$$

$$v = D(\delta B - A)/\delta B(1+D) \qquad \text{12b.}$$

And $\phi = \dfrac{(1-\alpha_1-\alpha_2)\beta}{\alpha_1(1-\beta)D + (1-\alpha_1-\alpha_2)\beta}$ 12c.

Where D is a constant and given by

$$D = \frac{(1-\alpha)\beta}{\alpha\alpha_1}\left[\frac{(\rho - n\alpha_2)Z - (n+\delta-\rho)(Y+\alpha_1\alpha_2)}{\rho Z - (n+\delta-\rho)Y}\right] \quad 12d.$$

Where $Z = (1-\alpha_2)[1-(1-\sigma)\{\beta(1-\alpha) + \frac{\alpha\alpha_1(1-\sigma)}{(1-\alpha_2)}\}]$ 12e.

And $Y = \alpha_1\{\alpha(1-\sigma)-1\} + \beta(1-\alpha)(1-\alpha_2)(1-\sigma)$ 12f.

Hence in this model the values of u, v and ϕ are endogenously determined. The model to be economically viable u, v and 1-u-v should be positive.

<u>The conditions for positive u, v and (1-u-v) are</u>:

When σ<1; the positivity of u and v requires the following condition:

$\delta B \geq A$

Or, $\delta(1-x) \geq n+\delta-\rho$

Or, $\rho \geq n+\delta x$ 13a.

From $(1-u-v) \geq 0$, we get $\frac{A}{\delta B} \geq 0$

Therefore the required conditions are: A and B must be positive. So, from the requirement that $A \geq 0$ and $B \geq 0$ we get 13b. and 13c. equations respectively

$n+\delta \geq \rho$ 13b.

And $1-x \geq 0$,

Or. $x \leq 1$ 13c.

Merging equation no. 13a.and 13b we get,

$n+\delta \geq \rho \geq n+\delta x$

This is the same condition that is required for positive B. Combining extreme left and extreme right side of the above inequality we in fact have 13c.When σ≥1 : The required conditions are the same as the previous case.

Now the positivity of D is also required for positive values of u and v.

The conditions required for positive D:

When σ<1; the sufficient condition $\alpha_1 > \alpha_1^*$

Where $\alpha_1^* = \dfrac{\alpha_2 + (1-\sigma)\beta(1-\alpha)(1-\alpha_2)}{1-(1-\sigma)\alpha}$.

Thus, combining the conditions we have the following growth path:

There exists positive, unique steady state growth rate for human capital consumption service and capital goods sectors.

The detailed derivation of the growth paths has been done in the appendix of the paper written by me and my co-authors, titled "Service Sector, Human Capital Accumulation and Endogenous Growth" which was published in Theoretical and Applied Economics Volume XXII (2015), No. 4(605), Winter, pp. 199-216.

Comparative static analysis:

We have done comparative static analysis on ϕ. Here 'ϕ' is the fraction of total unskilled labor force that is devoted in the commodity sector. α stands for the intensity of preference for commodity output. β is the service output elasticity of skilled labour. Differentiating ϕ with respect to α and β we get (detailed derivation is done in appendix),

$$\frac{\partial \phi}{\partial \alpha} > 0$$

Proposition 1: When the intensity of preference for commodity output rises, the fraction of total unskilled labor force engaged in the commodity sector also rises.

The reason behind such result is that when the intensity of preference for commodity output rises, the requirement for more commodity production also rises. As a result, the fraction of total unskilled labor force engaged in the commodity sector also rises.

$$\frac{\partial \phi}{\partial \beta} > 0$$

Proposition 2: When the service output elasticity of skilled labour increases, the fraction of total unskilled labor force engaged in the commodity sector also rises.

The reason behind such result is that as the two sectors are interdependent, Whenever the relative responsiveness of service output with respect to skilled labor rises, the share of unskilled labor force engaged in the commodity sector also rises so that the remaining share of unskilled labor who are engaged in service sector, decreases. The service sector become more efficient in this manner.

5 Conclusion:

This paper develops an endogenous growth model with commodity sector and service sector with Lucas type human capital accumulation function. This extension of Lucas model shows that that there exists unique steady state growth rate of human capital accumulation which works as the main driving force for the economy as a whole. It is found from the comparative static analysis that **when the intensity of preference for commodity output rises, the fraction of total unskilled labor force engaged in the commodity sector also rises and secondly, we have found when** the service output elasticity of skilled labour increases, **the fraction of total unskilled labor force engaged in the commodity sector also rises.**

Bibliography:

Arrow, K. J. (1962), "The economic implications of learning by doing", Review of Economic Studies, 29(3), 155-73.

Cass, D. (1965), "Optimum growth in an aggregative model of capital accumulation", Review of Economic Studies, 32(3), 233-240.

Koopmans, T. C. (1965), "On the concept of optimal economic growth", The Econometric Approach to Development Planning, ch 4, 225-87. North-Holland Publishing Co., Amsterdam.

Chakraborty et. al. (2015) "Service Sector, Human Capital Accumulation and Endogenous Growth" Theoretical and Applied Economics Volume XXII (2015), No. 4(605), Winter, pp. 199-216

Chand R. U. K (1983) "The Growth of the Service Sector in the Canadian Economy" Social Indicators Research, 13(4), 339-379.

Drandakis E.M.(1963), "Factor substitution in the two-sector growth model", Review of Economic Studies, 30 (2), 217-28.

Eswaran M. , Kotwal A. (2002) "The role of the service sector in the process of industrialisation. "Journal of development Economics 68 (2002) 401-420.

Grossman, G. and E. Helpman (1991), Innovation and Growth in the Global Economy, Cambridge: MIT Press.

Hahn, F.H. (1965), "On two-sector growth models", Review of Economic Studies, 32(4), 339-46.

Inada, K. (1963), "On a two-sector model of economic growth: comments and a generalization", Review of Economic Studies, 30(2),119-127.

Konan D. E & Maskus K.E (2006) “Quantifying the impact of services liberalization in a developing country.”Journal of Development Economics 81 (2006) 142– 162.

Kirn T.J (1987) “Growth and Change in the Service Sector of the U.S.: A Spatial Perspective” Annals of the Association of American Geographers, 77(3), 353-372.

Lee D. and Wolpin K.I.(2006) “Intersectoral Labor Mobility and the Growth of the Service Sector”, Econometrica, 74(1) 1-46.

Lucas, R. E (1988), “On the mechanics of economic development”, Journal of Monetary Economics, 22 (1), 3-42.

Marks D. (2006) “Reconstruction of the Service Sector in the National Accounts of Indonesia, 1900-2000: Concepts and Methods.” Economic Bulletin,23(3), 373-390.

Pugno M. (2006) “The service paradox and endogenous economic growth.”Structural Change and Economic Dynamics 17, 99-115.

Ramsey F.P. (1928), “A mathematical theory of saving”, Economic Journal, 38(152), 543-559.

Sasaki H. (2007)“The rise of service employment and its impact on aggregate productivity growth.” Structural Change and Economic Dynamics 18 (4) , 438–459.

Solow, R.M, (1956), “A contribution to the theory of economic growth”, Quarterly Journal of Economics, 70(1), 65-94.

Solow, R.M (2000) “Growth Theory AN EXPOSITION”, Newyork, Oxford, Oxford University Press

Swan, T.W., (1956), “Economic growth and capital accumulation,” Economic Record, 32, 334-61.

Takayama A.(1963), “On a two-sector model of economic growth: A comparative statics analysis”, Review of Economic Studies, 30(2), 95-104.

Takayama, A.(1965), “On a two-sector model of economic growth with technological progress”, Review of Economic Studies, 32(3), 251-62.

Uzawa, H. (1961), “On a two-sector model of economic growth”, Review of Economic Studies, 29(1), 117-124.

Uzawa, H. (1963), “On a two-sector model of economic growth: II”, Review of Economic Studies, 30(2), 105-118.

Uzawa, H (1965) “Optimum technical change in an aggregative model of economic growth”, International Economic Review, 6(1), 18-31.

Wood Peter A.(1990) “The service sector.” Geography, 75(4), 364-368.

Zhang W.B 2013 “Heterogeneous capital and consumption goods in a structurally generalized Uzawa’s model.”.Theoretical and Applied Economics, Volume XX 3(580), 31-35.

Appendix:

$$\phi = \frac{(1-\alpha_1-\alpha_2)\beta}{\alpha_1(1-\beta)D+(1-\alpha_1-\alpha_2)\beta}$$

if $\alpha_1 > \alpha_2$ and $(n+\delta-\rho) > 0$

$D = A\frac{(1-\alpha)\beta}{\alpha\alpha_1}$ Here A is not function of α and β

$$\phi = \frac{(1-\alpha_1-\alpha_2)\beta}{\alpha_1(1-\beta)D+(1-\alpha_1-\alpha_2)\beta}$$

$$D = \frac{(1-\alpha)}{\alpha\alpha_1}\left[\frac{(\rho-n\alpha_2)(1-\alpha_2)+(n+\delta-\rho)(1-\alpha_2)\alpha_1}{\rho(1-\alpha_2)+(n+\delta-\rho)\alpha_1}\right]$$

Where $Z = (1-\alpha_2)[1-(1-\sigma)\{\beta(1-\alpha)+\frac{\alpha\alpha_1(1-\sigma)}{(1-\alpha_2)}\}]$

$$Y = \alpha_1\{\alpha(1-\sigma)-1\}+\beta(1-\alpha)(1-\alpha_2)(1-\sigma)$$

When $\sigma = 1$,

$$D = \frac{(1-\alpha)\beta}{\alpha\alpha_1}\left[\frac{(\rho-n\alpha_2)(1-\alpha_2)+(1-\alpha_2)+(n+\delta-\rho)(1-\alpha_2)\alpha_1}{\rho(1-\alpha_2)+(n+\delta-\rho)\alpha_1}\right]$$

$$D = \frac{(1-\alpha)\beta}{\alpha\alpha_1}\left[\frac{\rho\{(1-\alpha_2)(1-\alpha_1)\}+(1-\alpha_2)n((\alpha_1-\alpha_2)+\delta\alpha_1(1-\alpha_2)}{\rho(1-\alpha_2)+(n+\delta-\rho)\alpha_1}\right]$$

Let $A = [\frac{\rho\{(1-\alpha_2)(1-\alpha_1)\} + (1-\alpha_2)n((\alpha_1 - \alpha_2) + \delta\alpha_1(1-\alpha_2)}{\rho(1-\alpha_2) + (n+\delta-\rho)\alpha_1}]$

So, $D = A\frac{(1-\alpha)\beta}{\alpha\alpha_1}$ Here A is not function of α and β

$$\phi = \frac{(1-\alpha_1-\alpha_2)\beta}{\alpha_1(1-\beta)D + (1-\alpha_1-\alpha_2)\beta}$$

if $\alpha_1 > \alpha_2$ and $(n+\delta-\rho) > 0$

Here A is not function of α and β

Differentiating D with respect to α,

$$\frac{\partial D}{\partial \alpha} = -(\frac{1}{\alpha^2})[\frac{A\beta}{\alpha_1}]$$

Therefore

$$\frac{\partial D}{\partial \alpha} < 0$$

Differentiating D with respect to β,

$$\frac{\partial D}{\partial \beta} = \frac{A(1-\alpha)}{\alpha\alpha_1}$$

$$\frac{\partial D}{\partial \beta} > 0$$

$$\phi = \frac{(1-\alpha_1-\alpha_2)\beta}{\alpha_1(1-\beta)D + (1-\alpha_1-\alpha_2)\beta} = \frac{M}{ND+M}$$

Here $M = (1-\alpha_1-\alpha_2)\beta \quad D = f(\alpha)$

$$\frac{\partial \phi}{\partial \alpha} = \frac{(ND+M)\frac{\partial M}{\partial \alpha} - M\frac{\partial(ND+M)}{\partial \alpha}}{(ND+M)^2}$$

Now as $\frac{\partial D}{\partial \alpha} < 0$, $\frac{\partial \phi}{\partial \alpha}$ >0

Therefore, $\frac{\partial \phi}{\partial \alpha} > 0$

$$\phi = \frac{(1-\alpha_1-\alpha_2)\beta}{\alpha_1(1-\beta)D+(1-\alpha_1-\alpha_2)\beta}$$

Or, $\phi = \dfrac{(1-\alpha_1-\alpha_2)}{\alpha_1 \frac{(1-\beta)}{\beta} D + (1-\alpha_1-\alpha_2)}$

Now, $D = A\dfrac{(1-\alpha)\beta}{\alpha\alpha_1}$

$$\phi = \frac{1}{\frac{A(1-\alpha)(1-\beta)}{\alpha(1-\alpha_1-\alpha_2)}+1} = \frac{1}{S(1-\beta)+1}$$ Where $S = \dfrac{A(1-\alpha)}{\alpha(1-\alpha_1-\alpha_2)}$

Using the division rule of differentiation, we derive

$\frac{\partial \phi}{\partial \beta}$ >0 ……………………finding 2

ECONOMIC ANNALS, Volume LXIV, No. 220 / January – March 2019
UDC: 3.33 ISSN: 0013-3264

https://doi.org/10.2298/EKA1920117G

*Senjuti Gupta**
*Bidisha Chakraborty***
*Tanmoyee Banerjee (Chatterjee)****

OPTIMAL TAX POLICY IN AN ENDOGENOUS GROWTH MODEL WITH A CONSUMABLE SERVICE GOOD

ABSTRACT: *The paper analyses the optimal tax policy in an endogenous growth model in a command economy, where the commodity output is produced with only physical capital, and skilled labour is the only input in producing the service good. In the benchmark model, per capita government expenditure is used to create human capital. Two cases are considered regarding taxation: in the first, tax is imposed on both commodity and service sectors, while in the second only the service sector is taxed. In each case the model derives the optimal tax rate and steady-state growth paths. In the first regime where both sectors are taxed we find the optimal tax rate on the service sector to be zero, but on commodity output it is positive. However, in the second regime there is also a unique optimal tax rate on the service sector to finance human capital accumulation. Comparing the growth rates in both cases we also observe that the imposition of tax on only the service sector instead of on both sectors yields a higher rate of growth if the population growth rate along with the marginal productivity of human capital is sufficiently high. We also show that when the service sector is taxed it may grow at a higher rate than the manufacturing sector. An extension of the benchmark model in which government spends tax revenue on accumulation of human capital as well as physical capital confirms that the optimal service tax rate is zero, but the optimal commodity tax rate is positive when both sectors are taxed.*

KEY WORDS: *taxation, government policy, endogenous growth, command economy, human capital accumulation.*

JEL CLASSIFICATION: E60, H21, O41

* Department of Economics, Government Girls' General Degree College, Kolkata, India
** Corresponding Author, Department of Economics, Jadavpur University, Kolkata, India, E-mail: bidisha.chakraborty@gmail.com
*** Department of Economics, Jadavpur University, Kolkata, India

1. INTRODUCTION

The choice of an optimal tax policy is an important issue in growth literature. The present paper focuses on the government's optimal tax policy in the presence of a consumable service sector. The development of endogenous growth theory has enabled policymakers to discover optimal fiscal policies in the growth model. To address the problems of optimal taxation a few assumptions are made. Following Slemrod (1990), it is assumed that all taxpayers are identical, so the government need not be concerned with the issues of vertical or horizontal equity. It is further assumed that tax rates can be raised without administrative cost. The basic problem of optimal tax policy literature is how to determine the tax rate that will maximize the economic growth rate, social welfare, or government revenue and leave the taxpayer as well off as possible. Around sixty years ago Ramsey (1927) showed that a uniform commodity tax system, which alters none of the relative prices of goods, was not optimal in general. Instead, the tax rate is negatively related to the consumption growth rate. Imposition of a lump-sum tax on the representative taxpayer is the first-best solution for optimal taxation, as the required revenue can be achieved without any efficiency cost. When there are very few restrictions, commodity taxation is optimal. The second-best solution for optimal taxation is the benign rule of uniform taxation (Slemrod1990). Slemrod(1990) carried out a detailed survey of existing literature on optimal tax policy.

There is a vast literature that also discusses the effects of various policies in endogenous growth models. Papers by Corlett and Hague(1953), Auerbach (1979) , Garcia-Castrillo and Sanso (2000), Kleven et.al(2000), Gomez (2003), Futagami, Morita, and Shibata (1993), Faig (1995), Dasgupta (1999), Chang (1999), Fernandez, Novales, and Ruiz (2004), Woo (2005), Chen and Lee (2007), Hollanders and Weel (2003), Greiner (2006) etc. shed light on this area. Given this background, the present study will try to find the government's optimal tax policy in an endogenous growth model in an economy with a consumable service good under the assumption that the government spends tax revenue to finance public education in order to accumulate human capital –similarly to Capolupo (2000),who investigates the long-run effects of government spending and taxation in an endogenous growth framework in which government spending on public education drives human capital accumulation. Several other papers consider the role in endogenous growth models of tax-financed government expenditure on public resources. Garcia-Castrillo and Sanso (2000) and Gomez (2003) design optimal fiscal policies in the Lucas (1988) model. Gomez (2003) also finds that atax-financed educational subsidy policy is optimal. However, Gomez' analysis (2003) does not finda lump sum tax to be optimal to finance the subsidy. Greiner (2008) examines the effects of fiscal policy in an endogenous growth model with two types of agent, skilled and unskilled, where human capital accumulation is a function of existing human capital the educational sector and public spending on education. The paper shows that a welfare-maximizing labour-income tax rate might exist even when a higher labour-income tax rate always raises the balanced growth rate.

Across the world, human capital and the education sector play a very important role in economic development and a lot of work has been done on the theory of human capital accumulation in growth economics. Hollanders and Weel (2003)address the role of public expenditure in human capital accumulation in a Lucas-type (1988) growth model. Greiner (2006) focuses on an endogenous growth model which is based on the assumption that human capital accumulation results from the investment of public resources, financed by imposing an income tax and issuing government bonds. Following Heckman (1976) and Rosen (1976), King and Rebelo (1990) try to discover the optimal accumulation of human capital and the effect of various taxation regimes on optimal accumulation. Their basic finding is that the cost of taxation on welfare is higher for endogenous growth models than in neoclassical models with exogenously given technical progress. The only study that deals with the service sector and optimal taxation is by Kleven et al.(2000). They find that market-produced services that are close substitutes for home-produced services should be given preference in an optimal tax system. The finding of this paper amends the classical Corlett-Hague (1953) rule for optimal commodity taxation and reveals that imposition of a lower tax rate on consumer services may be optimal in spite of the complementarily between services and leisure. Further, the study finds that when leisure can be equally substituted by services and other goods it is optimal to tax commodities uniformly, and when home production is absent the optimal tax structure will include a lower rate of tax on consumer services.

However, none of these growth models addresses the problems of the service sector along with the human capital accumulation function or discusses whether or not it is important to levy tax on service goods. In this paper, human capital is considered one of the most important factors in producing service output. Most of these services –education, health, public administration, banks, computer services, recreation, communications, financial services,and many others –require specialized know-how. A number of papers[1] have dealt with the importance of human capital in the service sector. Abowd et.al (2001) note that in service industries the service is fundamentally delivered by human capital.Kianto Hurmelinna-Laukkanen (2010) also find that service-oriented companies possess more human capital and renewal capital than product-oriented companies and focus more on intellectual capital creation. Messina (2004) considers the service sector to be characterized by relatively skill-oriented human-capital-intensive production compared to the manufacturing sector. According to an OECD(2000) study, the service sector employs a much higher share of university-educated workers than the goods sector, and in 1998 the ratio of university to non-university workers engaged in service industries was 0.24, whereas in the manufacturing sector the same ratio was .07. A briefing note by the Department for International Development (UK2008) also emphasizes the importance of human capital accumulation, saying that countries need to expand the human capital base in those professions whose services they are likely to export. Maroto Sánchez(2010) also acknowledges the role of human capital in the service sector. Simões and Duarte (2014), in the context of Portugal, show that modern progressive services register higher productivity levels and growth but demand higher levels of human capital to expand. Fang and Chao(2015) provide a detailed literature survey showing the positive impact of human capital in the development of tertiary industry in China. In their study of Shandong Province they show that the stock and level of human capital contributes positively to the development of tertiary industry. Thus, the literature on the service sector documents the importance of human capital as a service sector input.

Given this background, in the present paper we assume the existence of a hypothetical command economy where the only service sector input is human capital, which is accumulated through per capita government expenditure on the education sector. This is our benchmark model. Physical capital is used to produce commodity output only. Government expenditure is financed by tax revenue. We consider two tax regimes. In the first, tax is imposed on both consumption goods and service goods, while in the secondonly the service sector is taxed. We compare the steady-state growth paths of the two types of tax regime to discover the optimal tax policy. We also extend the model in order to consider the situation where government spends to accumulate human capital as well as physical capital in the above-mentioned tax regimes.

[1] Riley, 2012; Lucas, 1988; Mankiw et al., 1992; De La Fuente and Domenech, 2006

We find that in the benchmark model of a command economic regime, both human capital and commodity output have a positive, unique steady-state growth rate. In the first case where we consider tax on both the sectors, we find that the optimal tax rate for the service sector is zero, but the optimal tax rate for commodity output is positive. However, in the second case where tax revenue comes solely from a service tax, we find that there is a unique optimal tax rate for the service sector to finance human capital accumulation. Comparing the growth rates in both cases we also observe that taxing only the service sector instead of both sectors yields a higher rate of growth if the population growth rate along with the marginal productivity of human capital is sufficiently high. We also find that when the service sector is taxed to finance human capital accumulation it may grow at a higher rate than the manufacturing sector. In the case of the extended model where a fraction of government tax revenue is spent on human capital accumulation and another fraction goes to physical capital accumulation, when both sectors are taxed as in the benchmark model, the optimal tax on the service sector is still found to be zero. We also find that steady-state growth is the same under both tax regimes.

In this paper we are trying to find the optimal indirect tax on final goods and services. Existing theoretical papers on optimal indirect taxation show that final goods and services should be taxed uniformly, exempting intermediate goods. However, in practice value added tax, which is typically imposed on final goods and services, is imposed at different rates. In this paper, in a simplified model where human capital is used only to produce final services, while physical capital is used as the only input to produce final commodities, we offer an alternative theory of optimal policy. We suggest that the optimal policy should impose tax only on final commodity and not on services, irrespective of whether tax revenue sponsors only human capital accumulation or both human and physical capital accumulation. However, if tax is only imposed on services, even though it is not optimal, the economy may grow at a faster rate.

The rest of the paper is organised as follows. In section 2 the basic general model is presented. Section 3 discusses the optimal tax policy and steady-state growth paths and corresponding comparative static results under a command economic regime when tax is levied on both service and commodity sectors, modifies the model under the assumption that only service goods are being taxed, and comparesgrowth rates under the two tax regimes to find the optimal tax policy. Section 4 describesan extension of the benchmark model where tax revenue is spent on accumulation of human capital as well as physical capital. Section 5 concludes.

2. THE MODEL

This section describes the basic model for the functioning of an economy under a command economic regime.

Households, Firms, and Government

A closed economy model is considered that has two sectors, a commodity sector and a service sector. We assume that the output of the commodity sector is used for consumption or investment. The output of the service sector is fully consumed. The total labour force is homogeneous as far as skill is concerned. The commodity and the factor markets are characterized by perfect competition. Identical rational agents inhabit the economy. Production technology is subject to constant returns to scale. Preferences for the consumption of different combinations of commodity and service output are given by the following function, where *c* and *s* denote the flow of real per capita consumption of commodity and service outputs respectively.[2]

$$u(c) = \int_0^{\infty} \frac{(c^{\alpha} s^{1-\alpha})^{1-\sigma} - 1}{(1-\sigma)} e^{-\rho t} N(t) dt \tag{1}$$

Here, α is the parameter that measures the intensity of preference for commodity consumption and $(1-\alpha)$ measures the preference for service output consumption. Let ρ be the discount rate and σ the elasticity of marginal utility, the inverse of which is known as inter-temporal elasticity of substitution. Let N represents the total labour force or working population.

The commodity and service output production functions can be written as

$$y_c = AK \tag{2}$$

Following Das and Saha (2015) we assume

[2] Following Lucas (1988), we include *N(t)* in the utility function.

$$y_s = B(Nh) \tag{3}$$

where y_c and y_s are commodity and service outputs. K is the aggregate physical capital. Let the general skill level of a worker be h. The effective skilled work force in commodity production is Nh. A and B are the production technology parameters of commodity and service production functions that give the average as well as marginal productivity of each factor in the AK-type production function.

The population level is growing at an exponential rate in the following manner:

$$N(t) = N_0 e^{nt} \tag{4}$$

Here, N_0 stands for the population size during the initial time period. For simplicity, the initial population size is normalised, i.e., N_0=1. According to our assumption, government spends money on education to create human capital.

Following Glomm and Ravikumar (1992), Capolupo (2000), and Beauchemin (2001), we assume that human capital accumulation takes place through full-time public education. The human capital accumulation function can be written as

$$\dot{h} = \eta \frac{G}{N} \tag{5}$$

Here η is the technology parameter of human capital accumulation whose value is always positive, and G stands for government expenditure.

3. GROWTH RATES IN THE BENCHMARK MODEL UNDER DIFFERENT TAX REGIMES

3.1 Imposing tax on both commodity and service sectors

In this section we assume that both the commodity sector and the service sector are being taxed to finance government expenditure to build human capital. Let the tax rate levied per unit on service output production be τ_s and the tax rate imposed per unit on commodity output production be τ_k. Let the per unit price of service output be p_s and that of commodity output be 1. The balanced budget equation can be written as

$$G = T = p_s \tau_s y_s + \tau_K y_c \tag{6}$$

It is assumed that the disposable commodity output over aggregate consumption is accumulated as physical capital. The physical capital accumulation function is given by

$$\dot{K} = (1-\tau_k) y_c - Nc \tag{7}$$

Equation (7) also satisfies the feasibility constraint. The demand for production of goods is demand for consumption goods (*Nc*) and for service goods (*Ns*), investment demand ($\dot{K}$), and government demand for goods over tax revenue. On the other hand the supply of goods is commodity production and service production. Since theentire disposable service good is consumed and the government runs a balanced budget, equation (7) equals the feasibility constraint. We assume there is no depreciation of physical capital and human capital. The per unit price of service output p_s is obtained from the consumer's equilibrium condition by equating the marginal rate of service product substitution for commodity output with the ratio between service output price and commodity output price.

$$p_s = \frac{(1-\alpha)}{\alpha} . \frac{(\frac{c}{h})}{(1-\tau_s)B} \tag{8}$$

For simplicity, it is assumed that the commodity output is a numeraire good, which implies that the per unit price of the commodity output, i.e., p_c, should be 1.

After deducting the taxable amount, the remaining disposable service output value is equal to the expenditure incurred on service goods, as the service goods are totally consumed by the population. So the market clearing condition is

$$p_s(1-\tau_s) y_s = p_s s N \tag{9}$$

The social planner maximizes the present discounted utility value over the infinite time horizon defined by equation (1), subject to the constraints of physical and human capital.

In this case, the control variables are c, τ_s, τ_K and the state variables are *K* and *h*. The current value Hamiltonian function is formulated as

$$H = N(t)\left[\frac{(c^{\alpha}s^{1-\alpha})^{1-\sigma}-1}{(1-\sigma)}\right]+\theta_1\dot{K}+\theta_2\dot{h}$$

Substituting the value of the physical capital and human capital investment functions,we get

$$H = N(t)[\frac{[(c^{\alpha}s^{1-\alpha})^{1-\sigma}-1}{(1-\sigma)}]+\theta_1[(1-\tau_K)y_c-cN]+\theta_2\eta\frac{(p_s\tau_s y_s+\tau_K y_c)}{N} \tag{10}$$

where θ_1 and θ_2 are the shadow prices associated with $\dot{K}$ and h, which stand for physical capital investment and human capital accumulation.From the first-order conditions of the control variables and the two co-state equations, the growth rate of commodity output consumption and that of human capital accumulation and physical capital are solved along with the tax rates. The first-order conditions are:

$$\alpha c^{\alpha(1-\sigma)-1}(1-\tau_s)^{(1-\alpha)(1-\sigma)}B^{(1-\alpha)(1-\sigma)}h^{(1-\alpha)(1-\sigma)}N(t)-\theta_1 N(t)+\theta_2\eta\frac{(1-\alpha)\tau_s}{\alpha(1-\tau_s)}=0 \tag{11}$$

$$\theta_1=\frac{\theta_2\eta}{N} \tag{12}$$

$$N(t)c^{\alpha(1-\sigma)}B^{(1-\alpha)(1-\sigma)}h^{(1-\alpha)(1-\sigma)}(1-\alpha)(1-\tau_s)^{(1-\alpha)(1-\sigma)-1}+\theta_2\eta\frac{(1-\alpha)}{\alpha}c\frac{d}{d\tau_s}(\frac{\tau_s}{1-\tau_s})=0 \tag{13}$$

$$\dot{\theta}_1=\rho\theta_1-\left\{\theta_1(1-\tau_K)A+\theta_2\frac{\eta\tau_K}{N}(\frac{A}{N})\right\} \tag{14}$$

$$\dot{\theta}_2=\rho\theta_2-\left[N(t)c^{\alpha(1-\sigma)}(1-\tau_s)^{(1-\alpha)(1-\sigma)}B^{(1-\alpha)(1-\sigma)}(1-\alpha)h^{(1-\alpha)(1-\sigma)-1}\right] \tag{15}$$

Steady-state growth path and tax rate:

Proposition 1.

Under a command economic regime, human capital and consumption of commodity output and physical capital exhibit a positive, unique stead-state growth rate when tax is imposed on both sectors. Further, the optimal tax rate for the service sector is zero while that for commodity output is positive.

Proof:

(For detailed proof see Appendix 1.)

From first order conditions, we obtain the steady-state growth rate of*c, h, and K* and the uniquely determined values of tax rates.

$$\gamma_h = \gamma_c = \frac{(A-\rho)}{\sigma} > 0 \;\; A > \rho \tag{16}$$

$$\gamma_K = \gamma_h + n \tag{17}$$

$$\tau_K = \frac{(1-\alpha)(A-\rho)[\sigma(A-n)-(A-\rho)]}{A\sigma[(1-\alpha)(A-\rho)+\sigma\alpha(A-n)]} \tag{18}$$

$$\tau_s = 0 \tag{19}$$

$$k = \frac{K}{Nh} = \frac{(A-\rho)}{\sigma\tau_K A\eta} > 0 \Rightarrow A > \rho \tag{20}$$

Thus, when the rate of time preference (ρ) is lower than the marginal productivity of capital(A), the capital–labour ratio is always positive,[3] and this in turn implies that the economy grows at a positive rate at the steady state. From the investment function in equation (7) it is clear that the disposable income that is left after consuming the commodity output is invested in creating physical capital. As the future discount rate falls, individuals become more concerned with future consumption rather than present consumption. Therefore, more investment foregoes present consumption. As a result, future

[3] This is the standard assumption of the AK model.

consumption increases and present consumption decreases. Hence, the consumption growth rate and the output growth rate increase.

Further, $(\frac{c}{h})=\frac{(A-n)}{\eta}\frac{\alpha}{(1-\alpha)}>0 \Rightarrow A>n$ (21)

As the ratio of per capita commodity consumption to per capita skill level can never be negative, $A>n$. This condition for the positive value of per capita commodity consumption and the general skill level ratio require that the value of marginal capital productivity should be greater than the population growth rate. When the population growth rate is low, more output is left to be consumed by fewer individuals. This raises the commodity-consumption-to-skill ratio.

Equations (20) and (21) together with the condition $\sigma(A-n)>(A-\rho)$ imply that $0<\tau_K\leq 1$.

From equation (19), we observe that it is not optimal to tax the service sector. This result is very interesting. Auerbach (1979) explores the issue of optimal capital taxation and finds the optimal capital tax to be zero. Alternatively, Kleven et al.(2000) find that imposing a lower tax rate on consumer services may be optimal in spite of the complementarity between services and leisure. In our present paper, where household utility depends on commodity consumption and services consumption, we observe that if there is a possibility to tax commodity sector as well as service sector, it is optimal to tax only the commodity sector and not the service sector.

Next, we check the comparative static results corresponding to various parameters.

Differentiating the optimal commodity tax rate as given in (18) with respect to the inverse of inter-temporal elasticity of substitution, we find that

$$\frac{d\tau_K}{d\sigma}=\frac{A(A-\rho)(1-\alpha)[A(1-\alpha)(A-\rho)^2+\alpha\sigma(A-n)\{2(A-\rho)-\sigma(A-n)\}]}{\{A\sigma[(A-\rho)(1-\alpha)+\sigma\alpha(A-n)]\}^2}$$

The sufficient condition for $\frac{d\tau_K}{d\sigma} > 0$ is $A > \frac{2\rho - n\sigma}{2-\sigma}$. If the condition is not satisfied $\frac{d\tau_K}{d\sigma}$ may be positive or negative.

Further differentiating (16) with respect to σ gives $\frac{d\gamma_h}{d\sigma} < 0$

In this case, the growth rate of human capital γ_h always decreases for an increase in σ, but its impact on the optimal tax rate is ambiguous.

Differentiating (18) with respect to the rate of discount, we get

$$\frac{d\tau_K}{d\rho} = \frac{A\alpha\sigma^2(A-n)(1-\alpha)[2(A-\rho)-\sigma(A-n)]+(1-\alpha)^2(A-\rho)^2 A\sigma}{\{A\sigma[(1-\alpha)(A-\rho)+\alpha\sigma(A-n)]\}^2}$$

If, $\frac{(A-\rho)}{(A-n)} < \sigma < \frac{2(A-\rho)}{(A-n)}$

then $\frac{d\tau_K}{d\rho} > 0$ as well as τ_K is positive.

And $\frac{d\gamma_h}{d\rho} < 0$

As the discount rate rises, individuals become more concerned about present rather than future consumption. Thus, under a balanced budget the tax rate will rise that raises the future accumulation rate of human capital to be used as an input to produce service output in subsequent periods, for a rise in ρ if $2(A-\rho) > \sigma(A-n)$. However, irrespective of the movement in the tax rate, the growth rate of human capital accumulation will fall along with the rising values of the rate of time preference.

We note that the conditions for $\frac{d\tau_K}{d\rho} > 0$ and $\frac{d\tau_K}{d\sigma} > 0$ are the same. These conditions are likely to be satisfied if the values of ρ and σ are low.

Differentiating (18) with respect to the intensity of preference towards commodity consumption we get

$$\frac{d\tau_K}{d\alpha} = \frac{A\sigma^2(A-\rho)(A-n)[(A-\rho)-\sigma(A-n)]}{\{A\sigma[(A-\rho)(1-\alpha)+\sigma\alpha(A-n)]\}^2}$$

If $\tau_K > 0,\ A > \dfrac{\sigma n - \rho}{\sigma - 1}$

Therefore, $\dfrac{d\tau_K}{d\alpha} < 0$.

If individuals derive more utility from commodity consumption than service consumption it is optimal to reduce tax on commodity output. This result implies that as the intensity of preference toward service consumption increases, the value of τ_K rises.

3.2 When tax is imposed on only the service sector

In this section we consider the case where only the service sector is taxed. The tax revenue (equal to government expenditure) is spent to build human capital. Let the tax rate be τ_s, which is levied on per unit production of service output. Now the balanced budget equation can be written as

$$G = T = \tau_s y_s \tag{22}$$

In this model we assume that there is no depreciation of physical or human capital. Using equations (3), (5), and (6), the human capital accumulation function is given by

$$\dot{h} = \eta \frac{G}{N} = \eta \tau_s Bh \tag{23}$$

After deducting the taxable amount, the remaining disposable service output is totally consumed by the population. Thus the market clearing condition is derived as

$$s = (1-\tau_s)Bh \tag{24}$$

It is assumed that commodity output over aggregate consumption is accumulated as physical capital. The physical capital accumulation function is given by

$$\dot{K} = y_c - Nc \tag{25}$$

Equation (25) also satisfies the feasibility constraint, just like equation (7). The social planner in a command economy maximizes the value of utility defined by equation (1) subject to the physical capital accumulation and human capital accumulation constraints given by equations (23) and (25). The value of *s*, which denotes per capita consumption of service output in our model, is substituted by equation (24) in the following Hamiltonian function.

The current value Hamiltonian as given in (10) is maximised with respect to the control variables c and τ_s where the state variables are K and h. Here, θ_1 and θ_2 are the shadow prices associated with $\dot{K}$ and $\dot{h}$, which stand for physical capital investment and human capital accumulation.

$$H = N(t)[\frac{[c^{\alpha}\{(1-\tau_s)Bh\}^{1-\alpha}]^{1-\sigma}-1}{(1-\sigma)}] + \theta_1[AK - cN] + \theta_2 \eta\tau Bh \tag{26}$$

The first order conditions for the maximization of present discounted value of utility are given by:

$$\alpha c^{\alpha(1-\sigma)-1}(1-\tau_s)^{(1-\alpha)(1-\sigma)} B^{(1-\alpha)(1-\sigma)} h^{(1-\alpha)(1-\sigma)} = \theta_1 \tag{27}$$

$$N(t)c^{\alpha(1-\sigma)} B^{(1-\alpha)(1-\sigma)} h^{(1-\alpha)(1-\sigma)} (1-\alpha)(1-\tau_s)^{(1-\alpha)(1-\sigma)-1} = \theta_2 Bh\eta \tag{28}$$

$$\frac{\dot{\theta}_1}{\theta_1} = (\rho - A) \tag{29}$$

$$\frac{\dot{\theta}_2}{\theta_2} = \rho - B\eta \tag{30}$$

Steady-state growth path and tax rate:

Proposition 2: ***In a command economy, human capital and commodity output havea positive, unique steady-state growth rate. There also exists a unique optimal tax rate on the service sector to finance human capital accumulation.***

(For proof see Appendix 2.)

From first order conditions we obtain the growth rates of commodity output and human capital

$$\gamma^*{}_c = \frac{[(1-\alpha)(1-\sigma)(n+B\eta)-\rho]}{\sigma} + \frac{A[\sigma+\alpha(1-\alpha)(1-\sigma)^2]}{\{1-\alpha(1-\sigma)\}\sigma} \tag{31}$$

$$\gamma_h^* = \frac{A\alpha(1-\sigma)+\{1-\alpha(1-\sigma)\}(n+B\eta)-\rho}{\sigma} \tag{32}$$

The value of optimal tax rate is

$$\tau_s^* = \frac{A\alpha(1-\sigma)+\{1-\alpha(1-\sigma)\}(n+B\eta)-\rho}{B\eta\sigma} \tag{33}$$

Now we compare the human capital growth rate and commodity output growth rate.

Proposition 3*:* ***When only the service sector is taxed it will grow at a higher rate than the commodity sector if the sum of the population growth rate and the technology parameter of the service sector is higher than the technology parameter of the commodity sector.***

The comparison of γ_h and γ_c gives the following result:

$$\gamma_h^* - \gamma_c^* = (n+\eta B - A) \tag{34}$$

It implies that $\gamma_h^* < \gamma_c^*$ if and only if

$$A > n + B\eta \tag{35}$$

The reverse will be the case if $n + B\eta > A$

The condition implies that if the sum of the population growth and the weighted value (with the coefficient of human capital in the service output production function) of the technology parameter of human capital is more than the marginal productivity of physical capital, the growth rate of human capital accumulation and hence the service sector growth rate will be higher than the growth rate of commodity consumption. The result is intuitively obvious. In the model, human capital is used in the service production function, whereas physical capital is used in commodity production. Thus, if human capital becomes more efficient than physical capital the service sector will grow at a higher rate than the commodity sector, and vice versa. In developing countries like India, the service sector often grows at a much higher rate than the manufacturing sector (Bosworth, Collins, and Virmani, 2006; Banga and Goldar, 2007). Zuleta and Young (2013) explain this in terms of innovation in the manufacturing sector. They argue that as labour-saving innovation takes place in the manufacturing sector the labour force shifts to the service sector and consequently the service sector outperforms the manufacturing sector in contributing to the overall growth of the economy. Das and Saha (2015) argue that differences in returns to scale between the two sectors and employment frictions in manufacturing explain why the growth rate of the service sector may be higher. Our model tries to explain this fact in terms of population growth rate and the efficiency parameters of both the sectors. Since some developing countries have a high population growth rate they experience a disproportionate increase in service sector growth compared to manufacturing sector growth. If the service sector is taxed, services become more expensive to consume and individuals consume more commodity outputs, depleting physical capital and reducing manufacturing sector growth. Thus, taxing the service sector may yield unbalanced growth.

Next, we try to find how the tax rate and growth rates vary with respect to changes in different parameter values.

Differentiating the optimal service tax rate with respect to the inverse of inter-temporal elasticity of substitution, we find that

$$\frac{d\tau^*_s}{d\sigma} = \frac{-[(n+\eta B-A)(1-\alpha)+(A-\rho)]}{(B\eta\sigma)^2} \tag{36}$$

if $n+\eta B - A \geq 0$, and $A \geq \rho$, $\dfrac{d\tau_s}{d\sigma} \leq 0$.

As the inverse of inter-temporal elasticity of substitution, σ, falls, the optimal tax rate may increase if $A \geq \rho$ and $n + B\eta > A$. (See Appendix for detailed derivation.) This implies that as the inter-temporal elasticity of substitution increases (which is the same as a fall in σ), a representative consumer can easily substitute present consumption with future consumption. Thus, the present optimal tax rate for the service sector increases, because tax can finance education that can generate human capital in the future if $n + B\eta > A$ and $A \geq \rho$. Thus, when σ decreases, people are ready to forgo present consumption for future consumption and are willing to pay more tax when the service sector is more productive than the commodity sector and the time preference rate is not very high.

We now examine how the optimal service tax rate will respond when the technology parameter in human capital accumulation changes. Differentiating the optimal tax rate with respect to the technology parameter of human capital accumulation we find

$$\frac{d\tau^*_s}{d\eta} = -\frac{(B\sigma)}{(\eta B\sigma)^2}[(A-n)\{1-\alpha(1-\sigma)\}-(A-\rho)] \tag{37}$$

If $(A-n)\{1-\alpha(1-\sigma)\} < (A-\rho)$

Alternatively, $n > A - \dfrac{(A-\rho)}{\{1-\alpha(1-\sigma)\}}$

$$\frac{d\tau^*_s}{d\eta} > 0$$

If population growth is high, or above a critical level, then a rise in η, the technology efficiency parameter for human capital accumulation, may cause the tax rate to rise. If n is high, then per capita allocation of government spending on education is low. Thus, even when η rises, to increase the growth rate the optimal τ_s rises, and vice-versa.

Differentiating the optimal tax rate in a command economy with respect to the time preference rate, we find

$$\frac{d\tau^*_s}{d\rho} < 0$$

As the time preference rate rises, individuals become more concerned with present rather than future consumption. Thus, under a balanced budget, a tax rate increase that raises the future accumulation rate of human capital– which will be used as an input to produce commodity output in subsequent periods – will fall, against a rise in the time preference rate.

Now we will examine the changes in human capital accumulation and commodity consumption growth rates due to changes in different parameters.

The human capital growth rate is as follows:

$$\gamma^*_h = B\eta\tau_s$$

It is obvious from the human capital accumulation function that the response of γ^*_h to change in parameters α, ρ and σ, for example, will be same as the response of τ_s with respect to α, ρ and σ.

In this model the growth rate of human capital accumulation is positively related to the tax rate imposed on service output because the tax revenue is used to create human capital. Therefore, when the tax rate increases (decreases) due to an increase (decrease) of the parameters that we have considered in our analysis, the growth rate of human capital also increases (decreases) accordingly.

3.3 Comparison of growth rates

In this section we compare growth rates for the two different tax regimes discussed above.

Proposition 4: ***Taxing the service sector instead of taxing both sectors yields a higher growth rate if the population growth rate and the marginal productivity of human capital are sufficiently high. Otherwise, the reverse will happen.***

Proof: Comparing (16) and (32),we obtain

$$\gamma^*_h - \gamma_h = \frac{\{1-\alpha(1-\sigma)\}(n+B\eta-A)}{\sigma}$$

Therefore, the growth rate is higher when tax is imposed on the service sector rather than on both sectors if $n+B\eta>A$, and vice versa.

Note that this is the same condition we obtained for the service sector growing at a higher rate than the commodity sector. Thus, we can say that for $A < n + B\eta$, the service sector grows at a faster rate in the economy compared to when the commodity sector is taxed. Hence, imposition of tax on the service sector compared to taxing both sectors yields a higher growth rate. We know that A denotes the marginal product of capital in the commodity sector and B denotes the marginal product of human capital in the service sector. If the sum of the growth rate of the population and the marginal product of human capital in the service sector multiplied by the technology parameter in the human capital accumulation function ($B\eta$) is higher than A, then $\gamma_h^* > \gamma_h$. Thus, when the marginal product of capital to produce commodity output is relatively high, the economy experiences a higher growth rate if the commodity sector is taxed.

Finally, we consider a numerical example:

Let A be 1, B be 1, n be 0.05 and η be 1, then the growth rate when the service sector is taxed is higher than that when both sectors are taxed. But if we consider A to be 1, B to be 1, n to be 0.05, and η to be 0.5, then the growth rate when both sectors are taxed is higher than the growth rate when only the service sector is taxed.

4. EXTENSION OF THE BENCHMARK MODEL: GOVERNMENT SPENDS TO ACCUMULATE HUMAN AND PHYSICAL CAPITAL

In this section, we assume that government expenditure $G$is spent on accumulation of both human capital and physical capital. As a result, all other equations remaining unchanged, equations (5) and (7) are modified accordingly in the following way:

$$\dot{h} = \eta \frac{(\phi G)}{N} \tag{38}$$

and

$$\dot{K} = y_c + (1-\phi)G - Nc \tag{39}$$

Here, ϕ is the exogenously given fraction of *G* spent on human capital accumulation and *(1–ϕ)* is spent on physical capital accumulation. Here, *G* is given by Equation (6).

4.1.Government Expenditure is financed by taxing both commodity and service sectors

The current value Hamiltonian is given as[4]

$$H = N(t)[\frac{c^{\alpha(1-\sigma)}B^{(1-\alpha)(1-\sigma)}h^{(1-\alpha)(1-\sigma)}(1-\tau_s)^{(1-\alpha)(1-\sigma)}-1}{(1-\sigma)}]+$$
$$\theta_1[(1-\tau_K)AK+(1-\phi)\tau_K(AK)+\tau_s N\frac{(1-\alpha)}{\alpha}(\frac{(1-\phi)c}{(1-\tau_s)})-cN] \tag{40}$$
$$+\theta_2\eta\frac{\phi}{N}(\tau_K AK+\tau_s N\frac{(1-\alpha)}{\alpha}(\frac{c}{(1-\tau_s)}))$$

Here, the control variables are c, τ_K, and τ_s; K and h are the state variables and θ_1 and θ_2 are the co-state variables.

Using the first-order conditions of the optimization problem we find that

$$\tau_K = \frac{(1-\alpha)(A-\rho)[\sigma(A-n)-(A-\rho)]}{\sigma[(A+\phi-1)(1-\alpha)(A-\rho)+\sigma\alpha(A-n)\phi A]}$$

and $\tau_s = 0$. Note that if $\phi = 1$, the τ_K obtained in this extended model is same as that obtained in the basic model. We obtain that per capita consumption and human capital grow at the same constant rate given by $\gamma_c = \gamma_h = \frac{(A-\rho)}{\sigma}$.

Proposition 5: ***When government spends to accumulate human capital and physical capital and both sectors are taxed, under a steady state the optimal tax rate for services is τ_s=0 and for final commodities it is positive, and the steady-state growth rates are*** $\gamma_c = \gamma_h = \frac{(A-\rho)}{\sigma}$

(For proof see Appendix 3.)

[4] Detailed derivation of the model is given in Appendix 3

Thus, as in the previous case where tax revenue is spent solely on human capital accumulation, in this case where tax revenue is spent on both human and physical capital accumulation, the optimal tax rate for service goods is zero while that for final commodities is positive.[5] As summarized by Mankiw et al. (2009), existing theoretical papers on optimal indirect taxation, namely Diamond and Mirrlees (1971) and Atkinson and Stiglitz (1976), show that only final goods ought to be taxed and typically they ought to be taxed uniformly; taxes on intermediate goods should be avoided. Mankiw et al. (2009) also observe that in practice in many countries, value added taxes on goods and services that in principle exempt all intermediate goods are laden with exceptions and rules that violate the guidelines of optimal policy. This paper offers an alternative theory of optimal policy with a simplified model where human capital is used only in final services, while physical capital is the only input used to produce final commodities.

5. CONCLUSION

This paper constructs a two-sector endogenous growth model under a command economic regime in order to discover the optimal tax policy. Commodity output is produced with only physical capital, whereas skilled labour is the only input used to produce service output. Two tax regimes are considered. In the first regimeboth commodity goods and services are taxed. In the second regime only the service sector is taxed. We first consider the benchmark model where the tax revenue is invested to create human capital through government expenditure. Steady-state growth paths are studied under a command economic regime. The optimal tax rate and steady-state growth path are derived in each case. The growth rate is higher when tax is only imposed on the service sector rather than on both commodity and service sectors, provided the population growth rate and marginal productivity of human capital are sufficiently high. However, when both sectors are taxed the optimal tax on the service sector is zero while on commodity output it is positive. We also show that when the service sector is taxed it can grow at a higher rate than the manufacturing sector. Next, we extend the benchmark model to consider the case where tax revenue is spent on accumulating human capital as well as physical capital. In this case we also find that the optimal tax rate on final

[5] In this extended model, if only the service sector is taxed, along the steady-state balanced growth path the optimal service tax is found to be positive. Derivations are available from the authors on request.

commodities is positive but that on services is zero. In this paper we are trying to discover the optimal indirect tax on final goods and services. Existing theoretical papers on optimal indirect taxation show that only final goods and services should be taxed at a uniform rate and taxes should avoid intermediate goods. However, across countries the value added tax rate imposed on final goods and services differ. This paper offers an alternative theory of optimal policy in a simplified model where human capital is used only in final services while physical capital is only used as an input to produce final commodities. This paper finds that the optimal tax on final commodities is positive, while that on final services is zero, whether tax revenue is spent on only human capital accumulation or on both human and physical capital accumulation. However, taxing only services may yield higher growth.

REFERENCES.

Abowd, J. M., Haltiwanger, J., Lane, J., & Sandusky, K. (2001). Within and between firm changes in human capital, technology, and productivity. Paper presented at 2002 SOLE Meeting, Baltimore, MD, draft (December 2001).

Atkinson, A. B., & Stiglitz, J. E. (1976). The design of tax structure: direct versus indirect taxation. *Journal of Public Economics*, *6*(1–2), 55–75.

Auerbach, A. J. (1979). The optimal taxation of heterogeneous capital. *The Quarterly Journal of Economics*, *93*(4), 589–612.

Banga, R., & Goldar, B. (2007). Contribution of services to output growth and productivity in Indian manufacturing: pre-and post-reforms. *Economic and Political Weekly*, 2769–2777.

Beauchemin, K. R. (2001). Growth or stagnation? The role of public education. *Journal of Development Economics*, *64*(2), 389–416.

Bosworth B., Collins S. M., and Virmani A. (2006). Sources of Growth in the Indian Economy. *India Policy Forum, Global Economy and Development Program, The Brookings Institution*, 3(1), 1–69.

Capolupo, R. (2000). Output taxation, human capital and growth. *The Manchester School*, *68*(2), 166–183.

Chang, W. Y. (1999). Government spending, endogenous labor, and capital accumulation. *Journal of Economic Dynamics and Control*, *23*(8), 1225–1242.

Chen, B. L., & Lee, S. F. (2007). Congestible public goods and local indeterminacy: A two-sector endogenous growth model. *Journal of Economic Dynamics and Control*, *31*(7), 2486–2518.

Corlett, W. J., & Hague, D. C. (1953). Complementarity and the excess burden of taxation. *The Review of Economic Studies*, *21*(1), 21–30.

Das, S. P., &Saha, A. (2015). Growth of business services: A supply-side hypothesis. *Canadian Journal of Economics/Revue Canadiennedʼ Economique*, *48*(1), 83–109.

Dasgupta, D. (1999). Growth versus welfare in a model of nonrival infrastructure. *Journal of Development Economics*, *58*(2), 359–385

DFID (2008). The Contribution of Services to Development and the Role of Trade Liberalisation and Regulation.OECD Global Forum on International Investment OECD Investment Division www.oecd.org/investment/gfi-7. Accessed from *www.oecd.org/investment/globalforum/40302909.pdf*

Diamond, P. A., &Mirrlees, J. A. (1971). Optimal taxation and public production I: Production efficiency. *The American Economic Review*, *61*(1), 8–27.

Faig, M. (1995). A simple economy with human capital: transitional dynamics, technology shocks, and fiscal policies. *Journal of Macroeconomics*, *17*(3), 421–446.

Fernández, E., Novales, A., & Ruiz, J. (2004). Indeterminacy under non-separability of public consumption and leisure in the utility function. *Economic Modelling*, *21*(3), 409–428.

Futagami, K., Morita, Y., & Shibata, A. (1993). Dynamic analysis of an endogenous growth model with public capital. *The Scandinavian Journal of Economics*, 607–625.

De la Fuente, A., &Doménech, R. (2006). Human capital in growth regressions: how much difference does data quality make?*Journal of the European Economic Association*, 4(1), 1–36.

Garcia-Castrillo, P., & Sanso, M. (2000). Human capital and optimal policy in a Lucas-type model. *Review of Economic Dynamics*, *3*(4), 757–770.

Gómez, M. A. (2003). Optimal fiscal policy in the Uzawa-Lucas model with externalities. *Economic Theory*, *22*(4), 917–925.

Glomm, G., &Ravikumar, B. (1992). Public versus private investment in human capital: endogenous growth and income inequality. *Journal Of Political Economy*, *100*(4), 818–834.

Greiner, A. (2008). Human capital formation, public debt and economic growth. *Journal of Macroeconomics*, 30(1), 415–427.

Greiner, A. (2008). Fiscal policy in an endogenous growth model with human capital and heterogenous agents.*Economic Modelling*5(4): 643–657.

Heckman, J. J. (1976). A life-cycle model of earnings, learning, and consumption. *Journal Of Political Economy*,84(4, Part 2), S9–S44.

Hollanders, H. J. G. M., &terWeel, B. J. (2003). Skill-biased technological change: on endogenous growth, wage inequality and government intervention. In *Growth Theory And Growth Policy* (pp. 156–171). Routledge/Taylor & Francis Group.

Kianto, A., Hurmelinna-Laukkanen, P., &Ritala, P. (2010). Intellectual capital in service-and product-oriented companies. *Journal of Intellectual Capital*, *11*(3), 305–325.

King, R. G., & Rebelo, S. (1990). Public policy and economic growth: developing neoclassical implications. *Journal of Political Economy*, *98*(5, Part 2), S126–S150.

Kleven, H. J., Richter, W. F., &Sørensen, P. B. (2000). Optimal taxation with household production. *Oxford Economic Papers*, *52*(3), 584–594.

Lucas Jr, R. E. (1988). On the mechanics of economic development. *Journal of Monetary Economics*, *22*(1), 3–42.

Mankiw, N. G., Weinzierl, M., &Yagan, D. (2009). Optimal taxation in theory and practice. *Journal of Economic Perspectives*, *23*(4), 147–74.

Mankiw, N. G., Romer, D., & Weil, D. N. (1992). A contribution to the empirics of economic growth. *The Quarterly Journal of Economics*, *107*(2), 407–437.

Messina, J. (2005). Institutions and service employment: A panel study for OECD countries. *Labour*, *19*(2), 343–372.

Maroto Sánchez, A. (2010). Growth and productivity in the service sector: The state of the art. http://hdl.handle.net/10017/6558

OECD (2000) Employment in the Service Economy: a Reassessment. In *Employment Outlook*. Chapter 3. Paris. https://www.oecd.org/els/emp/2079561.pdf

Ramsey, F. P. (1927). A Contribution to the Theory of Taxation. *The Economic Journal*, *37*(145), 47–61.

Riley G. (2012). Economic Growth – The Role of Human & Social Capital, Competition & Innovation. http://www.tutor2u.net/economics/revision notes/a2-macro-economic-growth-capital.html Accessed April 16, 2014.

Rosen, S. (1976). A theory of life earnings. *Journal of Political Economy*, *84*(4, Part 2), S45–S67.

Simões, P. M. C., & Duarte, A. (2014). Human capital and growth in services economies: The case of Portugal. In *Structural Change, Competitiveness and Industrial Policy* (pp. 167–197). Routledge.

Slemrod, J. (1990). Optimal taxation and optimal tax systems. *Journal of Economic Perspectives*, 4(1), 157–178.

Woo, J. (2005). Social polarization, fiscal instability and growth. *European Economic Review*, 49(6), 1451–1477.

Received: April 23, 2018
Accepted: April 9, 2019

APPENDIX 1

Proof of Proposition 1.

The first order conditions are

$$\frac{dH}{dc}=0\Rightarrow \alpha c^{\alpha(1-\sigma)-1}(1-\tau_s)^{(1-\alpha)(1-\sigma)}B^{(1-\alpha)(1-\sigma)}h^{(1-\alpha)(1-\sigma)}N(t)-\theta_1 N(t)+\theta_2\eta\frac{(1-\alpha)\tau_s}{\alpha(1-\tau_s)}=0 \quad \text{A1.}$$

$$\frac{dH}{d\tau_k}=0\Rightarrow\theta_1=\frac{\theta_2\eta}{N} \quad \text{A2.}$$

$$\frac{dH}{d\tau_s}=0\Rightarrow N(t)c^{\alpha(1-\sigma)}B^{(1-\alpha)(1-\sigma)}h^{(1-\alpha)(1-\sigma)}(1-\alpha)(1-\tau_s)^{(1-\alpha)(1-\sigma)-1}+\theta_2\eta\frac{(1-\alpha)}{\alpha}c\frac{d}{d\tau_s}\left(\frac{\tau_s}{1-\tau_s}\right)=0 \quad \text{A3.}$$

$$\dot{\theta}_1=\rho\theta_1-\left\{\theta_1(1-\tau_K)A+\theta_2\frac{\eta\tau_K}{N}\left(\frac{A}{N}\right)\right\} \quad \text{A4.}$$

$$\dot{\theta}_2=\rho\theta_2-\left[N(t)c^{\alpha(1-\sigma)}(1-\tau_s)^{(1-\alpha)(1-\sigma)}B^{(1-\alpha)(1-\sigma)}(1-\alpha)h^{(1-\alpha)(1-\sigma)-1}\right] \quad \text{A5.}$$

Manipulating A1 and A2 gives:

$$\alpha c^{\alpha(1-\sigma)-1}(1-\tau_s)^{(1-\alpha)(1-\sigma)+1}B^{(1-\alpha)(1-\sigma)}h^{(1-\alpha)(1-\sigma)}=\theta_1\frac{(\alpha-\tau_s)}{\alpha} \quad \text{A6.}$$

From A3:

$$\frac{N(t)\alpha c^{\alpha(1-\sigma)-1}B^{(1-\alpha)(1-\sigma)}h^{(1-\alpha)(1-\sigma)}(1-\tau_s)^{(1-\alpha)(1-\sigma)+1}}{\eta}=\theta_2 \quad \text{A7.}$$

Using A2 in A4 we have

$$\frac{\dot{\theta}_1}{\theta_1}=(\rho-A) \quad \text{A8.}$$

Taking the log and differentiating A7 with respect to time *t*and using A2 and A6 we have

$$\frac{\dot{\theta}_2}{\theta_2} = \frac{\dot{\theta}_1}{\theta_1} + n = (\rho - A + n) \qquad \text{A9.}$$

Dividing A6byA7 and using A2 we have $(\alpha - \tau_s) = \alpha$ or

$$\tau_s = 0 \qquad \text{A10.}$$

Then equating A8andA9 and using A10

$$(\frac{c}{h}) = \frac{(A-n)}{\eta}\frac{\alpha}{(1-\alpha)} \qquad \text{A11.}$$

Since c/h>0, A>n.

This in turn implies $\gamma_h = \gamma_c$ A12.

Taking the logarithm of A6and using A8 gives

$$\gamma_h = \frac{(A-\rho)}{\sigma} \qquad \text{A13.}$$

From the model and using A10,

$$\gamma_h = \frac{\dot{h}}{h} = \eta\frac{G}{Nh} = \eta\frac{T}{Nh} = \tau_s p_s B(hN) + \tau_K (AK) = \tau_K Ak\eta \qquad \text{A14.}$$

Thus, $k = \frac{(A-\rho)}{\sigma\tau_K A\eta}$ A15.

For k to be positive, the required condition is

$$(A-\rho) > 0$$

Thus $\gamma_h = \gamma_c = \dfrac{(A-\rho)}{\sigma} > 0$

Further from A14, it is clear that at the steady state, $k = \dfrac{K}{Nh}$ must be a constant.

Thus, $\gamma_K = n + \gamma_h$ A16.

From investment function

$$\frac{\dot{K}}{K} = (1-\tau_k)A - \left(c\frac{N}{K}\right) \text{ or}$$

$$\gamma_K = (1-\tau_K)A - \left(\frac{c}{kh}\right) \qquad \text{A17.}$$

Equating A16 and A17 and replacing A11, A14, and A15 we have

$$\tau_K = \frac{(1-\alpha)(A-\rho)[\sigma(A-n)-(A-\rho)]}{A\sigma[(1-\alpha)(A-\rho)+\sigma\alpha(A-n)]} \qquad \text{A18.}$$

From A15, $(A-\rho) > 0$, thus $\tau_K \geq 0$ requires that $\sigma(A-n) > (A-\rho)$. Algebraicmanipulation shows $\tau_K \leq 1$ as

$$\tau_K = \frac{A\sigma(1-\alpha)(A-\rho) - [(1-\alpha)(A-\rho)(n\sigma + A-\rho)]}{A\sigma(1-\alpha)(A-\rho) + A\sigma^2\alpha(A-n)]} \leq 1$$

APPENDIX 2

Proof of Proposition 2.

The first order conditions are

$$\frac{dH}{dc} = 0 \Rightarrow \alpha c^{\alpha(1-\sigma)-1}(1-\tau_s)^{(1-\alpha)(1-\sigma)} B^{(1-\alpha)(1-\sigma)} h^{(1-\alpha)(1-\sigma)} = \theta_1 \quad \text{A2.1.}$$

$$\frac{dH}{d\tau_s} = 0 \Rightarrow N(t)c^{\alpha(1-\sigma)} B^{(1-\alpha)(1-\sigma)} h^{(1-\alpha)(1-\sigma)}(1-\alpha)(1-\tau_s)^{(1-\alpha)(1-\sigma)-1} = \theta_2 Bh\eta \quad \text{A2.2.}$$

$$\frac{\dot{\theta}_1}{\theta_1} = (\rho - A) \quad \text{A2.3}$$

$$\frac{\dot{\theta}_2}{\theta_2} = \rho - B\eta \quad \text{A2.4}$$

From A2.1 we have

$$\frac{\dot{\theta}_1}{\theta_1} = \left\{\alpha(1-\sigma)-1\right\}\gamma_c + (1-\sigma)(1-\alpha)B\eta\tau_s \quad \text{A2.5.}$$

Comparing A2.3 and A2.5

$$\rho - A = -\{1-\alpha(1-\sigma)\}\gamma_c + (1-\sigma)(1-\alpha)B\eta\tau_s$$

$$\text{or } \gamma_c = \frac{(1-\sigma)(1-\alpha)B\eta\tau_s + A - \rho}{\{1-\alpha(1-\sigma)\}} \quad \text{A2.6.}$$

From A2.2 we have

$$\{(1-\alpha)(1-\sigma)-1\}\gamma_h + \alpha(1-\sigma)\gamma_c + n = \frac{\dot{\theta}_2}{\theta_2} \quad \text{A2.7}$$

Comparing A2.4 and A2.7 we have

$$\{(1-\alpha)(1-\sigma)-1\}\gamma_h+\alpha(1-\sigma)\gamma_c+n=\rho-B\eta$$

Substituting the value of $\gamma_h=B\eta\tau_s$ andthat of γ_c from A2.6, we have

$$\{(1-\alpha)(1-\sigma)-1\}\eta\tau_s B+\alpha(1-\sigma)[\frac{(1-\sigma)(1-\alpha)B\eta\tau_s-\rho+A}{\{1-\alpha(1-\sigma)\}}]+n=\rho-B\eta \qquad \text{A2.8}$$

orsolving τ_s in terms of parameters:

$$\tau_s=\frac{\{1-\alpha(1-\sigma)\}(n+B\eta)+A\alpha(1-\sigma)-\rho}{B\eta\sigma} \qquad \text{A2.9.}$$

The optimal tax rate will lie between 0 and 1 if the following condition is satisfied.

$$(n+B\eta)[1-\alpha(1-\sigma)]+A\alpha(1-\sigma)-B\eta\sigma<\rho<\{1-\alpha(1-\sigma)\}(n+B\eta)+A\alpha(1-\sigma)$$

and $\gamma_h=B\eta\tau_s=\dfrac{\alpha(1-\sigma)[A-n-B\eta]+(n+B\eta-\rho)}{\sigma}$ A2.10.

From A2.6

$$\gamma_c=\frac{[(1-\alpha)(1-\sigma)(n+B\eta)-\rho]}{\sigma}+A\frac{[\sigma+\alpha(1-\alpha)(1-\sigma)^2]}{\sigma\{1-\alpha(1-\sigma)\}} \qquad \text{A2.11.}$$

From $\dot{K}=y_c-Nc$

$$\gamma_K=\gamma_c+n \qquad \text{A2.12.}$$

APPENDIX 3

Extended Model when both sectors are taxed:

$$u(c)=\int_0^{\infty}\frac{(c^{\alpha}s^{1-\alpha})^{1-\sigma}-1}{(1-\sigma)}e^{-\rho t}N(t)dt \tag{A3.1}$$

$$y_c = AK \tag{A3.2}$$

$$\mathrm{y_s} = \mathrm{B(Nh)} \tag{A3.3}$$

$$N(t) = N_0 e^{nt} \tag{A3.4}$$

$$\dot{h}=\eta\frac{(\phi G)}{N} \tag{A3.5}$$

$$G=T=\tau_K y_c + p_s\tau_s y_s \tag{A3.6}$$

From the market clearing condition

$$s=(1-\tau_s)Bh \tag{A3.7}$$

theinvestment function is asfollows:

$$\dot{K}=(1-\tau_K)y_c+(1-\phi)G-Nc \tag{A3.8}$$

From the consumer's equilibrium condition, the value of p_s is solved:

$$\frac{p_c}{p_s}=\frac{MU_c}{MU_s}=\frac{\alpha c^{\alpha(1-\sigma)-1}s^{(1-\alpha)(1-\sigma)}}{(1-\alpha)c^{\alpha(1-\sigma)}s^{(1-\alpha)(1-\sigma)-1}} \tag{A3.9}$$

It is assumed that the value of

$$p_c = 1$$

Therefore $p_s = \frac{(1-\alpha)}{\alpha}\frac{c}{(1-\tau_s)Bh}$ (A3.10)

The current value Hamiltonian function can be formulated as

$$H = N(t)[\frac{c^{\alpha(1-\sigma)}B^{(1-\alpha)(1-\sigma)}h^{(1-\alpha)(1-\sigma)}(1-\tau_s)^{(1-\alpha)(1-\sigma)}-1}{(1-\sigma)}] + \theta_1[(1-\tau_K)AK + (1-\phi)\tau_K AK + \tau_s\frac{(1-\alpha)}{\alpha}\frac{(1-\phi)cN}{(1-\tau_s)} - cN] + \theta_2\eta\frac{\phi}{N}(\tau_K AK + \tau_s\frac{(1-\alpha)}{\alpha}\frac{cN}{(1-\tau_s)}) \quad \text{(A3.11)}$$

The control variables are c, τ_K, τ_s and the state variables are K, h.

From the first order conditions of the control variables we get

$$\frac{dH}{dc} = 0$$

or $\alpha N c^{\alpha(1-\sigma)-1}B^{(1-\alpha)(1-\sigma)}h^{(1-\alpha)(1-\sigma)}(1-\tau_s)^{(1-\alpha)(1-\sigma)} + \theta_1\tau_s N\frac{(1-\alpha)}{\alpha}\frac{(1-\phi)}{(1-\tau_s)} + \theta_2\eta\phi\tau_s\frac{(1-\alpha)}{\alpha(1-\tau_s)} = \theta_1 N$ (A3.12)

$$\frac{dH}{d\tau_K} = 0$$

or $\theta_2\eta = \theta_1 N$ (A3.13)

Taking the logarithm of both sides and differentiating with respect to time,

$$\frac{\dot{\theta}_1}{\theta_1} + n = \frac{\dot{\theta}_2}{\theta_2} \quad \text{(A3.14)}$$

From $\frac{dH}{d\tau_s} = 0$

andsubstituting the value of θ_2 into the equation from equation (A3.13)

$$\alpha(1-\tau_s)^{(1-\alpha)(1-\sigma)+1}c^{\alpha(1-\sigma)-1}B^{(1-\alpha)(1-\sigma)}h^{((1-\alpha)(1-\sigma)} = \theta_1 \quad \text{(A3.15)}$$

Taking the logarithm of both sides and differentiating with respect to time,

$$\{\alpha(1-\sigma)-1\}\gamma_c + (1-\sigma)(1-\alpha)\gamma_h = -\frac{\dot{\theta}_1}{\theta_1} \tag{A3.16}$$

The co-state equation of the state variable *K* is

$$\dot{\theta}_1 = \rho\theta_1 - \frac{dH}{dK} \tag{A3.17}$$

Now $\frac{dH}{dK} = \theta_1(1-\tau_K)A + \theta_1(1-\phi)\tau_K A + \theta_2\eta\frac{\phi}{N}\tau_K A$ (A3.18)

Substituting this value from (A3.18) into equation (A3.17)

$$\dot{\theta}_1 = \theta_1(\rho - A)$$

or $\frac{\dot{\theta}_1}{\theta_1} = (\rho - A)$ (A3.19)

The other co-state equation is

$$\dot{\theta}_2 = \rho\theta_2 - \frac{dH}{dh} \tag{A3.20}$$

Now $\frac{dH}{dh} = Nc^{\alpha(1-\sigma)}(1-\tau_s)^{(1-\alpha)(1-\sigma)}B^{(1-\alpha)(1-\sigma)}(1-\alpha)h^{(1-\alpha)(1-\sigma)-1}$

$$\dot{\theta}_2 = \rho\theta_2 - \frac{dH}{dh}$$

or $\frac{\dot{\theta}_2}{\theta_2} = \rho - \frac{N(t)c^{\alpha(1-\sigma)}(1-\tau_s)^{(1-\alpha)(1-\sigma)}B^{(1-\alpha)(1-\sigma)}(1-\alpha)h^{(1-\alpha)(1-\sigma)-1}}{\theta_2}$ (A3.21)

Substituting the value of θ_2 from equation (A3.13) into equation (A3.15)

$$\frac{\dot{\theta}_2}{\theta_2} = \rho - \frac{\eta}{(1-\tau_s)\alpha}\left(\frac{c}{h}\right)(1-\alpha) \tag{A3.21.A}$$

From the human capital accumulation function we get

$$\gamma_h = \frac{\dot{h}}{h} = \eta\phi\tau_K Ak + \frac{\tau_s}{(1-\tau_s)}\frac{(1-\alpha)}{\alpha}\left(\frac{c}{h}\right) \tag{A3.22}$$

Proof of Proposition 5:

From equations (A3.14) and (A3.19) we get

$$\frac{\dot{\theta}_2}{\theta_2} = (\rho - A + n) \tag{A3.23}$$

Equating equation (A3.21.A) with(A3.23) we get

$$(\frac{c}{h}) = \frac{(A-n)(1-\tau_s)\alpha}{\eta(1-\alpha)} \tag{A3.24}$$

From equation (A3.24) it is clear that as $(\frac{c}{h})$ is constant, $\gamma_c = \gamma_h$

From equation (A3.16) and (A3.19) we get

$$\{\alpha(1-\sigma)-1\}\gamma_c + (1-\sigma)(1-\alpha)\gamma_h = (A-\rho)$$

or $\gamma_c[\{1-\alpha(1-\sigma)\}-(1-\alpha)(1-\sigma)] = (A-\rho)$

or $\gamma_c = \dfrac{(A-\rho)}{\sigma}$ (A3.25)

From equation (A3.12) and using equations (A3.13) and equation (A3.15) we obtain

$$\frac{\tau_s}{(1-\tau_s)\alpha} = 0 \text{ implying } \tau_s = 0$$

The growth rate of physical capital is

$$\gamma_K = (1-\tau_K)\frac{y_c}{K} + (1-\phi)\frac{G}{K} - \frac{cN}{K}$$

After simplification we get

$$\gamma_K = A(1-\phi\tau_K) + (\frac{c}{kh}) \qquad \text{(A3.26)}$$

Where $k = \frac{K}{Nh}$ in the steady state, γ_K is constant so $(\frac{c}{kh})$ should be constant.

We have already found that $\frac{c}{h}$ is constant.Therefore, k is constant.

Hence,

$$\gamma_K = n + \gamma_h = \frac{(A-\rho+n\sigma)}{\sigma} \qquad \text{(A3.27)}$$

Again from equation (A3.25) we get

$$\gamma_c = \gamma_h = \frac{(A-\rho)}{\sigma}$$

andfrom equation (A3.22)

$$\gamma_h = \eta\phi\tau_K Ak + \frac{\tau_s}{(1-\tau_s)}\frac{(1-\alpha)}{\alpha}(\frac{c}{h})$$

Since $\tau_s = 0$, therefore

$$\frac{(A-\rho)}{\sigma} = \eta\phi\tau_K Ak$$

Hence, $k = \frac{(A-\rho)}{\sigma\eta\phi A\tau_K}$ (A3.28)

Equating the value of γ_K from (A3.26) and (A3.27) and using (A3.24) and (A3.28) we obtain

the value of $\tau_K = \frac{\{(A-\rho)-\sigma(A-n)\}(1-\alpha)(A-\rho)}{\sigma[(1-\phi-A)(1-\alpha)(A-\rho)-(A-n)\alpha\sigma\phi A]}$ (A3.29)

Article

Service Good as an Intermediate Input and Optimal Government Policy in an Endogenous Growth Model

South Asian Journal of Macroeconomics and Public Finance
8(1) 57–91, 2019

DOI: 10.1177/2277978719837043
journals.sagepub.com/home/smp

Senjuti Gupta[1]
Bidisha Chakraborty[2]
Tanmoyee Banerjee (Chatterjee)[2]

Abstract

The present article considers an endogenous growth model in which the service output is used as intermediate good in commodity sector, tax is imposed on manufacturing product and the revenue earned is invested to create human capital. It is shown that there exists a unique, saddle path stable steady-state growth rate of human capital accumulation and a unique growth-maximizing tax rate. The optimal tax rate for the command economy is compared with growth-maximizing tax rate in competitive economy. A numerical analysis shows that the command economy will have a higher growth rate than the competitive economy. An extension of the model where households privately spend for accumulation of human capital yields the same growth rate as that of the command economy of the previous model.

[1] Department of Economics, Government Girls' General Degree College, Kolkata, West Bengal, India.
[2] Department of Economics, Jadavpur University, Kolkata, West Bengal, India.

Corresponding author:
Bidisha Chakraborty, Department of Economics, Jadavpur University, 188, Raja S.C. Mallick Road, Kolkata, West Bengal 700032, India.
E-mail: bidisha.chakraborty@gmail.com

Keywords

Intermediate good, endogenous growth, competitive economy, command economy, human capital accumulation

JEL Classification: E6, H2, O4

Introduction

The last few decades have experienced a rapid growth in the service sector, which has been reflected in an upward trend in the usage of service goods as consumption good as well as producer good (as intermediate input in production). The present study focuses on the service good as a producer good. According to Ishikawa (1992), producer services that have expanded with economic growth include business and professional services (such as management consulting, engineering consulting and data processing), financial and insurance services and real estate services. Banga and Goldar (2007) observed that in case of India, contribution of services input to output and productivity growth in manufacturing (organized) has increased substantially in the 1990s. Francois and Woerz (2008) pointed out that the importance of services in production as input rises with the level of development of an economy specially after the information technology revolution. Further, using a cross-country panel data analysis, they have found the evidence that the producer services (business services/communication services/financial services/insurance services/transportation services) are significantly present in the production of food, textile, leather, clothing, wood, paper, coke, chemicals, machinery, motor vehicles and electrical equipment. Das and Saha (2015) also showed that in the USA, the UK and Japan, the share of pure business services in the services sector as a whole has nearly or more than doubled in a span of over three decades 1970–2006. Behuria and Khullar (1994) documented the role of intermediate services in economic development in the context of Malaysia. They have observed that services are increasingly used as an input of production in various sectors. Thus, there are many empirical evidences showing the increasing importance of producer services in the production process of different goods.

Ishikawa (1992) theoretically developed a model where producer service is used as an intermediate good to the manufacturing sector, while service is produced using labour alone with constant returns to scale (CRS) technology. Ishikawa (1992) worked on a simple dynamic small open economy model, which allows for changes in both industrial structure and trade patterns during the process of economic growth. In this article, he has considered three sectors: manufacturing, agriculture and producer service, where producer service is an intermediate good in the manufacturing sector. In this model, learning by doing in the service sector is the source of endogenous growth, and whether the economy will flourish or not depends on the initial productivity of labour in the producer service sector. Thus, the producer service sectors play a crucial role in the model. Another theoretical model by Das and Saha (2015) also considers service as an intermediate input to explain the fast growth of service sector, which is sometimes greater than the manufacturing sector also. The article develops a two-sector closed economy model with manufacturing and service sectors. The analysis focuses on business services, while household services are also considered. The manufacturing output is produced with human capital and business service, and the service output solely depends on the human capital. It is argued that differences in returns to scale between the two sectors and employment frictions in manufacturing explain why the growth rate of the service sector may be higher. The model also features that within the service sector, the business services sub-sector may grow faster than the household services. The producer services are human capital intensive. As a result, contribution of education towards economic growth has gradually increased in recent years. Bosworth, Collins, and Virmani (2006) showed that in case of India, service sector has registered the largest improvements in the educational attainment of its workforce.[1]

Given the importance of the service good as an input to manufacturing sector, the present study hypothetically considers a two-sector endogenous growth model where service output is used as an input in the commodity manufacturing sector.[2] We consider human capital as one of the most important factors in producing service output.[3] We first assume

[1] The papers by Riley (2014), Lucas (1988), Mankiw, Romer, and Weil (1992), Fuente and Doménech, (2006), and so on discuss various issues related to human capital and service goods.

[2] As already mentioned, Francois and Woerz (2008) found a number of evidence that pointed towards using service good as an input in various industries. Apart from that, we can consider a simple dressmaker who uses sewing machine and tailoring services for production purpose. Alternatively, the fully automated electricity plants use machineries and engineering services to generate electricity.

[3] The papers by Moro (2007), Sekar, Delgado, and Ulu (2015), Barua and Pant (2014), Imbruno (2014), Miroudot, Lanz, and Ragoussis (2009), Psarianos (2002), and so on have discussed the matters related to various aspects of intermediate goods other than service good in the context of closed or open economies.

public education system, and hence, human capital is generated through government expenditure on education. This model is considered as the basic model in our article. In addition, the article develops the command economy version of the basic model to consider the issues of optimal taxation in the presence of producer services. Finally, we build up another model where household allocates a fraction of their income for human capital investment. This version of the model does not incorporate government sector like the other version. This analysis helps us to compare the features of growth process of the competitive economy under government intervention vis-à-vis the case where government does not interfere.

Contribution of this article is to incorporate public education system for human capital formation when human capital is used to generate producer services.[4] The article contributes to existing literature by considering the issue of optimal taxation in the presence of producer services in the endogenous growth model. After the emergence of goods and service tax, many countries, such as Canada, France, the UK, New Zealand, Malaysia, Singapore, India and many more, are still struggling to rationalize the tax rate structure. A comparison of tax rates by countries is difficult as tax laws in most countries are extremely complex, and the tax burden falls differently on different groups in each country and subnational unit. Different tax rates are levied on goods and services in different countries. Thus, the article contributes to the literature by finding out optimal and growth-maximizing tax policy in the competitive and command economy where service sector output is used as an input in the manufacturing sector. Given the present scenario of service-led growth, our article contributes to the literature by linking the issue of public expenditure-led education to the issue of service sector's contribution to economic growth. Next, we compare this to the situation where human capital formation is undertaken privately by the households in the presence of producer services. To best of our knowledge, we did not come across any paper that has done this exercise.

[4] The spending of government expenditure on public resources, through taxation to create both human capital and physical capital, in endogenous growth models has also been analysed in various studies, such as by Garcia-Castrillo and Sanso (2000), Gomez (2003), Futagami, Morita, and Shibata (1993), Faig (1995), Dasgupta (1999), Fernández, Novales, and Ruiz (2004), Woo (2005), Tsoukis and Miller (2003), Chen and Lee (2007), Hollanders and Weel (1999), Greiner (2006), and so on. However, these models did not include the issue of service good as an intermediate product.

We find some interesting results. The results show that under competitive economy framework, in the basic model where government imposes tax on commodity sector to finance human capital accumulation that is used in the production of producer service, the growth rate depends on the rate of taxation, and a unique growth rate maximizing tax rate will exist. This growth rate is saddle path stable. However, the existence of tax on commodity in the competitive market is creating a distortion in the model. Further, a numerical analysis shows that the command economy will have a higher growth rate than the competitive economy. The first best solution is obtained when households privately spend for accumulation of human capital. The command economy growth rate, after endogenizing the tax rate, is found to be the same as the first best solution.

The rest of the article is organized as follows: in the second section, the basic model is presented; in sub-section 'Households, Firms and Government' assumptions of the model are described. Sub-section 'Decentralized Economy: The Basic Model' presents the basic model in competitive economy framework. Sub-section 'Command Economy: The Basic Model' presents the command economy version of the basic model. The third section presents an extension where households privately invest for human capital formation. The comparison of tax rates for basic model under competitive and command economy framework is done with a numerical analysis in the fourth section. Finally, the fifth section concludes the article.

Basic Model

This section discusses the basic assumptions of the model and derives the growth path under competitive and command regime.

Households, Firms and Government

This article considers a hypothetical closed economy model with two sectors, namely commodity sector and service sector. The service sector produces producer service, which is exclusively used as an intermediate input in producing commodity output. The total labour force is homogeneous as far as skill is concerned. Identical rational agents inhabit the economy. Production technology is subject to CRS. The household sector chooses the path of per capita consumption of commodity output by maximizing the present discounted value of utility over the infinite time horizon, ρ being the discount rate and σ being the elasticity of marginal utility; inverse of σ is known as inter-temporal elasticity of substitution. N represents the total labour force or working population. Preferences over consumption are given by the following function where 'c' denotes flow of real per capita consumption of commodity output:

$$u(c) = \int_0^{\infty} \frac{(c^{1-\sigma} - 1)}{(1-\sigma)} e^{-\rho t} N(t)\, dt \tag{1}$$

Here, we assume that the output in the commodity sector can be used for consumption or investment purposes. The commodity output is produced using physical capital and producer service good. The producer service output is a function of human capital and physical capital. Both the production functions are Cobb–Douglas type. Here 'K' stands for the level of physical capital. Let α and β be the commodity output elasticity of physical capital and service output elasticity of skilled labour, respectively. The commodity and service output production functions can be written as:

$$Y_C = A\{(1-\varphi)K\}^{\alpha} Y_s^{1-\alpha} \tag{2}$$

$$Y_s = B(Nh)^{\beta}(\varphi K)^{1-\beta} \tag{3}$$

where Y_c and Y_s are the flow of commodity output and service output, respectively. It is obvious that $(1 - \alpha)$ measures the commodity output elasticity of service product. Similarly, $(1 - \beta)$ measures the service output elasticity of physical capital. The level of population is growing at an exponential rate in the following manner:

$$N(t) = N_0 e^{nt} \tag{4}$$

where N_0 is the population size at initial time period. It is assumed that the initial amount of population $N_0 = 1$. Further, we assume that the general skill level of a worker is h. Skill is accumulated through education. The aggregate effective skilled labour input in commodity production is Nh. Let φ be the fraction of physical capital that is allocated to the service sector. The remaining $(1-\varphi)$ fraction is engaged in producing commodity output. In the present section, it is assumed that government spends money on working population to create human capital. We did not assume any allocation of time between production and skill accumulation by the skilled individual. Hence, in this model, an individual simultaneously works and accumulates skill. Skill accumulation may be assumed to take place through government sponsored on job training of workers or apprenticeship programmes.

Following Beauchemin (2001), Cardak (2004), Tanaka (2003), Glomm and Ravikumar (2001), we assume per capita government expenditure as an input in the production process of human capital in the basic model. The findings by Blankenau, Simpson, and Tomljanovich (2007) based on pooled data from 1960 to 2000 for 80 countries support a positive relationship between public education expenditure and human capital formation in developed countries. In most of the developing countries too, governments play key roles in fostering education through providing free primary education, highly subsidized secondary education, research funding and student financial assistance. Because of the 'non-rival' nature of the skill, it is assumed that there is no diminishing return to G in skill accumulation.

The human capital accumulation can be written as:

$$\dot{h} = \eta \frac{G}{N} \tag{5}$$

Here, η is the technology parameter of human capital accumulation and G is the government expenditure on education. It is further assumed that only the commodity sector is being taxed. Let the tax rate be τ which is levied on per unit of commodity output. Even in the study of Futagami et al. (1993), the accumulation rate of public capital is proportional to the tax revenue or equivalently government expenditure.[5]

The balanced budget equation can be written as follows:

$$\mathrm{G} = \mathrm{T} = \tau \mathrm{Y}_C \tag{6}$$

A part of disposable income is consumed, and the rest is invested to form physical capital. Hence, the physical capital accumulation function is given by

$$\dot{K} = (1-\tau)\, Y_C - cN = (1-\tau)(rK + wNh) - cN \tag{7}$$

[5] If instead of assuming direct government expenditure as an input in human capital accumulation, we assume that government expenditure is used to finance the wage rate of the specialized labour (teachers) used to generate human capital, endogenous growth rate is obtained, but growth maximizing tax rate cannot be found out.

In the decentralized economy, the households own all capital. It can be easily verified that $Y_C = rK + wNh$.[6] The final product is produced by a representative firm that maximizes profit. The objective of the economy is to maximize the present discounted value of utility over the infinite time horizon defined by Equation (1) subject to the wealth accumulation constraint. The next section presents the competitive economy equilibrium.

Decentralized Economy: The Basic Model

The objective of an individual consumer is to maximize present discounted value of utility over the time horizon choosing the consumption path. The current value Hamiltonian for this particular problem is given as follows:

$$H = \frac{c^{1-\sigma}-1}{(1-\sigma)}N(t) + \theta[(1-\tau)(rK + wNh) - cN] \tag{8}$$

In competitive economy, a representative household chooses c, the flow of consumption. So, c is the decision variable, K is a state variable and θ is the shadow price of physical capital. While solving this Hamiltonian function, tax rate τ is considered to be given as per the decentralized regime.

The first-order optimality conditions for maximization of Hamiltonian is given by

$$c^{-\sigma} = \theta \tag{9}$$

The equation of motion of co-state variable is given by

$$\frac{\dot{\theta}}{\theta} = \rho - (1-\tau)r \tag{10}$$

The profit of the producers for the commodity sector and service is:

$$\pi_c = p_c Y_C - r(1-\varphi)K - p_s Y_s \tag{11}$$

$$\pi_s = p_s Y_s - (r\varphi K) - (wNh) \tag{12}$$

[6] For proof, see Appendix A.

Here, r is the rate of interest, w is the real wage rate and p_s is the per unit price of service output. It is assumed that the commodity output is numeraire commodity, which implies that per unit price of commodity output, p_c, is unity.

Both the output and the factor markets are characterized by perfect competition. Hence, equating the value of the marginal product of each factor input to its return and using profit maximization condition, we get the following expressions:

From profit maximization of final consumption good sector

$$r = A\alpha((1-\varphi)K)^{\alpha-1}Y_s^{1-\alpha} \tag{13a}$$

$$p_s = A((1-\varphi)K)^{\alpha}(1-\alpha)Y_s^{-\alpha} \tag{14}$$

From profit maximization of producer service sector

$$r = p_s B(hN)^{\beta}(1-\beta)(\phi K)^{-\beta} \tag{13b}$$

which equivalently in intensive form is

$$r = \alpha A(1-\hat{\varphi})^{\alpha-1}B^{1-\alpha}\hat{\varphi}^{(1-\beta)(1-\alpha)}k^{-\beta(1-\alpha)} \tag{13c}$$

$$p_s = A((1-\varphi)K)^{\alpha}(1-\alpha)Y_s^{-\alpha} = AB^{-\alpha}(1-\phi)^{\alpha}(1-\alpha)\phi^{\alpha(\beta-1)}k^{\alpha\beta}$$

$$w = p_s B\beta(Nh)^{\beta-1}(\phi K)^{1-\beta} = p_s B\beta(\phi k)^{1-\beta} \tag{15}$$

Here k denotes the physical capital per unit of skill and is defined by $k = \frac{K}{hN}$. From the aforementioned system of equations using no arbitrage condition and equating (13a) and (13b), the value of φ is found as follows:

$$\hat{\varphi} = \frac{(1-\alpha)(1-\beta)}{1-\beta(1-\alpha)} \tag{16}$$

The steady-state growth paths in market economy is defined as the path along which c, h, K grow at constant rate, and the value of φ is time-independent. The growth rate of human capital accumulation and that of per unit commodity output consumption and the growth rate of physical capital are given by

$$\gamma_h^{comp} = \eta\tau A\{(1-\hat{\varphi})\}^{\alpha} B^{1-\alpha}(\hat{\varphi})^{(1-\beta)(1-\alpha)} k^{1-\beta(1-\alpha)} \tag{17}$$

$$\gamma_c^{comp} = \frac{(1-\tau)\alpha A(1-\hat{\varphi})^{\alpha-1} B^{1-\alpha}\hat{\varphi}^{(1-\beta)(1-\alpha)} k^{-\beta(1-\alpha)} - \rho}{\sigma}$$
$$= \frac{(1-\tau)r-\rho}{\sigma} \tag{18}$$

$$\gamma_K^{comp} = n + \gamma_h^{comp} \tag{19}$$

where γ_x stands for growth rate of the variable x.

Along the steady state, $\gamma_c = \gamma_h$. Equating γ_c, γ_h from Equations (17) and (18), the following equation is obtained in terms of k, τ and other parameters. τ is considered to be given in the competitive economy.

$$\sigma\eta\tau A\{(1-\hat{\varphi})\}^{\alpha} B^{1-\alpha}(\hat{\varphi})^{(1-\beta)(1-\alpha)} k^{1-\beta(1-\alpha)} + \rho = (1-\tau)\alpha A(1-\hat{\varphi})^{\alpha-1} B^{1-\alpha}\hat{\varphi}^{(1-\beta)(1-\alpha)} k^{-\beta(1-\alpha)} \tag{20}$$

Let $f(k)$ = *L.H.S* of Equation (20), where $f' > 0$. $f(k)$ is depicted by *I–J* curve in Figure 1. $g(k)$ = *R.H.S* of Equation (20), where $g' < 0$. $g(k)$ is depicted by *LM* in Figure 1.

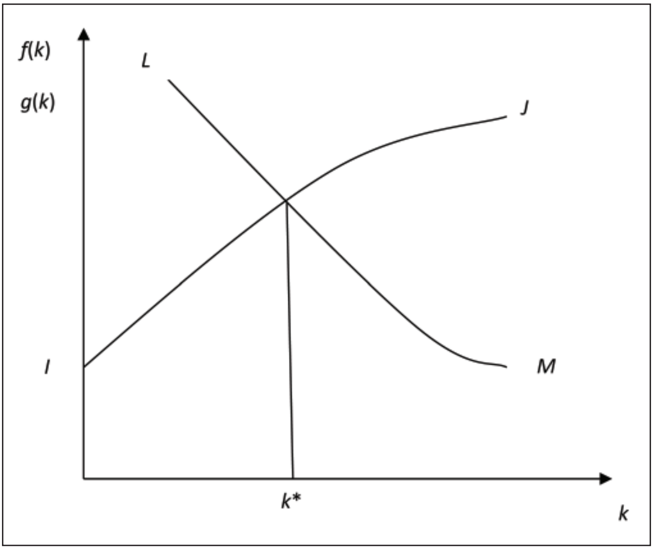

Figure 1. Determination of Equilibrium k^* in Decentralized Economy

Source: The authors.

Diagrammatically, it is shown that there exists unique value of k that satisfies Equation (20) and that can be found out in terms of τ and other parameters.

In Figure 1, *LM* and *IJ* represent $g(k)$ and $f(k)$ functions from Equation (20), respectively. The equilibrium value of k is given by k^* in the figure.

In Figure 1, k^* is the equilibrium value for k in competitive economy. Hence, there exists a unique solution of k, given tax rate τ in competitive framework. Consequently, the growth rates of human capital, commodity output and that of physical capital can be solved endogenously.

Proposition 1: *There exists positive, unique steady-state growth rate for human capital, physical capital and production and consumption of commodity output in competitive economy.*

It is found that

$$\frac{dk}{d\tau} = -\frac{[\alpha + \sigma\eta k]}{[\sigma\eta\tau(1-\beta(1-\alpha)) + (1-\tau)\alpha\beta(1-\alpha)k^{-1}]} < 0 \tag{21}$$

Thus, with an increase in the tax rate, the ratio of physical capital to human capital decreases. An increased tax rate implies enhanced government expenditure for human capital accumulation, and human capital grows more rapidly. On the other hand, as the tax is imposed on commodity output, it hampers physical capital accumulation. Thus, increased tax rate implies lower growth of production and consumption of commodity. As a result, the value of physical capital that is allocated per head human capital, that is, k falls for an increase in τ.

Differentiating Equations (17) and (18) with respect to tax rate gives the following results:

$$\frac{\partial\gamma_h}{\partial\tau} = \frac{\eta A\{(1-\hat{\varphi})^{\alpha} B^{1-\alpha}(\hat{\varphi})^{(1-\beta)(1-\alpha)}\} k^{(1-\beta(1-\alpha))}(\beta(1-\alpha)-\tau)}{[\sigma\eta\tau(1-\beta(1-\alpha))k + (1-\tau)\alpha\beta(1-\alpha)]} \tag{22}$$

$$\frac{\partial\gamma_c}{\partial\tau} = \frac{\alpha A\{(1-\hat{\varphi})\}^{\alpha-1} B^{1-\alpha}(\hat{\varphi})^{(1-\beta)(1-\alpha)}\} k^{(1-\beta(1-\alpha))}\eta(\beta(1-\alpha)-\tau)}{[\sigma\eta\tau(1-\beta(1-\alpha))k + (1-\tau)\alpha\beta(1-\alpha)]} \tag{23}$$

From the aforementioned equation, we find that the relationship with growth rates and τ will depend on the tax rate. Further, the growth rates are maximized for the tax rate $\tau^* = \beta(1-\alpha)$.[7] This tax rate is

[7] Second-order conditions for maximization are checked and satisfied.

equal to indirect elasticity of human capital in the production of final consumption good.

Proposition 2: *There exists a unique growth-maximizing tax rate for the competitive economy.*

It is also found that

$$\frac{dk}{d\eta} = -\frac{\sigma\tau k}{[\sigma\eta\tau(1-\beta(1-\alpha)) + (1-\tau)\alpha\beta(1-\alpha)k^{-1}]} < 0 \quad (24)$$

From Equation (18), we see that γ_c is negatively related to k. Since k is negatively related to η, the steady-state growth rate of consumption is positively related to η. As the technological efficiency of education sector increases, per capita physical capital–human capital ratio in steady state decreases, but the growth rate of consumption, human capital and aggregate physical capital increases. This is obvious because as education sector becomes more efficient, it can generate more human capital. Hence, the ratio of per capita physical capital to human capital declines.

A rise in technological efficiency of education sector will boost up the growth of human capital. This will in turn raise the service output; as a result, commodity output will also experience a rise in growth rate.

Stability Analysis of the Basic Model

Dividing both sides of Equation (7) by K, we get

$$\gamma_K = \frac{\dot{K}}{K} = (1-\tau)(\frac{y_c}{K}) - \frac{cN}{K}$$

Using Equations (2), (3) and definition of $k = \frac{K}{hN}$, we have

$$\frac{\dot{K}}{K} = B^{(1-\alpha)}(1-\tau)A(1-\varphi)^{\alpha}k^{-\beta(1-\alpha)}\varphi^{(1-\alpha)(1-\beta)} - (\frac{c}{kh})$$

Let $(\frac{c}{h}) = x$

Using Equations (2), (3), (5) and (6), we derive

$$\gamma_h = \frac{\dot{h}}{h} = \eta A\tau(1-\varphi)^{\alpha}B^{(1-\alpha)}\varphi^{(1-\beta)(1-\alpha)}k^{1-\beta(1-\alpha)}$$

Now, $\frac{\dot{k}}{k} = \frac{\dot{K}}{K} - \frac{\dot{h}}{h} - n$

Hence,

$$\dot{k} = B^{(1-\alpha)}(1-\tau)A(1-\varphi)^{\alpha}k^{1-\beta(1-\alpha)}\varphi^{(1-\alpha)(1-\beta)} - (\frac{c}{h}) - \eta A\tau(1-\varphi)^{\alpha}B^{(1-\alpha)}\varphi^{(1-\beta)(1-\alpha)}k^{2-\beta(1-\alpha)} - nk \tag{25}$$

From Equation (18), we have

$$\dot{c} = \frac{c}{\sigma}[(1-\tau)A\alpha(1-\varphi)^{\alpha-1}B^{1-\alpha}k^{-\beta(1-\alpha)}\varphi^{(1-\beta)(1-\alpha)} - \rho] \tag{26}$$

As $(\frac{c}{h}) = x$

$$\frac{\dot{c}}{c} - \frac{\dot{h}}{h} = \frac{\dot{x}}{x}$$

Therefore, the system of dynamic equation of the present model is as follows:

$$\dot{x} = x[\{\frac{(1-\tau)\alpha A(1-\varphi)^{\alpha-1}B^{1-\alpha}\varphi^{(1-\beta)(1-\alpha)}k^{-\beta(1-\alpha)} - \rho}{\sigma}\} - \eta A\tau(1-\varphi)^{\alpha}B^{(1-\alpha)}\varphi^{(1-\beta)(1-\alpha)}k^{1-\beta(1-\alpha)}] \tag{27}$$

$$\dot{k} = AB^{(1-\alpha)}(1-\tau)(1-\varphi)^{\alpha}k^{1-\beta(1-\alpha)}\varphi^{(1-\alpha)(1-\beta)} - x - \eta A\tau(1-\varphi)^{\alpha}B^{(1-\alpha)}\varphi^{(1-\beta)(1-\alpha)}k^{2-\beta(1-\alpha)} - nk \tag{28}$$

If profit-maximizing conditions and no arbitrage conditions are assumed to be satisfied at every point of time, φ is always a constant. We are not getting any dynamics of φ.

At steady state, $\dot{k} = 0$. Hence, from Equation (28), we get

$$x = AB^{(1-\alpha)}(1-\tau)(1-\varphi)^{\alpha}k^{1-\beta(1-\alpha)}\varphi^{(1-\alpha)(1-\beta)} - \eta A\tau(1-\varphi)^{\alpha}B^{(1-\alpha)}\varphi^{(1-\beta)(1-\alpha)}k^{2-\beta(1-\alpha)} - nk \tag{29}$$

Now, $\frac{dx}{dk} = 0$ at $k = \hat{k}$ and $\frac{d^2x}{dk^2} < 0$. Hence, x curve given by Equation (29) is maximized at $k = \hat{k}$. In Equation (27), setting $\dot{x} = 0$, we get a fixed value of $k = k^*$.We can represent $\dot{x} = 0$ and $\dot{k} = 0$ curves in x–k plane and graphically illustrate the transitional dynamics.

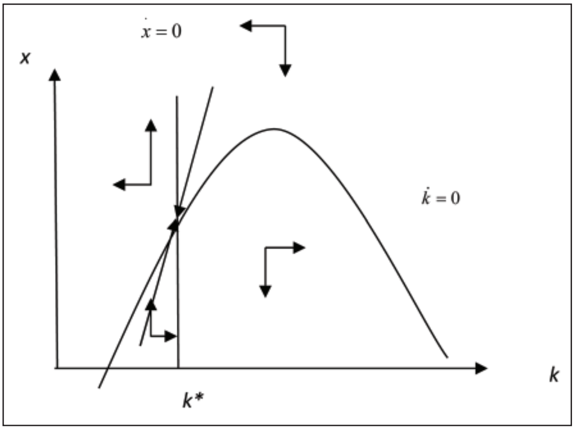

Figure 2. Stability Analysis of the Basic Model

Source: The authors.

From the above figure, we observe that like the Ramsey model, the steady state obtained in this model is saddle path stable.

Proposition 3: *The equilibrium growth rate is saddle path stable.*

Command Economy: The Basic Model

In this section, we discuss the same problem in command economy set up. There are no external effects and imperfect competition in this model. But, in the competitive economy, individual considers tax rate as given, and thus, individual agents consider human capital accumulation function as given while maximizing the present discounted value of utility. In the command economy, the social planner takes into account the human capital accumulation function while optimizing the welfare of the society, deciding tax rate and allocating resources optimally. The objective of the social planner is to maximize the present discounted value of utility defined by Equation (1) subject to the constraints given by Equations (5)–(7). The Hamiltonian function is given by the following equation:

$$H = \frac{N}{(1-\sigma)}(c^{1-\sigma} - 1) + \theta_1[(1-\tau)A\{(1-\varphi)K\}^{\alpha}B^{1-\alpha}(Nh)^{\beta(1-\alpha_1)}$$
$$(\varphi K)^{(1-\beta)(1-\alpha)} - cN] + \theta_2[\eta\frac{\tau}{N}A\{(1-\varphi)K\}^{\alpha}B^{1-\alpha}(Nh)^{\beta(1-\alpha)}$$
$$(\varphi K)^{(1-\beta)(1-\alpha)}] \quad (30)$$

where θ_1 and θ_2 are the shadow prices associated with $\dot{K}$ and $\dot{h}$ which stand for physical investment and human capital accumulation. Here, the decision variables of the social planner are c, ϕ, τ and the state variables are K and h. From the first-order conditions, the growth rates of commodity output production, human capital and physical capital are solved.

The first-order optimality conditions are as follows:

$$c^{-\sigma} = \theta_1 \tag{31}$$

$$\frac{dH}{d\varphi} = 0$$

or

$$\begin{aligned}&\{(1-\beta)(1-\alpha)\varphi^{(1-\beta)(1-\alpha)-1}(1-\phi)^{\alpha}\\&+\alpha(1-\phi)^{\alpha-1}(-1)\varphi^{(1-\beta)(1-\alpha)}\}\\&[AK^{\alpha}B^{1-\alpha}(Nh)^{\beta(1-\alpha)}K^{(1-\beta)(1-\alpha)}][\theta_1(1-\tau)+\theta_2\eta\frac{\tau}{N}]=0\end{aligned} \tag{32}$$

$$\frac{dH}{d\tau} = 0$$

or

$$\frac{\theta_1}{\theta_2} = \frac{\eta}{N} \tag{33}$$

The equations of motion of co-state variables are as follows:

$$\begin{aligned}\frac{\dot{\theta}_1}{\theta_1} &= \rho-(1-\tau)A(1-\varphi)^{\alpha}\{1-\beta(1-\alpha)\}B^{1-\alpha}(Nh)^{\beta(1-\alpha)}\\&\varphi^{(1-\beta)(1-\alpha)}K^{\{\alpha+(1-\beta)(1-\alpha)-1\}}\\&+\frac{\theta_2}{\theta_1}\eta\frac{\tau}{N}A(1-\varphi)^{\alpha}B^{(1-\alpha)}(Nh)^{\beta(1-\alpha)}\varphi^{(1-\beta)(1-\alpha)}\\&\{1-\beta(1-\alpha)\}K^{\{\alpha+(1-\beta)(1-\alpha)-1\}}\end{aligned} \tag{34}$$

$$\begin{aligned}\frac{\dot{\theta}_2}{\theta_2} &= \rho-A(1-\varphi)^{\alpha}B^{1-\alpha}\beta(1-\alpha)h^{\beta(1-\alpha)-1}\\&\varphi^{(1-\beta)(1-\alpha)}(\frac{K}{Nh})^{1-\beta(1-\alpha)}\end{aligned} \tag{35}$$

Steady-State Growth Path Under Command Economy: The Basic Model

From the first-order optimality conditions, we derive the steady-state growth rates. The growth rate of per capita commodity output is given by

$$\gamma_c = \frac{\{1-\beta(1-\alpha)\}A(1-\varphi)^{\alpha}B^{1-\alpha}\varphi^{(1-\beta)(1-\alpha)}k^{-\beta(1-\alpha)}-\rho}{\sigma} \tag{36}$$

The growth rate of human capital accumulation is given by the following equation:

$$\gamma_h = \eta\tau A(1-\varphi)^{\alpha}B^{1-\alpha}(\varphi)^{(1-\beta)(1-\alpha)}k^{1-\beta(1-\alpha)} \tag{37}$$

Since along the steady state as γ_c is constant (followed from Equation (36)), k is also constant.

Therefore, $\gamma_k = 0$. Here, $k = \frac{K}{Nh}$. Taking logarithm of both sides of the aforementioned equation,

$\gamma_k = \gamma_K - n - \gamma_h$. As $\gamma_k = 0$, the growth rate of aggregate physical capital in steady state is given by $\gamma_K = \gamma_h + n$

The fraction of the physical capital that is allocated to produce service output is

$$\phi_{command} = \frac{(1-\beta)(1-\alpha)}{1-\beta(1-\alpha)} \tag{38}$$

Note that φ in command economy is the same as that obtained in competitive economy. The reason of the aforementioned finding is the absence of imperfect competition or any kind of external effects in this model. Using the value of $\phi_{command}$ and Equation (13c) in Equation (36), we get $\gamma_c = \frac{r-\rho}{\sigma}$. This the first best value for the growth of per capita commodity output. A comparison of this growth rate with that of the competitive economy (given in Equation [18]) reveals that in the competitive economy, a distortion appears in the growth rate due to imposition of the tax.

Given the value of $\phi_{command}$ and using the co-state equation and steady-state equilibrium conditions, we obtain unique solution of k from the following equation:

$$n = A(1-\phi_{command})^{\alpha} B^{1-\alpha} \phi_{command}^{(1-\beta)(1-\alpha)} k^{-\beta(1-\alpha)} \\ [\{1-\beta(1-\alpha)\} - k\beta(1-\alpha)] \tag{39}$$

Let $h(k)$ = *R.H.S* of the aforementioned equation. Here, $h' < 0$. The existence of the unique value of k is shown diagrammatically in Figure 2. In Figure 3, the growth rate of population n and $h(k)$ is plotted on the vertical axis, and the value of k is plotted along the horizontal axis. From the figure, it is quite obvious that k has a unique value at steady state. In the same figure, $h(k)$ intersects the line of growth rate of population n, at E for equilibrium value of k. Let it be $\hat{k}$. Note that $\hat{k}$ does not depend on τ

In Figure 3, population growth is depicted by AB. CD represents function $h(k)$ from Equation (39). $\hat{k}$is the equilibrium value for k in command economy.

Given the equilibrium value of k, that is, $\hat{k}$, the value of optimal tax rate τ can be solved from the following equation which is obtained by using a steady-state equilibrium condition where the growth rates of human capital and consumption of commodity are equal to each other:

$$\hat{k}^{1-\beta(1-\alpha)} A(1-\phi_{command})^{\alpha} B^{1-\alpha} \phi_{command}^{(1-\beta)(1-\alpha)} \sigma\eta\tau \\ = \{1-\beta(1-\alpha)\} \hat{k}^{-\beta(1-\alpha)} A(1-\phi_{command})^{\alpha} B^{1-\alpha} \\ \phi_{command}^{(1-\beta)(1-\alpha)} - \rho \tag{40}$$

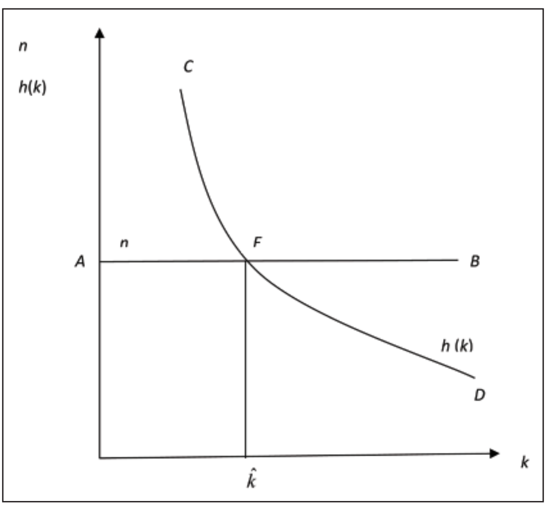

Figure 3. Determination of Optimal *k* in Command Economy

Source: The authors.

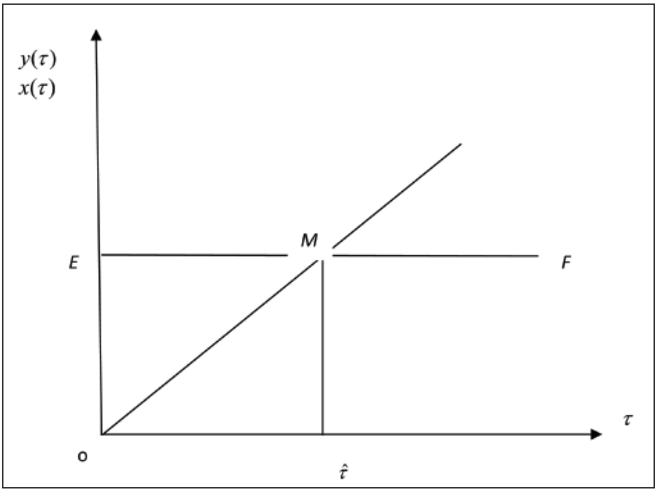

Figure 4. Determination of Optimal Tax rate in Command Economy

Source: The authors.

Let $x(\tau)$ be the LHS of Equation (40) and $y(\tau)$ be the RHS of Equation (40), where $x' > 0$ and $y' = 0$. In Figure 4, $x(\tau)$ intersects $y(\tau)$ at point M for unique τ.

In Figure 4, OH depicts the function $y(\tau)$ and EF represents $x(\tau)$ from Equation (40). $\hat{\tau}$ is the optimal tax rate in the command economy.

After obtaining the values of $\hat{k}$ and $\hat{\tau}$ at steady state, the values of growth rates can be derived. In steady state, the growth rate of consumption of commodity output and that of human capital accumulation are equal which is given by the following equation:

$$\gamma_h = \gamma_c = \left[\frac{\rho \hat{k} \eta \hat{\tau}}{\{1 - \beta(1-\alpha)\} - \hat{k} \eta \hat{\tau} \sigma} \right] \tag{41}$$

Proposition 4: *There exists positive, unique steady-state growth rate of human capital and that of consumption and production of commodity output in the command economy. There also exists a unique optimal tax rate.*

In the following section, we discuss another extension of the basic model.

Extension of the Basic Model

Household internalizes the government sector to itself and sets aside a part of their income for education.

In this section, we assume that there is no role of government, and household invests a fraction of their income in human capital education. In this case, all other equations remaining unchanged, the human capital and physical capital function are as follows:

$$\dot{h} = \frac{\eta\psi(whN + rK)}{N}$$

where ψ is the fraction of income invested for education; $0 < \psi < 1$

$$\dot{K} = \{(1-\psi)(whN + rK) - Nc\}$$

The Hamiltonian function can be formulated as:

$$\begin{aligned} H = \frac{c^{1-\sigma}}{(1-\sigma)}N + \theta_1[(1-\psi)(rK + wNh) - cN] \\ + \theta_2[\eta\psi\frac{(whN + rK)}{N}] \end{aligned} \tag{42}$$

Here, c, ψ are the decision variables and K and h are the state variables.[8]

We can derive the values of w, r, p_s using the profit maximization conditions like the basic model described in section 'Households, Firms and Government'. Using the no arbitrage condition, the values for φ and ψ are found as:

$$\left.\begin{aligned} \hat{\varphi} &= \frac{(1-\alpha)(1-\beta)}{1-\beta(1-\alpha)} \\ \hat{\psi} &= \frac{n-\rho+w\eta}{\eta\sigma(w+rk)} \end{aligned}\right\} \tag{43}$$

The growth rate of commodity sector is found as:

$$\gamma_c = \frac{n-\rho+w\eta}{\sigma} = \frac{r-\rho}{\sigma} \tag{44}$$

[8] Detailed derivation of this model is available with the author.

Thus, in case of private spending, we obtain the first best solution as equilibrium outcome in the absence of any distortion due to taxation.

$$r - w\eta = n \tag{44a}$$

where $r = \alpha A(1-\hat{\varphi})^{\alpha-1}B^{1-\alpha}\hat{\varphi}^{(1-\beta)(1-\alpha)}k^{-\beta(1-\alpha)}$

Replacing the values of w and r, we get Equation (45) that uniquely defines k in terms of the parameters.

$$A(1-\phi)^{\alpha}(1-\alpha)B^{1-\alpha}k^{-\beta(1-\alpha)}\varphi^{\alpha\beta-\alpha-\beta}[(1-\beta)-\eta\beta(\phi k)] = n \tag{45}$$

Let $\Gamma(k) = A(1-\phi)^{\alpha}(1-\alpha)B^{1-\alpha}k^{-\beta(1-\alpha)}\varphi^{\alpha\beta-\alpha-\beta}[(1-\beta)-\eta\beta(\phi k)]$

It can be shown that $\Gamma'(k) < 0$. Hence, there exists a unique k that satisfies Equation (45). Hence, using this, we find that

$$\frac{dk}{d\eta} = -\frac{[\beta(\phi k)]}{[\eta\beta\phi(1-\beta(1-\alpha)) + (1-\alpha)(1-\beta)\beta k^{-1}} < 0 \tag{46}$$

Thus, in the model with private spending too, we observe that k is negatively related to η. This result is the same as found in Equation (24), under competitive framework for basic model. Therefore, when the households are privately spending for accumulation of human capital, as the technological efficiency of education sector increases, per capita physical capital in steady state will decrease.

Using Equation (44), we observe that

$$\frac{d\gamma_c}{d\eta} = \frac{1}{\sigma}\frac{dr}{dk}\frac{dk}{d\eta} > 0 \quad \text{as } \frac{dr}{dk} < 0.$$

Hence, we conclude that in the model with producer services, when household spends a part of their income for accumulation of human capital, an increase in efficiency of education technology will cause the growth rate of per capita consumption to improve. This result is also similar to the result obtained in the basic model discussed in section ‘Basic Model’.

Numerical Analysis of Basic Model with Sector-specific Inputs

In this section, we develop a simpler version of the generalized model. Here, we assume that human capital is used only in service sector, and physical capital is employed only in the manufacturing sector. The general model is simplified by assuming $\beta = 1$.

The production functions are modified in the following manner:

$$Y_c = AK^{\alpha} Y_s^{1-\alpha} \tag{47}$$

$$Y_s = B(Nh) \tag{48}$$

Using the production functions, the human capital accumulation function is as follows:

$$\gamma_h = \frac{\dot{h}}{h} = \eta\left(\frac{G}{Nh}\right) = \eta\left(\frac{\tau y_c}{Nh}\right) = \eta\tau AB^{1-\alpha}k^{\alpha} \tag{49}$$

The investment function, utility function, balanced budget equation and growth path of population remain the same as the original model.

Given this assumption, section 'Competitive Economy' derives the steady-state growth path in competitive economy and section 'Command Economy' elaborates the same for a command economy. A comparative static analysis is done in section 'Comparative Static Results'.

Competitive Economy

In market economy, an individual consumer maximizes present discounted value of utility (over the infinite horizon) by choice of the consumption path subject to the wealth accumulation constraint. By using the current value Hamiltonian function, the problem of dynamic optimization is solved. The current value Hamiltonian for this particular problem is as follows:

$$H = \frac{N}{(1-\sigma)}(c^{1-\sigma} - 1) + \theta[(1-\tau)(rK + wNh) - cN]$$

In this problem, c is the decision variable, K is the one and only state variable and θ is the shadow price of physical capital. While solving this Hamiltonian function, tax rate τ is considered to be given throughout the analysis.

Steady-state Growth Path

The model results show that along the steady-state growth path, c, h and K grow at constant rate, and the growth rate of human capital and that of per unit commodity output consumption are given by

$$\gamma_h = \eta\tau A B^{1-\alpha} k^{\alpha} \tag{50}$$

$$\gamma_c = (1-\tau)\frac{A\alpha B^{1-\alpha} k^{\alpha-1}}{\sigma} - \frac{\rho}{\sigma} \tag{51}$$

The input prices, that is, r, w and p_s are found from the profit-maximizing conditions

$$r = A\alpha B^{1-\alpha} k^{\alpha-1}$$
$$w = p_s B$$
$$p_s = A(1-\alpha)B^{-\alpha}k^{\alpha}$$

In steady state, the growth rate of commodity output and that of human capital accumulation are equal, and equating these two expressions, we have

$$(1-\tau)\frac{A\alpha B^{1-\alpha} k^{\alpha-1}}{\sigma} - \frac{\rho}{\sigma} = \eta\tau A B^{1-\alpha} k^{\alpha} \tag{52}$$

As τ is given in competitive economy, the value of physical capital per skilled labour, that is, k is solved from the aforementioned equation.

Using Equation (35), we also find that

$$\frac{dk}{d\tau} = \frac{-[\alpha + \sigma\eta k]}{\alpha[\sigma\eta\tau + (1-\tau)(1-\alpha)k^{-1}]} < 0$$

To determine the growth-maximizing tax rate in competitive economy, the growth rate γ_c is maximized with respect to τ. The first-order condition is given as follows:

$$\frac{d\gamma_c}{d\tau} = 0$$

Using Equation (33), the level of tax rate that maximizes the growth rate in competitive framework is obtained. Let the level of tax rate be τ^{**}, and it is found that

$$\tau^{**} = (1 - \alpha) \tag{53}$$

The second-order condition that is required for growth maximization is $\frac{d^2\gamma_c}{d\tau^2} < 0$, and this condition is satisfied.

Proposition 5: *If human capital is the only input of service sector, then growth-maximizing tax rate in competitive economy is equal to the output elasticity of service in producing commodity output.*

In the present framework, in the competitive economy, the growth-maximizing tax rate is found to be the same as the output elasticity of manufacturing product with respect to service good. In this model, commodity sector uses service output as an input, which in turn is produced using human capital. Human capital accumulation depends on government per capita expenditure on education sector and financed by tax on commodity output. Hence, growth is maximized when tax rate is equal to the output elasticity of manufacturing product with respect to service good.

Command Economy

In the command economy, optimum solution is obtained by maximizing the following current value Hamiltonian

$$H = \frac{N}{(1-\sigma)}(c^{1-\sigma} - 1) + \theta_1 \dot{K} + \theta_2 \dot{h} \tag{54}$$

where θ_1 and θ_2 are shadow prices associated with $\dot{K}$ and $\dot{h}$ which stand for physical investment and human capital accumulation.

Here c and τ are the decision variables and K, h are state variables.

The growth rate of per capita commodity output is

$$\gamma_c = \frac{A\alpha k^{\alpha-1} B^{1-\alpha} - \rho}{\sigma} \tag{55}$$

The growth rate of human capital accumulation is

$$\gamma_h = \frac{\dot{h}}{h} = \eta \tau A B^{1-\alpha} k^{\alpha} \tag{56}$$

At steady state, $\gamma_h = \gamma_c$. Substituting the values, we get

$$\sigma \eta \tau A B^{1-\alpha} k^{\alpha} = A \alpha k^{\alpha-1} B^{1-\alpha} - \rho \tag{57}$$

Using the first-order conditions and the co-state equations, we get the following equation that solves k in terms of parameters.

$$n = AB^{1-\alpha} k^{\alpha-1} \alpha - A k^{\alpha} B^{1-\alpha} (1-\alpha)\eta \tag{58}$$

Here, we get a non-linear solution of k. For obtaining the value of tax rate in command economy and to compare it with that of competitive economy which maximizes growth rate, the model is made simpler by assuming $\alpha = \frac{1}{2}$.

The value of k is

$$(\hat{\hat{k}}) = \frac{(\sqrt{n^2 + A^2 B \eta} - n)^2}{A^2 B \eta^2} \tag{59}$$

Substituting the value of $\alpha = \frac{1}{2}$ into Equation (58), the following equation is obtained:

$$n = AB^{\frac{1}{2}} (\hat{\hat{k}})^{-\frac{1}{2}} (\frac{1}{2}) - A (\hat{\hat{k}})^{\frac{1}{2}} B^{\frac{1}{2}} (\frac{1}{2}) \eta \tag{58$'$}$$

Substituting the equilibrium value of k, that is, $(\hat{\hat{k}})$ in Equation (57), the value of optimal tax rate is solved. The optimal tax rate is

$$\tau_{command} = \frac{A(\frac{1}{2})(\hat{\hat{k}})^{-\frac{1}{2}} B^{\frac{1}{2}} - \rho}{\eta A B^{\frac{1}{2}} (\hat{\hat{k}})^{\frac{1}{2}} \sigma} = \frac{\gamma_c}{\eta A B^{\frac{1}{2}} (\hat{\hat{k}})^{\frac{1}{2}}} \tag{60}$$

Now the value of tax rate must be positive, and its value must be less than the one which implies $0 \leq \tau_{command} \leq 1$. From Equation (44), it is clear that $\tau_{command} \geq 0$ if γ_c is positive as all the other variables in the expression are assumed to be positive by default.

Therefore, the required condition for positive value of tax rate is

$$\gamma_c \geq 0 \tag{61}$$

Substituting the value of $\alpha = \frac{1}{2}$ into the commodity production function, it is found that $A(\frac{1}{2})(\hat{\hat{k}})^{-\frac{1}{2}}B^{\frac{1}{2}}$ is the expression of marginal productivity of physical capital.

The aforementioned condition implies that the value of marginal productivity of capital should be higher than the rate of time preference for tax rate to be positive. It is because the use of human capital is solely to increase future production. If individuals discount future more heavily compared to present marginal productivity of capital, it is meaningless to invest in human capital.

For $\tau_{command} \leq 1$, the required condition is

$$A(\frac{1}{2})(\hat{\hat{k}})^{-\frac{1}{2}}B^{\frac{1}{2}} \leq \rho + \eta A B^{\frac{1}{2}}(\hat{\hat{k}})^{\frac{1}{2}}\sigma$$

Using Equation (58′), we obtain

$$n - \rho \leq A B^{\frac{1}{2}}(\hat{\hat{k}})^{\frac{1}{2}}\eta(\sigma - \frac{1}{2}) \tag{62}$$

or

$$\mathrm{n} - \rho \leq (\sqrt{\mathrm{n}^2 + \mathrm{A}^2\mathrm{B}\eta} - \mathrm{n})(\sigma - \frac{1}{2})$$

Therefore, for $\tau_{command} \leq 1$

or

$$\frac{\mathrm{n} - \rho}{(\sqrt{\mathrm{n}^2 + \mathrm{A}^2\mathrm{B}\eta} - \mathrm{n})} + \frac{1}{2} \leq \sigma \tag{63}$$

Thus, in general model, the steady-state growth rates of human capital, commodity consumption and that of physical capital are obtained endogenously under both competitive and command economic regimes. Considering the tax rate as given in competitive frame, the values of k, ϕ are determined. In command economy, it is clear from the model that optimal tax rate exists. In the sector-specific input model along with the uniquely determined steady-state growth rates for human capital, physical capital and commodity consumption, the value of growth-maximizing tax rate under competitive regime and the optimal tax rate under command economy are also derived. The value of growth-maximizing tax rate in competitive economy is equal to the value of output elasticity of service in producing final output (α), and its value is assumed to be constant for the model under consideration. However, it is obvious from the expression of optimal tax rate (derived in earlier section) that the value of it depends on different parameters. In the following section, the comparative static analysis is done to study the impact of different parameters on optimal tax rate obtained in command economy framework.

Comparative Static Results

Differentiating optimal tax rate in command economy in this special case with respect to rate of time preference, we find

$$\frac{d\tau_{command}}{d\rho} = -\frac{1}{\eta AB^{1-\alpha}(k)^{\alpha}\sigma} < 0 \tag{64}$$

As rate of time preference (discount rate) rises, individuals become more concerned for present consumption rather than future consumption. So, under balanced budget, tax rate that raises the future accumulation rate of human capital which will be used as an input to produce commodity output in subsequent periods will fall for a rise in rate of time preference.

Now, we study how the optimal tax rate will respond when the technology parameter in human capital accumulation changes. Differentiating optimal tax rate with respect to technology parameter of human capital accumulation, we find

$$\frac{d\tau_{command}}{d\eta} = \frac{-\frac{dk}{d\eta}\alpha[(1-\alpha)+\sigma\eta k]}{\sigma k^2 \eta} - \frac{\tau}{\eta} \tag{65}$$

where

$$\frac{dk}{d\eta} = \frac{-k^{\alpha}}{(\alpha k^{\alpha-2} + \eta\alpha k^{\alpha-1})} < 0 \tag{66}$$

In numerical simulation done in the next section, we find $\frac{d\tau_{command}}{d\eta} > 0.$

This result is intuitively obvious. As efficiency of education sector η rises, marginal benefit from investing one unit for accumulation of human capital increases. Hence, it is optimal to increase tax rate.

Differentiating optimal tax rate with respect to the inverse of inter-temporal elasticity of substitution, we find that

$$\frac{d\tau_{command}}{d\sigma} = -\frac{\tau_{command}}{\sigma} < 0 \tag{67}$$

where σ stands for the inverse of inter-temporal elasticity of substitution. As inter-temporal elasticity of substitution increases, representative consumer can easily substitute present consumption by future consumption, and optimal tax rate increases because tax can finance education that can generate human capital in future. That human capital can be used for service production, and service is again used for commodity output production in future. So when σ decreases, people are ready to forgo present consumption for future consumption and willing to pay more tax.

Proposition 6: *The optimal tax rate decreases as the discount rate (ρ) increases and/or the elasticity of marginal utility and inverse of which is known as inter-temporal elasticity of substitution (σ)increases. The optimal tax rate increases as efficiency parameter of human capital accumulation (η) increases.*

Numerical Example

This section gives a numerical example to substantiate the results obtained in section 'Extension of the Basic Model'. Here, we consider a special case of specific factor model with $\alpha = 1/2$.

Under $\alpha = \frac{1}{2}$ assumption, the ratio of physical capital to human capital, growth-maximizing tax rate, growth rate of commodity output and growth rate of human capital under competitive economy are as follows:

$$k_{competitive} = \left[\frac{-\rho + \sqrt{\rho^2 + 4(.125)A^2 B\sigma\eta}}{\sigma\eta A B^{\frac{1}{2}}}\right]^2$$

$$\tau_{competitive} = (1 - \alpha) = (1 - .5) = .5$$

$$\gamma_c^{competitive} = \frac{A(.25)B^{\frac{1}{2}}k^{-\frac{1}{2}}_{competitive}}{\sigma} - \frac{\rho}{\sigma}\gamma_h^{competitive} = \eta(.5)AB^{\frac{1}{2}}k^{\frac{1}{2}}_{competitive}$$

Under $\alpha = \frac{1}{2}$ assumption, the ratio of physical capital to human capital, growth-maximizing tax rate, growth rate of commodity output and growth rate of human capital obtained under command economic regime are as follows:

$$k_{Command} = \frac{(\sqrt{n^2 + A^2 B\eta} - n)^2}{A^2 B\eta}$$

$$\tau_{command} = \frac{A(.5)k^{-\frac{1}{2}}_{command}B^{\frac{1}{2}} - \rho}{\eta AB^{\frac{1}{2}}k^{\frac{1}{2}}_{command}\sigma}$$

$$\gamma_c = \frac{A(.5)k^{-\frac{1}{2}}_{command}B^{\frac{1}{2}} - \rho}{\sigma}$$

$$\gamma_h = \frac{\dot{h}}{h} = \eta\tau_{command}AB^{\frac{1}{2}}k^{\frac{1}{2}}_{command}$$

A few diagrammatic representations have been shown on the basis of the numerical analysis.

Numerically, it has been found that for $n = 0.01$, $A = 0.5$, $B = 0.5$, $\eta = 0.05$, $\sigma = 2.1$ and $0.05 \leq \rho \leq 0.1$ $\frac{d\tau_{command}}{d\rho} < 0$ which is illustrated in Figure 5. In this figure, we see that the optimal tax rate in command economy falls with the increase in values of rate of preference.

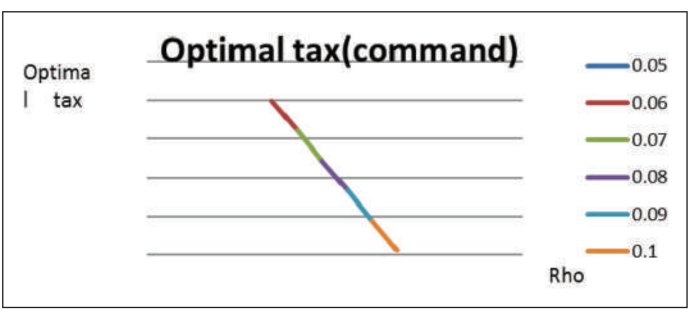

Figure 5. Relationship Between Optimal Tax Rate and ρ

Source: The authors.

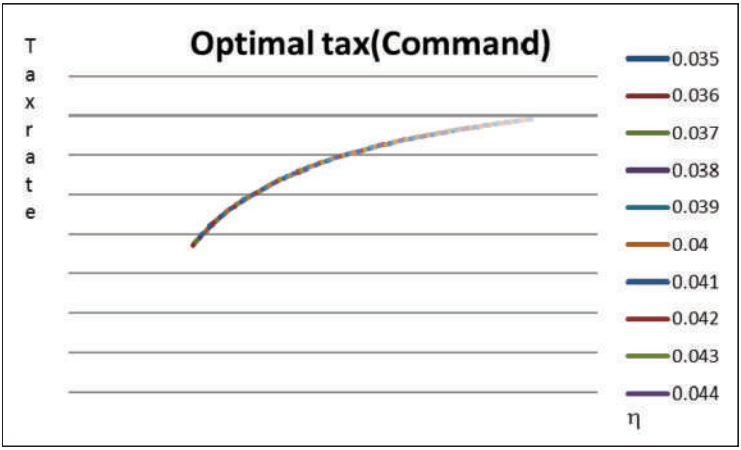

Figure 6. Relationship Between Optimal Tax Rate and η

Source: The authors.

Second, numerically, it is found that for n = 0.01, A = 0.5, B = 0.5, $\rho = 0.07$, $\sigma = 2.5$ and for the range $0.035 \leq \eta \leq 0.131$, the value of tax rate increases as η, that is, $\frac{d\tau_{command}}{d\eta} \geq 0$. The result is shown in Figure 6.

Finally, it is observed that for n = 0.01, A = 0.5, B = 0.5, ρ = 0.07, $\eta = 0.05$ and $1.5 \leq \sigma \leq 2.46$, $\frac{d\tau_{command}}{d\sigma} < 0$, that is, the value of tax rate decreases as σ rises (see Figure 7).

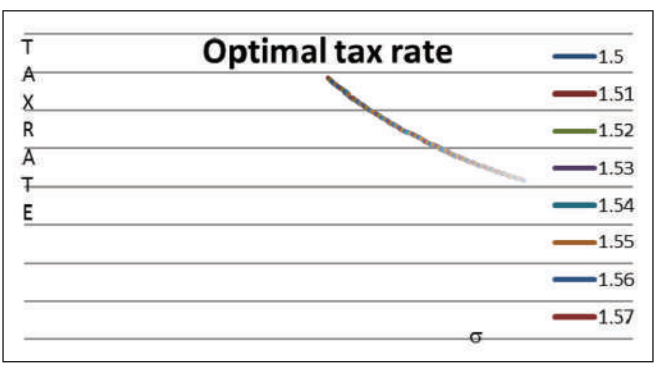

Figure 7. Relationship Between Optimal Tax Rate and σ

Source: The authors.

The value of the growth-maximizing tax rate under competitive economy rate is constant, that is, 0.5 here. Theoretically, it is derived that under certain assumptions, its value does not depend on any of the parameters of η, σ and ρ. Therefore, in every case, in earlier figures, the growth-maximizing tax rate will be a horizontal line with respect to the changing values of any parameter under consideration. The growth-maximizing tax rate in competitive economy is constant and depending on variation of different parameters, such as η, σ and ρ, it may be higher than the optimal tax rate of the command economy or the other way round.

Finally, we compare the growth rates for command and competitive economies and try to find how they vary with different parameters. In the following two figures, the growth rates of human capital under two economic regimes are plotted along the vertical axis, and the values of the parameter under consideration are plotted along the horizontal axis. The dotted line represents the growth rate of command economy, whereas the solid one denotes the growth rate of competitive economy.

Figure 8 shows the pattern of growth path of human capital in two different economic regimes due to change in value of technology parameter of human capital, that is, η. It is found that the growth rate in command economy is higher than that of the competitive economy.

In Figure 9, comparison is done between growth rates under command and competitive framework with variation in rate of time preference. The growth rate in command economy is higher than that of the competitive economy.

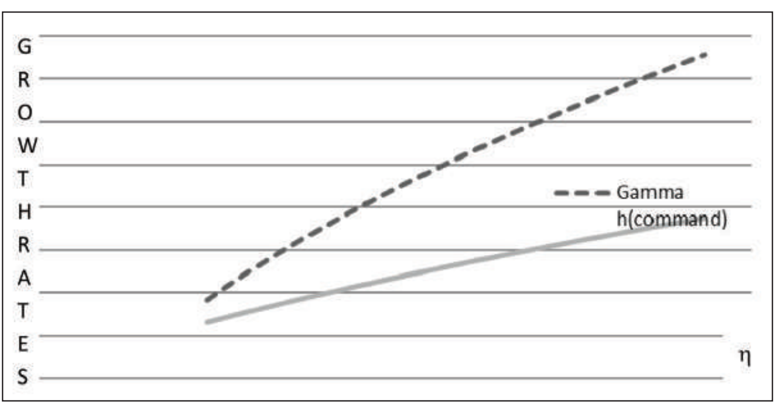

Figure 8. Comparison Between Growth Rates with Respect to η

Source: The authors.

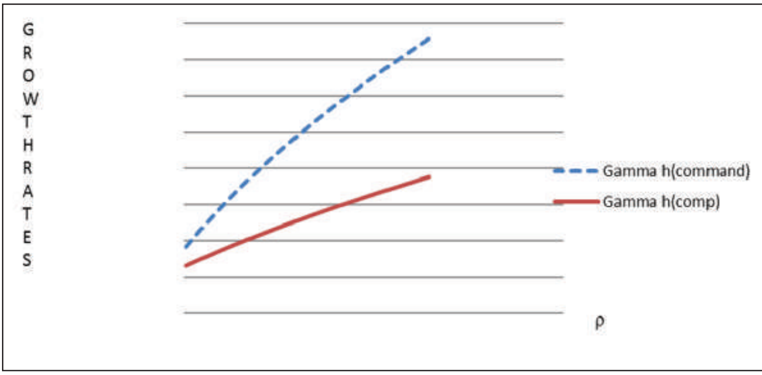

Figure 9. Comparison Between Growth Rates with Respect to ρ

Source: The authors.

Thus, from Figure 9, it is observed that the command economy has higher growth rate than that of competitive economy under this numerical specification. This result is found because in command economy, tax is chosen by the social planner optimally, whereas in decentralized economy, tax rate is considered to be exogenously given by the optimizing agents. Then, the growth rate in competitive economy is maximized with respect to tax rate. After substituting this growth by maximizing tax rate, competitive economy growth rate is obtained. Under command economic regime, the cost of taxation is being equalized with the benefit of taxation by the social planner at the margin. In competitive economy, the decisions taken are disjoint. Hence, follows the above result.

Conclusion

In this article, an endogenous growth model is considered with producer service. The service output is used as an intermediate good in commodity sector. Human capital is used to produce service good. Initially, we assume that accumulation of human capital depends on the government expenditure on education sector. The government levies tax on the commodity output. This model is considered as the basic model in the article. In this framework, we observe that there exists a unique saddle path stable steady-state growth rate of human capital accumulation, which works as the source of growth for all other sectors of the economy. Also, we observe in the competitive framework, a unique growth-maximizing tax rate exists. We also compare the optimal tax rates for the command economy with growth-maximizing tax rate in competitive economy under the assumption that the physical capital is specific to commodity manufacturing sector, and human capital is specific to producer service sector. It is found that the growth-maximizing tax rate in competitive economy is constant, and depending on the variation of different parameters, it may be higher than the optimal tax rate of the command economy or the other way around. Further, the tax rate of the command economy increases when the efficiency of human capital accumulation technology rises. However, the optimal tax rate decreases as the discount rate of utility and the elasticity of marginal utility increase. Finally, the numerical analysis shows that in the presence of producer service, the command economy will have a higher growth rate than the competitive economy even after imposition of growth-maximizing tax rate in competitive economy. We also attempt another extension of the model where it is assumed that households privately spend for accumulation of the human capital. In this case, we obtain the first best solution as the equilibrium rate of growth in the absence of distortion due to taxation. This same growth rate is also yielded by command economy after endogenizing the tax rate. In addition, like the basic model as the technological efficiency of the education sector improves, the growth of per capita consumption will improve.

Acknowledgement

We are indebted to the anonymous referees for their valuable comments.

Declaration of Conflicting Interests

The authors declared no potential conflicts of interest with respect to the research, authorship and/or publication of this article.

Funding

The authors received no financial support for the research, authorship and/or publication of this article.

Appendix A

To Prove

$$rK + whN = Y_c$$

From Equations (13b), (14) and (15), substituting the value of r, w and p_s in the LHS of the above equation, we get

$$p_s B(Nh)^{\beta-1}\beta(\phi K)^{1-\beta}hN + p_s B(Nh)^{\beta}(1-\beta)(\phi K)^{-\beta}K$$

$$= p_s B(Nh)^{\beta}K^{1-\beta}\phi^{-\beta}[\beta\phi + (1-\beta)]$$

$$= p_s B(Nh)^{\beta}K^{1-\beta}\phi^{-\beta}[B\frac{(1-\alpha)(1-\beta)}{1-\beta(1-\alpha)} + (1-\beta)]$$

$$= p_s B(Nh)^{\beta}K^{1-\beta}\phi^{-\beta}[\frac{(1-\beta)}{1-\beta(1-\alpha)}]$$

$$= p_s \frac{(1-\beta)}{1-\beta(1-\alpha)} B(Nh)^{\beta}K^{1-\beta}\phi^{-\beta}$$

$$= [A(1-\phi)^{\alpha}(1-\alpha)B^{-\alpha}k^{\alpha\beta}\phi^{-\alpha(1-\beta)}]\{\frac{(1-\beta)}{1-\beta(1-\alpha)}B(Nh)^{\beta}K^{1-\beta}\phi^{-\beta}\}$$

$$= \frac{AB(Nh)^{\beta(1-\alpha)}(1-\phi)^{\alpha-1}B^{-\alpha}\phi^{(1-\alpha)(1-\beta)}K^{\alpha+(1-\alpha)(1-\beta)}\alpha}{\{1-\beta(1-\alpha)\}}$$

$$= AB^{1-\alpha}K^{\alpha+(1-\alpha)(1-\beta)}\phi^{(1-\alpha)(1-\beta)}(Nh)^{\beta(1-\alpha)}\frac{(1-\phi)^{\alpha}}{(1-\phi)\{1-\beta(1-\alpha)\}}$$

Now

$$1-\phi = 1-\frac{(1-\alpha)(1-\beta)}{1-\beta(1-\alpha)} = \frac{1-\beta(1-\alpha)-(1-\alpha)(1-\beta)}{1-\beta(1-\alpha)}$$

Therefore,

$$= AB^{1-\alpha}K^{\alpha+(1-\alpha)(1-\beta)}\phi^{(1-\alpha)(1-\beta)}(Nh)^{\beta(1-\alpha)}\frac{(1-\phi)^{\alpha}}{(1-\phi)\{1-\beta(1-\alpha)\}} =$$

$$\frac{Y_c}{1-\beta(1-\alpha)-(1-\alpha)+\beta(1-\alpha)} = Y_c(\text{proved})$$

References

Banga, R., & Goldar, B. (2007). Contribution of services to output growth and productivity in Indian manufacturing: Pre- and post-reforms. *Economic and Political Weekly*, *42*(26), 2769–2777.

Barua, A., & Pant, M. (2014). Trade and wage inequality: A specific factor model with intermediate goods. *International Review of Economics and Finance, 33*(C), 172–185.

Beauchemin, K. R. (2001). Growth or stagnation? The role of public education. *Journal of Development Economics*, *64*(2), 389–416.

Behuria, S., & Khullar, R. (1994). *Intermediate services and economic development: The Malaysian example*. Retrieved from https://www.adb.org/publications/intermediate-services-and-economic-development-malaysian-example

Blankenau, W. F., Simpson, N. B., & Tomljanovich, M. (2007). Public education expenditures, taxation, and growth: Linking data to theory. *American Economic Review*, *97*(2), 393–397.

Bosworth, B., Collins, S. M., & Virmani, A. (2006). Sources of growth in the Indian economy. *India Policy Forum*, *3*(1), 1–69. Retrieved from https://www.brookings.edu/wp-content/uploads/2016/07/2006_bosworth.pdf

Cardak, B. A. (2004). Education choice, endogenous growth and income distribution. *Economica*, *71*(281), 57–81.

Chen, B. L., & Lee, S. F. (2007). Congestible public goods and local indeterminacy: A two-sector endogenous growth model. *Journal of Economic Dynamics and Control*, *31*(7), 2486–2518.

Das, S. P., & Saha, A. (2015). Growth of business services: A supply-side hypothesis. *Canadian Journal of Economics/Revue canadienned'économique*, *48*(1), 83–109. doi:10.1111/caje.12120

Dasgupta, D. (1999). Growth versus welfare in a model of nonrival infrastructure. *Journal of Development Economics*, *58*(2), 359–385.

De la Fuente, A., & Doménech, R. (2006). Human capital in growth regressions: How much difference does data quality make? *Journal of the European Economic Association*, *4*(1), 1–36.

Faig, M. (1995). A simple economy with human capital: Transitional dynamics, technology shocks, and fiscal policies. *Journal of Macroeconomics*, *17*(3), 421–446.

Fernández, E., Novales, A., & Ruiz, J. (2004). Indeterminacy under non-separability of public consumption and leisure in the utility function. *Economic Modelling*, *21*(3), 409–428.

Francois, J., & Woerz, J. (2008). Producer services, manufacturing linkages, and trade. *Journal of Industry, Competition and Trade*, *8*(3–4), 199–229.

Futagami, K., Morita, Y., & Shibata, A. (1993). Dynamic analysis of an endogenous growth model with public capital. *The Scandinavian Journal of Economics*, *95*(4), 607–625.

Garcia-Castrillo, P., & Sanso, M. (2000). Human capital and optimal policy in a Lucas-type model. *Review of Economic Dynamics*, *3*(4), 757–770.

Glomm, G., & Ravikumar, B. (2001). Human capital accumulation and endogenous public expenditures. *Canadian Journal of Economics/Revue canadienned'économique*, *34*(3), 807–826.

Gomez, M. A. (2003). Optimal fiscal policy in the Uzawa-Lucas model with externalities. *Economic Theory*, *22*(4), 917–925.

Greiner, A. (2006). Human capital formation, public debt and economic growth. *Journal of Macroeconomics*, *30*(1), 415–427.

Hollanders, H. J. G. M., & ter Weel, B. J. (1999). Skill-biased technical change: On endogenous growth, wage inequality and government intervention. In H. Hagemann & S. Seiter (Eds.), *Growth theory and growth* policy (pp. 156–171). London, UK: Routledge.

Imbruno, M. (2014). *Trade liberalization, intermediate inputs and firm efficiency: Direct versus indirect modes of import*. Nottingham Centre for Research on Globalisation and Economic Policy, University of Nottingham, Nottingham, UK.

Ishikawa, J. (1992). Learning by doing, changes in industrial structure and trade patterns, and economic growth in a small open economy. *Journal of International Economics*, *33*(3–4), 221–244.

Lucas, R. E., Jr. (1988). On the mechanics of economic development. *Journal of Monetary Economics*, *22*(1), 3–42.

Mankiw, N. G., Romer, D., & Weil, D. N. (1992). A contribution to the empirics of economic growth. *The Quarterly Journal of Economics*, *107*(2), 407–437.

Miroudot, S., Lanz, R., & Ragoussis, A. (2009). *Trade in intermediate goods and services* (OECD Trade Policy Working Paper No. 93). Paris: OECD.

Moro, A. (2007). *Intermediate goods and total factor productivity* (Economics Working Papers we076034). Universidad Carlos III de Madrid. Departamento de Economía. Madrid, Spain.

Psarianos, I. N. (2002). Fiscal policy in an endogenous growth model with horizontally differentiated intermediate goods. *Spoudai*, *52*(4), 18–41.

Riley, G. (2014). *Economic growth-the role of human & social capital, competition & innovation*. Retrieved from http://www.tutor2u.net/economics/revisionnotes/a2-macro-economic-growth-capital.html

Sekar, M., Delgado, D. R., & Ulu, M. F. (2015). *Imported intermediate goods and product innovation: Evidence from India* (Working Papers 1537). Research and Monetary Policy Department, Central Bank of the Republic of Turkey, Turkey.

Tanaka, R. (2003). Inequality as a determinant of child labour. *Economics Letters*, *80*(1), 93–97.

Tsoukis, C., & Miller, N. J. (2003). Public services and endogenous growth. *Journal of Policy Modeling*, *25*(3), 297–307.

Woo, J. (2005). Social polarization, fiscal instability and growth. *European Economic Review*, *49*(6), 1451–1477.

Bell-CHSH violation under global unitary operations: Necessary and sufficient conditions

Nirman Ganguly, Amit Mukherjee, Arup Roy, Some Sankar Bhattacharya, Biswajit Paul, and Kaushiki Mukherjee

https://doi.org/10.1142/S0219749918500405

< Previous

Abstract

The relation between Bell-CHSH violation and factorization of Hilbert space is considered here. That is, a state which is local in the sense of the Bell-CHSH inequality under a certain factorization of the underlying Hilbert space can be Bell-CHSH nonlocal under a different factorization. While this question has been addressed with respect to separability, the relation of the factorization with Bell-CHSH violation has remained hitherto unexplored. We find here that there is a set containing density matrices, which do not exhibit Bell-CHSH violation under any factorization of the Hilbert space brought about by global unitary operations. Using the Cartan decomposition of $SU(4)$, we characterize the set in terms of a necessary and sufficient criterion based on the spectrum of density matrices. Sufficient conditions are obtained to characterize such density matrices based on their bloch representations. For some classes of density matrices, necessary and sufficient conditions are derived in terms of bloch parameters. Furthermore, an estimation of the volume of such density matrices is achieved in terms of purity. The criterion is applied to some well-known class of states in two qubits. Since both local filtering and global unitary operations influence the Bell-CHSH violation of a state, a comparative study is made between the two operations. The inequivalence of the two operations (in terms of increasing Bell-CHSH violation) is exemplified through their action on some classes of states.

Keywords: Bell-CHSH ▪ global unitory operation

PACS: 03.67.Ac, 03.67.Mn

back

Nonequilibrium Quantum Transport Physics in Nanosystems
Felix A Buot, World Scientific Book, 2009

Maximum violation of Wigner inequality for two-spin entangled states with parallel and antiparallel polarizations
Yan Gu et al., International Journal of Quantum Information, 2018

A simple entanglement criterion of two-qubit system
Chao-Ying Zhao et al., International Journal of Modern Physics B, 2019

Eigenvalues, absolute continuity and localizations for periodic unitary transition operators
Tatsuya Tate, Infinite Dimensional Analysis, Quantum Probability and Related Topics, 2019

A recursive approach for geometric quantifiers of quantum correlations in multiqubit Schrödinger cat states
M. Daoud et al., International Journal of Modern Physics B, 2015

Researchers demonstrated violation of Bell's inequality on frequency-bin entangled photon pairs
Phys.org, 2017

Quantum test strengthens support for EPR steering
Phys.org

Big Blue's Big Leap: Quantum center takes on 53 qubit system
by Nancy Cohen et al., TechXplore.com, 2019

Research opens the way to new treatments for chronic pain and cancer
MedicalXpress, 2016

A sliding mode control scheme for nonlinear positive Markov jumping systems
by Ingrid Fadelli et al., TechXplore.com, 2019

Monthly Notices of the ROYAL ASTRONOMICAL SOCIETY

MNRAS **480,** L116–L120 (2018) doi:10.1093/mnrasl/sly136
Advance Access publication 2018 July 27

The flux distribution of individual blazars as a key to understand the dynamics of particle acceleration

Atreyee Sinha,[1†] Rukaiya Khatoon,[2⋆] Ranjeev Misra,[1] Sunder Sahayanathan,[3] Soma Mandal,[4] Rupjyoti Gogoi[2] and Nilay Bhatt[3]

[1]*Inter-University Center for Astronomy and Astrophysics, Post Bag 4, Ganeshkhind, Pune-411007, India*
[2]*Tezpur University,Napaam-784028, Assam, India*
[3]*Astrophysical Sciences Division, Bhabha Atomic Research Centre, Mumbai - 400085, India*
[4]*Government Girls' General Degree College, Kolkata-700023, West Bengal, India*

Accepted 2018 July 24. Received 2018 July 24; in original form 2018 April 12

The observed lognormal flux distributions in the high-energy emission from blazars have been interpreted as being due to variability stemming from non-linear multiplicative processes generated dynamically from the accretion disc. On the other hand, rapid minute scale variations in the flux point to a compact emitting region inside the jet, probably disconnected from the disc. In this work, we show that linear Gaussian variations of the intrinsic particle acceleration or escape time-scales can produce distinct non-Gaussian flux distributions, including lognormal ones. Moreover, the spectral index distributions can provide confirming evidence for the origin of the variability. Thus, modelling of the flux and index distributions can lead to quantitative identification of the micro-physical origin of the variability in these sources. As an example, we model the X-ray flux and index distribution of Mkn 421 obtained from ∼9 yr of MAXI observations and show that the variability in the X-ray emission is driven by Gaussian fluctuations of the particle acceleration process rather than that of the escape rate.

Key words: acceleration of particles – galaxies: active – BL Lacertae objects: general – BL Lacertae objects: individual: Mkn 421.

1 INTRODUCTION

Blazars are a special class of radio-loud active galactic nuclei (AGNs) and their observed broad-band spectra are dominated by non-thermal emission arising from radiative cooling of relativistic electron distributions in powerful Doppler-boosted jets (Urry & Padovani 1995). Additionally, blazar luminosity is observed to vary over time-scales of years down to minutes and at all wavelengths across the electromagnetic spectrum. Despite many decades of observations, the cause of the underlying variability is poorly understood. The dominance of the non-thermal emission further hinders our understanding of the accretion disc-jet connection in these sources.

Irrespective of the origin, emission from blazars has been found to be stochastic in nature, similar to that seen in other AGNs and Galactic X-ray binaries (McHardy et al. 2006; Chatterjee et al. 2012; Nakagawa & Mori 2013; Sobolewska et al. 2014). Since the past decade, much work has been done to understand the flux distribution of the lightcurves. For a linear stochastic process, a Gaussian distribution of the flux is to be expected, with the width of the distribution determining the flux variation. However, for the case of the eponymous blazar BL Lac, a lognormal flux distribution was clearly evident in the long-term X-ray light curves, with the average amplitude of variability being proportional to the flux level (Giebels & Degrange 2009). Henceforth, this behaviour has been witnessed even in other blazars, and at different timescales and wavelengths (H.E.S.S. Collaboration 2010; Chevalier et al. 2015; Kushwaha et al. 2016; Sinha et al. 2016, 2017; Shah et al. 2018). Such properties were initially observed in the X-ray emission of the galactic black hole binary Cygnus X-1 (Uttley & McHardy 2001), and are usually interpreted as arising from multiplicative processes which originate in the accretion disc (Lyubarskii 1997; Uttley, McHardy & Vaughan 2005; McHardy 2010). However, minute time-scale variability as seen in many blazars (Gaidos et al. 1996; Aharonian et al. 2007; Albert et al. 2007; Paliya et al. 2015) is difficult to originate from the disc (Narayan & Piran 2012), and strongly favours the variability to originate within the jet.

On the other hand, additive processes can also result in such distributions under specific scenarios. Biteau & Giebels (2012) studied the statistical properties of the mini jets-in-a-jet model of Giannios, Uzdensky & Begelman (2009) and showed that the total flux from randomly oriented mini jets will converge to an α-stable

⋆ E-mail: rukaiyakhatoon12@gmail.com
† Now at: APC, AstroParticule et Cosmologie, Université Paris Diderot, CNRS/IN2P3, CEA/Irfu, Observatoire de Paris, Sorbonne Paris Cité, 10, rue Alice Domon et Léonie Duquet, 75205 Paris Cedex 13, France.

distribution. Further, inclusion of experimental uncertainties can imitate such a distribution as a lognormal one. In this work, we provide an alternate interpretation of the non-Gaussian signatures seen in blazar variability through linear fluctuations of the underlying particle acceleration and/or the diffusive escape rate of the emitting electrons. Such small Gaussian perturbations propagate to produce non-linear flux distributions and linear flux-rms relations at high frequencies. This can explain the lognormal behaviour in both the long term stationary time series and during blazar flares, while reproducing the observed flux-rms relations. Finally, this study is used to interpret a plausible cause of variability in light curves obtained from the MAXI observations for the brightest TeV blazar, Mkn 421.

2 PERTURBATION ON THE INTRINSIC TIME-SCALES

We consider a scenario where the non-thermal electrons responsible for the blazar emission are accelerated at a shock front (AR; the acceleration region). Subsequently, they diffuse downstream (CR; the cooling region), at a rate ${\tau_e}^{-1}$, where they radiate through synchrotron and inverse Compton (IC) mechanisms (Kirk, Rieger & Mastichiadis 1998; Sahayanathan 2008) The kinetic equation describing evolution of the electrons in the AR can be written as (Kardashev 1962)

$$\frac{\partial n(\gamma,t)}{\partial t}+\frac{\partial}{\partial\gamma}\left[\left(\frac{\gamma}{\tau_a}-A\gamma^2\right)n(\gamma,t)\right]+\frac{n(\gamma,t)}{\tau_e}=Q(\gamma), \qquad (1)$$

where, γ/τ_a is the electron acceleration rate and $A\gamma^2$ is the radiative loss rate.[1] Together, they govern the maximum attainable Lorentz factor of the accelerated electrons, $\gamma_{max}=\frac{1}{A\tau_a}$. The steady state solution of equation (1) for a mono-energetic electron injection, $Q(\gamma)=Q_0\delta(\gamma-\gamma_0)$, will be

$$n_0(\gamma)=Q_0\tau_a\gamma^{-1-\frac{\tau_a}{\tau_e}}\left(1-\frac{\gamma}{\gamma_{max}}\right)^{\frac{\tau_a}{\tau_e}-1}\left(\frac{1}{\gamma_0}-\frac{1}{\gamma_{max}}\right)^{-\frac{\tau_a}{\tau_e}}. \qquad (2)$$

After injection into the CR, the evolution of these particles is governed by

$$\frac{\partial n_s(\gamma,t)}{\partial t}=\frac{\partial}{\partial\gamma}[B\gamma^2 n_s(\gamma,t)]+\frac{n(\gamma,t)}{\tau_e}-\frac{n_s(\gamma,t)}{t_e}, \qquad (3)$$

where first term on the right hand side of equation (3) describes the radiative loss rate in the CR, and the last term is the escape of electrons from CR at a rate ${t_e}^{-1}$. The steady state solution of the above equation will be a broken power law, with indices τ_a/τ_e + 1 and τ_a/τ_e + 2, and a break at energy $1/Bt_e$. Since the indices of the particle spectrum do not depend on the intrinsic time-scales of the CR, this will not introduce any additional non-linearity in the temporal behaviour. Moreover, as the radiative loss rate is $\propto\gamma^2$, the resultant photon spectrum will again be a broken power law with indices $\tau_a/2\tau_e$ and $(\tau_a+\tau_e)/2\tau_e$ respectively. The narrow width of the single particle emissivity due to synchrotron and inverse Compton emission mechanisms, with respect to the power-law electron distribution, further ensures that the photon spectrum will retain the temporal behaviour of the underlying particle distribution. In addition, the shape of the flux distribution due to synchrotron and inverse Compton scattering of an external photon field will be similar to that of electron number density since the corresponding emissivities are proportional to the number density. On the other hand, for synchrotron self-Compton process, the emissivity will depend on the square of the electron distribution (Sahayanathan, Sinha & Misra 2018) and hence the variance of the distribution will be twice as that of the electron distribution.

[1]Here, the radiative loss includes both synchrotron and inverse Compton processes happening at Thomson regime. For high electron and target photon energies the Compton scattering process will happen at Klein–Nishina regime and the loss rate will be different. However, here we confine or study within the low-energy domain where Thomson approximation is valid.

2.1 Gaussian perturbation on τ_a

A small perturbation in the acceleration time-scale can introduce variation in the accelerated particle number density. If we quantify this variation in τ_a as

$$\tau_a=\tau_{a0}+\Delta\tau_a, \qquad (4)$$

where τ_{a0} corresponds to the mean acceleration timescale, the change in the number density can be expressed as

$$\bar{n}(\gamma)=\bar{n}_0(\gamma)+\Delta\bar{n}(\gamma), \qquad (5)$$

where $\bar{n}_0$ is the steady state solution (equation 2) corresponding to $\tau_a=\tau_{a0}$. Substituting equations (4) and (5) in the steady state form of equation (1), the fractional variability in $\bar{n}(\gamma)$ can then be obtained as

$$\frac{\Delta\bar{n}(\gamma)}{\bar{n}(\gamma)}=f(\gamma)\frac{\Delta\tau_a}{\tau_a}+g(\gamma)\frac{\Delta\tau_a}{\tau_e}, \qquad (6)$$

where

$$f(\gamma)=\left(\frac{1}{1-\gamma/\gamma_{max}}\right) \qquad (7)$$

$$g(\gamma)=\log\frac{\gamma_0(1-\gamma/\gamma_{max})}{\gamma(1-\gamma_0/\gamma_{max})}-\frac{\gamma/\gamma_{max}}{1-\gamma/\gamma_{max}}+\frac{\gamma_0/\gamma_{max}}{1-\gamma_0/\gamma_{max}}. \qquad (8)$$

From equation (6), it is evident that the variability in $\bar{n}(\gamma)$ is a linear combination of Gaussian and lognormal terms. The relative amplitudes of these terms are decided by the functions $f(\gamma)$ and $g(\gamma)$. For the case $\gamma_{max}\to\infty$, the lognormal term dominates when $\gamma\gg\gamma_0\exp(\tau_e/\tau_a)$. Also in this case, the standard deviation of a normally distributed τ_a will be approximately $\tau_e/\log(\gamma_0/\gamma)$ times that of $\log\bar{n}(\gamma)$. Since the variability in photon index will be equal to $\Delta\tau_a/2\tau_e$, the standard deviation of the logarithm of the photon flux distribution will be $2|\log(\gamma_0/\gamma)|$ times the index distribution (in case of synchrotron and external Compton processes).

To quantify the deviation of $n(\gamma,t)$ from a Gaussian, we simulate its temporal behaviour by solving equation (1) numerically using finite difference scheme. Gaussian perturbations of varying widths (σ_{τ_a}) are then introduced in τ_a and the time series spanning over 5000 points of $n(\gamma)$ is computed for each case at different values of γ. The values of γ_0 and γ_{max} are kept fixed at 10 and 10^5 respectively. The generated time series are then investigated for various statistical properties.

In Fig. 1(a), we plot the skewness of the accelerated electron distribution (κ_n) as a function of σ_{τ_a}/τ_a for different values of γ. Since the fractional variation in the blazar spectral index during different flux states is 15 per cent approximately (see Section 3), we extend σ_{τ_a}/τ_a variation up to 0.25. At low-electron energies ($\gamma\approx30$) the skewness of the distribution is negligible indicating a symmetric distribution. However, the distributions drift towards highly tailed ones for increasing electron energies, thus implying a deviation from Gaussianity. To investigate whether the skewed high-energy electron distribution reflects a lognormal behaviour, we plot in Fig. 1(c), the skewness of the logarithm of the number density

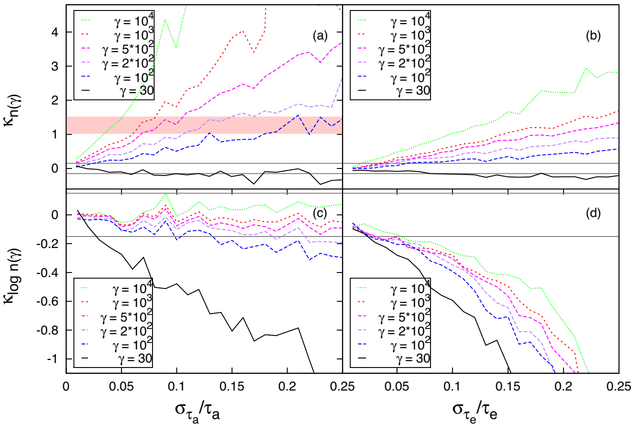

Figure 1. Skewness (κ) of the simulated particle distribution as a function of σ_{τ_a}/τ_a and σ_{τ_e}/τ_e is shown in (a) and (b), whereas the skewness of the logarithm of the distribution as a function of σ_{τ_a}/τ_a and σ_{τ_e}/τ_e is shown in (c) and (d). The solid line corresponds to electron with Lorentz factor $\gamma = 30$ (black), dashed line to $\gamma = 10^2$ (blue), dashed line to $\gamma = 2 * 10^2$ (purple), dashed line to $\gamma = 5 * 10^2$ (magenta), short dashed line to $\gamma = 10^3$ (red) and dotted line $\gamma = 10^4$ (green). The grey lines show the 3-σ ($3\sqrt{15/N}$) error range (Press et al. 1992). The pink band shows the 1-σ error range for the observed value for Mkn421 (Section 3).

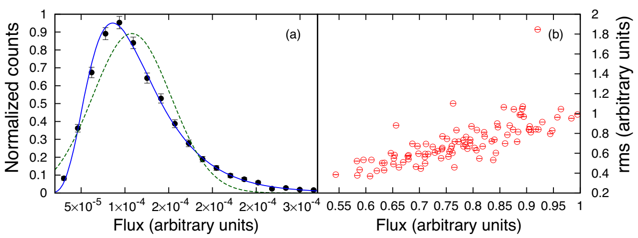

Figure 2. (a) Histogram of the simulated particle number density for $\sigma_{\tau_a}/\tau_a = 0.1$ and $\gamma = 10^3$. The dashed green line represents the best-fitting Gaussian and the solid blue line represents the best-fitting lognormal PDF. (b) The flux-rms scatter plot obtained by dividing the simulated time series into 50 equal time bins. A strong positive correlation is clearly evident ($\rho = 0.83$, $P = 4 \times 10^{-26}$).

($\kappa_{\log n}$) as a function of σ_{τ_a}/τ_a. Here, the skewness is negligible for increasing electron energies suggesting a possible drift towards a lognormal distribution. To confirm this, we further fit the normalized distribution of the number densities with Gaussian and lognormal probability density functions (PDFs). We find that a lognormal PDF significantly fits the distribution better at high-electron energies. In Fig. 2(a), we show the normal and lognormal fit to the electron distribution corresponding to $\gamma = 10^3$ and $\sigma_{\tau_a}/\tau_a = 0.1$. Clearly, the fit statistics is better for a lognormal with a reduced chi-square, $\chi^2_{\rm red} \approx 1.1$ for 17 degrees of freedom (dof), than a Gaussian ($\chi^2_{\rm red} \approx 20.9$ for 17 dof) PDF. The lognormal behaviour of the number density n at large γ lets us express the skewness of the distribution as

$$\kappa_n = \left(2 + e^{\sigma^2_{\log n}}\right)\sqrt{e^{\sigma^2_{\log n}} - 1}, \tag{9}$$

where $\sigma_{\log n}$ is the standard deviation of $\log n$ which can be approximated as

$$\sigma_{\log n} \approx \frac{g(\gamma)}{\tau_e}\sigma_{\tau_a}. \tag{10}$$

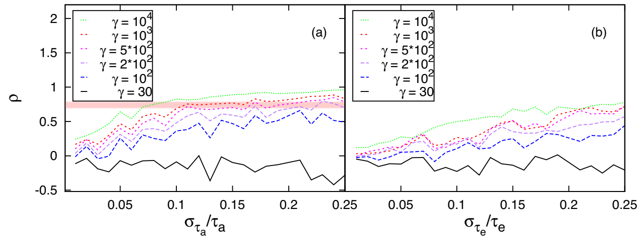

Figure 3. Spearman's rank correlation coefficient ρ of the flux-rms scatter plot as a function of (a) σ_{τ_a}/τ_a and (b) σ_{τ_e}/τ_e. The legends are same as in Fig. 1. The pink band shows the 1-σ ($0.6325/\sqrt{N-1}$) error range for the observed value for Mkn421 (Section 3).

The energy dependence of $\sigma_{\log n}$ will cause the skewness (κ_n) to increase with energy which in turn can be an indicator for the energy of the emitting electrons. It is evident from equations (9) and (10) that for $\sigma_{\tau_a} \to 0$, the distribution of n will closely reflect a Gaussian behaviour.

A necessary feature of a lognormal behaviour is a linear dependence of the average flux on its excess (rms) variation (Vaughan et al. 2003). Consistently, the electron number density at high energies should reflect this behaviour and to examine this, we compute the average number density and its variation, for a given γ and σ_{τ_a}/τ_a, by dividing the corresponding time series into 50 equal time bins. In Fig. 2(b), we show the distribution of the average number density and its variation for $\gamma = 10^3$ and $\sigma_{\tau_a}/\tau_a = 0.1$. A Spearman's rank correlation study shows these quantities are significantly correlated with correlation coefficient $\rho = 0.83$ with null hypothesis probability $P = 4 \times 10^{-26}$. In Fig. 3(a), we plot the correlation coefficient with respect to σ_{τ_a}/τ_a for different values of γ. It can be noted that the correlation improves with the increasing value of γ, thereby supporting a lognormal behaviour.

2.2 Gaussian perturbation on τ_e

In addition to the acceleration rate, the observed photon spectral index will also depend on the confinement time of the electron distribution within AR. In other words, a variation in the escape timescale in AR can introduce non-linearity in the electron distribution. To study this effect, we quantify the variation in escape time-scale (τ_e) in AR as

$$\tau_e = \tau_{e0} + \Delta\tau_e \tag{11}$$

and the corresponding change in the electron number density as

$$\tilde{n}(\gamma) = \tilde{n}_0(\gamma) + \Delta\tilde{n}(\gamma), \tag{12}$$

where $\tilde{n}_0$ is the steady state solution (equation (2)) corresponding to $\tau_e = \tau_{e0}$. Following the procedure similar to the case of τ_a (Section 2.1), substituting equations (11) and (12) in the steady state form of equation (1), the fractional variability in $\tilde{n}(\gamma)$ can then be obtained as

$$\frac{\Delta\tilde{n}}{\tilde{n}} = \tau_a\frac{\Delta\tau_e}{\tau_e^2}f(\gamma), \tag{13}$$

where

$$f(\gamma) = \log\frac{\gamma(1-\gamma_0/\gamma_{max})}{\gamma_0(1-\gamma/\gamma_{max})}. \tag{14}$$

It is evident from equation (13), that while the resultant distribution will be neither normal nor lognormal, it will be a skewed one. Additionally, since the particle index $p \sim \frac{\tau_a}{\tau_e}$, the distribution of the spectral indices will also be skewed.

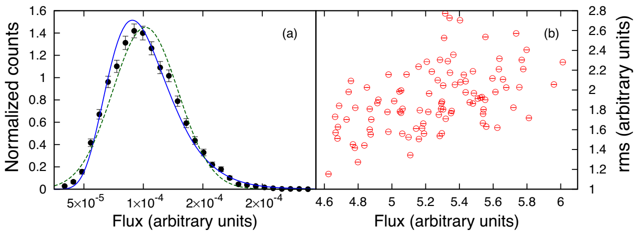

Figure 4. (a) Histogram of the simulated particle number density for $\sigma_{\tau_e}/\tau_e = 0.1$ and $\gamma = 10^3$. The dashed green line represents the best-fitting Gaussian and the solid blue line, the best-fitting lognormal PDF. (b) The flux-rms scatter plot obtained by dividing the simulated time series into 50 equal time bins. A weak positive correlation is seen ($\rho = 0.26$, $P = 0.0071$).

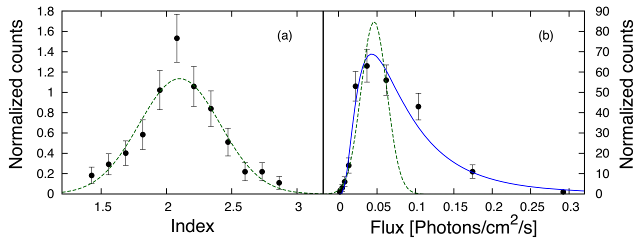

Figure 5. Histograms of the 10 d binned X-ray (a) spectral index at 2–10 keV and (b) 2–20 keV flux of Mkn 421 spanning over 9 yr. The dashed green line corresponds to the best-fitting Gaussian function, whereas the solid blue line corresponds to the best-fitting lognormal one.

To further quantify the effect on the electron number density due to a Gaussian fluctuation in τ_e, we simulate the temporal behaviour of $n(\gamma, t)$ by solving equation (1) numerically (Section 2.1). In Fig. 1(b), we show the skewness of the particle distribution (κ_n) as a function of σ_{τ_e}/τ_e for different values of γ. The distributions are highly tailed for increasing values of γ supporting a non-Gaussian behaviour. A similar behaviour is also observed in case of the skewness of the logarithm of the number density ($\kappa_{\log n}$) which is shown in Fig. 1(d). These studies suggest that the resultant electron number density distribution is significantly skewed; however, it is neither normal nor lognormal.

We also perform the Anderson Darling test on the distribution of the electron number density for various γ. Consistent with our earlier study, both Gaussian and lognormal fits are strongly rejected. In Fig. 4(a), we show the normalized histogram of the electron number density for $\gamma = 10^3$ and $\sigma_{\tau_e}/\tau_e = 0.1$ fitted with Gaussian and lognormal PDFs. Our fit result suggests both of these PDFs cannot represent the given distribution with $\chi^2_{\rm red} \approx 6.7$ (dof=28) for the Gaussian PDF and $\chi^2_{\rm red} \approx 3.7$ (dof = 28) for lognormal one. To study the flux-rms relation, we divide the temporal evolution of the number density into 50 equal time bins (Section 2.1), the average number density and its rms variation corresponding to each bin is determined. In Fig. 4(b), we show their distribution for the case of $\gamma = 10^3$ and $\sigma_{\tau_e}/\tau_e = 0.1$. A Spearman's rank correlation study suggests mild positive correlation between these quantities with $\rho = 0.26$ and $P = 0.0071$. The variation of the flux-rms correlation coefficient with respect to σ_{τ_e}/τ_e is shown in Fig. 3(b) for different values of γ. The correlation improves with increasing value of γ; however, it is less significant than the case of the Gaussian perturbation on τ_a.

3 DISCUSSION

The flux-rms relation of individual blazars or the skewness shown by the distribution of the flux are interpreted by several authors as arising from multiplicative processes, favouring a variability stemming from the disc. Alternatively, Biteau & Giebels (2012) demonstrated that such behaviour can also arise from a collection of randomly oriented mini jets within the jet. They showed that the flux from a randomly oriented mini jet will follow a Pareto distribution which preserves the flux-rms relation. Further, the total flux due to several randomly oriented mini jets will be a sum of Pareto distributions that converge to an α-stable distribution. The resultant flux distribution still holds the flux-rms relation; however, will neither be normal nor lognormal one. Nevertheless, inclusion of experimental uncertainties may imitate the distribution as a lognormal one.

In this work, we show that small temporal fluctuations in the intrinsic time-scales in the AR is capable of producing particle distributions with non-Gaussian signatures and significant flux-rms correlations. The novelty of this work is that it connects the long term temporal behaviour of the blazars with the relatively shorter time-scales of the acceleration process, and provide clues on electron energies responsible for the emission. To highlight this, we study the X-ray observations of the blazar Mkn 421 by *MAXI* satellite, spanning over 9 yr ranging from 2009 to 2018 (Matsuoka et al. 2009). While the integrated counts obtained from a 10 d binned light curve showed a lognormal behaviour with $\chi^2_{\rm red} \approx 1.43$ for 7 dof and $\sigma = 0.33 \pm 0.02$ over a Gaussian one with $\chi^2_{\rm red} \approx 9.84$ for 7 dof (Fig. 5b), the spectral indices estimated from the hardness ratio between 4–10 keV and 2–4 keV fluxes were normally distributed with $\chi^2_{\rm red} \approx 0.81$ for 10 dof, mean $m_p = 2.1 \pm 0.022$ and standard deviation $\sigma_p = 0.31 \pm 0.096$ (Fig. 5a). This suggests that the plausible physical process responsible for the observed flux variation is associated with the fluctuations in the particle acceleration rate. The fractional variation in acceleration time-scale can then be identified from σ_p and m_p of the index distribution as $\sigma_{\tau_a}/\tau_a \approx 0.148 \pm 0.046$. A comparison of Fig. 1(a) with this value and the observed skewness of $\kappa = 1.27 \pm 0.24$ suggests the emission to originate from electrons with γ range $\sim 10^2$–10^3. From Fig. 3(a), we see that this value of γ is consistent with the observed correlation co-efficient $\rho = 0.74 \pm 0.04$. However, this estimate of γ is significantly lower than the electron energies obtained through the broad-band spectral modelling of the source using synchrotron and inverse Compton emission mechanisms (Donnarumma et al. 2009; Abdo et al. 2011; Sinha et al. 2016; Zhu et al. 2016). This discrepancy can be associated with the low value of the injection Lorentz factor γ_0 which is fixed at 10 for this study. From equations (8), (9), and (10), it is evident that the skewness is a function of γ_0/γ rather than γ alone. For a given κ, higher values of γ_0 can result in large γ values that may be consistent with the ones obtained through spectral modelling.

While the lognormal distribution obtained from the light curve of blazars are generally integrated over a certain energy band, here we have quantified the distributions at some fixed electron energy. However, to be consistent with the observations, we verified our results for integrated number densities between different electron energies. We found that our results remain qualitatively similar to that obtained for the case of mono-energetic electron, being strongly dominated by the number counts at the lower energies.

4 CONCLUSION

Through this work, we show that non-Gaussian flux distributions observed in blazars can be associated with the perturbations in the intrinsic time-scales of the main particle acceleration region.

A lognormal flux distribution with the spectral indices showing a Gaussian behaviour can be attributed to the fluctuations in the acceleration rate, whereas fluctuations in the electron escape rate can cause flux/index distributions which significantly differ from Gaussian and lognormal ones. Given well sampled multiwavelength lightcurves, this study can be effectively utilized to identify the underlying physical processes, specifically in estimating the fractional fluctuations in the intrinsic time-scales and also the typical electron energies responsible for emission in the different frequency bands. In addition, by a comparison of the flux distributions at different energies (e.g X-ray and gamma-ray), it is possible to identify whether the emission is associated with similar electron energies and thus, constrain spectral models.

ACKNOWLEDGEMENTS

We are thankful to the anonymous referee for valuable comments and suggestions. SM is thankful to ISRO (ISRO/RES/2/404/15-16) and RK is thankful to CSIR, New Delhi (03(1412)/17/EMR-II) for financial support. RG would like to thank IUCAA, Pune for associateship.

REFERENCES

Abdo A. A. et al., 2011, ApJ, 736, 131
Aharonian F. et al., 2007, ApJ, 664, L71
Albert J. et al., 2007, ApJ, 669, 862
Biteau J., Giebels B., 2012, A&A, 548, A123
Chatterjee R. et al., 2012, ApJ, 749, 191
Chevalier J., Kastendieck M. A., Rieger F. M., Maurin G., Lenain J. P., Lamanna G., 2015, in 34th International Cosmic Ray Conference (ICRC2015). p. 829
Donnarumma I. et al., 2009, ApJ, 691, L13
Gaidos J. A. et al., 1996, Nature, 383, 319
Giannios D., Uzdensky D. A., Begelman M. C., 2009, MNRAS, 395, L29
Giebels B., Degrange B., 2009, A&A, 503, 797
H.E.S.S. Collaboration, 2010, A&A, 520, A83
Kardashev N. S., 1962, Sov. Astron., 6, 317
Kirk J. G., Rieger F. M., Mastichiadis A., 1998, A&A, 333, 452
Kushwaha P., Chandra S., Misra R., Sahayanathan S., Singh K. P., Baliyan K. S., 2016, ApJ, 822, L13
Lyubarskii Y. E., 1997, MNRAS, 292, 679
Matsuoka M. et al., 2009, PASJ, 61, 999
McHardy I., 2010, in Belloni T., ed., Lecture Notes in Physics , Springer Verlag, Berlin p. 203
McHardy I. M., Koerding E., Knigge C., Uttley P., Fender R. P., 2006, Nature, 444, 730
Nakagawa K., Mori M., 2013, ApJ, 773, 177
Narayan R., Piran T., 2012, MNRAS, 420, 604
Paliya V. S., Böttcher M., Diltz C., Stalin C. S., Sahayanathan S., Ravikumar C. D., 2015, ApJ, 811, 143
Press W. H., Teukolsky S. A., Vetterling W. T., Flannery B. P., 1992, Numerical recipes in FORTRAN. The art of scientific computing, Cambridge Univ. Press, Cambridge
Sahayanathan S., 2008, MNRAS, 388, L49
Sahayanathan S., Sinha A., Misra R., 2018, RAA, 18, 035
Shah Z., Mankuzhiyil N., Sinha A., Misra R., Sahayanathan S., Iqbal N., 2018, preprint (arXiv:1805.04675)
Sinha A. et al., 2016, A&A, 591, A83
Sinha A., Sahayanathan S., Acharya B. S., Anupama G. C., Chitnis V. R., Singh B. B., 2017, ApJ, 836, 83
Sobolewska M. A., Siemiginowska A., Kelly B. C., Nalewajko K., 2014, ApJ, 786, 143
Urry C. M., Padovani P., 1995, PASP, 107, 803
Uttley P., McHardy I. M., 2001, MNRAS, 323, L26
Uttley P., McHardy I. M., Vaughan S., 2005, MNRAS, 359, 345
Vaughan S., Edelson R., Warwick R. S., Uttley P., 2003, MNRAS, 345, 1271
Zhu Q., Yan D., Zhang P., Yin Q.-Q., Zhang L., Zhang S.-N., 2016, MNRAS, 463, 4481